University of Bath

PHD

Some aspects of the chemistry of co-ordinated alkynes

Walker, Alan Philip

Award date:
1995

Awarding institution:
University of Bath

Link to publication

Alternative formats
If you require this document in an alternative format, please contact:
openaccess@bath.ac.uk

Copyright of this thesis rests with the author. Access is subject to the above licence, if given. If no licence is specified above, original content in this thesis is licensed under the terms of the Creative Commons Attribution-NonCommercial 4.0 International (CC BY-NC-ND 4.0) Licence (https://creativecommons.org/licenses/by-nc-nd/4.0/). Any third-party copyright material present remains the property of its respective owner(s) and is licensed under its existing terms.

Take down policy
If you consider content within Bath's Research Portal to be in breach of UK law, please contact: openaccess@bath.ac.uk with the details. Your claim will be investigated and, where appropriate, the item will be removed from public view as soon as possible.

Download date: 05. May. 2023

Some Aspects of the Chemistry of Co-ordinated Alkynes.

Submitted by Alan Philip Walker
for the degree of Ph.D.
of the University of Bath
1995

COPYRIGHT

Attention is drawn to the fact that the copyright of this thesis rests with its author. This copy of the thesis has been supplied on the condition that anyone who consults it is understood to recognise that its copyright rests with its author and that no quotation from the thesis and no information derived from it may be published without the prior written consent of the author.

This thesis may be made available for consultation within the University Library and may be photocopied or lent to other libraries for the purposes of consultation.

UMI Number: U541588

All rights reserved

INFORMATION TO ALL USERS
The quality of this reproduction is dependent upon the quality of the copy submitted.

In the unlikely event that the author did not send a complete manuscript
and there are missing pages, these will be noted. Also, if material had to be removed,
a note will indicate the deletion.

UMI U541588
Published by ProQuest LLC 2013. Copyright in the Dissertation held by the Author.
Microform Edition © ProQuest LLC.
All rights reserved. This work is protected against
unauthorized copying under Title 17, United States Code.

ProQuest LLC
789 East Eisenhower Parkway
P.O. Box 1346
Ann Arbor, MI 48106-1346

UNIVERSITY OF BATH
LIBRARY
21 23 AUG 1996
PhD
510540

Memorandum

The work described in this thesis was carried out by the author between October 1992 and September 1995 within the School of Chemistry at the University of Bath, under the supervision of Professor Michael Green. Unless otherwise indicated the work is original and has not been submitted for any other degree.

Summary

The formation and reactivity of alkyne complexes of molybdenum and tungsten form the basis of the work described in this thesis.

Chapter one is a general introductory chapter describing the synthesis and reactivity of various types of alkyne complexes, mainly of molybdenum and tungsten, and the interest they have raised in recent years. The conversion of these alkyne complexes into η^1-vinyl and η^2(3e)-vinyl complexes is discussed and the role of these vinyl complexes as reaction intermediates.

Chapter two is concerned with the synthesis of η^4(5e)-butadienyl ligands. These are derived from the neutral bis-alkyne complexes of molybdenum with the formula $[XMo(\eta^2\text{-}RC_2R)_2(\eta\text{-}C_5H_5)]$. The η^4(5e)-butadienyl molybdenum complex $[BrMo{=}C(Et)\text{-}\eta^3\text{-}\{C(Et)C(Et)CHEt\}(OH_2)(\eta{-}C_5H_5)][BF_4]$ is described and has been structurally identified by X-ray crystallography. Its formation from the bis-alkyne complex is discussed and it is postulated that an η^2(3e)-vinyl complex is an intermediate in the reaction. Substitution reactions on the η^4(5e)-butadienyl complex are described, as is a deprotonation reaction leading to a diene complex $[ClMo\{\eta^4\text{-}CHMe{=}C(Me).C(Me){=}C{=}CH_2\}\{P(OMe)_3\}(\eta{-}C_5H_5)]$.

Chapter three discusses the synthesis of pentamethylcyclopentadienyl bis-alkyne complexes of tungsten and molybdenum. A modification of an earlier cyclopentadienyl molybdenum synthesis by Beck is used to synthesise bis-alkyne complexes direct from $[Mo(CH_3)(CO)_3(\eta{-}C_5Me_5)]$. It is shown that these complexes have similar chemistry to their cyclopentadienyl analogues, but there is a difference found in their reactivity. Some four-electron donor alkyne complexes of molybdenum are synthesised and reported. Also the synthesis of a heptamethylindenyl complex of molybdenum is described.

Chapter four contains all the experimental procedures and experimental data for the complexes described in chapters two and three.

Acknowledgements

Firstly, I would like to express my gratitude to Professor Michael Green for giving me the opportunity of researching under his supervision for my three years at Bath University.

I would like to thank Dr Mary Mahon for the crystal structure determinations carried out at Bath University. I would also like to thank Dr Tom McGrath for two crystal structure determinations and the EHMO calculations carried out at Heriot-Watt University, and Mr Rhodri Thomas for his assistance with these. Also Sue Wingate for some preliminary experiments.

Special thanks must go to the technical staff within the department, especially Ahmed Sheibani, Robert Stevens and Alan Carver, who provided excellent support services. Thanks to Dr Nick Carr, Dr Stephen Dossett, Dr Tom McGrath, Jackie McInnes, Chris Butters, Simon Rumble, Georg Brauers, Claire Beddows, Gareth Cairns and all the other people who have worked in 2.31, who have made my time here so enjoyable.

I thank the E.P.S.R.C (S.E.R.C) for financial support over the three years.

Finally, I would like to thank some special people who deserve to be named here! Emma Lenz for not being **BAD!** in any way what so ever, all "the gang" at Clarence Terrace, Phillip "P" Perks for being the best mate in the world, and my parents for their support and encouragement over the years.

Abbreviations.

M	:	Metal Atom
L	:	Ligand
X	:	Halide
R	:	Alkyl Group
Ar	:	Aryl Group
Me	:	Methyl Group
Et	:	Ethyl Group
Bu	:	Butyl Group
Ph	:	Phenyl Group
s	:	Secondary
t	:	Tertiary
o	:	Ortho
MeCN		Acetonitrile
THF	:	Tetrahydrofuran
η-C_5H_5; Cp	:	η^5-Cyclopentadienyl
η-C_5Me_5; Cp*	:	η^5-Pentamethylcyclopentadienyl
η^5-C_9Me_7, Ind*	:	η^5-Heptamethylindenyl
Δ	:	Reflux
ν	:	Frequency
NMR	:	Nuclear Magnetic Resonance
Relating to NMR		
J	:	Coupling Constant, Hz
N	:	$\lvert J_{AX} + J_{AX'} \rvert$, Virtual Coupling Constant, Hz
s	:	Singlet
d	:	Doublet
t	:	Triplet
q	:	Quartet
m	:	Multiplet
br	:	Broad
u	:	Unresolved

v	:	Virtual
IR	:	Infra Red
Relating to IR		
ν	:	Frequency
	:	
Relating to Mass Spectra		
FAB	:	Fast Atom Bombardment
M	:	Mass of Parent Ion
Relating to X-ray Diffraction		
a, b, c	:	Unit Cell Length in Å
α, β, γ	:	Angles Between Pairs of Sides
Z	:	Number of Molecules in Unit Cell
U	:	Volume of Unit Cell in $Å^3$
D_c	:	Density in gcm^{-3}
F(000)	:	Total Number of Electrons in Unit Cell
μ(Mo-K_α)	:	Linear Absorbance Coefficient for Molybdenum K_α Radiation

Contents

List of New Complexes or Complexes Synthesised *Via* New Methods.

(21b) $[BrMo{=}C(Et)\text{-}\eta^3\text{-}\{C(Et)C(Et)CHEt\}(OH_2)(\eta\text{-}C_5H_5)][BF_4]$

(24) $[Mo(\eta^2\text{-}PhCH_2C_2CH_2Ph)_2(CO)(\eta\text{-}C_5H_5)][BF_4]$

(25) $[Mo(\eta^2\text{-}PhCH_2C_2CH_2Ph)_2(NCMe)(\eta\text{-}C_5H_5)][BF_4]$

(26) $[BrMo(\eta^2\text{-}PhCH_2C_2CH_2Ph)_2(\eta\text{-}C_5H_5)]$

(27) $[BrMo{=}C(Et)\text{-}\eta^3\text{-}\{C(Et)C(Et)CH(Et)\}(NCMe)(\eta\text{-}C_5H_5)][BF_4]$

(28) $[BrMo{=}C(Et)\text{-}\eta^3\text{-}\{C(Et)C(Et)CH(Et)\}\{P(OMe)_3\}(\eta\text{-}C_5H_5)][BF_4]$

(29) $[BrMo{=}C(Et)\text{-}\eta^3\text{-}\{C(Et)C(Et)CH(Et)\}(PMe_3)(\eta\text{-}C_5H_5)][BF_4]$

(31) $[I_2Mo{=}C(Et)\text{-}\eta^3\text{-}\{C(Et)C(Et)CHEt\}(\eta\text{-}C_5H_5)]$

(32) $[BrIMo{=}C(Et)\text{-}\eta^3\text{-}\{C(Et)C(Et)CHEt\}(\eta\text{-}C_5H_5)]$

(35) $[IMo{=}C(Et)\text{-}\eta^3\text{-}\{C(Et)C(Et)CHEt\}(NCMe)(\eta\text{-}C_5H_5)][BF_4]$

(36) $[ClIMo{=}C(Et)\text{-}\eta^3\text{-}\{C(Et)C(Et)CHEt\}(\eta\text{-}C_5H_5)]$

(37) $[Br_2Mo{=}C(Et)\text{-}\eta^3\text{-}\{C(Me)C(Me)CH(Me)\}(\eta\text{-}C_5H_5)]$

(38) $[BrClMo{=}C(Et)\text{-}\eta^3\text{-}\{C(Me)C(Me)CH(Me)\}(\eta\text{-}C_5H_5)]$

(39) $[ClMo{=}C(Me)\text{-}\eta^3\text{-}\{C(Me)C(Me)CHMe\}(OH_2)(\eta\text{-}C_5H_5)][CF_3SO_3]$

(45) $[BrMo\{\eta^4\text{-}CHEt{=}C(Et).C(Et){=}C{=}CHMe\}\{P(OMe)_3\}(\eta\text{-}C_5H_5)]$

(46) $[IMo\{\eta^4\text{-}CHEt{=}C(Et).C(Et){=}C{=}CHMe\}(CO)(\eta\text{-}C_5H_5)]$

(48) $[Mo(\eta^2\text{-}MeC_2Me)_2(CO)(\eta\text{-}C_5Me_5)][BF_4]$

(49) $[Mo(\eta^2\text{-}PhC_2Ph)_2(CO)(\eta\text{-}C_5Me_5)][BF_4]$

(51) $[Mo(\eta^2\text{-}MeC_2Me)_2(NCMe)(\eta\text{-}C_5Me_5)][BF_4]$

(52) $[BrMo(\eta^2\text{-}MeC_2Me)_2(\eta\text{-}C_5Me_5)]$

(60) $[Mo(\eta^2\text{-}PhC_2Ph)\{P(OMe)_3\}_2(\eta\text{-}C_5Me_5)][BF_4]$

(61) $[Mo(\eta^2\text{-}PhC_2Ph)(CO)(PMe_3)(\eta\text{-}C_5Me_5)][BF_4]$

(63) $[W(CO)_2(NCMe)_2(\eta\text{-}C_5Me_5)][BF_4]$

(64) $[W(\eta^3\text{-}C_3H_5)(CO)_2(\eta\text{-}C_5Me_5)]$

(65) $[W(\eta^2\text{-}MeC_2Me)_2(CO)(\eta\text{-}C_5Me_5)][BF_4]$

(66) $[W(\eta^2\text{-}EtC_2Et)_2(CO)(\eta\text{-}C_5Me_5)][BF_4]$

(67) $[W(\eta^2\text{-}MeC_2Me)_2(NCMe)(\eta\text{-}C_5Me_5)][BF_4]$

(69) $[Mo(\eta^3\text{-}C_3H_5)(CO)_3(\eta^5\text{-}C_9Me_7)]$

1. General Introduction

1.1 Alkynes as Ligands in Transition Metal Complexes.

Since the mid 1970's there has been a large interest in metal alkyne chemistry. Previous to this time, it was thought that generally alkynes were analogous to alkenes, being two-electron σ-donor/π-acceptor ligands. Consequently little attention was paid to the bonding involved in a transition metal-alkyne complex. This surmise was supported by the known alkyne complexes of the 1960's, in which analogous reactivity between alkyne and alkene complexes of late transition metals was observed[1-4] (Figure 1.1).

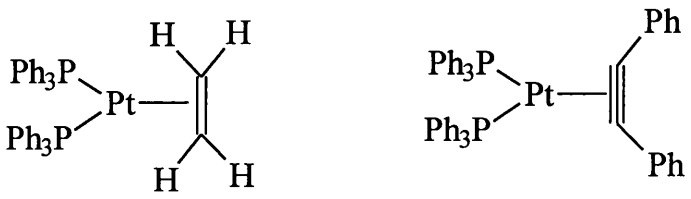

Figure 1.1. Analogous alkene and alkyne complexes of platinum.

Occasionally rigorous application of the 18-electron rule was not always possible for some transition metal complexes. It was not until a supposedly 14-electron tungsten species was first reported by Tate and Augl[5,6] in 1963 that the possibility of alkyne ligands stabilising a metal complex to greater extent than just a two-electron donor, as in an alkene complex, was considered.

Reaction of $[W(CO)_3(MeCN)_3)]$ with diphenylacetylene or 3-hexyne led to the formation of a neutral, yellow complex with the formula $[W(\eta^2\text{-}RC_2R)_3(CO)]$ (eq.1.1).

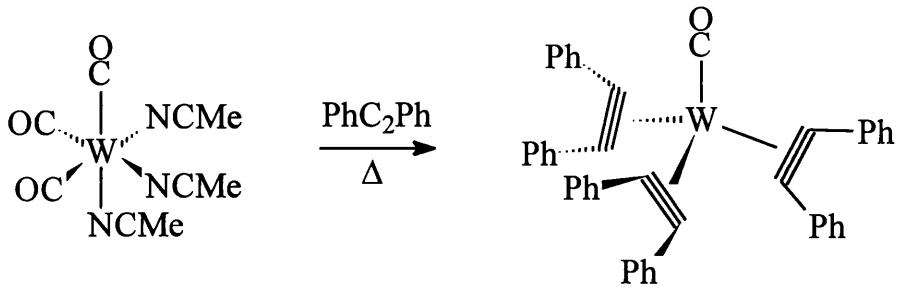

(I) **(II)** eq.1.1

Spectroscopic data suggested that all of the three alkyne ligands were identical, but each end of the alkyne ligand was in a different environment. The pseudo-tetrahedral structure of (**II**) shown in eq.1.1 was suggested. In order to satisfy the 18-electron rule, each alkyne would need to donate $3\,1/3$ electrons to the metal centre, bearing in mind that they are all equivalent on the NMR time-scale. This situation could be explained by a rapidly alternating system of two four-electron donor alkyne ligands and one two-electron donor alkyne. These conclusions were subsequently supported by the determination of the structure of (**II**) by X-ray crystallography,[7] which confirmed the C_{3v} symmetry of the molecule and a study of the orbital interactions by King.[8] This latter study showed that there was no possibility for the third alkyne to donate four electrons owing to orbital interactions. This led to the prediction that $[W(\eta^2\text{-}RC_2R)_3]$ was not stable and therefore required the CO ligand to stabilise the complex.

1.2 Bonding of the Four-Electron Donor Alkyne to a Transition Metal Centre.

The side on co-ordination of alkynes can be described by the four orbital interactions shown in Figure 1.2.

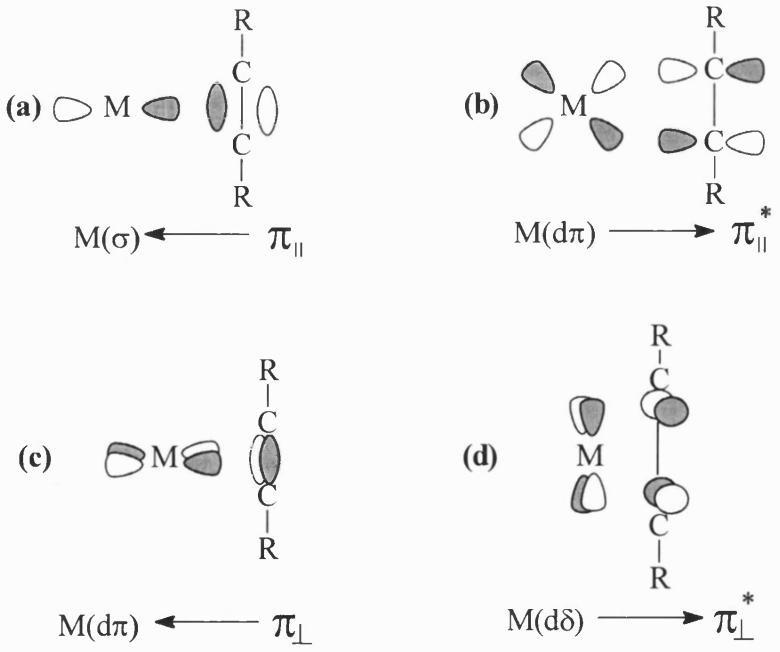

Figure 1.2. Orbital interactions involved in metal-alkyne bonding.

These interactions are dependent on the oxidation state of the metal, the nature of the auxiliary ligands on the metal and the substituents on the alkyne ligand itself. The σ-$\pi_{\|}$ donation (a) (ligand-metal) exhibits the greatest overlap. The dπ-$\pi_{\|}^{*}$ (b) and dπ-$\pi_{\perp}$ (c) are similar in energy and the dσ-$\pi_{\perp}^{*}$ (d) is negligible. Interactions (a) and (b) are usually bonding, (c) can be bonding when the metal atom has vacant dπ orbitals or anti bonding when the dπ orbitals are filled (d^{10} late transition metals).[9] The number of electrons donated by an alkyne ligand depends on the availability of filled or vacant orbitals and the energy levels of interactions (a) to (c). The bonding of a two-electron donor alkyne may be regarded as analogous to the metal-alkene bonding as described by the Dewar-Chatt-Duncanson model.[10,11] The interactions involved are the donation from the alkyne($\pi_{\|}$) to the vacant metal σ acceptor orbital (a) and acceptance ($\pi_{\|}^{*}$) from a filled dπ orbital (b). The bonding for a four-electron donor alkyne involves, in addition to the two interactions described for a two-electron donor, a donation from the filled $\pi_{\perp}$ orbitals to an empty dπ orbital (c). Four-electron donor alkynes are net electron donors, whereas two-electron donor alkynes can be net donors or acceptors.

1.3 Spectroscopic and Structural Features of Alkyne Complexes.

It has now been established that alkynes can donate more than two electrons and where there is more than one alkyne ligand bonded to a metal centre, the number of electrons donated per alkyne does not necessarily have to be an integer (e.g.(**II**) in eq.1.1).

Templeton[12,13] first noted the systematic relationship between the $^{13}C\{^{1}H\}$ NMR chemical shift of the contact carbons of the alkyne ligands and N, the effective number of electrons donated per alkyne ligand, for a number of molybdenum(II) and tungsten(II) complexes. A graph plotting N against carbon chemical shift clearly shows the correlation (Figure 1.3).

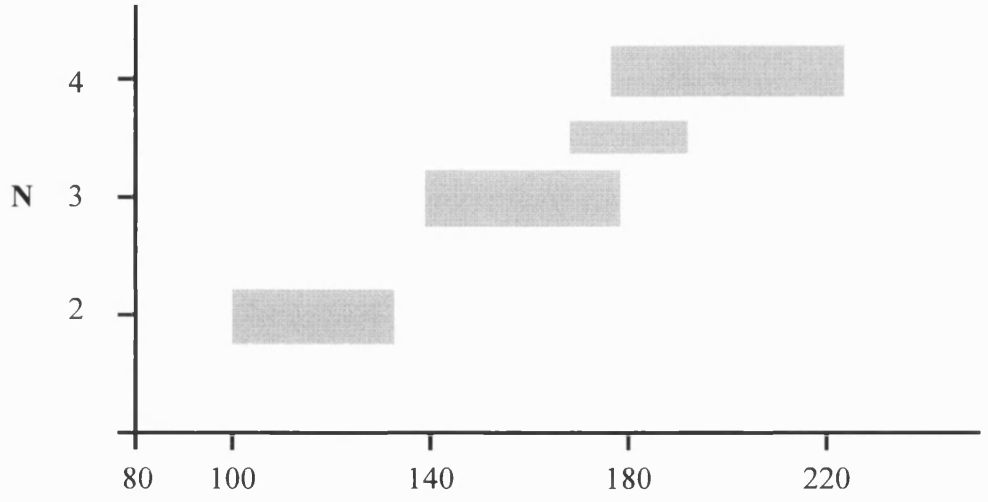

Figure 1.3. Graph showing the relationship between N and carbon chemical shift.

The signals for two-electron donor alkyne ligands fell in the range 100 to 130 ppm, three-electron donor alkyne signals were in the range 140 to 180 ppm and four-electron donor alkynes were in the range 175 to 230 ppm. Examples of $3_{1/3}$ donation such as (**II**) fell in the range 170 to 190 ppm, which is consistent with this correlation.

To a lesser extent, as it is only applicable to terminal alkynes, ^{1}H NMR can be used to determine the extent of electron donation of an alkyne ligand. The alkyne protons in $[Mo(\eta^2\text{-}HC_2H)(\eta\text{-}C_5H_5)_2]$[9] resonate at 7.7 ppm (two-electron donor), whereas the protons in $[Mo(\eta^2\text{-}HC_2H)(CO)(PPh_3)(\eta\text{-}C_5H_5)]^+$ (four-electron donor)[14] resonate at 12.9 and 12.0 ppm.

In general the side on co-ordination of alkynes and other multiply bonded species, gives rise to a reduction in the bond order of the ligand. This leads to an increase in the C-C bond length. This is observed for alkyne ligands that have been structurally identified by X-ray crystallography. This feature is not, however, a sensitive indicator of the extent of electron donation. The C-C bond lengths obtained fall somewhere in between the values for a non-complexed doubly or triply bonded system.[15] The linearity of the alkyne ligand is deformed with a bending of the substituents away from the metal, but again this is not a sensitive indicator of the

extent of electron donation. The metal-carbon distances do, however, give some useful information. Table 1.1 gives some examples of M-C and C-C distances.

Table 1.1. Structural parameters for some group 6 complexes.

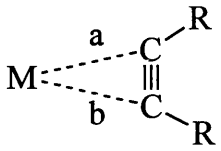

N	Complex	$\frac{a+b}{2}$ (Å)	C-C (Å)
0	C=C	---	1.34
0	C≡C	---	1.20
2	$[Mo(\eta^2\text{-}PhC_2Ph)(\eta\text{-}C_5H_5)_2]$	2.14	1.27
3	$[ClW(\eta^2\text{-}CF_3C_2CF_3)_2(\eta\text{-}C_5H_5)]$	2.06	1.28
3	$[IMo(\eta^2\text{-}MeC_2Me)_2(\eta\text{-}C_5H_5)]$	2.06	1.27
3 1/3	$[W(\eta^2\text{-}PhC_2Ph)_3(CO)]$	2.06	1.30
4	$[Mo(\eta^2\text{-}MeC_2Me)(PMe_3)_2(\eta\text{-}C_5H_5)][BF_4]$	2.02	1.31
4	$[W(\eta^2\text{-}HC_2H)(CO)(S_2CNEt_2)_2]$	2.03	1.29

Although not definitive (some overlap is observed), it is possible to define some ranges for M-C bond lengths. N = 4 donors fall within 2.03 ± 0.03Å, N= 3 donors fall within 2.07 ± 0.02Å and N = 2 donors fall within 2.15 ± 0.02Å.

1.4 Preparation of Mono- and Bis-Alkyne Complexes.

After the preparation of $[W(\eta^2\text{-}PhC_2Ph)_3(CO)]$, further investigations showed that this complex was not unique in its ability to donate more than two electrons to the metal centre. The most significant observations made by Templeton and others in section 1.3 were obtained by studies on alkyne complexes of molybdenum and tungsten in the +2 oxidation state. The concept of the four-electron donor alkyne

was established unequivocally by work carried out on these complexes. The main approaches to their synthesis are detailed in Figure 1.4.[15-20]

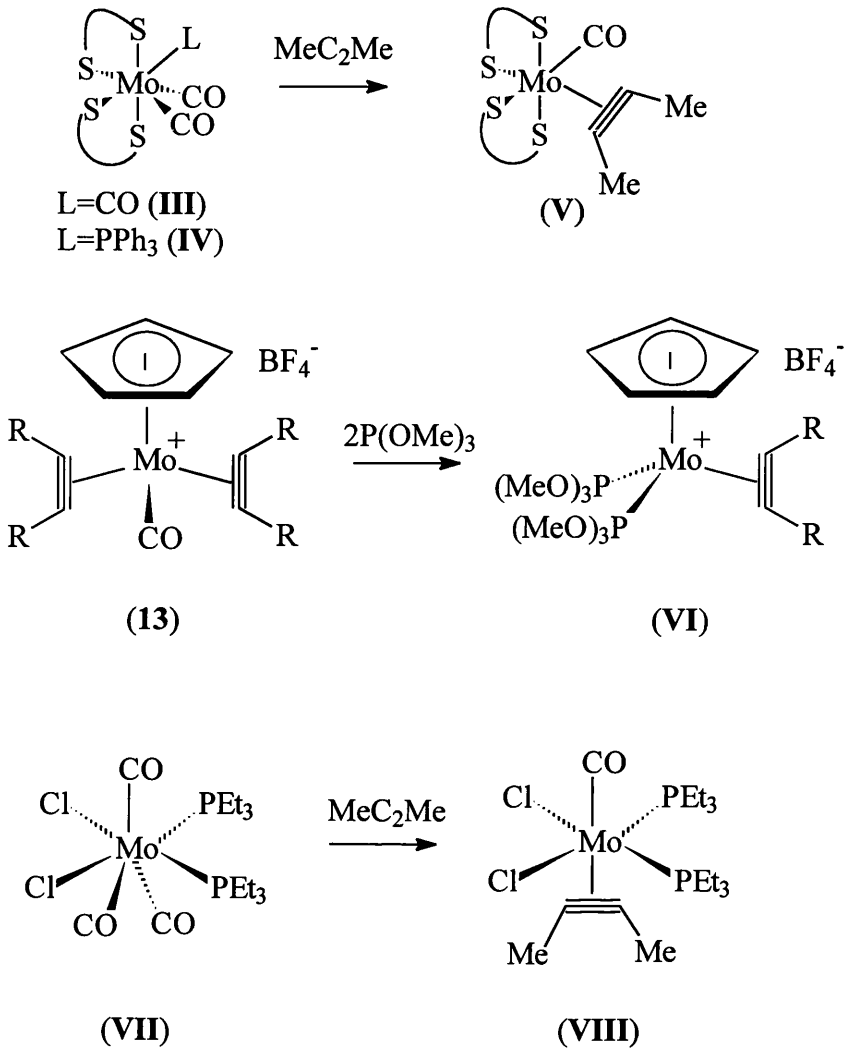

Figure 1.4. Preparative methods for four-electron donor alkyne complexes.

Many variations of alkyne (terminal, with electron donating and withdrawing substituents) complexes have been synthesised, but there is no general methodology for their preparation.

Three-electron donor alkyne complexes also form an important group of complexes, and are precursor complexes for the work described in this thesis. The donation in these bis-alkyne complexes may be seen as a rapidly alternating 4 + 2 system similar to complex (**II**). The bis-alkyne complexes of molybdenum can be

synthesised by a number of ways. The oxidative cleavage of $[Mo(CO)_3(\eta\text{-}C_5H_5)]_2$ using $Ag[BF_4]$ in the presence of alkyne,[21] substitution of MeCN and CO ligands from $[Mo(CO)_2(NCMe)_2(\eta\text{-}C_5H_5)][BF_4]$[22] and protonation of $[Mo(CH_3)(CO)_3(\eta\text{-}C_5H_5)]$ and subsequent addition of alkyne[23] (Figure 1.5).

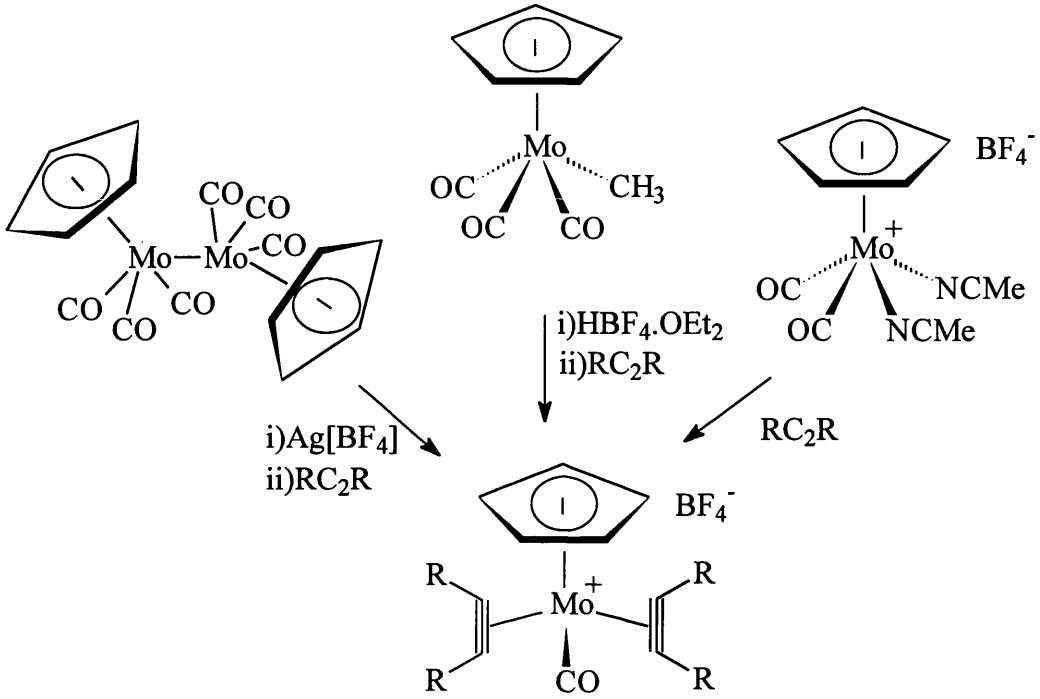

(13)

Figure 1.5. Synthetic routes to bis-alkyne complexes of molybdenum.

There are also examples of N = 3 donor alkyne complexes to the immediate right[24] and left[25] of the d^6 metal series (Figure 1.6).

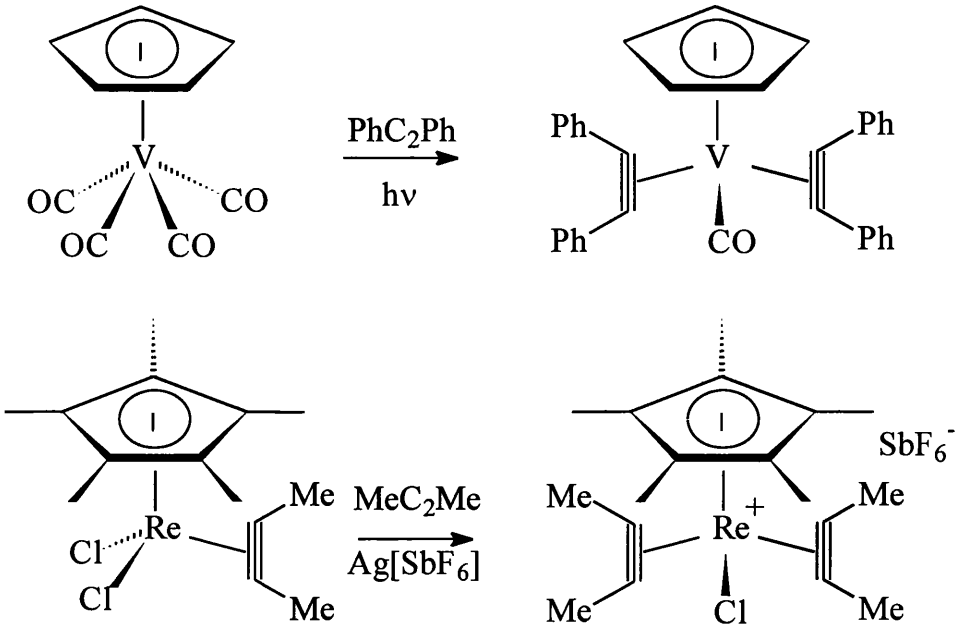

Figure 1.6. Other bis-alkyne complexes of the transition metals.

1.5 Reactions of Molybdenum(II) and Tungsten(II) Alkyne Complexes to Give η^1*-Vinyl and* η^2*(3e)-Vinyl Ligands.*

With a wide range of alkyne complexes where the alkyne ligand donates more than two electrons now established, further work was carried out to assess the reactivity of these complexes.

The formation of vinyl ligands was an area which has received a lot of interest. There are several methods described for the preparation of η^1-vinyl ligands from various functional groups. Alkyne,[26-28] acetylide[29] and alkene[30] complexes have all been used to create these ligands (Figure 1.7).

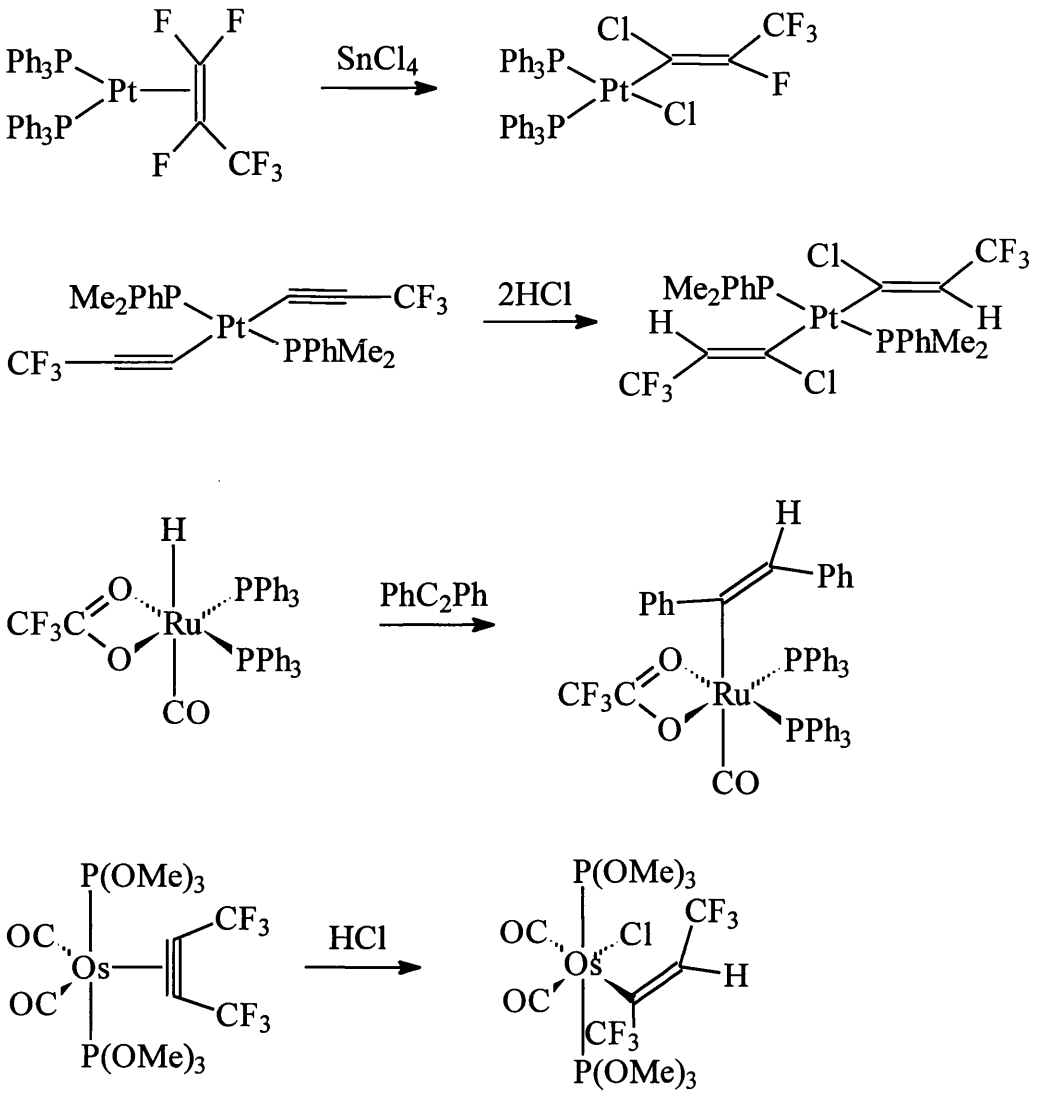

Figure 1.7 Preparation of η^1-vinyl ligands.

From these examples it can be seen that there are many ways to synthesise these ligands. They can also be synthesised by nucleophillic attack on an alkyne ligand[31,32] (eq.1.2).

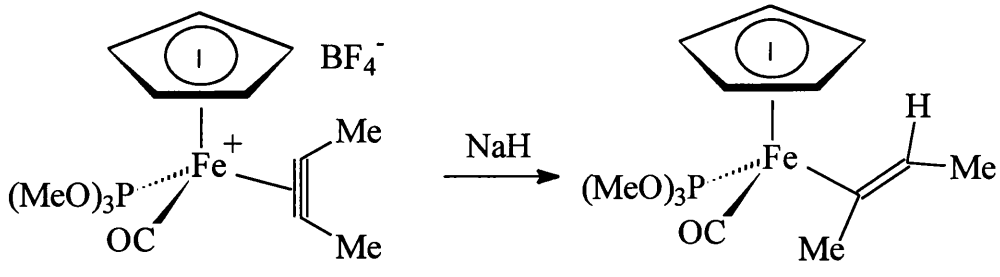

(IX) **(X)** eq.1.2

In complex (**IX**) the alkyne ligand is functioning as a two-electron donor. If the same reaction was attempted with a four-electron donor alkyne ligand, formation of an η^1-vinyl ligand would be unlikely as this would result in an unstable 16e complex. This was seen to be the case as other stable types of complexes were formed. The reactions of the analogous molybdenum cations to (**IX**) which contain a four-electron donor alkyne ligand illustrate this. Reaction of (**XI**) with $Na[BH_4]$ in the presence of $P(OMe)_3$, gave an η^1-vinyl complex[33] (eq.1.3).

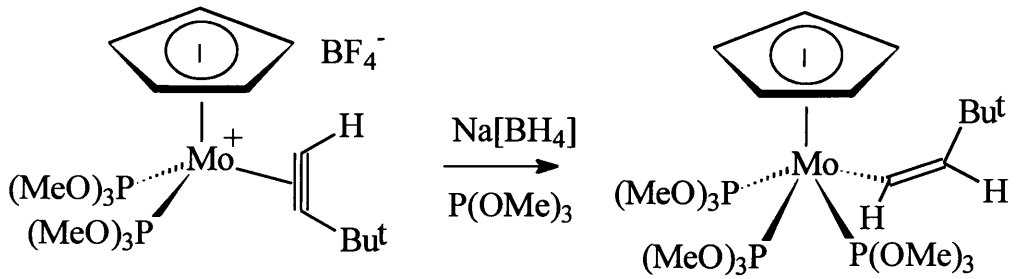

(**XI**) (**XII**) eq.1.3

The generation of the η^1-vinyl ligand was made possible by the incorporation of the extra molecule of $P(OMe)_3$, to give an 18e complex. When (**XI**) was reacted with just Ph_2CuLi, a very interesting result was obtained.[34] This reaction led to a stable complex containing a three-electron donor ligand (eq.1.4).

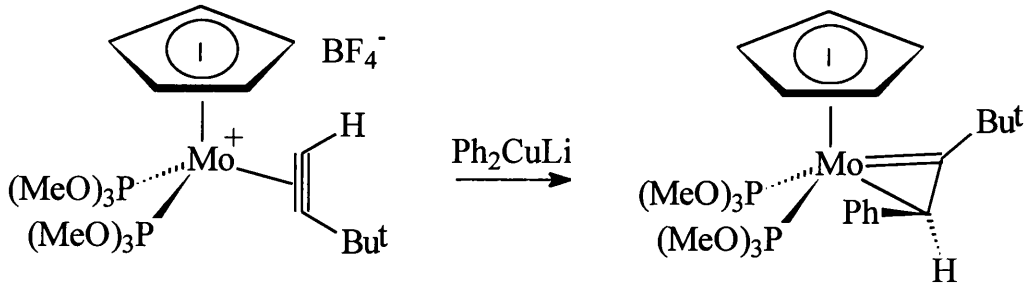

(**XIII**) (**XIV**) eq.1.4

The three-electron donor ligand contained in this complex has been described variously as a metallocyclopropene, cyclic alkylidene and an η^2(3e)-vinyl ligand.

The final description, that of an η^2(3e)-vinyl ligand, shall be used here, as it emphasises a link between it and the η^1-vinyl bonding mode. Many of the subsequent investigations into the η^2(3e)-vinyl ligand have been directed towards the interchange between these two modes of bonding (Figure 1.8).

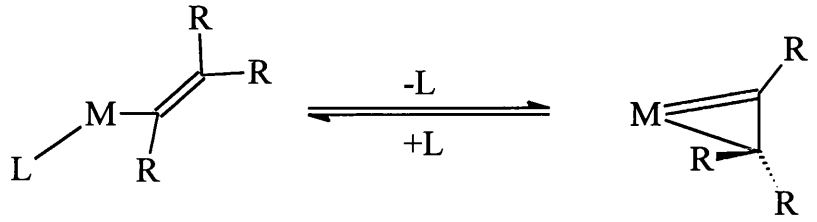

Figure 1.8. The reversible conversion of an η^1-vinyl ligand to an η^2(3e)-vinyl ligand.

The change from η^2 to η^1 bonding would allow associative reaction pathways, whilst retaining a stable 18e configuration. A significant result in this area was a reaction between the bis-alkyne complex (**13**) and Me_2CuLi. This could have led to three possible complexes: a neutral complex containing an η^1-vinyl ligand and a four-electron donor alkyne ligand, a neutral complex with an η^2(3e)-vinyl ligand and a two-electron donor alkyne or a coupled product. The product obtained was in fact an η^1-vinyl complex[35] (eq.1.5).

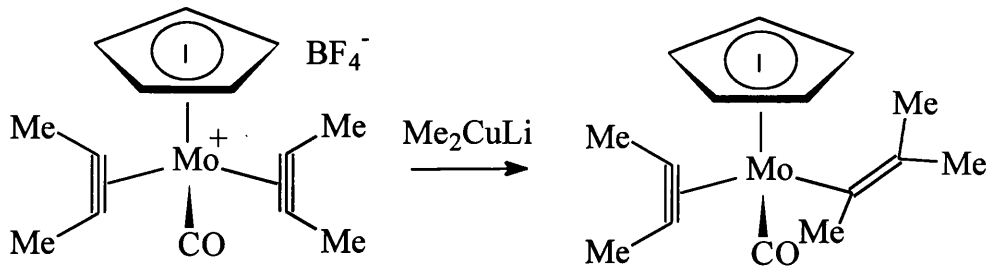

(**13**) (**XV**) eq.1.5

The first reported example of an η^2(3e)-vinyl complex was by Kreissel *et al*[36-39] (eq.1.6).

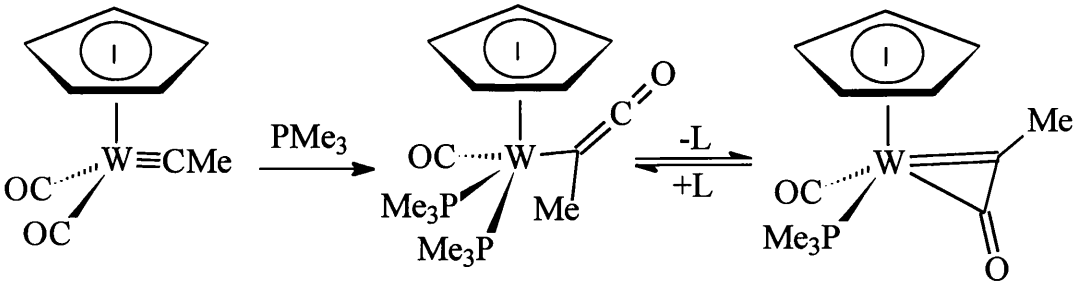

(XVI) **(XVII)** **(XVIII)** eq.1.6

In this case the η^1 to η^2 conversion was reversible. Reaction of **(XVIII)** with CO produced the bis-carbonyl analogue via a ligand incorporation/expulsion mechanism. This reversibility is not a general feature of the chemistry of the η^2(3e)-vinyl ligand.

1.6 η^2(3e)-Vinyl Ligands as Reaction Intermediates.

The chemistry of the η^2(3e)-vinyl ligand developed by M. Green and co-workers has highlighted their role as intermediates. The synthesis of π-allyl and carbyne complexes from alkyne complexes of molybdenum can be traced through η^2(3e)-vinyl intermediates.

When the η^2(3e)-vinyl complex **(XIX)** was left to stand in a toluene solution for 3 days at room temperature, a rearrangement to an isomeric π-allyl complex occurred (Figure 1.9).

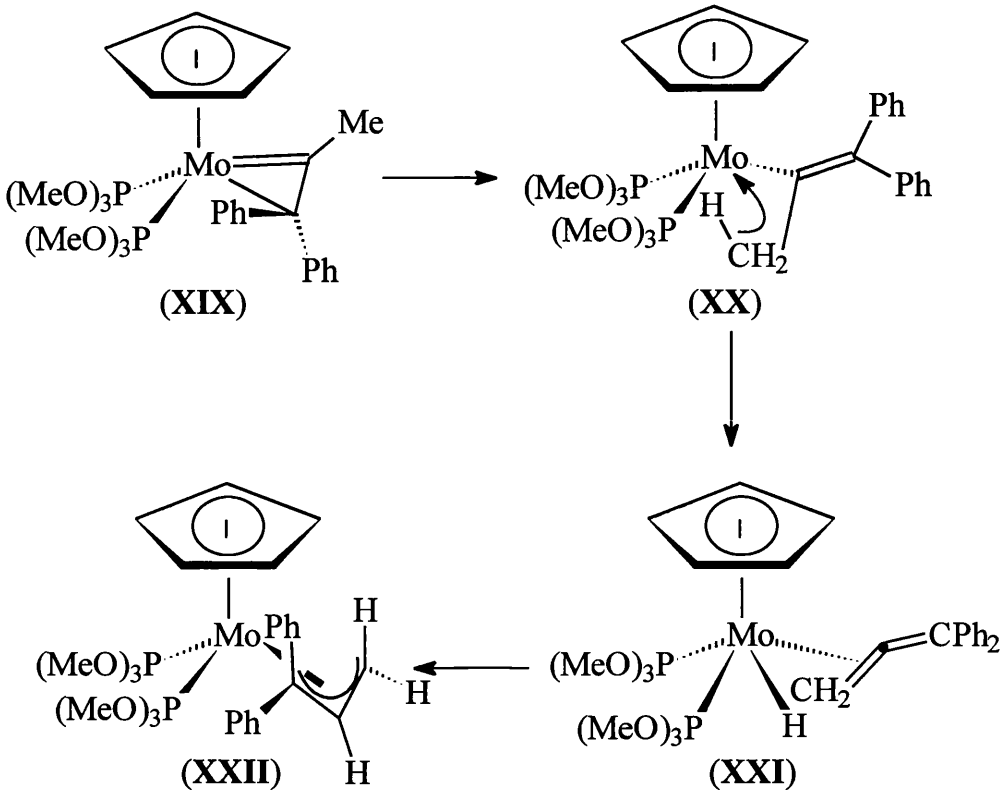

Figure 1.9. Isomerisation of an η^2(3e)-vinyl complex to a π-allyl complex.

The mechanism of an η^1-vinyl ligand isomerising to a π-allyl ligand had been studied previously.[40,41] This rearrangement in Figure 1.9. required only one additional step, the η^2 to η^1 switch in bonding mode of the vinyl ligand. This rearrangement was achieved *via* the elimination of a β (methyl) hydrogen from the η^1-vinyl complex (**XX**) to give the hydrido allenyl complex (**XXI**). Rotation about the double bond followed by hydrogen migration on to the central carbon atom gave the π-allyl complex (**XXII**). There are some reactions where alkyne complexes are converted to π-allyl complexes,[35,40,42] where no intermediate can be isolated. It may be the case that a short lived η^2(3e)-vinyl intermediate may be involved.

There is also an example of an η^2(3e)-vinyl ligand rearranging to an alkylidyne ligand in the presence of PhIO[43] (Figure 1.10).

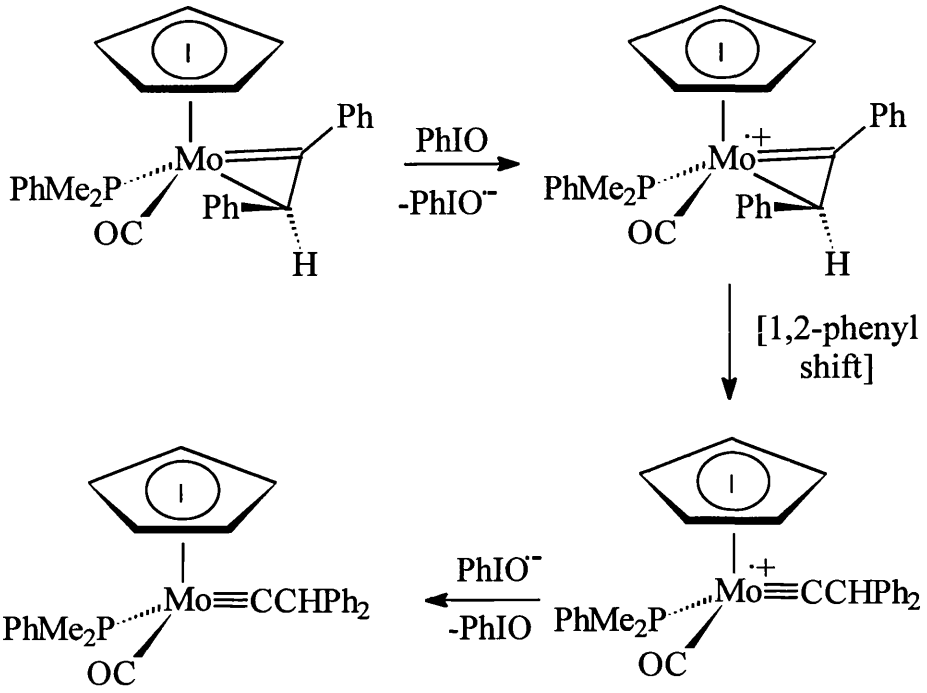

Figure 1.10. Rearrangement of an η^2(3e)-vinyl ligand to an alkylidyne ligand.

The original aim of the reaction was to convert a co-ordinated CO molecule to unco-ordinated CO_2 molecule with the iodosobenzene *via* oxygen transfer. It is suggested that the electron rich η^2(3e)-vinyl complex undergoes a one electron transfer reaction with PhIO to give a radical cation which transforms *via* a 1,2-phenyl shift into the alkylidyne.

1.7 Preparation of η^2(3e)-Vinyl Ligands from Alkyne Complexes.

Green and co-workers have undertaken extensive studies of η^2(3e)-vinyl complexes. They concentrated on reaction of H^-, alkyl and aryl nucleophiles with four-electron donor alkyne complexes of molybdenum with the general molecular formula $[Mo(\eta^2\text{-}RC_2R')\{P(OMe)_3\}_2(\eta\text{-}C_5H_5)][BF_4]$. When the alkyne Bu^tC_2H was used an η^2(3e)-vinyl or η^1-vinyl complex was formed on reaction with nucleophiles, depending on whether excess $P(OMe)_3$ was present (see eq.1.3). Reaction of $[Mo(\eta^2\text{-}PhC_2Ph)\{P(OMe)_3\}_2(\eta\text{-}C_5H_5)][BF_4]$ with $K[BHBu^s{}_3]$ gave the

η^2(3e)-vinyl complex (**XXIII**). Further reaction with the weak acid C_6F_5SH gave the co-ordinated *cis* and *trans* stilbene (Figure 1.11).

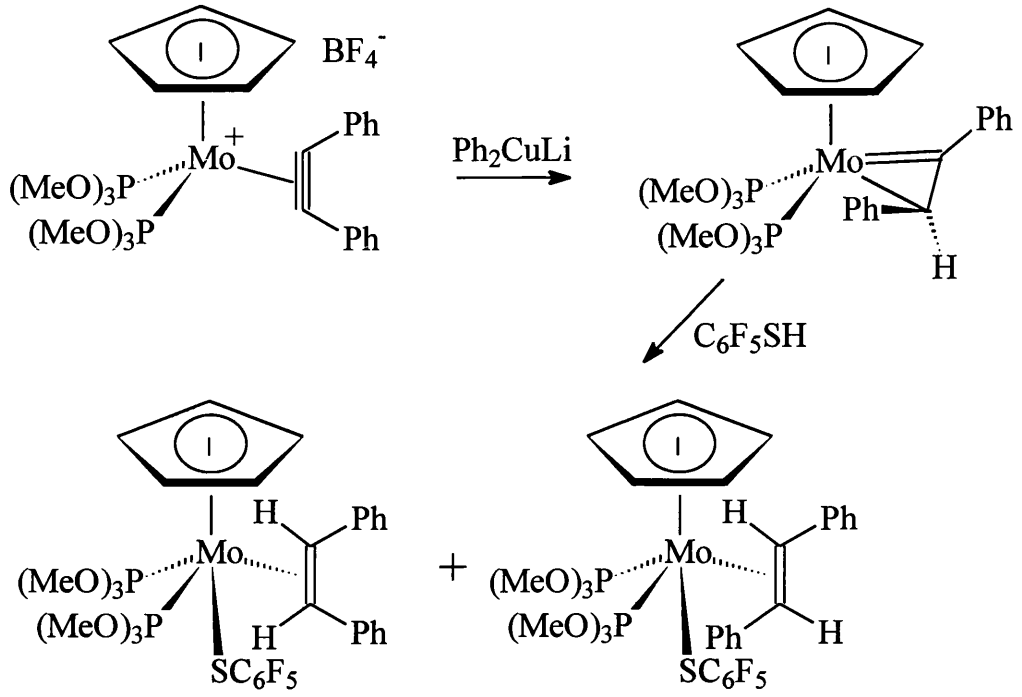

Figure 1.11. Conversion of an η^2(3e)-vinyl ligand to an alkene.

This indicated that there was a slight negative charge on the carbene carbon atom $M^{\delta+}=C^{\delta-}$, as in a Schrock type system.[44-46] Further investigations showed that the eventual product obtained on reaction of a four-electron donor alkyne complex of the type (**XIII**) with nucleophiles depended on the substituents on the alkyne ligand and the nature of the nucleophile itself. Some examples of this are given in Figure 1.12.

Ln = $\{P(OMe)_3\}_2(\eta\text{-}C_5H_5)$

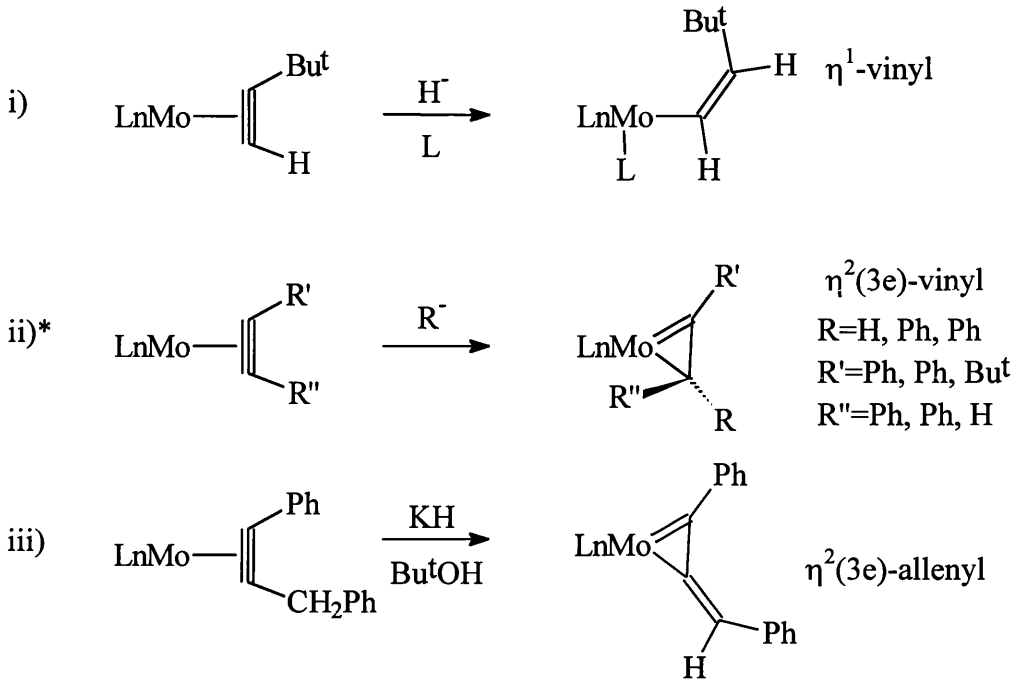

* Many other combinations of R, R' and R" also produced this result.

Figure 1.12. Formation of η^1-vinyl and η^2(3e)-vinyl complexes from alkyne ligands.

The η^2(3e)-vinyl complexes gave characteristic $^{13}C\{^1H\}$ NMR chemical shifts for the Mo=C carbon atom C_α. Typically these were in the range of 250.0 to 290.0 ppm. This is compared to the singly bonded atom C_β which usually gives rise to a signal in the range 30.0 to 50.0 ppm. In the η^2(3e)-vinyl complexes that have been structurally identified, the Mo=C_α double bonds are in the range 1.94 to 1.96Å and the Mo-C_β bonds in the range 2.25 to 2.30Å. The C_α to C_β bonds are usually around 1.45Å. Previously determined values for Mo=C bonds (1.83 to 2.06Å), Mo-C single bonds (2.20 to 2.40Å) and C-C single bonds (1.45 to 1.55Å) suggest that there is little delocalisation about the metallocycle.

1.8 The Bonding of an η^2(3e)-Vinyl Ligand to a Transition Metal Centre.

Studies have shown the main orbitals used by the CH_2=CH^- fragment (a non complexed η^2(3e)-vinyl ligand) in bonding to a metal centre.[34,47] The most important fact gained from these studies was that the orbitals involved in bonding for an η^2(3e)-vinyl ligand are similar to those employed by a four-electron donor alkyne ligand. The frontier orbitals of the metal fragment,[48,49] one empty σ orbital, one empty and one filled π orbital and one filled σ orbital, are well matched for the incoming η^2(3e)-vinyl ligand (Figure 1.13.).

The σ and $\pi_\perp$ of the CH_2=CH^- fragment (analogous to those of an alkyne) are filled and donate to the metal π orbitals, whilst the $\pi_\parallel$* can be used for back donation. The σ orbital is bonding with respect to C_α=C_β and its occupancy is decreased on complexation with the metal centre. The $\pi_\parallel$* orbital is antibonding with respect to the C_α=C_β bond and its occupancy is increased on complexation with the metal centre. Both these interactions give rise to a CH_2=CH^- fragment with a reduced bond order with respect to the C_α=C_β bond.

The main difference between alkyne and η^2(3e)-vinyl bonding to a metal centre is the localised nature of the $\pi_\perp$ in the η^2(3e)-vinyl ligand, which is located at the C_α atom. The $\pi_\perp$ orbital also lies at a higher energy to the corresponding alkyne orbital and is better matched to the π orbital of the metal centre. On complexation the strong bonding interaction between the metal centre and C_α results in a Mo=C_α double bond.

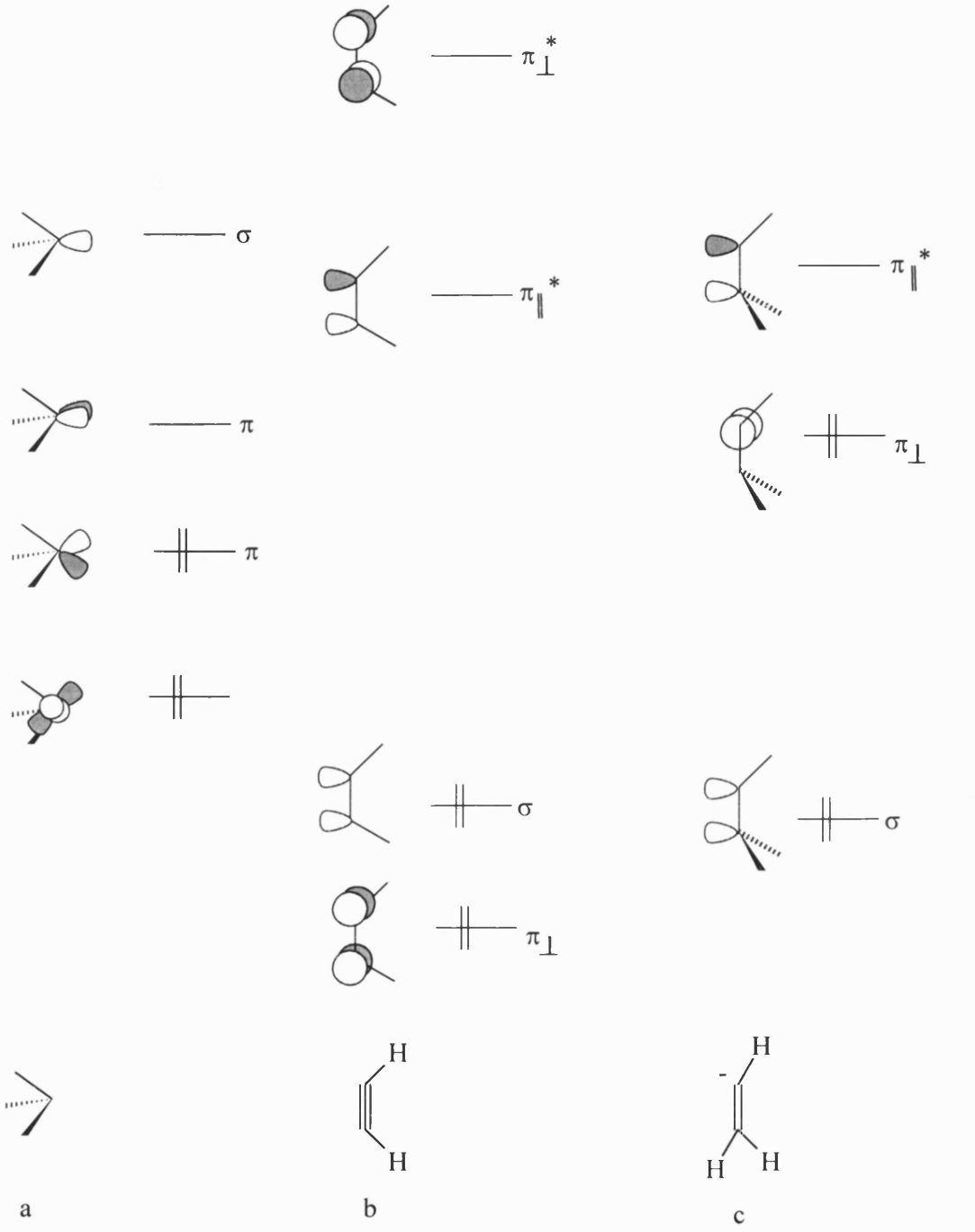

Figure 1.13. Frontier molecular orbitals for a) $[Mo\{P(OMe)_3\}_2(\eta\text{-}C_5H_5)]$ b) HC≡CH and c) $CH_2{=}CH^-$ fragments.

Another consequence of the similarity in energy of the two orthogonal π orbitals is the observed equivalence of the two phosphite environments in complexes of the type (ii) in Figure 1.12, where the two substituents on the C_β atom are the same. A fluxional process was described which accounted for this equivalence. This was a windscreen wiper type motion as opposed to a full rotation[34] (Figure 1.14).

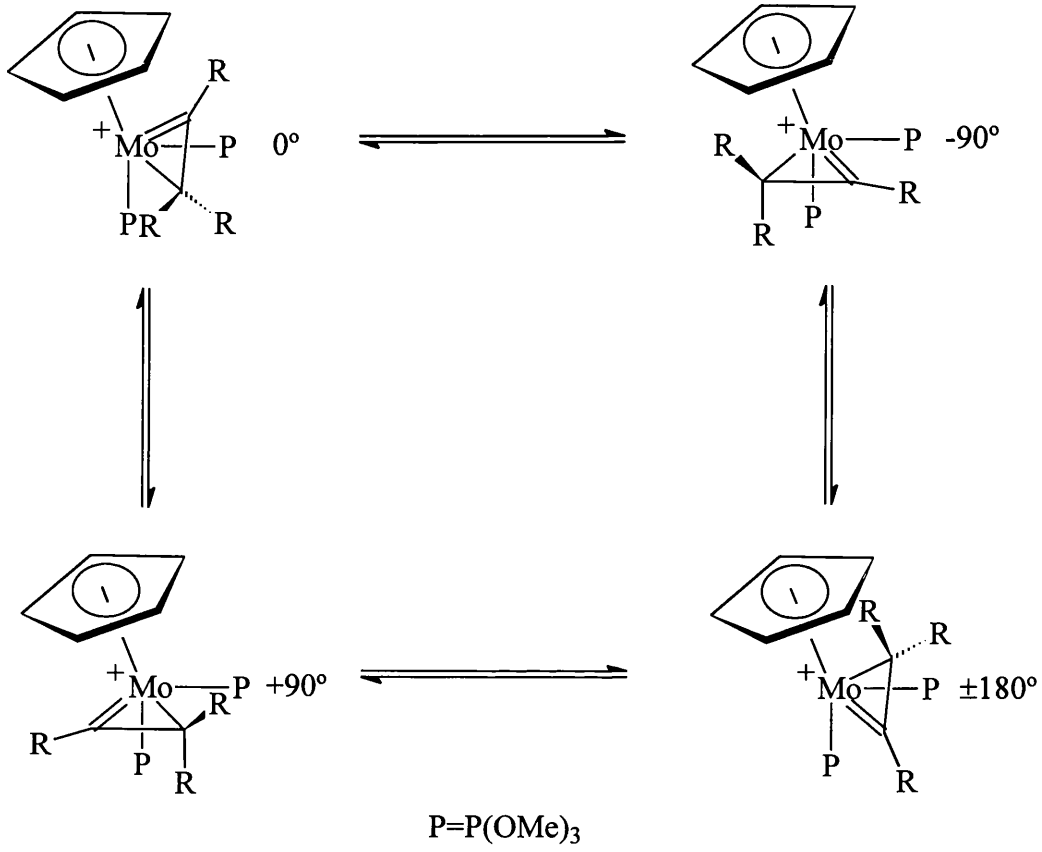

Figure 1.14. Windscreen wiper type motion of an η^2(3e)-vinyl ligand.

This windscreen wiper type of motion is a low energy process compared to a full 180° rotation. If the two substituents on the C_β atom were inequivalent then the two phosphite environments would not be made equivalent by this process.

2. Formation and Reactivity of η^4(5e)-Butadienyl Complexes of Molybdenum

2.1 Review of η^4(5e)-Butadienyl Complexes.

In 1984 it was shown for the first time that the butadienyl ($C_4R_5^-$) ligand could function as an η^4(5e)-system[50] rather than the familiar η^3(3e)-mode.[51,52] Reaction of the η^4(4e)-cyclobutadiene cation (**1**) with K[BHBu$^s_3$] was found to give the red complex (**2**), which was shown to have the illustrated structure by X-ray crystallography. It was suggested that (**2**) was formed by a conrotatory ring-opening of an η^3(3e)-cyclobutenyl intermediate (eq.2.1).

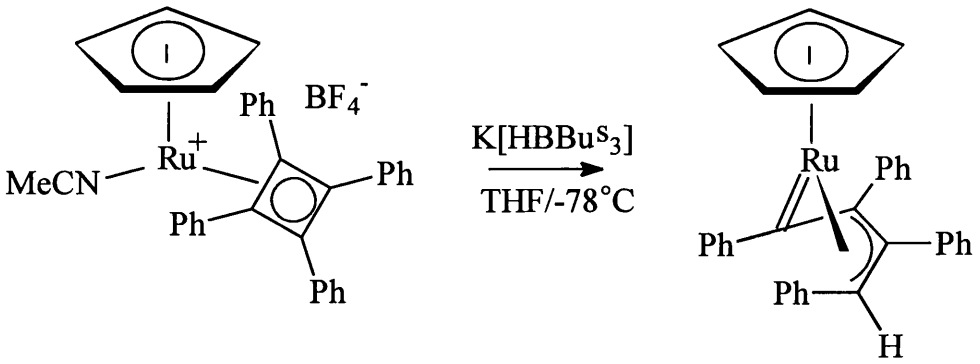

(**1**) (**2**) eq.2.1

An important feature of this complex (**2**) was a low field signal in the $^{13}C\{^1H\}$ NMR spectrum ascribed to the Ru=C bond (δ 246.0), which was characteristic of an alkylidene type carbon. This low field signal is prominent in all η^4(5e)-butadienyl complexes. The X-ray structure of (**2**) showed a Ru=C bond length of 1.896(5)Å, consistent with double bond character. It also showed characteristic bond lengths for a delocalised η^3-(3e)-allyl group for the remaining three Ru-C bonds.[53,54]

Following this report, Templeton *et al*[55] described a second example of an η^4(5e)-butadienyl complex, formed by acid induced coupling of two PhC_2Ph units at tungsten and molybdenum centres (eq.2.2).

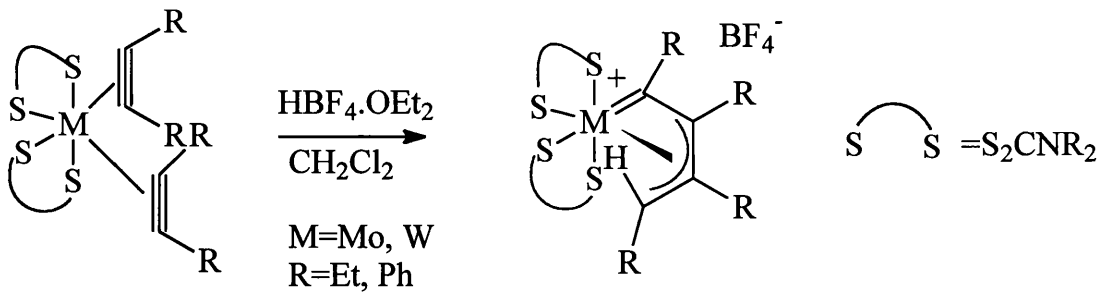

(3) (4) eq.2.2

An oxo-derivative of (**4**) was synthesised and the structure determined to confirm that an η^4(5e)-butadienyl ligand was present. From the X-ray structure of the oxo tungsten complex it was clear that there was a delocalised η^3(3e)-allyl moiety in the butadienyl ligand. Again the characteristic low field ^{13}C chemical shifts of the alkylidenes were observed, (δ 270.0 W, 279.8 Mo). Further reaction of these complexes (**4**) with NaS_2CNEt_2 and $HBF_4.OEt_2$ resulted in formation of an η^3(4e)-vinylcarbene complex (**6**) *via* an η^2(3e)-vinyl intermediate (**5**) (eq.2.3).

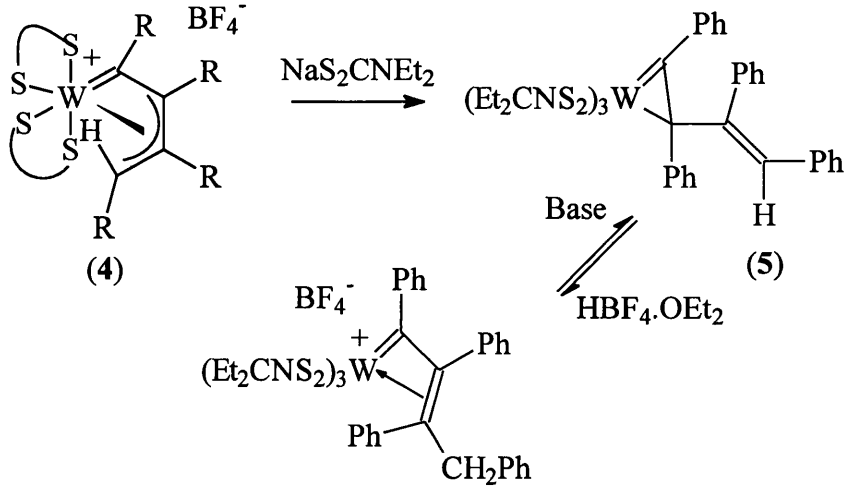

eq.2.3

These two examples of η^4(5e)-butadienyl complexes both contain allylcarbene moieties. This, however, is only one possible bonding mode. Figure 2.1 shows another bonding formalism.

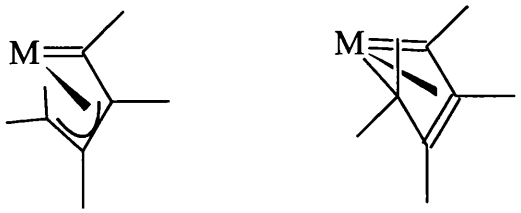

A **B**

Figure 2.1. Depiction of the possible bonding modes for an η^4(5e)-butadienyl ligand.

Some examples of formalism (**B**) have been described by Davidson *et al.*[56,57,58,59] These were formed by reaction of an η^2(3e)-vinyl ligand (**7**) and an incoming alkyne ligand (eq.2.4).

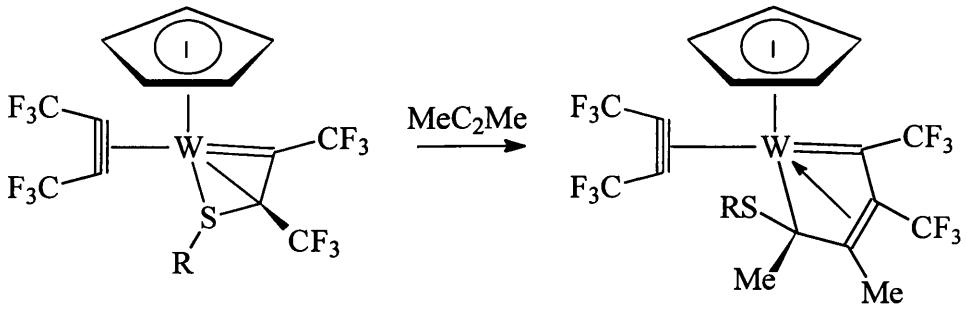

(**7**) (**8**) eq.2.4

This was proved when the X-ray structure of one of these complexes was solved. It clearly showed a η^4(5e)-butadienyl complex. The allylcarbene formalism (**A**) did not fit in with the bond parameters. The best description was a more localised M-C σ bond and M-alkene π bond, i.e. formalism (**B**).

Recently, two interesting η^4(5e)-butadienyl complexes of rhenium have been reported. Reaction of $[Br_2Re(\eta^2\text{-}RC_2Ph)(\eta\text{-}C_5H_5)]$ (**9**) (R=Me or Ph) with two equivalents of $Ag[BF_4]$ and *o*-diphenylphosphinostyrene (dpps)[60] gave a complex (**10**) formed apparently through coupling of the alkyne and the alkene moiety present in the dpps (eq.2.5).

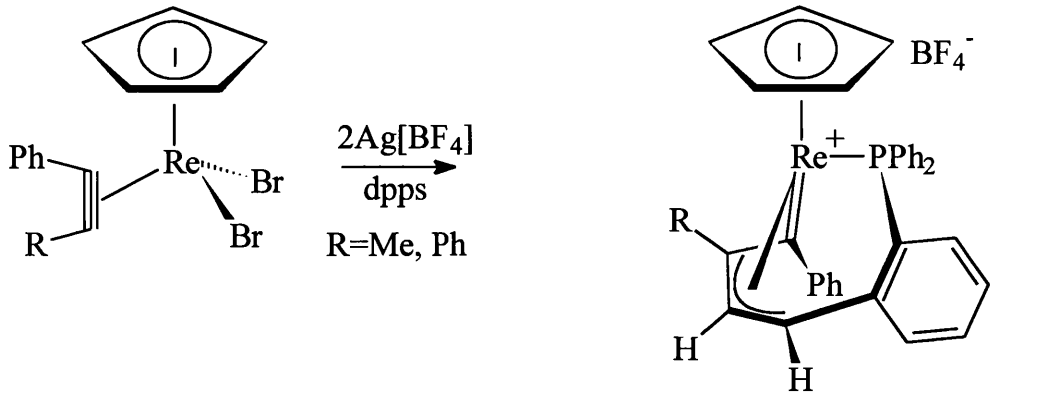

(**9**) (**10**) eq.2.5

Again an X-ray structure of complex (**10**) confirmed the allylcarbene, i.e. formalism **A**, nature of the η^4(5e)-butadienyl ligand.

Recently, an alternative bonding configuration for the η^4(5e)-butadienyl ligand has been established. Reaction of the cationic bis-alkyne complex of rhenium (**11**) with $Li[BHEt_3]$[61] gave the η^4(5e)-butadienyl complex (**12**) (eq.2.6).

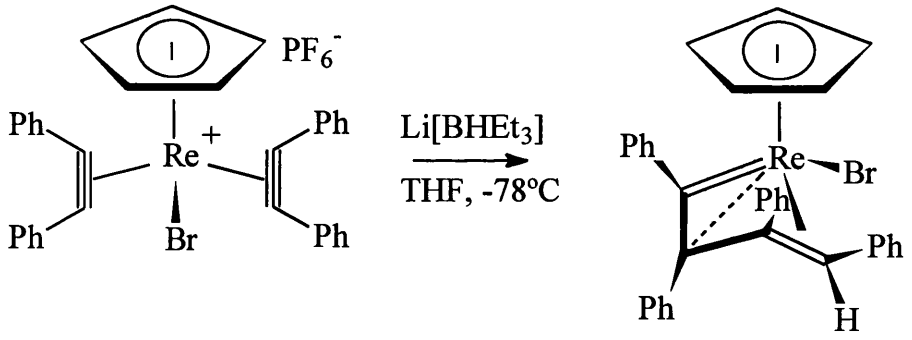

(**11**) (**12**) eq.2.6

An X-ray structure determination showed that the η^4(5e)-butadienyl fragment adopts an unusual *transoid* conformation, as opposed to the familiar *cisoid* conformation encountered before. As illustrated there is also an interesting 'bent' carbon to rhenium bond present in the molecule.

Very recently, the first examples of niobium η^4(5e)-butadienyl complexes[62] were reported by Etienne and co-workers. These were formed by reaction of a mono-

alkyne hydrotris(3,5-dimethylpyrazolyl)borate complex of niobium (**13**) with an allyl Grignard reagent to give the η^4(5e)-butadienyl complex (**14**) (eq.2.7).

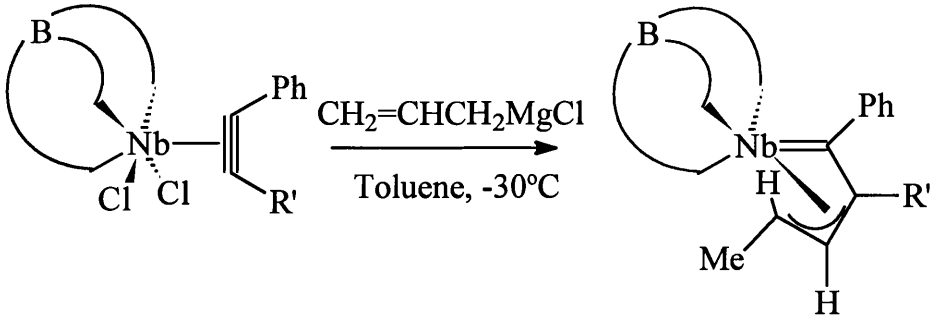

(**13**) (**14**) eq.2.7

This was the first report of the reaction of an allyl group and an alkyne coupling to give an allylcarbene. The allylcarbene structure was confirmed by an X-ray structure determination on (**14**, R′=Ph).

Finally, in a preliminary study it was found that a group of η^4(5e)-butadienyl complexes are formed by reaction of bis-alkyne complexes of molybdenum (**15**) with $HBF_4.OEt_2$ and subsequent addition of (two-electron) donor ligands[63] (**17**) (eq.2.8).

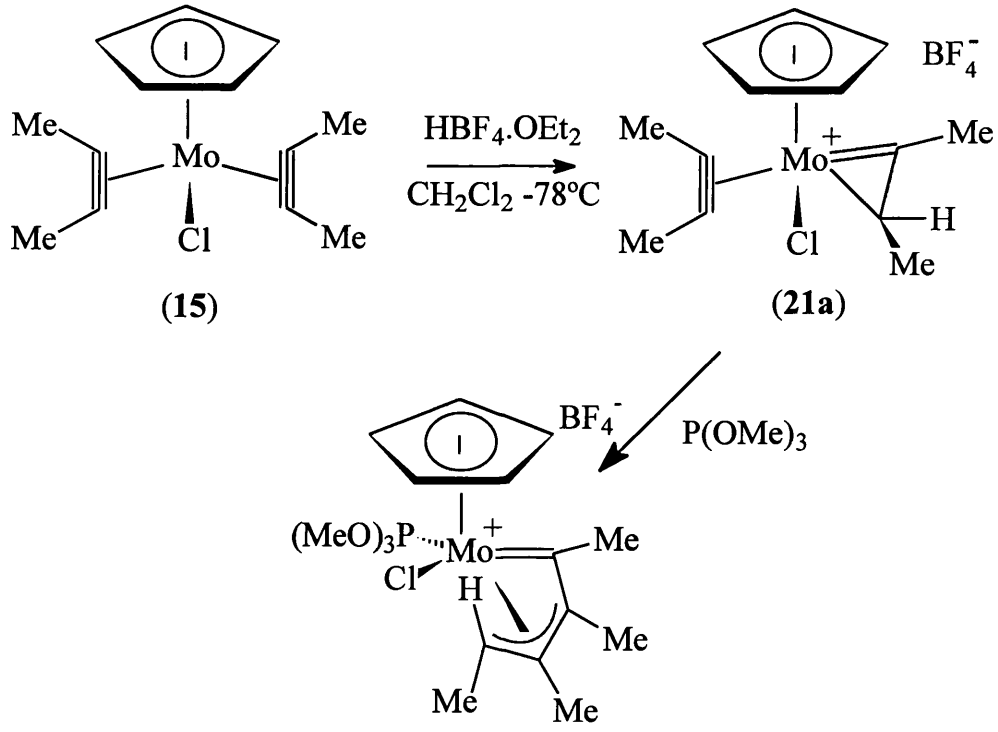

(**15**) (**21a**)

(**17**) eq.2.8

There was uncertainty as to the actual structure of the η^2(3e)-vinyl complex (**16**) as the $^{13}C\{^1H\}$ NMR data seemed to suggest a two-electron donor alkyne ligand, when a four-electron donor alkyne was needed to fulfil the requirements of the 18-electron rule. There were also inconsistencies between the methyl and ethyl substituted complexes, it appeared that some of these complexes coupled to give η^4(5e)-butadienyl complexes and others did not. It is this final group of η^4(5e)-butadienyl complexes that this thesis will be dealing with, describing work directed towards understanding these interesting reactions.

2.2. Protonation of Neutral Bis-Alkyne Cyclopentadienylmolybdenum Halogen Complexes.

Bis-alkyne complexes of molybdenum are usually prepared by oxidative cleavage, with $Ag[BF_4]$, of the molybdenum dimer $[Mo(CO)_3(\eta\text{-}C_5H_5)]_2$ (**18**) in the presence of the desired alkyne[21] (eq.2.9).

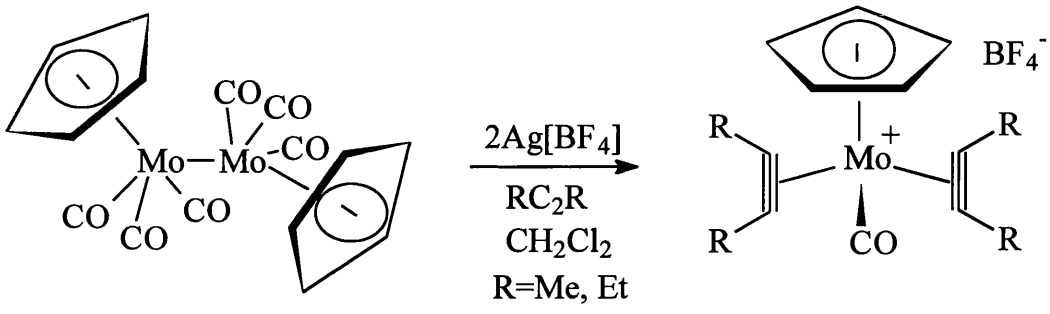

(18) **(19)** eq.2.9

The yields in this type of reaction are typically very good (70-80%). The CO complexes (**19**) are quantitatively converted to MeCN complexes (**20**) by refluxing in MeCN in the presence of a small amount of free alkyne[18] for several hours (eq.2.10).

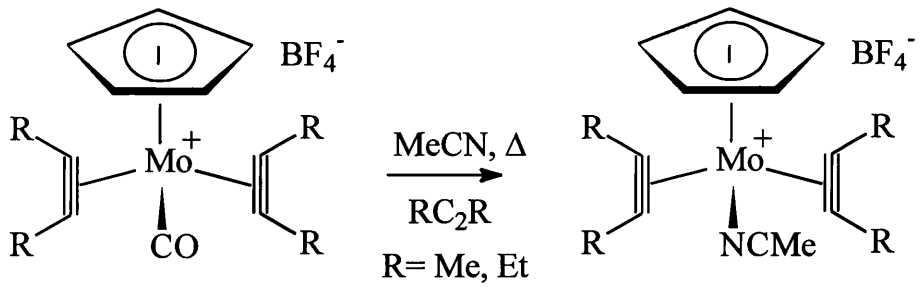

(19) **(20)** eq.2.10

The presence of a small amount of free alkyne is necessary in order to suppress a competing reaction involving the irreversible loss of an alkyne ligand to give the MeCN/CO complex.

The halo-complexes (**15**) can be made from the MeCN complexes (**20**) by refluxing in THF with anhydrous lithium halide for 1 to 2 hours (eq.2.11).

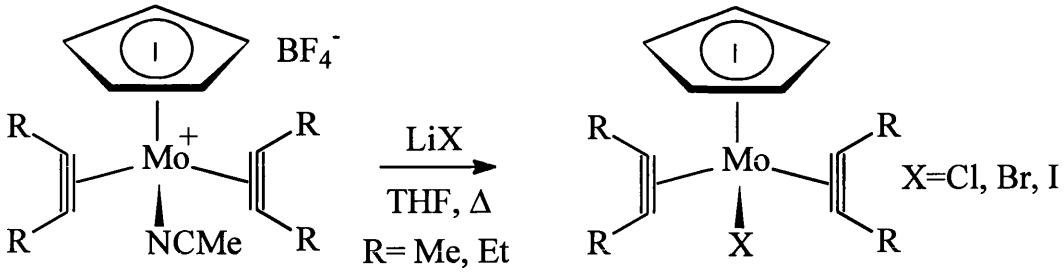

(**20**) (**15**) eq.2.11

These yellow/orange complexes were purified by column chromatography and obtained in moderate yields (45-55%). In all the alkyne complexes mentioned here the alkyne ligands formally donate 3 electrons each to make up the required 18-electrons (N=3 donors). This arrangement in reality is a rapidly alternating 4 + 2 system (see Chapter 1).

It had been found by Woolhouse[64] and Fries[65] that low temperature protonation of certain of these halo complexes with $HBF_4.OEt_2$ (-78°C) in CH_2Cl_2 produced a colour change from yellow/orange to cherry red. The resulting air sensitive, pink/purple cationic complexes could be isolated by addition of Et_2O. This protonation reaction only worked for complexes where R was an alkyl group e.g. 2-butyne[64], 3-hexyne[66] and 4,4-dimethyl-2-pentyne[65] This is presumably because the electron donating effect of the alkyl groups is needed to allow the protonation to occur. With phenyl substituted alkynes no reaction occurs with the acid. The methyl (**21a**) and ethyl (**21b**) substituted cations were tentatively identified as η^2(3e)-vinyl/η^2(4e)-alkyne complexes (eq. 2.12).

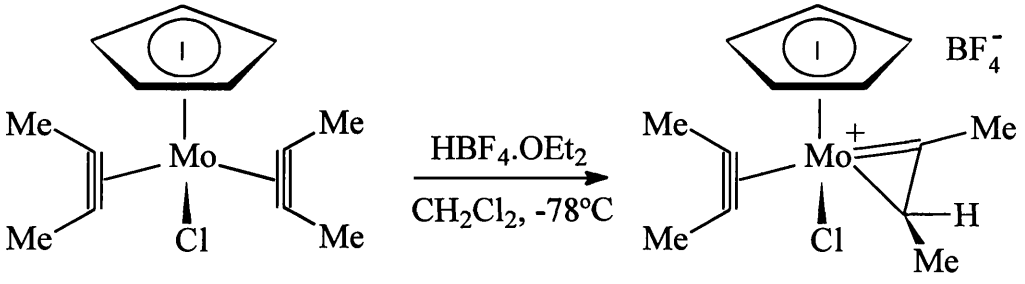

(15) **(21a)** eq.2.12

These cations were found to be reactive towards halide anions and donor ligands.[64] The presumed complex (**21a**, R=Me X=Cl) was treated with LiCl in a (1:1) mixture of THF/CH_2Cl_2 at room temperature for 1hr. Upon work-up, this reaction gave a purple coloured neutral product (**22**). The NMR data for this complex showed similar features to that of (**21a**), i.e. a broad ^1H NMR spectrum and a low field resonance (291.3 ppm) for the carbene carbon atom. This led to the suggestion that the product (**22**) was a neutral η^2(3e)-vinyl/η^2(4e)-alkyne complex as illustrated (eq.2.13).

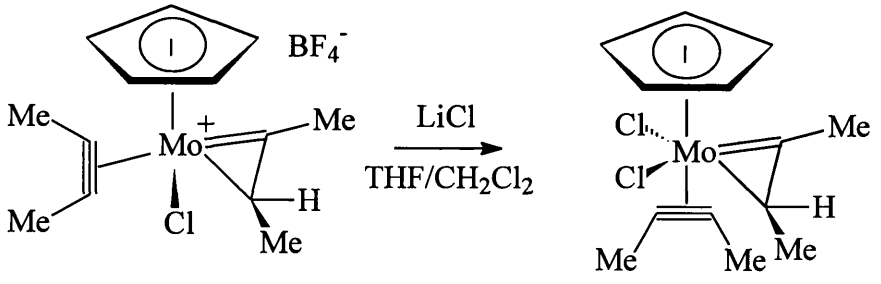

(21a) **(22)** eq.2.13

It was found that (**21a**) reacted with $P(OMe)_3$. Complex (**21a**) and $P(OMe)_3$ were stirred in CH_2Cl_2 for 1hr at room temperature, causing a colour change from purple to orange. It was thought that addition of this two-electron donor ligand would allow the alkyne ligand to function as a two-electron donor in agreement with the 18-electron rule. The isolated product (**23**) was analysed as a 1:1 adduct. Again the ^1H NMR spectrum was broad and the $^{13}C\{^1H\}$ NMR spectrum showed a low field

signal (305.2 ppm). At first it was thought that this was an example of an η^2(3e)-vinyl/η^2(4e)-alkyne complex (eq.2.14).

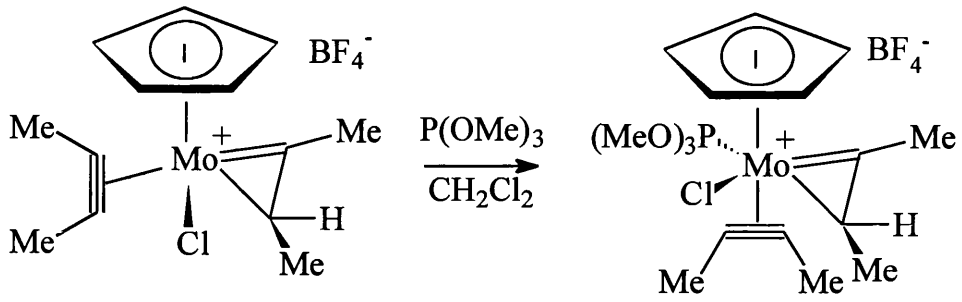

(21a) **(23)** eq.2.14

However, crystals suitable for X-ray structure determination were obtained for the bromo-analogue of (**23**) and the resulting structure determination was shown[66] to be that displayed in Figure 2.3. This was the first example of a family (see later) of structurally characterised η^4(5e)-butadienyl-cyclopentadienyl complexes of molybdenum derived from bis-alkyl substituted alkynes.

Thus, not only was there a problem relating to the structure of (**21a**), but also it was now clear that a carbon-carbon coupling reaction could occur, leading to the formation of an η^4(5e)-butadienyl ligand (Figure 2.2.)

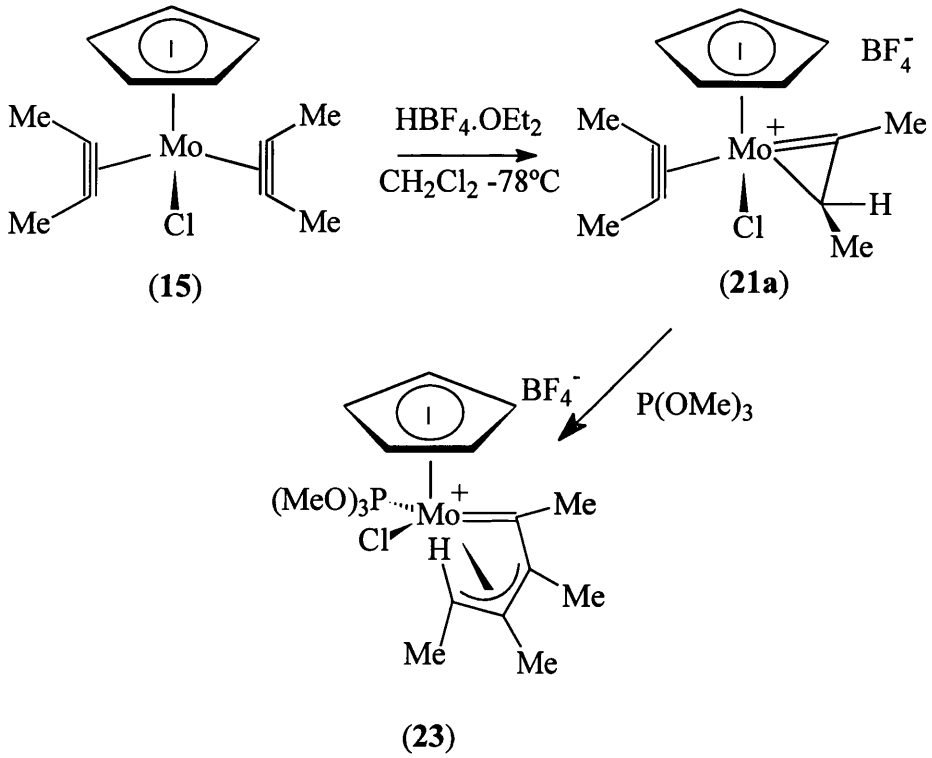

(15) **(21a)**

(23)

Figure 2.2. Formation of an η^4(5e)-butadienyl complex of molybdenum.

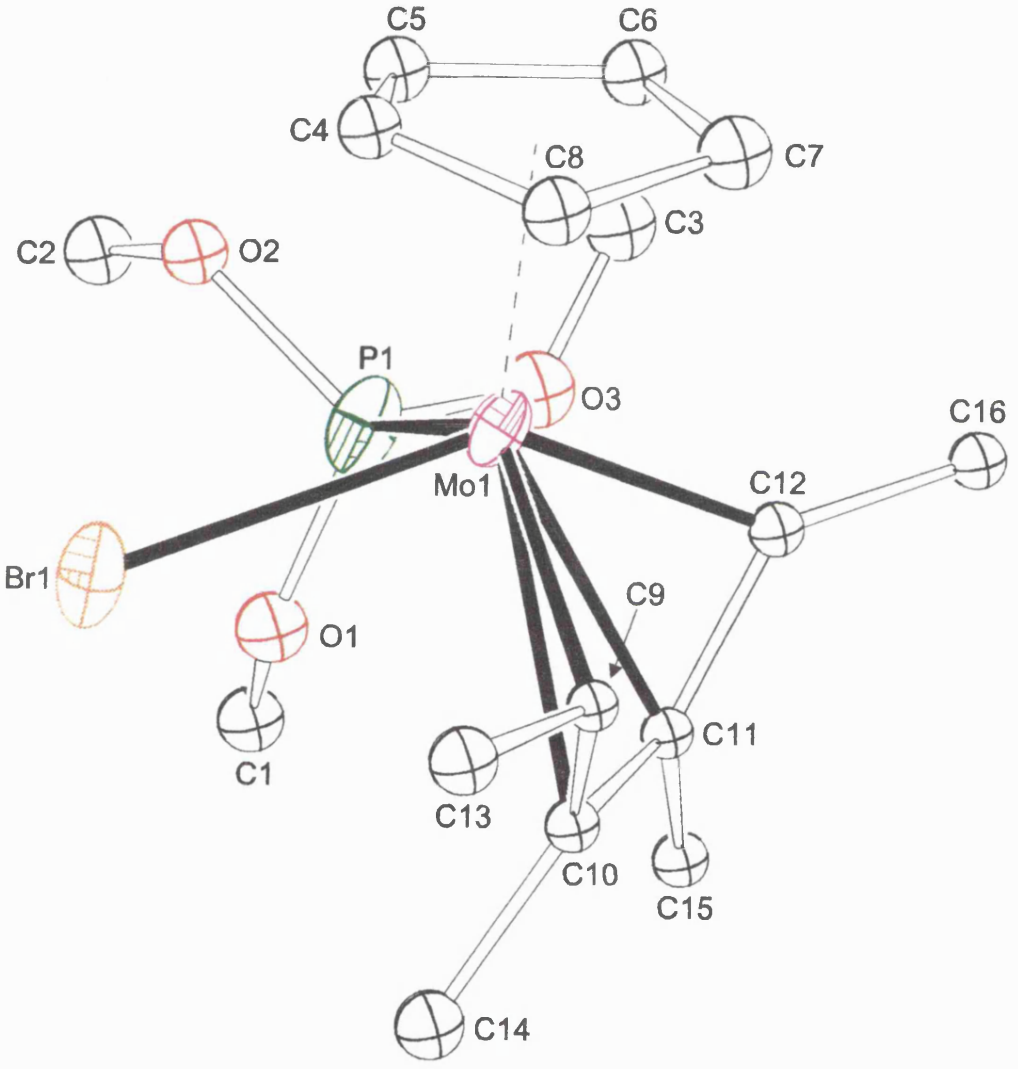

Figure 2.3. ORTEX representation of [BrMo=C(Me)-η^3-{C(Me)C(Me)CHMe}{$P(OMe)_3$}(η-C_5H_5)][BF_4]. Hydrogen atoms ommited for clarity.

Returning to the question of the identity of the cations (**21a**) and (**21b**), the ^{1}H NMR spectra of these complexes showed the presence of one isomer, as indicated by the presence of only a singlet resonance for the Cp ligand. These spectra were broad especially in the CH_2 region for 3-hexyne derived complexes i.e. (**21b**), and even recording spectra at low temperatures did not improve the broadness of the peaks.

The most important spectroscopic feature of these complexes was the very low field chemical shifts of the carbene carbon atom in the $^{13}C\{^{1}H\}$ NMR spectrum. These were typically in the range of 297 to 305 ppm and, as mentioned previously this feature was taken as evidence of an η^2(3e)-vinyl group which had been encountered before.[67] The carbons to which the proton from the $HBF_4.OEt_2$ had become attached came in the region of 71 to 80 ppm, which meant that the resonances in the range 108 to 118 ppm and 130 to 138 ppm had to be assigned, if the η^2(3e)-vinyl/η^2(4e)-alkyne structure was correct, to the alkyne contact carbons. As mentioned earlier, Templeton[13] showed that there was a correlation between the carbon NMR chemical shift of the alkyne contact carbons, and the number of electrons formally donated. In order to possess a stable 18-electron electronic configuration, complexes of the type (**21**) require the alkyne ligand to formally donate four electrons. This would lead to alkyne contact carbon resonances in the range 180 to 230 ppm. The values actually observed lay in the two-electron donor region (100 to 130 ppm). This was obviously an important discrepancy in the data for this compound and it was vital that an explanation was found. This was the starting point for this study.

The first explanation for these anomolous observations which we considered was the possibility of a "non-innocent" co-ordinating [BF_4] ligand. Evidence for this anionic counter ion co-ordinating had been known for some time,[68] and therefore a possible structure for (**21a**) is shown in Figure 2.4, which would explain the apparent two-electron donation from the alkyne ligand.

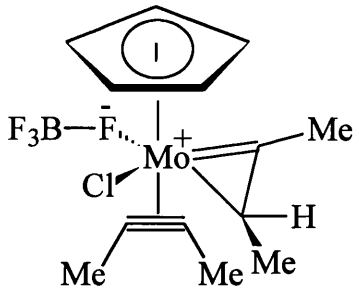

Figure 2.4. A co-ordinated [BF_4] complex with a two-electron donor alkyne ligand.

The [BF_4] anion would be linked through a fluorine atom to the metal centre, thus allowing the alkyne to formally donate two electrons. Where the [BF_4] is non-innocent, the low temperature ^{19}F spectra of examples of these complexes clearly show two different fluorine environments. The ^{19}F spectrum for the presumed η^2(3e)-vinyl/η^2(4e)-alkyne complex (**21b**) was recorded at 185K. Only two singlets, corresponding to the ^{11}B and ^{10}B isotopomers of the free [BF_4], were observed. This clearly pointed to a free [BF_4] anion and therefore some other explanation was needed for the high field ^{13}C resonance of the presumed η^2(4e)-alkyne.

Since attempts to obtain crystals suitable for X-ray crystallography studies of complexes (**21a**) and (**21b**) had been previously unsuccessful, efforts to explain the apparent structural uncertainties were made by synthesising the dibenzyl substituted complexes (**24**, **25** and **26**) (eq.2.15), using the methods mentioned previously, in the hope of making an η^2(3e)-vinyl/η^2(4e)-alkyne complex which would be easier to crystallise.

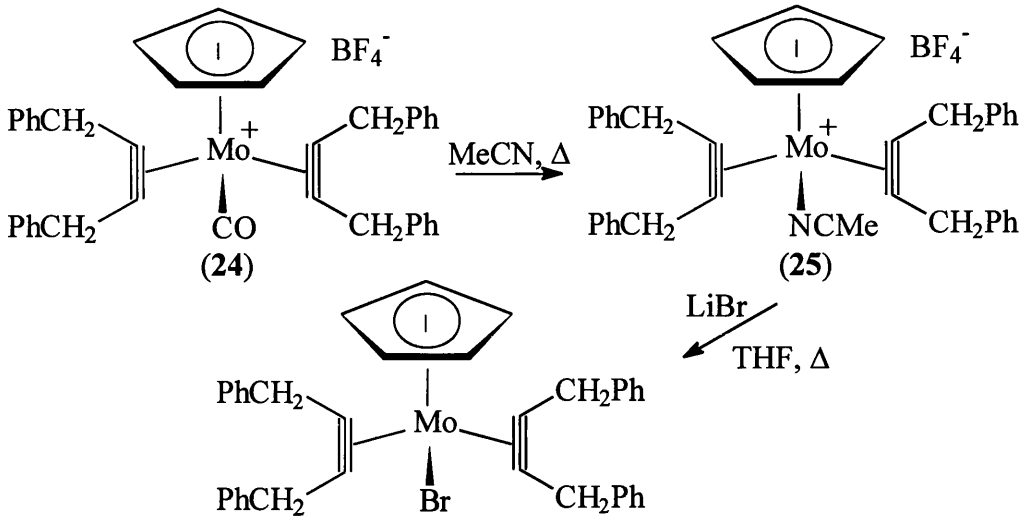

(**26**) eq.2.15

These complexes were obtained in exactly the same manner as for other complexes of this type as shown in eq.2.15, the reactions proceeding in good yield. However, protonation of (**26**) was not selective, the reaction leading to a number of different compounds.

Thus the problem of the uncertainty of the complexes of the type (**21**) still remained, and while this was so, any detailed and full explanation of this chemistry was impossible. It was obviously of great importance to establish firmly the structure of these complexes, and resolve the contradictions observed in the data gathered on them. The methyl substituted complexes of type (**21a**) were virtually insoluble in CH_2Cl_2 and other solvents which are commonly used. Efforts were made to obtain crystals of (**21b**) suitable for X-ray structure determination. Eventually after several failed attempts, a suitable crystal was obtained by layer diffusion (CH_2Cl_2/pentane) at room temperature and the structure of [BrMo=C(Et)-η^3-{C(Et)C(Et)CHEt}(OH_2)(η-C_5H_5)][BF_4] (**21b**) determined (Figure 2.5).

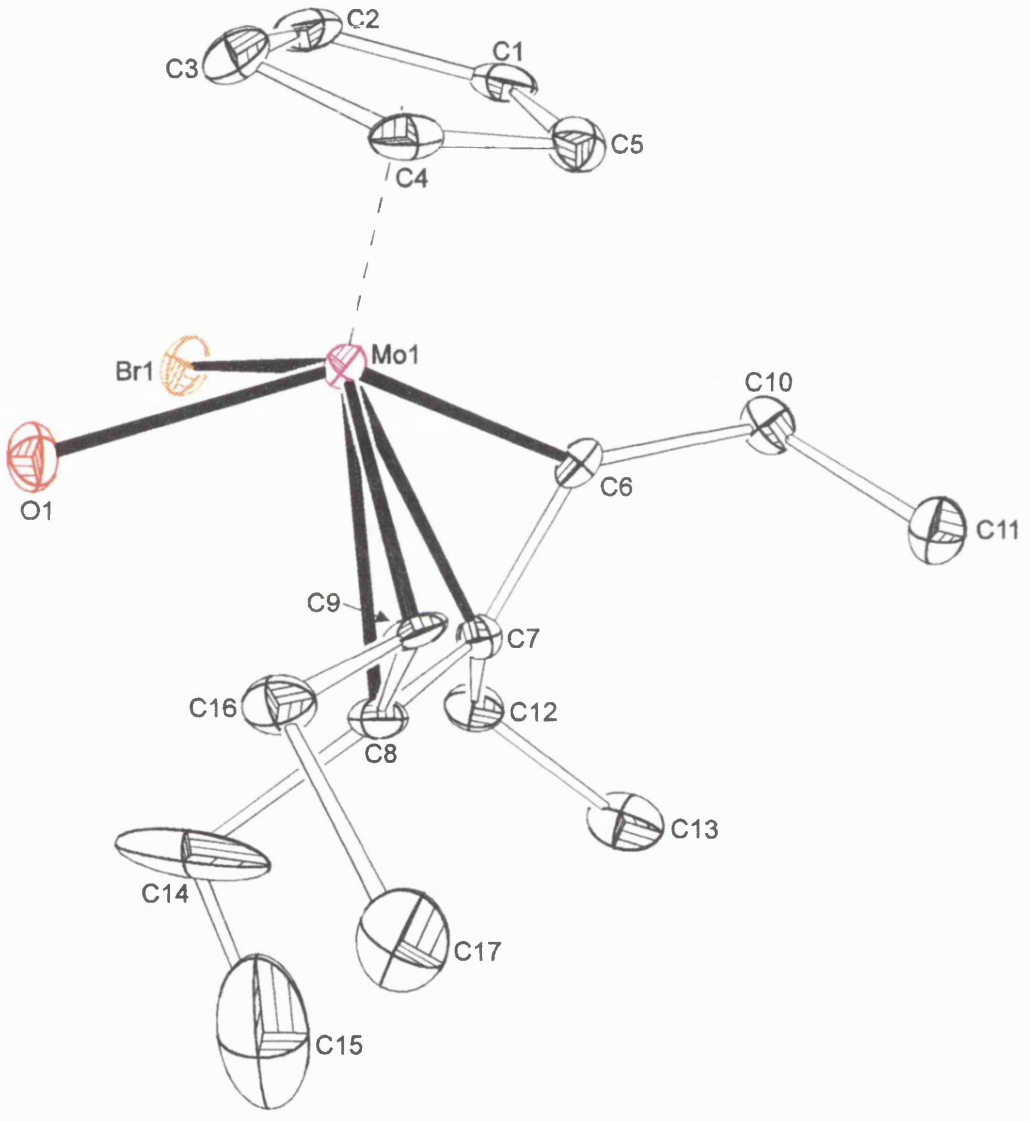

Figure 2.5. ORTEX representation of [BrMo=C(Et)-η^3-{C(Et)C(Et)CHEt}(OH_2)(η-C_5H_5)][BF_4]. Hydrogen atoms omitted for clarity.

The structure determination showed that (**21b**) was not the expected η^2(3e)-vinyl/η^2(4e)-alkyne complex, instead the complex contained an η^4(5e)-butadienyl ligand in the anti-supine conformation and a co-ordinated molecule of H_2O. The Mo=C double bond was present (1.933(9)Å) and the C-C bond lengths at 1.467(14)Å, 1.405(14)Å and 1.452(14)Å were similar to those found in the previously determined structure of (**26**). The H_2O ligand was found to be in a *trans* position relative to the Mo=C bond (C6-Mo1-O1=142.8(4)°) (see Table 2.1.).

It was clear that the previous interpretation of the NMR data for (**21a**) and (**21b**) suggesting the presence an η^2(3e)-vinyl ligand and an alkyne ligand was incorrect. With hindsight it was easy to see how the error was made. The two central carbon atoms in the η^4(5e)-butadienyl ligand gave resonances which lay in the range of two-electron donor alkyne ligands, and therefore could easily be misinterpreted as alkyne contact carbon resonances. This structure determination was an important breakthrough which dispelled all the uncertainties and discrepancies that had previously left so much of what was taking place a mystery.

The structure explained the discrepancy of the electron count at the metal centre, as there was not in fact an alkyne ligand present. This compound was an 18 electron complex, the source of water in the reaction probably being the $HBF_4.OEt_2$. The co-ordinated H_2O molecule gives a very broad signal at approximately 4.0 ppm in the ^{1}H NMR spectrum, which is often very difficult to see. The mass spectrum shows only the parent ion minus a molecule of H_2O, which is probably lost in the process of recording the spectrum.

An interesting additional structural feature worthy of note is the very close F-O distances (in the range of 2.68Å - 2.98Å) indicating hydrogen bonding between the [BF_4] anion and the co-ordinated water molecule. Unfortunately the two hydrogen atoms of the H_2O could not be located, but the F-O distances show, without doubt, strong interactions. This hydrogen bonding between [BF_4] anion and H_2O, has been observed previously in molybdenum complexes.[69] A packing diagram clearly shows these interactions in Figure 2.6. Other relevant bond distances and bond angles for (**21b**) are given in Table 2.1.

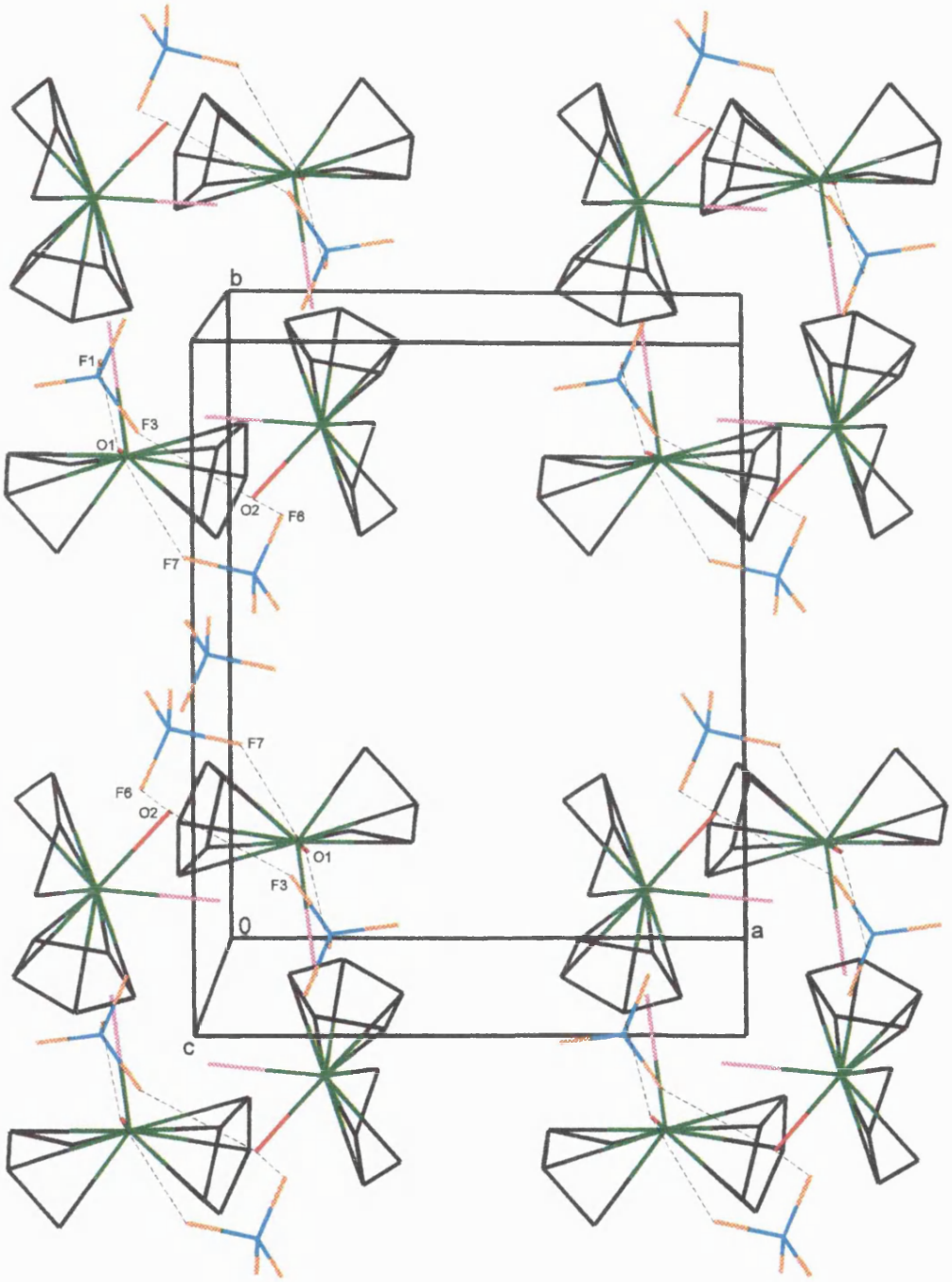

Figure 2.6. Packing diagram of [BrMo=C(Et)-η^3-{C(Et)C(Et)CHEt}(OH_2)(η-C_5H_5)][BF_4]. Ethyl groups omitted for clarity.

Table 2.1. Selected bond lengths (Å) and angles (°) for the aqua-complex [BrMo=C(Et)-η^3-{C(Et)C(Et)CHEt}(OH_2)(η-C_5H_5)][BF_4] (**21b**).

Bond	Bond length (Å)
Mo-C6	1.933(9)
Mo-C7	2.341(10)
Mo-C8	2.414(10)
Mo-C9	2.294(10)
C6-C7	1.467(14)
C7-C8	1.405(14)
C8-C9	1.452(14)

Bond Angle	Angle (°)
Mo-C6-C7	86.1(6)
C6-C7-C8	115.7(9)
C7-C8-C9	116.3(9)
Mo-C9-C8	76.6(6)
C6-Mo-Br1	97.2(3)
C6-Mo-O1	142.8(4)

The torsion angle C6-C7-C8-C9 is -11.18°, a slight deviation from planarity for the C_4 backbone of the η^4(5e)-butadienyl ligand.

2.3 Discussion of the Coupling Mechanism for an η^2(3e)-Vinyl Ligand and an Alkyne.

With the structural identity of (**21b**), and by analogy that of (**21a**), revealed it was now possible to consider the details of the reaction paths followed in the formation of the η^4(5e)-butadienyl ligand.

On addition of $HBF_4.OEt_2$ (-78°C) to an alkyl substituted bis-alkyne complex (**15**) an η^2(3e)-vinyl substituted complex is probably formed, which upon warming reacts with the alkyne ligand to give an η^4(5e)-butadienyl complex. This reaction is either promoted by co-ordination of a molecule of H_2O, or the H_2O co-ordinates after the coupling has occurred. In simple terms as shown in Figure 2.7, the coupling may be depicted as a Dötz[70] type reaction between a co-ordinated alkyne and the metal to carbon double bond (i.e. the carbene moiety) present in the η^2(3e)-vinyl ligand.

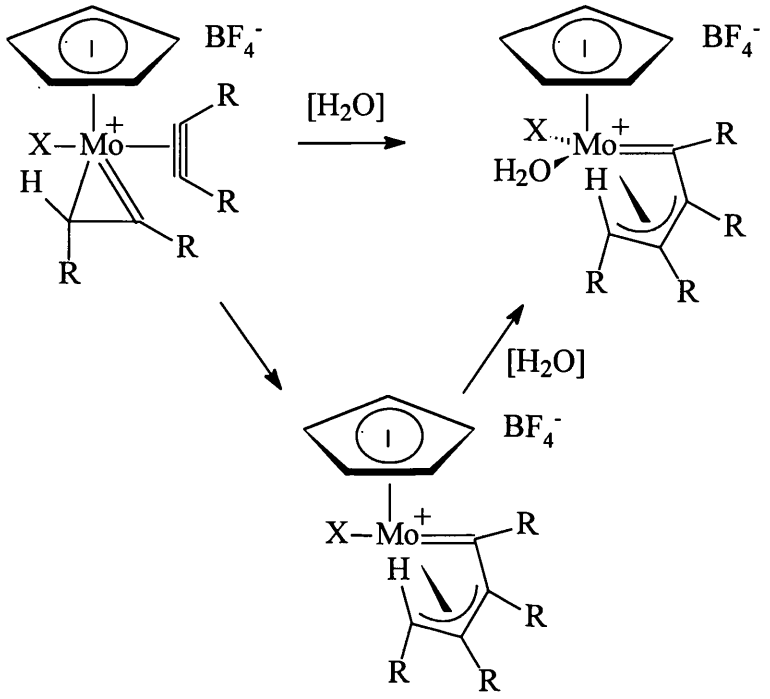

Figure 2.7 The Dötz type alkyne/carbene coupling mechanism.

In calculations by Hofmann[71] *et al* on a chromium system $[(OC)_5Cr{=}CH_2(HC_2H)]$, a model for the important step in the Dötz reaction, it was shown that there is a preferred orientation, where the alkyne ligand is out of the plane of the metal-carbon double bond (Figure 2.8).

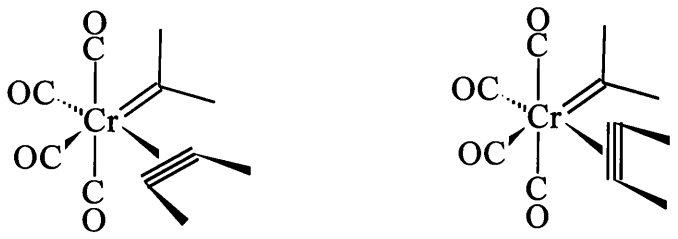

Disfavoured Favoured

Figure 2.8. The preferred orientation for a Dötz coupling to occur.

However, before examining the details of this idea it was vitally important to know more about the electronic structure of the starting materials $[XMo(\eta^2\text{-}RC_2R)_2(\eta\text{-}C_5H_5)]$ (X=Cl, Br, I). In particular, information was needed about the possible site for a charge controlled protonation reaction. Thus, in order to provide molecular

parameters for an EHMO (Extended Hückel Molecular Orbital) calculation the crystal structure of the bis-alkyne complex (**15** X=I, R=Me) was examined. A single crystal was obtained by layer diffusion methods (CH_2Cl_2/hexane) at room temperature and the resulting structure is shown in Figure 2.9. The alkyne ligands lie parallel to the Mo-I vector and also the plane of the Cp ligand.
Relevant bond distances and bond angles for [IMo(η^2-MeC_2Me)$_2$(η-C_5H_5)] (**15**) are given in Table 2.2.

Table 2.2. Selected bond lengths (Å) and bond angles (°) for the bis-alkyne complex [IMo(η^2-MeC_2Me)$_2$(η-C_5H_5)] (**15**).

Bond	Bond length (Å)
Mo-C12	2.06(1)
Mo-C13	2.05(1)
Mo-C22	2.07(1)
Mo-C23	2.04(1)
C22-C23	1.23(1)
C12-C13	1.27(1)

Bond Angle	Angle (°)
C24-C23-C22	143.8(7)
C21-C22-C23	141.7(6)
C14-C13-C12	144.8(7)
C11-C12-C13	141.0(7)

Once this structure had been obtained it was then possible to perform EHMO calculations to determine the preferred site of protonation (calculations performed using the extended Hückel iterative method on the CAChe system using the standard STO-3G basis set and a Wolfenburg-Helmholtz constant, k, of 1.75. The EHT parameters in the CAChe library are based upon experimental data).[72] Table 2.3 shows the charge density on selected atoms of complex (**15**).

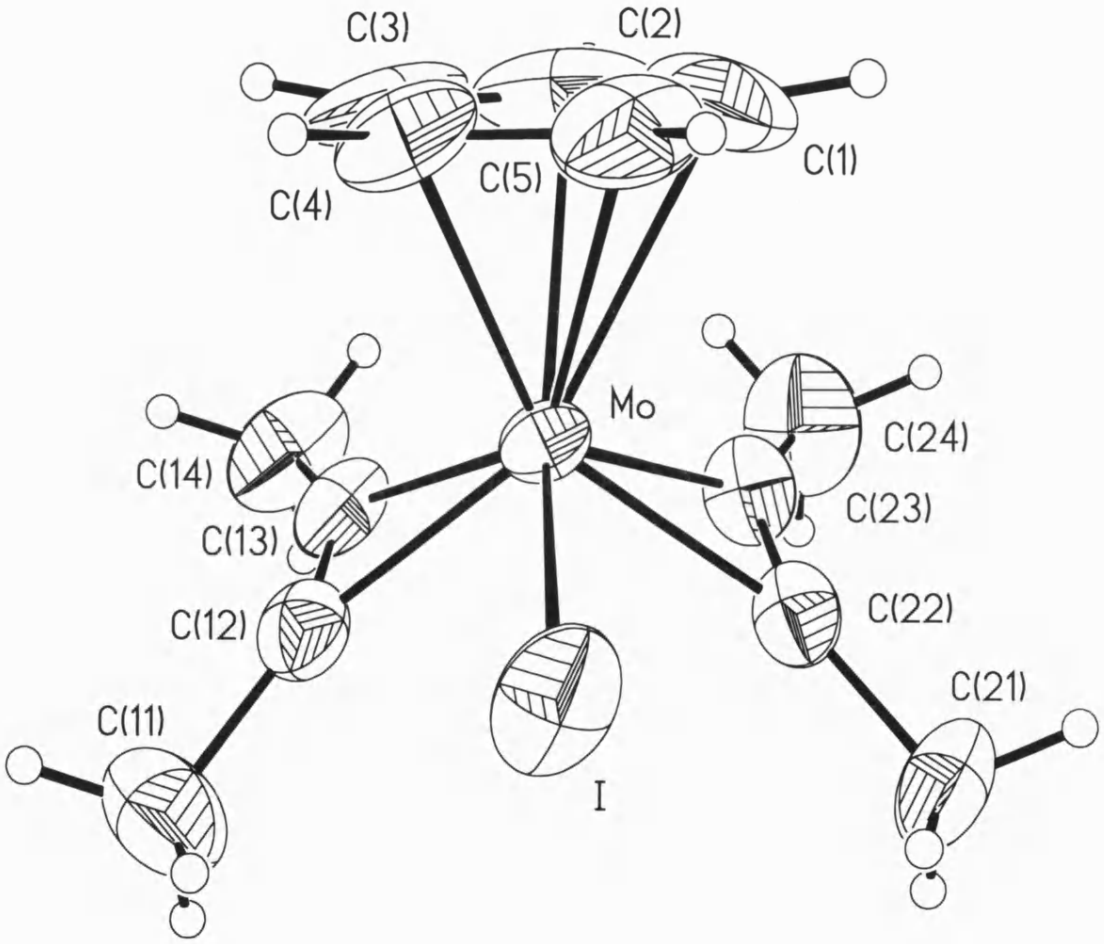

Figure 2.9. ORTEP representation of [IMo(η^2-MeC_2Me)$_2$(η-C_5H_5)] (**15**).

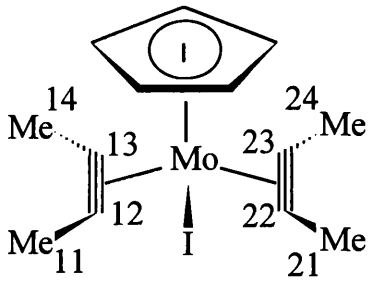

Atom	Charge
C11	-0.0829
C12	**-0.4887**
C13	-0.3459
C14	-0.0867
C21	-0.0815
C22	**-0.4900**
C23	-0.3482
C24	-0.0874

Table 2.3. Charge densities on selected carbon atoms of (**15**).

Assuming the protonation reaction is charge controlled, this shows that the protonation probably occurs at the carbon atoms closest to the iodine atom (C12 and C22). On the basis of space filling diagrams[73] (Figure 2.11) of this complex it might be expected that proton attack will occur from below (i.e. from the face opposite the Cp ligand.). Such a reaction path would therefore give the η^2(3e)-vinyl complex illustrated in Figure 2.10.

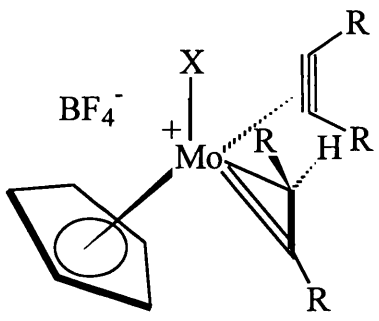

Figure 2.10. Representation of the η^2(3e)-vinyl complex obtained upon protonation of (**15**).

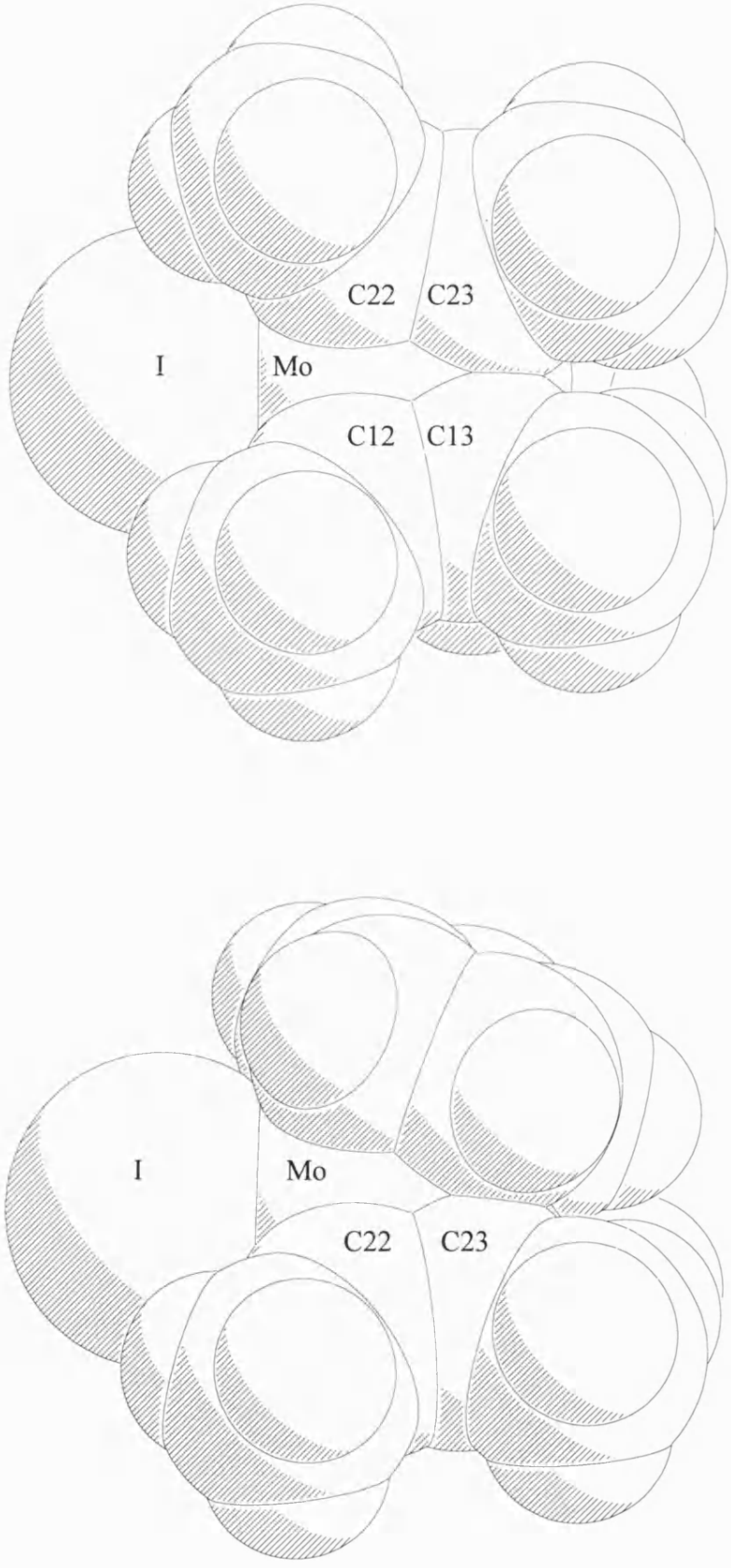

Figure 2.11. Space filling diagrams of (**15**), showing sites of $HBF_4.OEt_2$ attack.

Thus as is illustrated both the η^2(3e)-vinyl and alkyne ligands lie parallel to the Mo-X bond, and the double bond of the η^2(3e)-vinyl ligand is orthogonal to the alkyne ligand. If a coupling reaction took place as is thought to occur in the Dötz reaction, the resultant η^4(5e)-butadienyl ligand would be in the prone conformation, rather than the observed supine conformation, also the hydrogen substituent on the η^4(5e)-butadienyl ligand would be in a pseudo-anti position (eq.2.16).

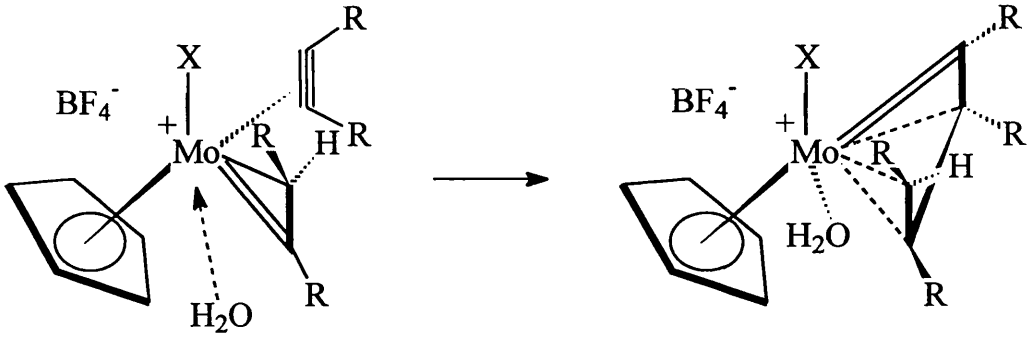

eq.2.16

One way of achieving the supine conformation, is to postulate a 180° rotation of the η^2(3e)-vinyl ligand. As mentioned in Chapter 1 a direct rotation is disfavoured, but the required rotation can be accomplished by means of two 90° rotations (Figure 2.12).

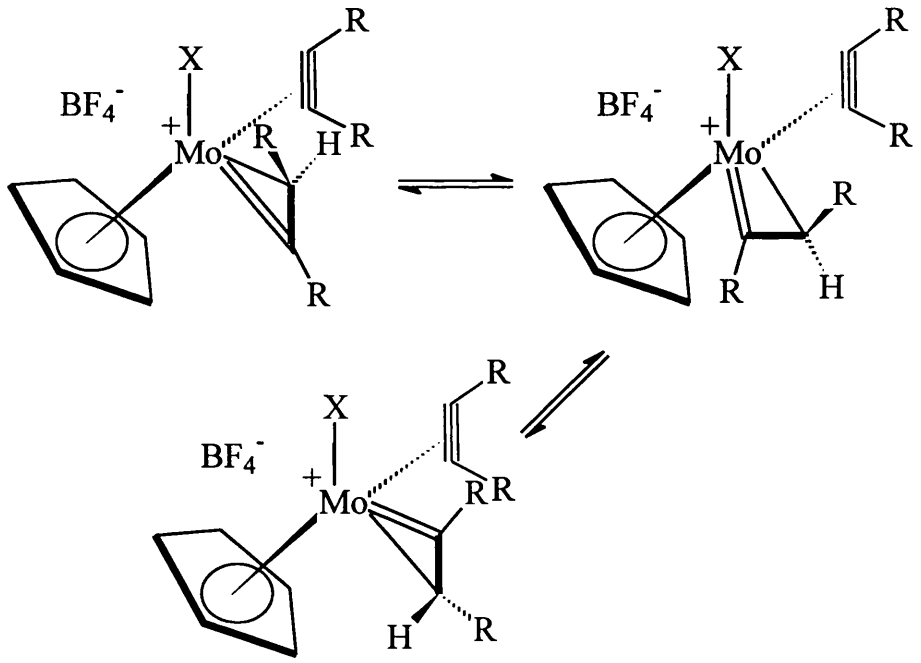

Figure 2.12. Rotation of the η^2(3e)-vinyl ligand to facilitate supine conformation of the η^4(5e)-butadienyl ligand.

However, if this complex were now to couple via a Dötz reaction, the syn-supine conformation would be obtained. This is not the observed orientation, i.e. anti-supine, and in order to achieve an anti-supine conformation protonation would have to occur on the same face as the Cp ligand and the iodine atom. Such a process is obviously unlikely on steric grounds. There is, however, an alternative way of accessing the η^2(3e)-vinyl/η^2(4e)-alkyne cation needed to generate the anti-supine η^4(5e)-butadienyl ligand, and that is to invoke a steric factor in the protonation reaction. As is shown in Table 2.3, there is also an appreciable negative charge on the alkyne carbon atoms C13 and C23, i.e. those contact carbons *trans* to the iodo ligand, and therefore protonation could be directed to these carbons by steric interactions with the incoming $HBF_4.OEt_2$ molecule. Indeed, examination of the space filling model (Figure 2.11.) clearly shows that not only is the preferred direction of attack remote from the Cp ligand but also on the alkyne carbons remote from the iodo-ligand. Thus, the cation shown in Figure 2.13 might be expected to be formed stereoselectively.

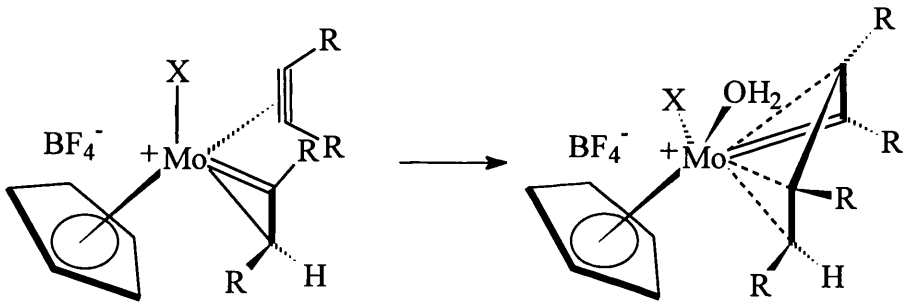

Figure 2.13. Formation of the anti-supine conformation of an η^4(5e)-butadienyl ligand.

With regards to the coupling reaction between the η^2(3e)-vinyl and the η^2(4e)-alkyne there are a number of other possible orientations of the reacting ligands. These are shown in Figure 2.14 along with the resulting *cisoid* η^4(5e)-butadienyl ligand, which would be obtained.

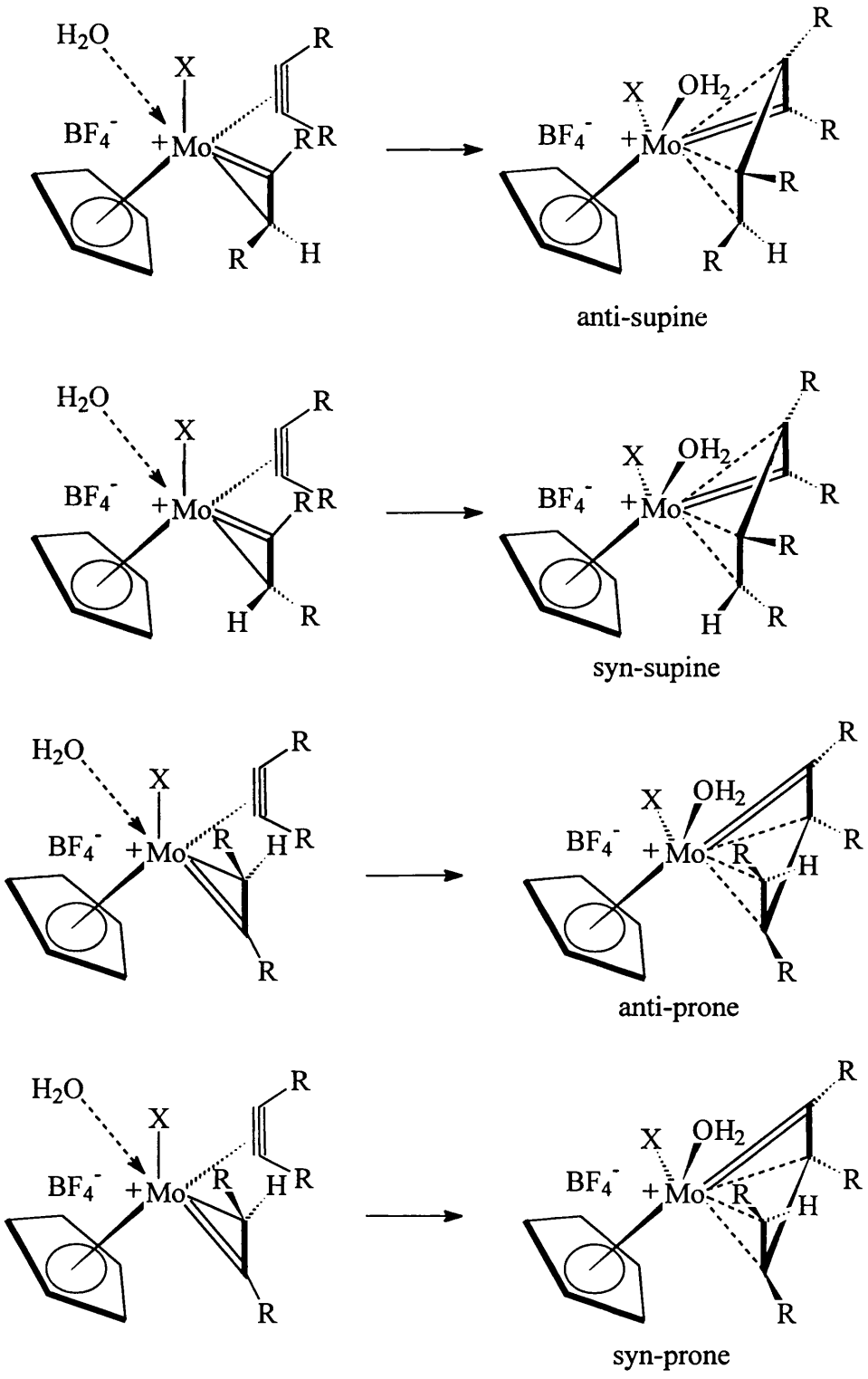

Figure 2.14. Possible *cisoid* orientations of the η^4(5e)-butadienyl ligand.

It should also be mentioned here that in theory a *transoid* conformation may be adopted as was seen with complex (**12**), but this has not been observed in the case

of these molybdenum complexes. The configurations which would have been obtained if the *transoid* configurations were observed are shown in Figure 2.15.

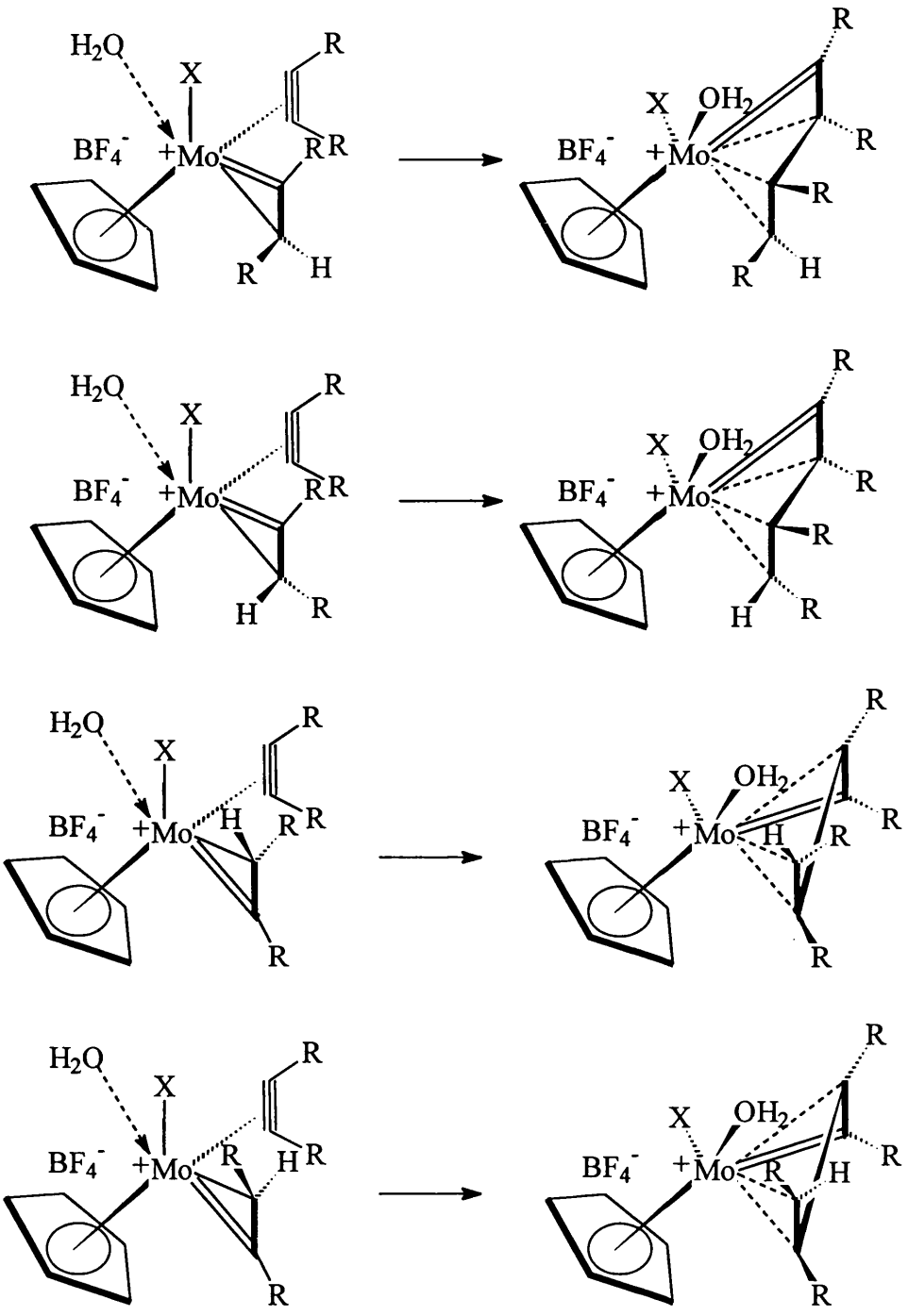

Figure 2.15. Possible *transoid* orientations of the η^4(5e)-butadienyl ligand.

Thus in summary, this analysis provides a possible insight into the mechanism of formation of the anti-supine η^4(5e)-butadienyl ligand. Isolation of the presumed

η^2(3e)-vinyl/η^2(4e)-alkyne intermediate complex would greatly strengthen our understanding of this mechanism, but the difficulties involved in isolating such a reactive complex have, so far, proved insurmountable.

2.4 The Synthesis and Reactivity of the Acetonitrile Complex [BrMo=C(Et)-η^3-{C(Et)C(Et)CHEt}(NCMe)(η-C_5H_5)][BF_4] (27).

In the light of the discovery of the aqua complexes of the type [BrMo=C(Et)-η^3-{C(Et)C(Et)CHEt}(OH_2)(η-C_5H_5)][BF_4] (**21b**), it was obviously interesting to examine the reactivity of this complex and the related methyl substituted system (**21a**) with various donor ligands.

The reaction of the methyl substituted analogue (**21a**) with MeCN gave a very low yield product which, despite once being obtained in a crystalline form suitable for X-ray structure determination by Nation,[66] was found not to be reproducible.

However, stirring (**21b**) in MeCN for 1hr caused a colour change from purple to orange and, upon work-up, an orange complex[65] (more stable than the methyl substituted version) was isolated (eq.2.17). The NMR data for the MeCN complex were very similar to that of the aqua-complex (**21b**), however, in order to confirm the stereochemistry of (**27**) a single crystal was obtained, using diffusion layer techniques (MeCN/Et_2O) at room temperature, and an X-ray diffraction study was undertaken.

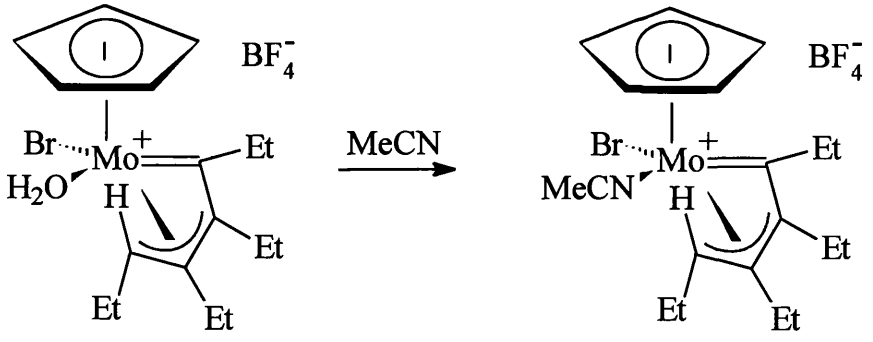

(**21b**) (**27**) eq.2.17

The structure of (**27**) is shown in Figure 2.16. Relevant bond distances and bond angles for (**27**) are given in Table 2.4.

Table 2.4. Selected bond lengths (Å) and bond angles (°) for the acetonitrile complex [BrMo=C(Et)-η^3-{C(Et)C(Et)CHEt}(NCMe)(η–C_5H_5)][BF_4] (**27**).

Bond	Bond length (Å)
Mo-C11	1.925(8)
Mo-C10	2.335(8)
Mo-C9	2.431(8)
Mo-C8	2.324(8)
C11-C10	1.447(9)
C10-C9	1.390(9)
C9-C8	1.440(10)

Bond Angle	Angle (°)
Mo-C11-C10	86.5(5)
C11-C10-C9	115.1(6)
C10-C9-C8	117.8(6)
Mo-C8-C9	76.5(3)
C11-Mo-N1	138.9(2)
C11-Mo-Br1	96.2(3)

The torsion angle C8-C9-C10-C11 is 8.8(8)°, a slight deviation from planarity for the C_4 backbone of the η^4(5e)-butadienyl ligand.

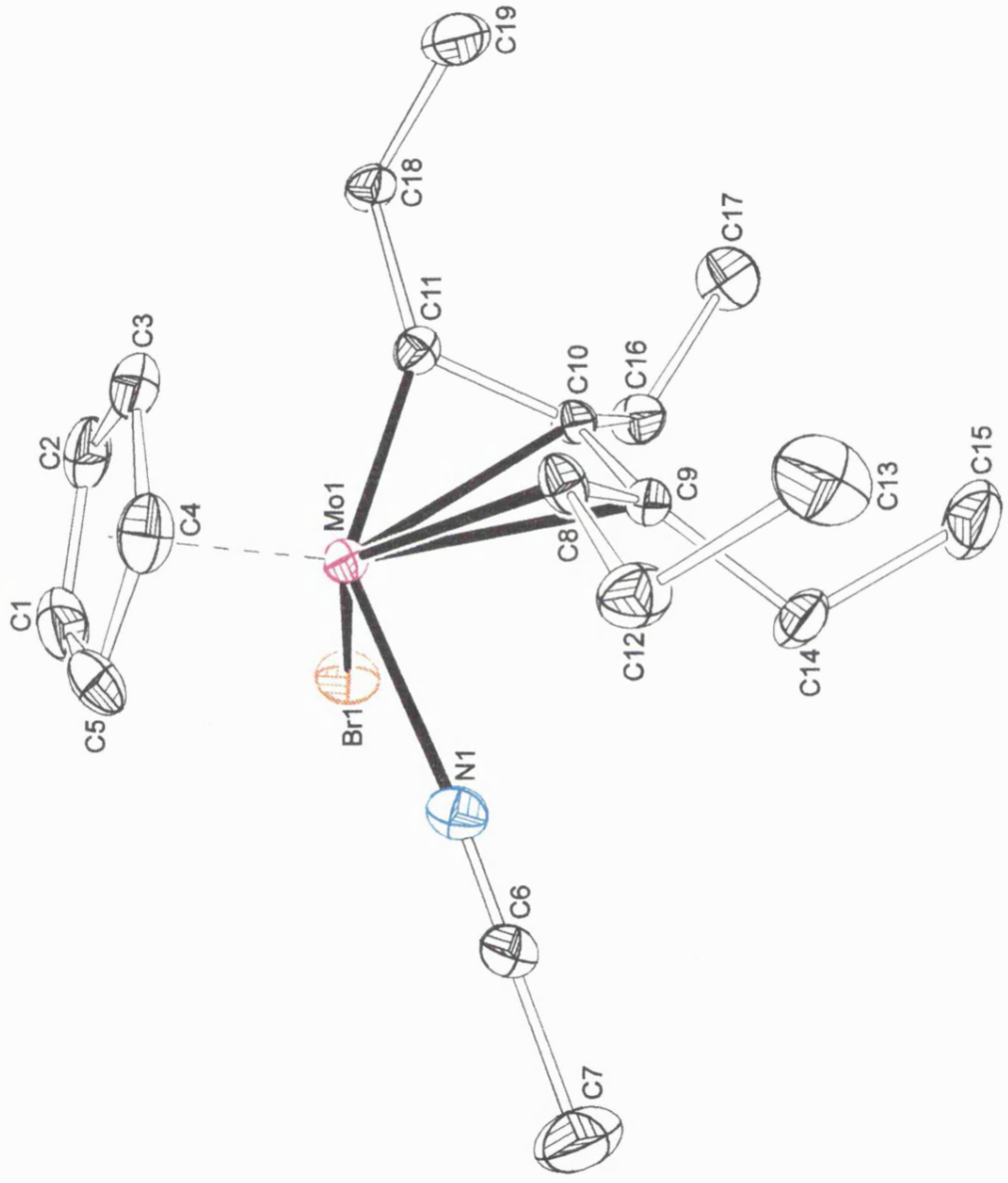

Figure 2.16. ORTEX representation of [BrMo=C(Et)-η^3-{C(Et)C(Et)CHEt}(NCMe)(η-C_5H_5)][BF_4]. Hydrogen atoms omitted for clarity.

The bond lengths and angles within the η^4(5e)-butadienyl ligand are consistent with those obtained for the analogous aqua-complex. Interestingly, the MeCN ligand adopts the same site (*trans* to the Mo=C double bond: C11-Mo1-N1=138.9(2)°) as did the H_2O molecule which it displaced.

An explanation was clearly needed for the stereochemistry of this reaction, i.e. retention of configuration, and for the earlier observation that reaction of the aqua-complex (**21a**), with $P(OMe)_3$ affords the η^4(5e)-butadienyl complex (**26**), in which the $P(OMe)_3$ ligand lies *cis* to the Mo=C double bond. Why was the H_2O ligand replaced by MeCN with retention, whereas replacement of H_2O with $P(OMe)_3$ involves inversion ?

A possible explanation is to assume that the rate determining step involves dissociative loss of H_2O to give a co-ordinately unsaturated cation, which reacts on different faces with MeCN and $P(OMe)_3$ (see Figure 2.17).

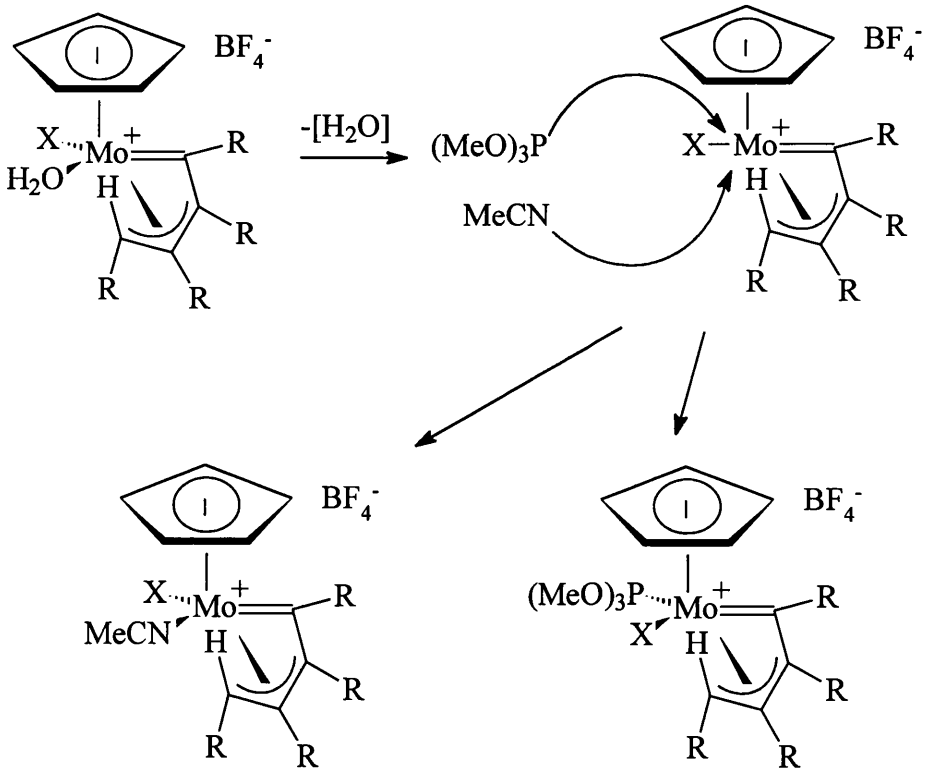

Figure 2.17. S_N1 type reaction for displacement of H_2O with 2e donor ligand.

With a supply of the stereochemically defined MeCN complex, it was now possible to explore further displacement reactions. The lability of the MeCN ligand was first established by the fact that an exchange occurs with d_3-MeCN in solution, producing a resultant complex with no complexed MeCN signal, but a signal for free MeCN in the ^1H NMR spectrum.

The first attempt to displace the MeCN ligand was made with CO. This, surprisingly, proved to be unsuccessful. After 3 hours of bubbling CO through a CH_2Cl_2 solution of (**27**), only the unreacted starting material was recovered.

Complex (**27**) was then reacted with $P(OMe)_3$. After 2 hours stirring of a CH_2Cl_2 solution of (**27**) and $P(OMe)_3$ at room temperature, a pink solid (**28**) was obtained, and identified by comparison of its NMR spectra with that obtained by direct reaction of $P(OMe)_3$ with the aqua-complex (**21b**)[65] (eq. 2.18).

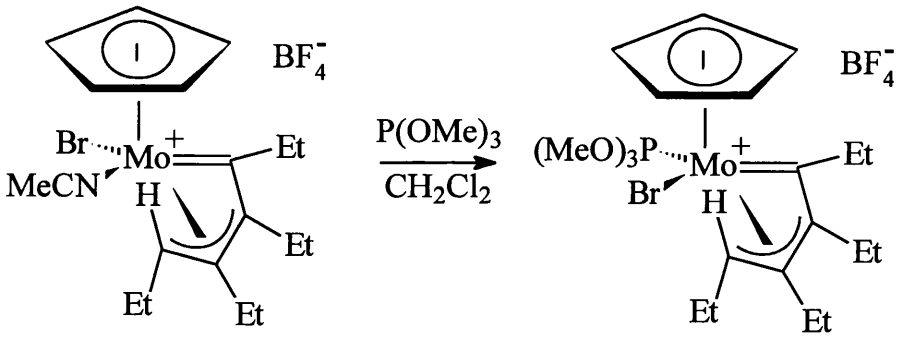

(**27**) (**28**) eq.2.18

This proved to be the same complex as was obtained by direct reaction of the aqua-complex (**21b**) and $P(OMe)_3$, and therefore displacement of MeCN had the same stereochemical conseqences as the displacement of H_2O. In both cases the position of the two-electron donor ligand had altered to become *cis* to the Mo=C double bond. (A discussion of the preference for a *cis* or *trans* site for various ligands will be entered into in the next section.)

A similar reaction was examined with PMe_3 by reaction at room temperature in CH_2Cl_2, giving a pink solid (**29**) in one isomeric form (eq.2.19).

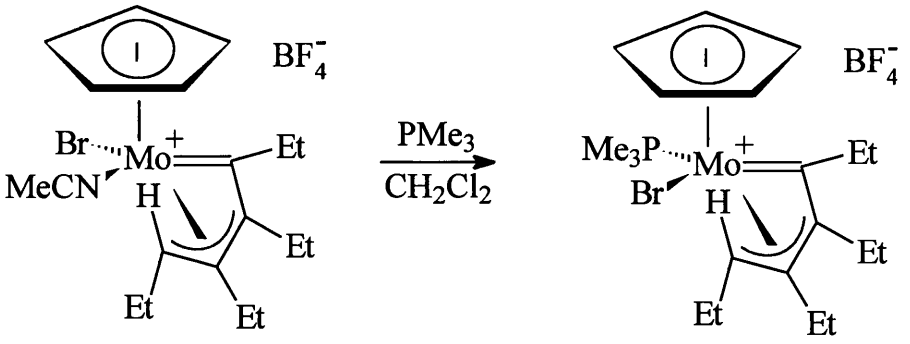

(**27**) (**29**) eq.2.19

This was an interesting result which will be discussed in more depth in the next section. Displacement of the MeCN ligand was also attempted with PPh_3, but only the unreacted starting material was recovered.

The reaction of the MeCN complex (**27**) with bromide anion had been examined before.[65] This complex proved to be identical to that previously prepared and structurally characterised by Nation[66] by reaction of what is now known to be the aqua-complex (**21b**) and LiBr.

Addition of LiBr to a THF/CH_2Cl_2 solution of (**27**) and stirring at room temperature for 1hr, gave the purple complex (**30**) (eq.2.20).

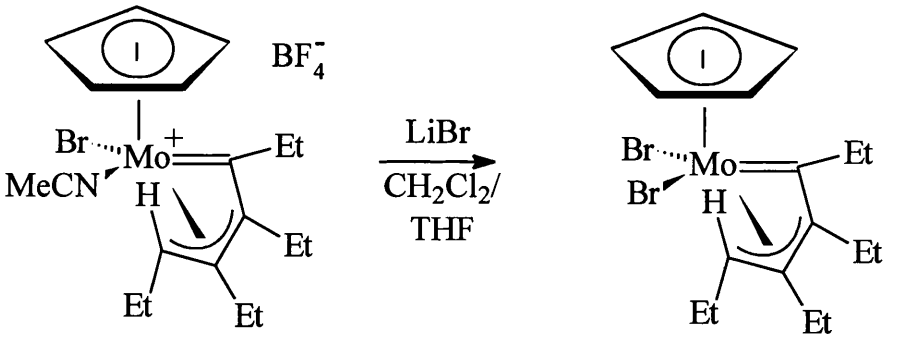

(**27**) (**30**) eq.2.20

Addition of LiCl to (**27**) was also attempted following the same procedure. The resulting product, however, gave broad NMR spectra and inconclusive mass spectrum data. Consequently its exact nature could not be established.

In contrast, reaction of (**27**) with excess LiI in THF/CH_2Cl_2 at room temperature did lead to the identifiable products (**31**) and (**32**) (eq.2.21).

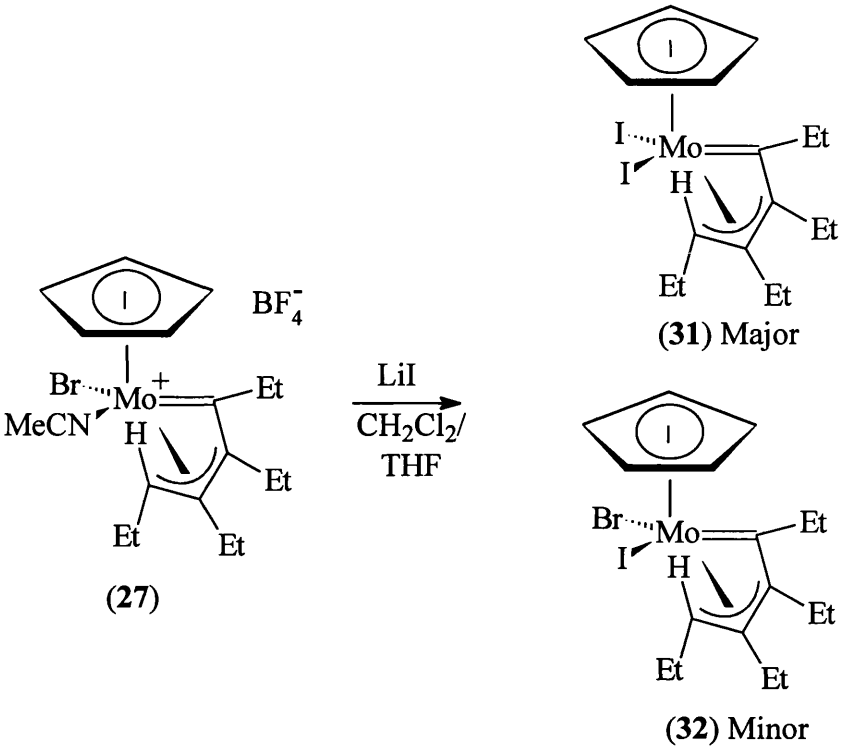

(**27**)

(**31**) Major

(**32**) Minor

eq.2.21

The bis-iodo complex had been synthesised previously,[65] by an analogous method (reaction of the iodo/aqua complex with LiI in THF/CH_2Cl_2 at room temperature) to (**25**) (eq.2.14) and comparison of the NMR data showed that this compound was indeed present, as opposed to there being two isomers of the bromo-iodo species (the stereochemistry of (**32**) is uncertain, and it may well be that the two halide atoms have the opposite configuration). This was confirmed by the mass spectrum of the mixture. This substitution of halide atoms by other higher atomic weight halide atoms has been shown before. A recent example of this was shown by Herrmann *et al*[74] in a dichloro-rhenium system (**33**), in which the chloride ligands were displaced by bromide and iodide (**34**) (eq.2.22).

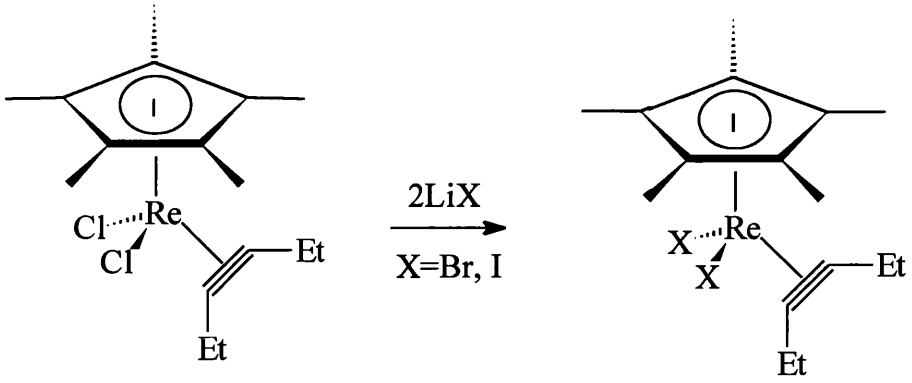

(**33**) (**34**) eq.2.22

In order to see if it was possible to perform one of these reactions without substitution occurring, the iodo-complex (**35**) was synthesised by an analogous route to (**27**) and reacted with LiCl in THF/CH_2Cl_2 at room temperature to give (**36**) (eq.2.23).

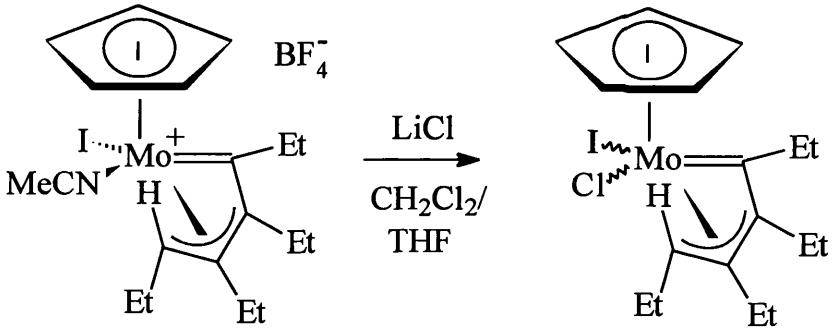

(**35**) (**36**) eq.2.23

The iodide was not displaced by excess chloride and this gave the desired iodide/chloride product. At present the configuration of the halide atoms is unknown but this question could be resolved by an X-ray structure determination.

Thus in conclusion, the MeCN complex has similar overall reactivity to the aqua-complex. There is, however, a difference in the lability and not all the substitution reactions that work with the aqua-complex are successful when applied to the MeCN complex.

The substitution reactions of the MeCN complexes may be explained by a variation on the dissociative mechanism (Figure 2.18.) in which the MeCN ligand is to a

degree still associated to the metal centre, unlike the case with the H_2O ligand. In other words the molybdenum centre still retains a 'memory' of the MeCN ligand when associative attack begins by the phosphorus ligand. Such an associative mechanism explains the failed reaction with PPh_3, owing to steric crowding , and the isolation of only the *cis* isomer of the PMe_3 complex

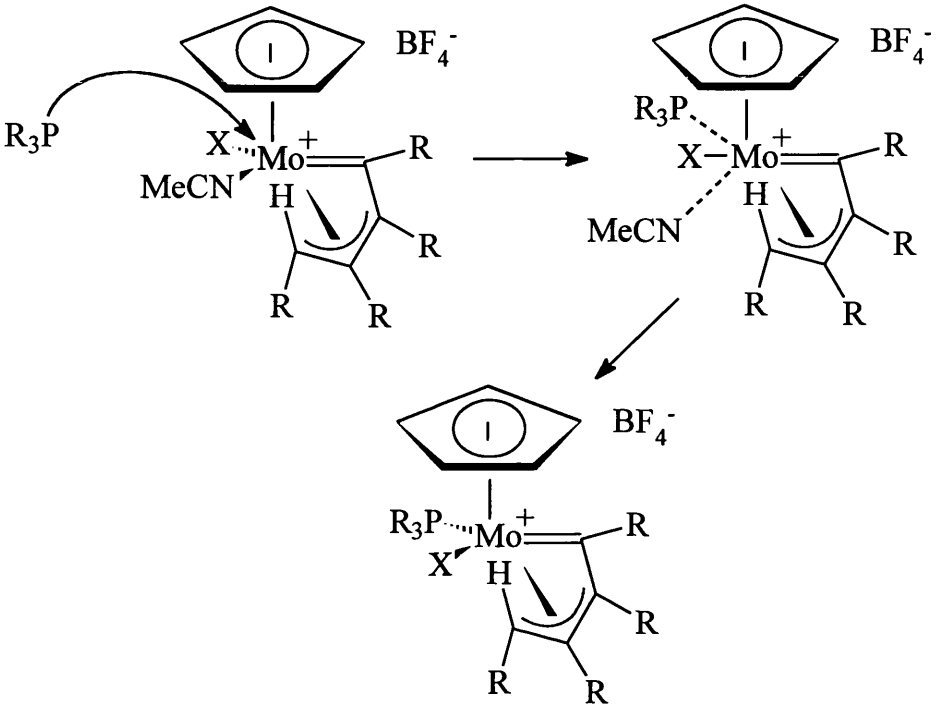

Figure 2.18. Associative mechanism for the displacement of the MeCN ligand.

As mentioned earlier, the MeCN ligand can be replaced by d_3-MeCN giving the same ^1H NMR spectrum, with the exception of the MeCN peak. This is probably due to a thermodynamic process resulting in the observation of only the *trans* isomer of the deuterated MeCN complex.

2.5 The Synthesis of Two-Electron Donor Phosphorus Substituted η^4(5e)-Butadienyl Complexes.

As described previously, η^4(5e)-butadienyl complexes with phosphorus co-ordinated ligands can be synthesised. Originally it was thought that these complexes containing $P(OMe)_3$ and PPh_3 ligands were formed from reaction of the η^2(3e)-vinyl/η^2(4e)-alkyne cations (**21a**) and (**21b**). However, these precursors are now known to be aqua complexes, and therefore we now know their synthesis involves a displacement reaction, i.e. displacement of H_2O by PR_3. In extending the reaction to PMe_3, it was found that treatment of (**21b**) with PMe_3 in CH_2Cl_2 led to the formation of two isomeric complexes (**29a**) and (**29b**) in the ratio 6:1.

The two isomers gave very similar NMR spectra which meant that the isomers only differed in the position of the phosphorus ligand. Any change in the position of the H atom on the allyl part of the η^4(5e)-butadienyl ligand would lead to a major difference in the ^{1}H NMR spectra of these complexes. The two isomers (**29a**) and (**29b**) are depicted in eq.2.24.

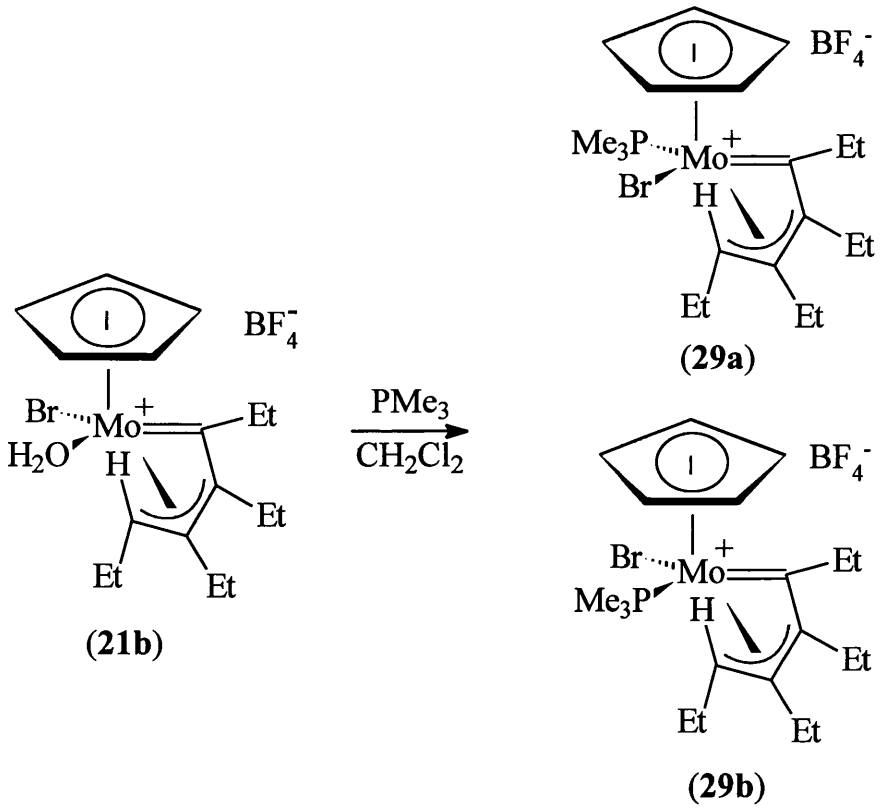

(**21b**)

(**29a**)

(**29b**)

eq.2.24

Unfortunately there was no way of deciding which of (**29a**) and (**29b**) was the major isomer. The answer to this problem came from the previously mentioned reaction of the MeCN complex (**27**) with PMe_3 (eq.2.19). On stirring (**27**) and PMe_3 in CH_2Cl_2 for 1hr, a pink complex was obtained. This proved to be only one isomer, which, on comparison of the NMR data was found to be identical to the major isomer formed in the reaction of the aqua-complex. Crystals suitable for X-ray structure determination were obtained by layer diffusion (CH_2Cl_2/hexane), the resulting structure is shown in Figure 2.19. Relevant bond distances and bond angles for (**29a**) are given in Table 2.5, and are consistent with the MeCN and aqua η^4(5e)-butadienyl complexes.

Table 2.5. Selected bond lengths (Å) and bond angles (°) for the trimethylphosphine complex [BrMo=C(Et)-η^3-{C(Et)C(Et)CHEt}(PMe_3)(η-C_5H_5)][BF_4] (**29a**).

Bond	Bond length (Å)
Mo-C9	1.930(9)
Mo-C8	2.341(9)
Mo-C7	2.467(9)
Mo-C6	2.331(10)
C9-C8	1.434(11)
C8-C7	1.400(12)
C7-C6	1.429(12)

Bond Angle	Angle (°)
Mo-C9-C8	86.9(5)
C9-C8-C7	117.7(8)
C8-C7-C6	118.1(8)
Mo-C6-C7	77.6(5)
C9-Mo-P1	92.4(3)
C9-Mo-Br1	140.6(2)

The phosphorus ligand was shown to be in the *cis* position relative to the Mo=C bond (C9-Mo1-P1=92.4(3)°). The torsion angle C6-C7-C8-C9 is -8.4(10)°, a slight deviation from planarity for the C_4 backbone of the η^4(5e)-butadienyl ligand.

It would be expected that the same intermediate would be formed by either dissociative loss of water from (**21b**), or dissociative loss of MeCN from (**27**), and therefore the capture of this intermediate by PMe_3 should lead to the same isomer distribution in both cases, however, as explained earlier (section 2.4) it is likely in the reaction (**27**) going to (**29a**) the MeCN, although dissociated from the cationic

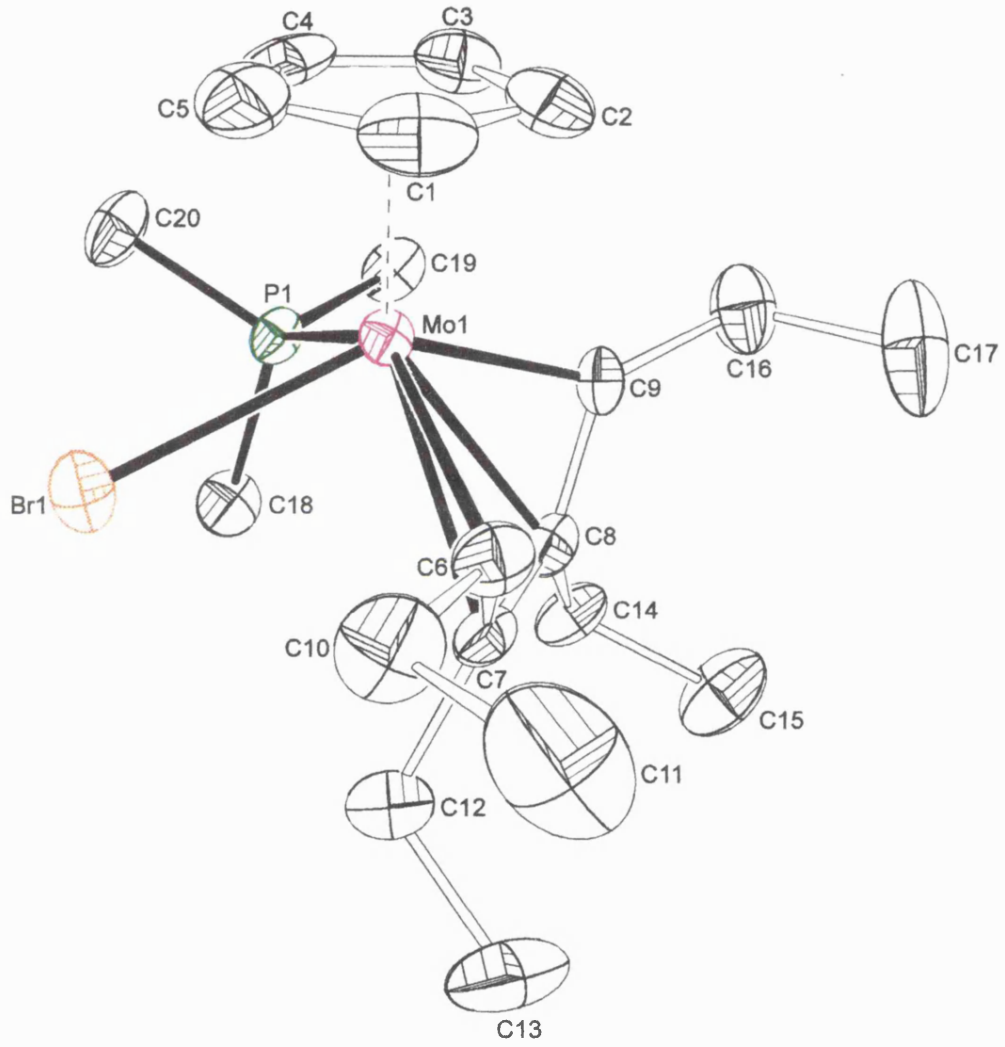

Figure 2.19. ORTEX representation of [BrMo=C(Et)-η^3-{C(Et)C(Et)CHEt}(PMe_3)(η-C_5H_5)][BF_4]. Hydrogen atoms omitted for clarity.

molybdenum centre, is still in close proximity and, therefore, the PMe_3 is directed exclusively *cis* to the Mo=C bond.

Returning to the question of the stereochemistry of the substitution reaction, it can now be seen that phosphorus ligands adopt a *cis* conformation (except for the small amount of (**29b**) in eq.2.24) in these η^4(5e)-butadienyl complexes. The aqua and MeCN complexes on the other hand adopt a *trans* conformation. If the mechanism in the substitution of H_2O is as suggested in Figure 2.16, both *cis* and *trans* sites are available. This means that the phosphorus ligands have a clear preference for the *cis* position over the *trans*, and the MeCN and H_2O ligands have a preference for the *trans*. There are two factors which are involved in which site is occupied. These are steric factors and electronic factors. In the case of phosphorus ligands steric factors could be very important. Figure 2.20 shows a representation of the Tolman[75] cone angle for a ligand.

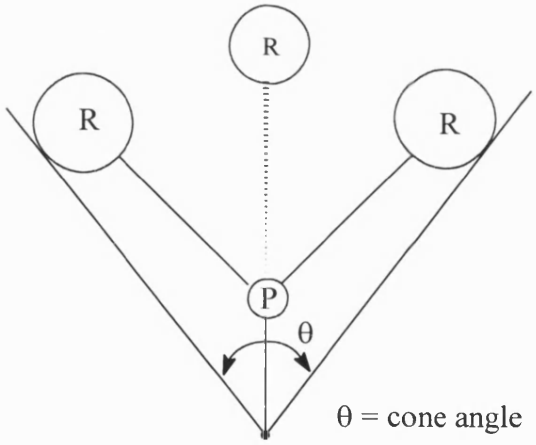

Figure 2.19. Diagram of the Tolman cone angle.

This cone angle gives us a measure of the steric bulk of a ligand. The values for $P(OMe)_3$, PMe_3 and PPh_3 are 108°, 118° and 145° respectively. As mentioned previously, *cis* and *trans* (relative to Mo=C bond) isomers of the PMe_3 complex are obtained on reaction of PMe_3 with (**21**), whereas the $P(OMe)_3$ complex is only found as the *cis* isomer. The preference of $P(OMe)_3$ for the *cis* position clearly can not be attributed to purely steric factors, as it has less steric bulk than PMe_3, which has been shown to occupy the *trans* position. The explanation for this preference

for a *cis* position is probably electronic factors. The superior π-accepting ability of $P(OMe)_3$ would create a competition for electron density between itself, the Mo=C double bond and the η^3(3e)-allyl moiety. The $P(OMe)_3$ is therefore incorporated into the *cis* site where any such conflict would be minimised. It should be noted here that PMe_3 does have some π-accepting ability[76], which could account for the fact that the majority of the PMe_3 also adopts a *cis* position. H_2O and MeCN occupy the *trans* position as they are pure σ-donors, and there is no conflict for electron density on the metal.

2.6 The Synthesis and Reactivity of the Bis-Halogen Complexes [X_2Mo=C(R)-η^3-{C(R)C(R)CHR}(η-C_5H_5)].

The final class of these η^4(5e)-butadienyl complexes, which have been studied, are the bis-halogen complexes. As seen previously, these complexes can be formed directly from the MeCN complexes (eq.2.20, 2.21, 2.23) and what were previously thought to be the η^2(3e)-vinyl/η^2(4e)-alkyne complexes, and are now known to be the aqua-complexes (eq.2.25).

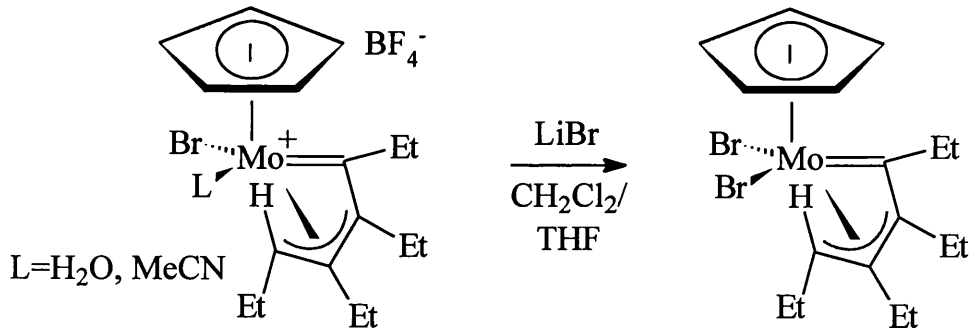

(21b), (27) **(30)** eq.2.25

The structure of complex (**30**) was determined by Nation.[66] It is important to emphasize now that a complex mentioned earlier (**22**), that was synthesised by Woolhouse,[64] is obviously an η^4(5e)-butadienyl complex (eq. 2.26).

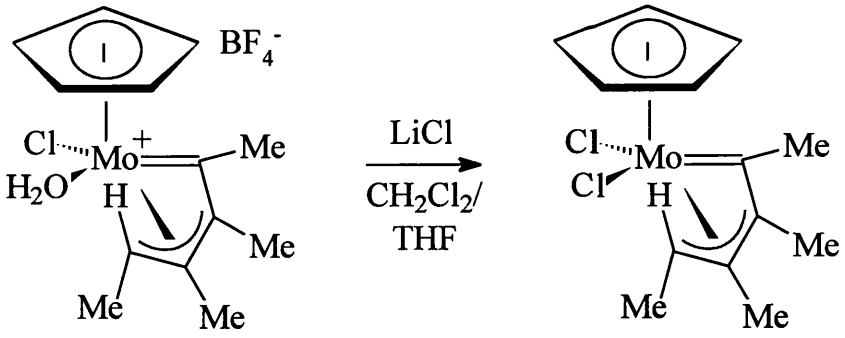

(21a) **(22)** eq.2.26

As described before in the case of the MeCN complexes, addition of LiBr to a CH_2Cl_2/THF (1:1) solution of **(21a)** at room temperature causes a darkening of the solution. This leads to two products, **(37)** the bis-bromo complex and **(38)** the bromo/chloro complex (eq.2.27).

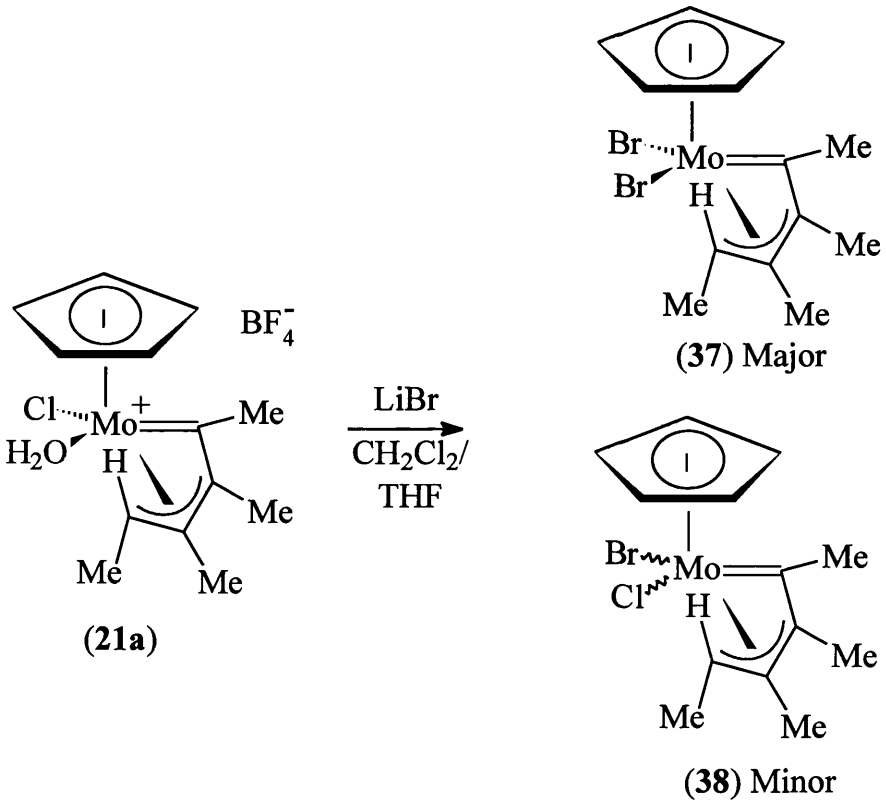

(21a)

(37) Major

(38) Minor

eq.2.27

Once formed these bis-halogen complexes can be converted back to cationic η^4(5e)-butadienyl complexes by reaction with $Ag[BF_4]$ in the presence of a two-

electron donor ligand such as PR_3 and MeCN in CH_2Cl_2 after stirring for 2hrs at room temperature e.g. eq. 2.28.

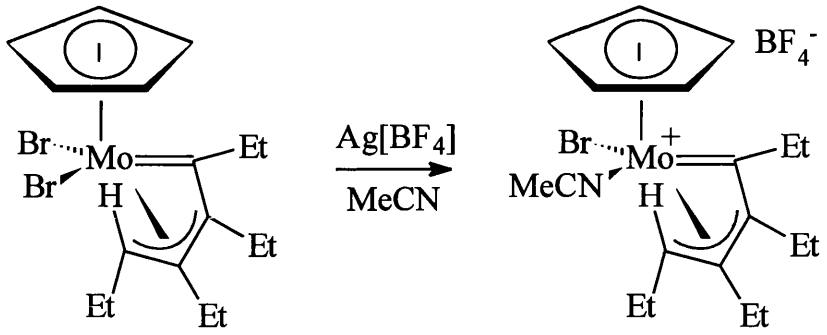

(30) **(27)** eq.2.28

These cationic complexes are found to adopt their preferred orientation i.e. *cis* or *trans* as evidenced by their NMR spectra. The aqua-complex (**39**) can be generated by reaction of $Ag[BF_4]$[64] or $Ag[O_3SCF_3]$ in good yields (90%) (eq.2.29).

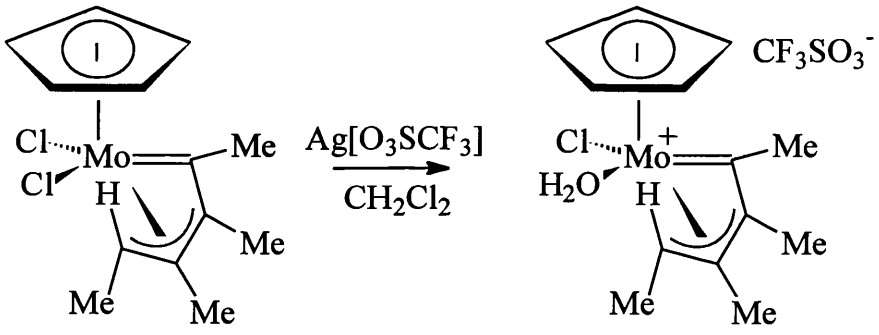

(25) **(39)** eq.2.29

The H_2O probably comes from the very hygroscopic $Ag[BF_4]$ and $Ag[O_3SCF_3]$ salts, which unavoidably come into contact with air.

2.7 Comparison of ^{13}C-NMR and X-ray Structural Data for η^4(5e)-Butadienyl Ligands.

The $^{13}C\{^1H\}$ NMR resonances for the *cisoid* backbone of the η^4(5e)-butadienyl ligands synthesised in this work are all remarkably similar, differing by only ± 5 ppm irrespective of the alkyl groups on the ligand itself. The relevant chemical shift data are summarised in Table 2.6.

Table 2.6. Selected $^{13}C\{^1H\}$ NMR data for some η^4(5e)-butadienyl ligands.

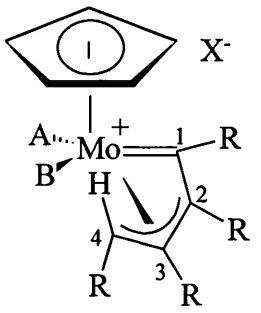

	A=Br B=H_2O R=Et X=BF_4	A=Cl B=H_2O R=Me X=BF_4	A=Br B=Br R=Et	A=Cl B=Cl R=Me	A=Br B=MeCN R=Et X=BF_4	A=PMe_3 B=Br R=Et X=BF_4
C_1	298.4	306.6	295.3	291.3	297.4	299.1
C_2	137.8	135.6	136.7	134.2	140.2	132.7
C_3	117.9	118.0	113.8	113.6	119.3	111.7
C_4	79.3	73.8	74.5	70.0	75.9	77.5

All the complexes have the characteristically low field shift for the Mo=C at approximately 290.0 to 307.0 ppm. This is observed for other types of η^4(5e)-butadienyl ligands, although usually at slightly higher field.

Until now the η^4(5e)-butadienyl complexes in this chapter have been described as allyl carbenes. Tables 2.7 and 2.8 show selected bond lengths and bond angles respectively for the η^4(5e)-butadienyl complexes described here and examples of *cisoid* rhenium and ruthenium complexes containing the η^4(5e)-butadienyl ligand i.e. [Re=C(Ph)-η^3-{C(Me)CHCHC$_6$H$_4$PPh$_2$-*o*}(η-C$_5$H$_5$)][BF_4] and [Ru=C(Ph)-η^3-{C(Ph)C(Ph)CHPh}(η-C$_5$H$_5$)]). The rhenium and ruthenium complexes have

Table 2.7. Bond lengths (Å) for some η^4(5e)-butadienyl complexes.

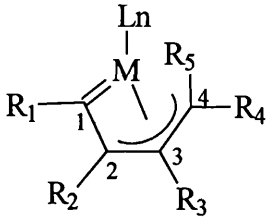

Complex						Bond Length (Å)						
(LnM)	R_1	R_2	R_3	R_4	R_5	M-C1	M-C2	M-C3	M-C4	C1-C2	C2-C3	C3-C4
(η-C_5H_5)Ru (**2**)	Ph	Ph	Ph	H	Ph	1.896(5)	2.204(5)	2.152(4)	2.154(6)	1.419(5)	1.435(7)	1.445(7)
(η-C_5H_5)(PPh_2Ar)Re (**10**)	Ph	Me	H	Ar	H	1.936(12)	2.222(13)	2.216(13)	2.172(14)	1.427(16)	1.415(18)	1.441(16)
(η-C_5H_5)(H_2O)BrMo (**21b**)	Et	Et	Et	Et	H	1.933(9)	2.341(10)	2.414(10)	2.294(10)	1.467(14)	1.405(14)	1.452(14)
(η-C_5H_5)(MeCN)BrMo (**27**)	Et	Et	Et	Et	H	1.925(8)	2.335(8)	2.431(8)	2.324(8)	1.447(9)	1.390(9)	1.440(10)
(η-C_5H_5)(PMe_3)BrMo (**29**)	Et	Et	Et	Et	H	1.930(9)	2.341(9)	2.467(9)	2.331(10)	1.434(11)	1.400(12)	1.429(12)
(η-C_5H_5)Br_2Mo (**30**)	Et	Et	Et	Et	H	1.897(21)	2.310(24)	2.464(22)	2.281(25)	1.42(3)	1.45(3)	1.44(3)
(η-C_5H_5){$P(OMe)_3$}BrMo (**23**)	Me	Me	Me	Me	H	1.938(16)	2.352(19)	2.443(22)	2.336(23)	1.40(3)	1.40(3)	1.34(3)

Table 2.8. Bond angles (°) for some η^4(5e)-butadienyl complexes.

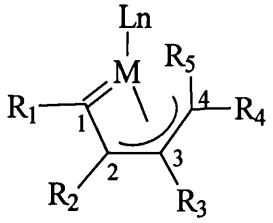

Complex						Bond	Angles	(°)		
(LnM)	R_1	R_2	R_3	R_4	R_5	M-C1-C2	C1-C2-C3-	C2-C3-C4	M-C4-C3	C1-C2-C3-C4
(η-C_5H_5)Ru (**2**)	Ph	Ph	Ph	H	Ph	81.9(3)	119.4(3)	119.4(3)	70.3(3)	---
(η-C_5H_5)(PPh_2Ar)Re (**10**)	Ph	Me	H	Ar	H	81.2(7)	117.6(10)	122.0(11)	72.5(8)	11.4
(η-C_5H_5)(H_2O)BrMo (**21b**)	Et	Et	Et	Et	H	86.1(6)	115.7(9)	116.3(9)	76.6(6)	-11.2
(η-C_5H_5)(MeCN)BrMo (**27**)	Et	Et	Et	Et	H	86.5(5)	115.1(6)	117.8(6)	76.5(3)	8.8(8)
(η-C_5H_5)(PMe_3)BrMo (**29**)	Et	Et	Et	Et	H	86.9(5)	117.7(8)	118.1(8)	77.6(5)	-8.4(10)
(η-C_5H_5)Br_2Mo (**30**)	Et	Et	Et	Et	H	87(1)	115(2)	115(2)	80(2)	-4.9
(η-C_5H_5){$P(OMe)_3$}BrMo (**23**)	Me	Me	Me	Me	H	88(1)	114(2)	122(2)	78(1)	-4.4

C1-C2, C2-C3 and C3-C4 bond lengths of approximately the same length. The molybdenum complexes (**21b**), (**27**) and (**29**) shown tend to have a shorter C2-C3 bond length (this is not the case for (**23**) and (**30**), but the errors quoted for these structures are significantly larger than for the structures described in this work). This indicates that the bonding in these moieties is more complex than a delocalised allyl fragment. It may be that the actual bonding in the cationic complexes mentioned here has some contribution from canonical form **B** shown in Figure 2.20. This would have the effect of shortening the C2-C3 bond.

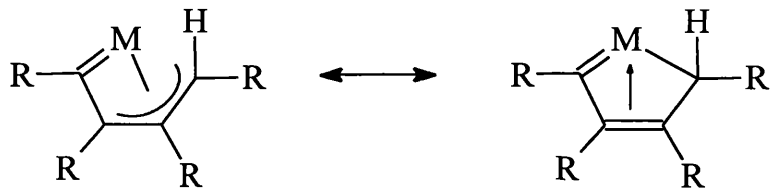

(**A**) (**B**)

Figure 2.20. Resonance forms of the η^4(5e)-butadienyl ligand.

The bond angles for the η^4(5e)-butadienyl moieties are very similar for all the examples shown here. These η^4(5e)-butadienyl ligands are essentially all planar, with slight deviations (±10°) present in all these moieties.

2.8. Reactions of η^4(5e)-Butadienyl Complexes.

In a preliminary study by Woolhouse, it was found[78] that reaction of the stereochemically defined η^4(5e)-butadienyl cationic complex (**26**) with K[BHBu$^s_3$] at 0°C in THF gave a mixture of products which were identified on the basis of the NMR data as a 3:1 mixture of the 1,3-diene complex (**40**) and a species which was depicted as the η^4-bonded vinyl allene complex (**41**) (eq.2.30).

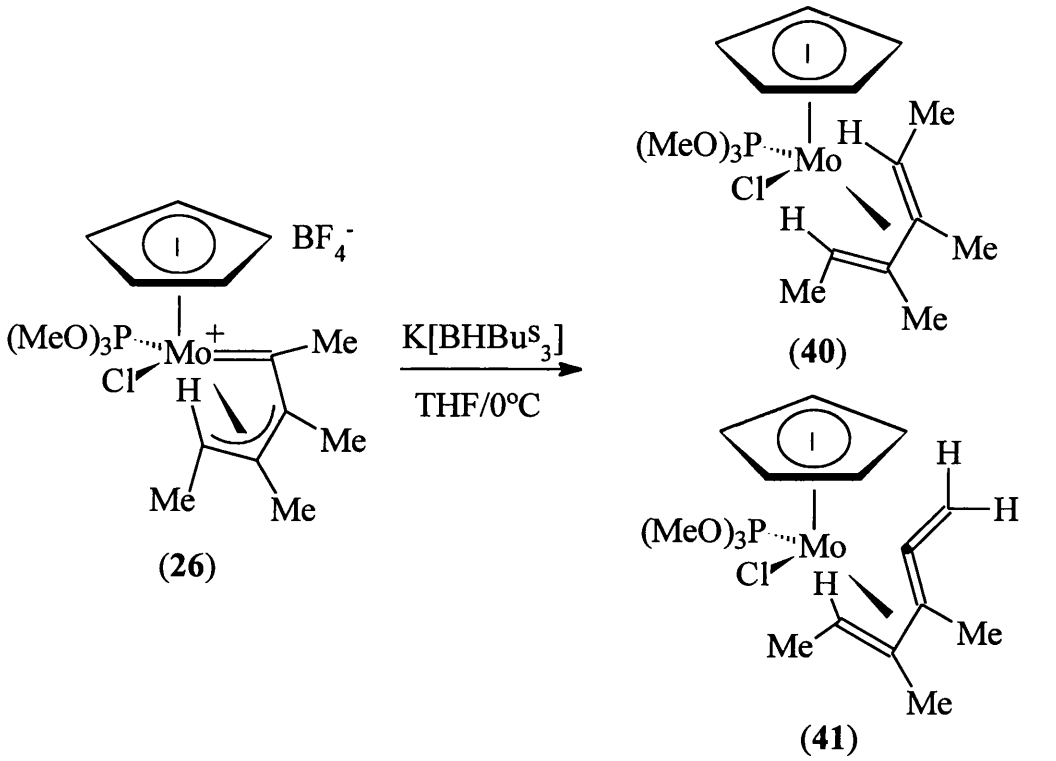

eq.2.30

It was found that (**40**) could be formed selectively by reacting (**26**) with the less basic source of 'H$^-$', the aluminium hydride Bu$^s_2$AlH.

In an attempt to selectively form (**41**) the reaction of (**26**) with the bulky base Li[N(SiMe$_3$)$_2$] in THF at -78°C was examined. This led to the formation (52% yield) of a very air sensitive, purple, hydrocarbon soluble complex. Examination of the ^{1}H, ^{13}C{^{1}H} and ^{31}P{^{1}H} NMR spectra of the complex suggested that the product (**41**) had one of the two structures illustrated in eq.2.31.

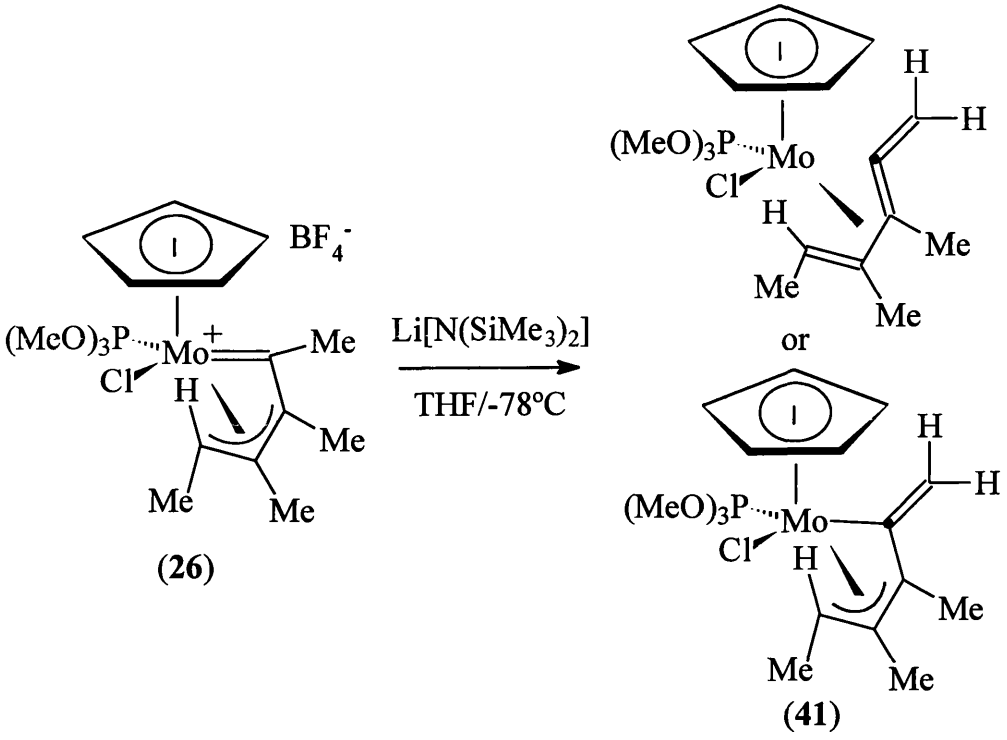

eq.2.31

In order to clarify this structural problem, a single crystal X-ray diffraction study was carried out with a suitable crystal obtained on low temperature (-30°C) crystallisation from a pentane solution. The resultant structure is illustrated in Figure 2.21, selected bond lengths and bond angles are listed in Table 2.8.

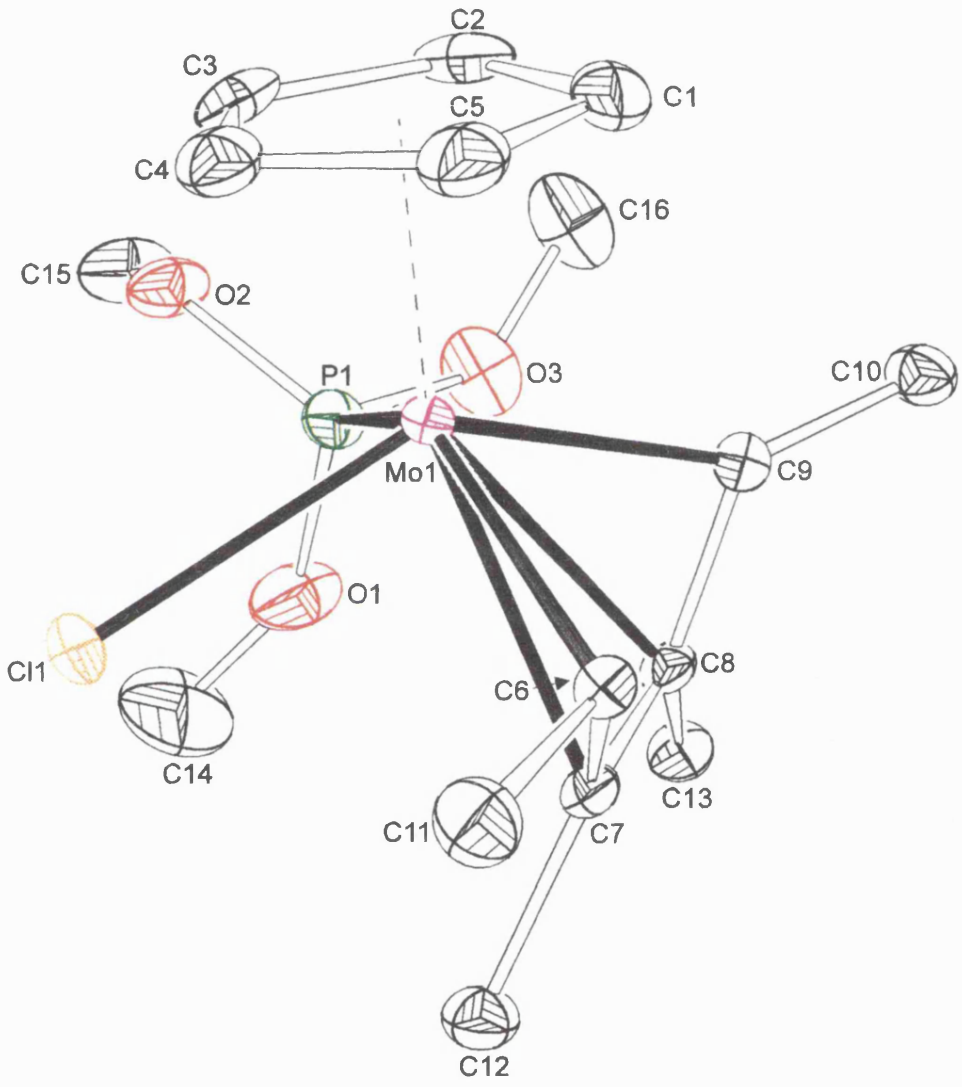

Figure 2.21. ORTEX representation of [ClMo{η^4-CHMe=C(Me).C(Me)=C=CH_2}{$P(OMe)_3$}(η-C_5H_5)] Hydrogen atoms omitted for clarity.

Table 2.8. Selected bond lengths (Å) and bond angles (°) for the trimethylphosphite complex [ClMo{η^4-CHMe=C(Me).C(Me)=C=CH_2}{$P(OMe)_3$}(η-C_5H_5)] (**41**).

Bond	Bond length (Å)
Mo-C9	2.106(9)
Mo-C8	2.380(9)
Mo-C7	2.437(9)
Mo-C6	2.313(9)
C9-C10	1.341(11)
C9-C8	1.433(11)
C8-C7	1.404(11)
C7-C6	1.450(11)

Bond Angles	Angles (°)
Mo-C9-C8	82.2(4)
C9-C8-C7	115.3(7)
C8-C7-C6	116.8(7)
Mo-C6-C7	76.9(4)
C9-Mo-P1	88.9(3)
C9-Mo-Cl1	138.9(2)

The molecule contains an η-$C_5H_5MoCl\{P(OMe)_3\}$ fragment bonded to a C_5-ligand in the anti-supine conformation, which can be described as a methylene substituted molybdenacyclopent-3-ene. This description follows from a comparison of the internal bond parameters of (**41**) 1.433(11), 1.404(11), 1.450(11)Å (a short C8-C7 bond) with those of the zirconium complex (**42**)[77] (Figure 2.22).

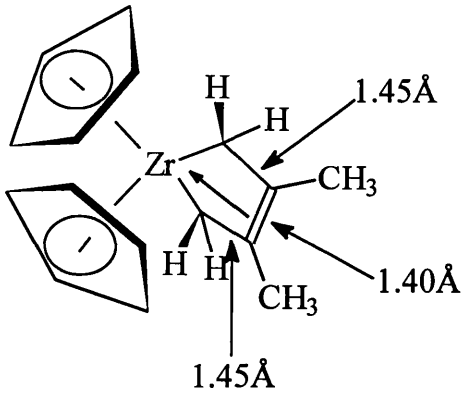

"Metallacyclopentene"

(**42**)

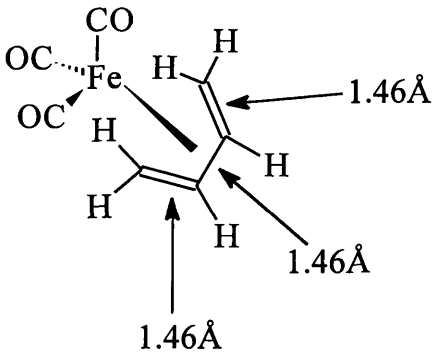

"π-complex"

(**43**)

Figure 2.22. Examples of metallocyclopentene and π complexes of dienes.

The iron complex (**43**) is included as an example of a π-diene complex, in which the internal bond lengths are approximately equal.

Figure 2.23 shows the orbital interactions involved between the diene ligand and a transition metal centre.

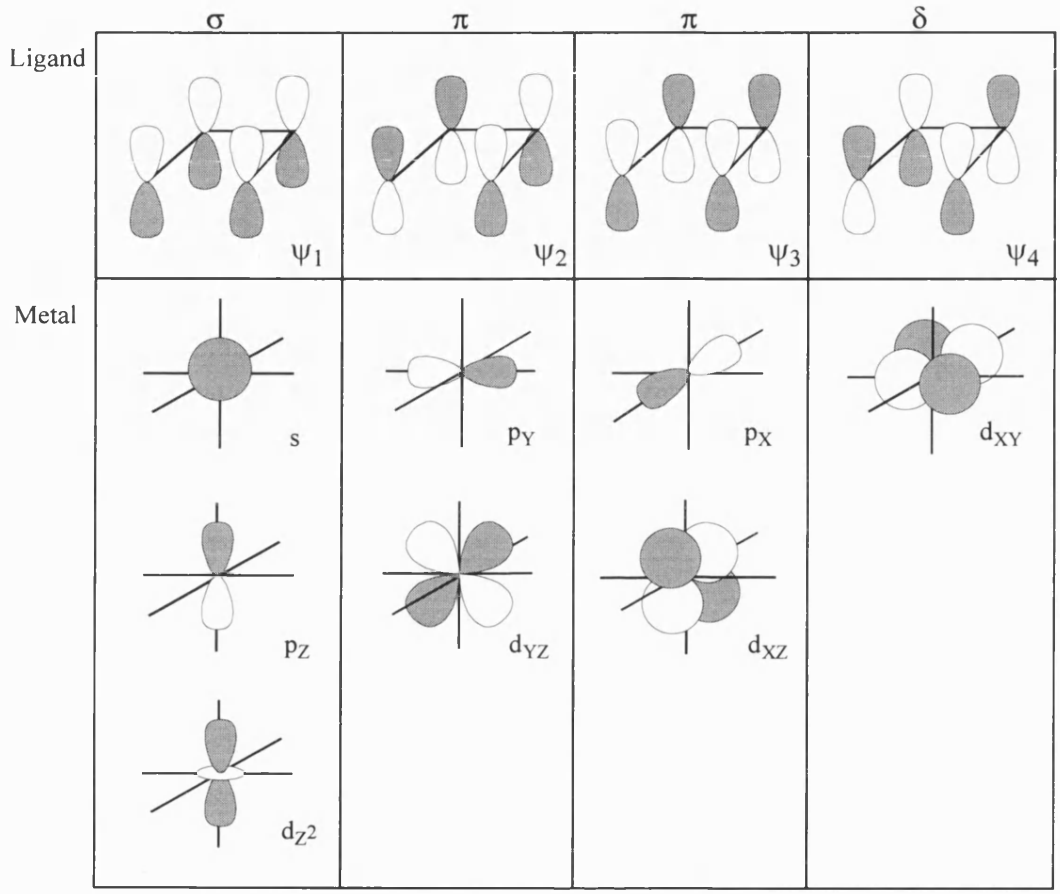

Figure 2.23. Orbitals involved in bonding between a transition metal and a diene.

The consequence of electron density being received into ψ_2 and ψ_3 is a lengthening of the bonds C8-C9 and C6-C7, and a shortening of the bond C8-C7. This results in the formation of a metallocyclopentene (Figure 2.24).

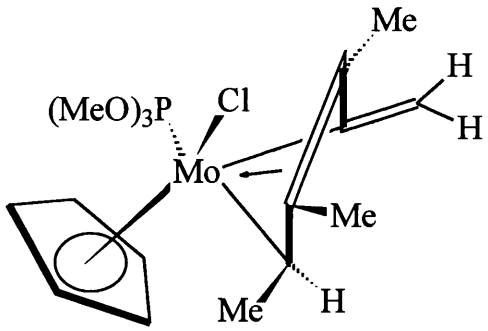

Figure 2.24. Metallocyclopentene character of (**41**).

With the X-ray data available for complex (**41**), it was now possible to perform an EHMO calculation to determine the site of protonation. (calculations performed using the extended Hückel iterative method on the CAChe system using the standard STO-3G basis set and a Wolfenburg-Helmholtz constant, k, of 1.75. The EHT parameters in the CAChe library are based upon experimental data).[72] Table 2.10 shows the charge density on selected atoms of complex (**41**).

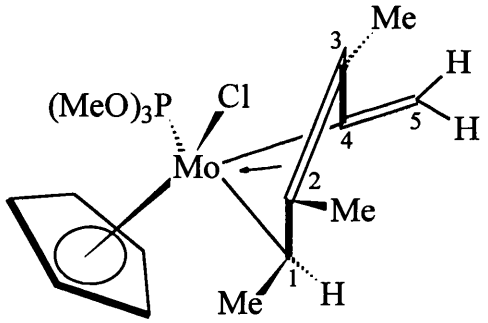

Atom	Charge
C1	-0.3796
C2	-0.0321
C3	-0.1296
C4	**-0.4041**
C5	**-0.3914**

Table 2.10. Charge densities on selected atoms of (**41**).

This calculation suggests that protonation, if it is *via* a charge controlled reaction, would occur on C4 or C5.

Complex (**41**) was found to be selectively reprotonated[78] (at C5) with $HBF_4.OEt_2$ at low temperature (-78°C) in CH_2Cl_2, to regenerate the starting material (**26**) (eq.2.32).

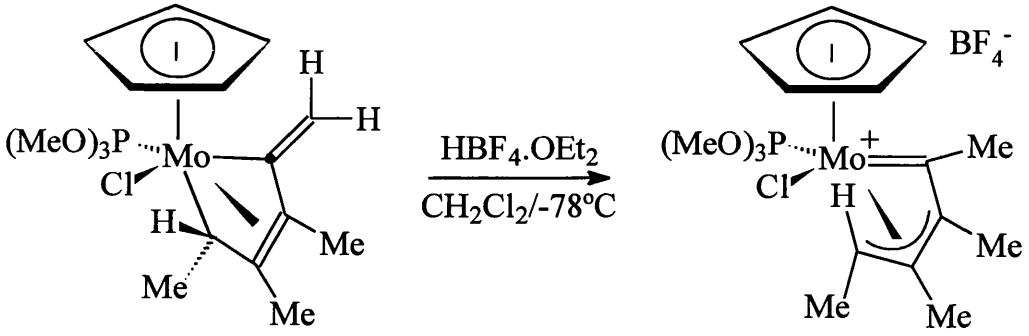

(**41**) (**26**) eq.2.32

The same deprotonation reaction was also carried out on the ethyl substituted analogue (**44**) with $Li[N(SiMe_3)_2]$ in THF at -78°C. This leads to the formation of two isomers in a ratio of 7:3 (**45a**) and (**45b**) (eq.2.33).

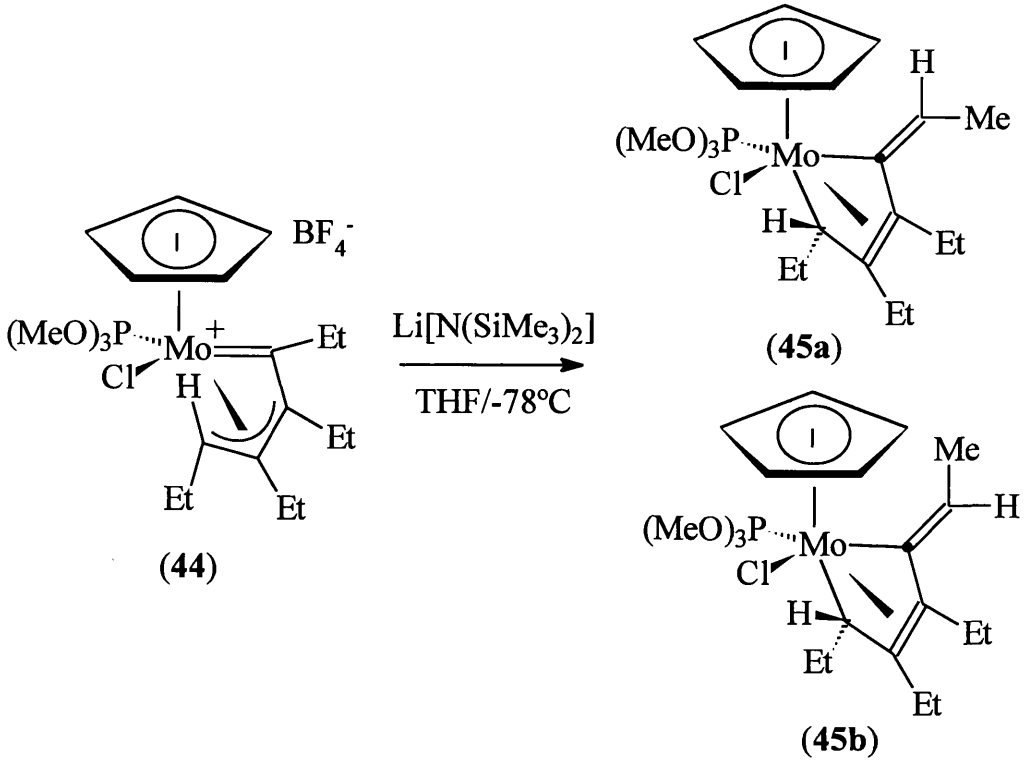

(**44**)

eq.2.33

In the light of the deprotonation reaction to give complex (**45**), it was also considered to be possible that the same reaction might occur with the bis-halogen complexes. Reaction of (**31**) with $Li[N(SiMe_3)_2]$ in THF at -78°C produced a colour change, but decomposition occured upon warming to room temperature. The reaction was repeated , but this time CO was bubbled through the reaction mixture as it warmed up. This gave, upon work up, an orange complex in low yield (16%) (**46**) (eq.2.34).

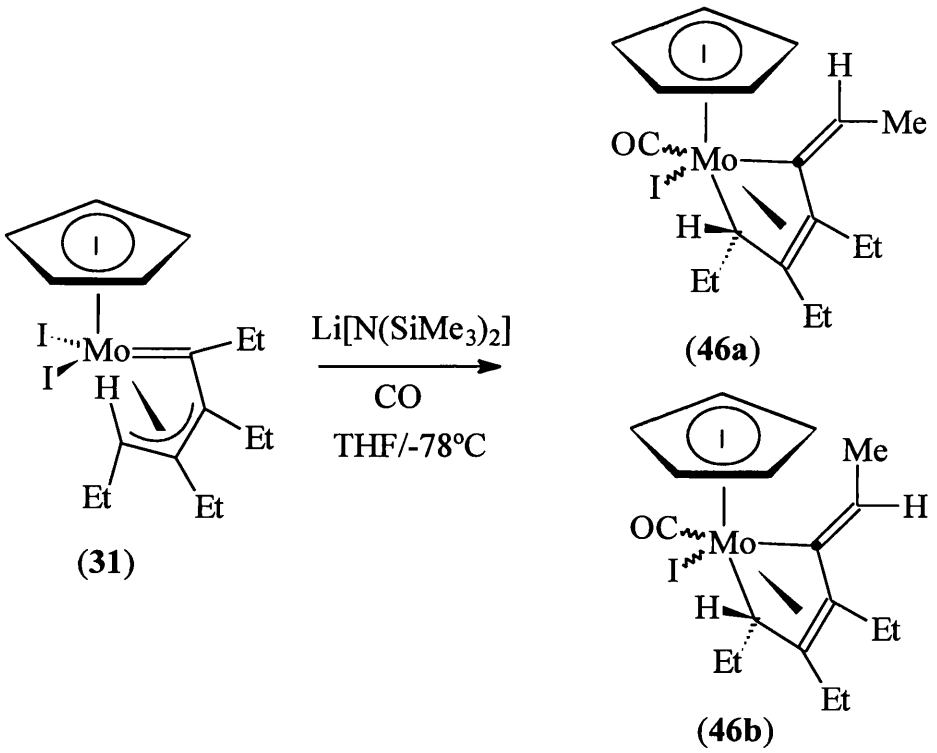

(**31**)

(**46a**)

(**46b**)

eq.2.34

Complex (**46**) gave very similar ^1H and $^{13}C\{^1H\}$ NMR spectra to (**45**) and it is thought that a dehydrohalogenation had occurred. Further attempts to isolate the deprotonated intermediate failed, as this was probably an unstable 16e complex formed by elimination of LiI from the 18-electron anionic molybdenum complex. Only the CO complex was stable enough to be isolated. Unfortunately time constraints prevented further analysis and reactions, such as protonation with $HBF_4.OEt_2$.

2.9 Conclusions.

The existence of the aqua complex (**21b**) has been established and this has removed the difficulties in reconciling the NMR data with the previously suggested structure. Important uncertainties about the stereochemistry of some of these η^4(5e)-butadienyl complexes have been resolved. There are still other reactions of interest that need to be investigated and merit more attention. An in depth theoretical study of the bonding involved in these η^4(5e)-butadienyl complexes certainly warrants attention.

3. Tungsten and Molybdenum Alkyne Complexes Containing the Pentamethylcyclopentadienyl Ligand.

3.1 Synthesis of a Neutral Bis-Alkyne Pentamethylcyclopentadienyl Complex of Molybdenum.

In our efforts to determine the structure of complex (**21**) in the previous chapter, it was decided to attempt to synthesise the pentamethylcyclopentadienyl analogue in the hope of producing a more soluble complex for the purposes of obtaining a single crystal for X-ray crystallography.

The first step was to synthesise the η-C_5Me_5 substituted starting material $[Mo(CH_3)(CO)_3(\eta\text{-}C_5Me_5)]$ (**47**), which was accomplished by using literature methods.[79] An extension of the synthesis reported for Cp chemistry by Beck[23] (protonation at low temperature and addition of alkyne) to the η-C_5Me_5 system gave the bis-alkyne carbonyl complexes (**48**) and (**49**) (eq.3.1).

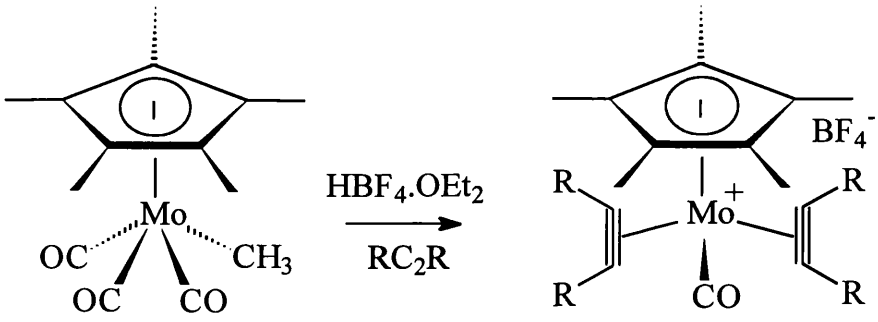

(**47**) (**48**), (**49**) eq.3.1

Complexes (**48** R=Me) and (**49** R=Ph) were obtained as yellow/orange powders in excellent yields (95%+). Complex (**48**) was also synthesised from the allyl complex[80] (**50**) (eq.3.2), but the overall yield was much lower than from the mono methyl complex (**47**).

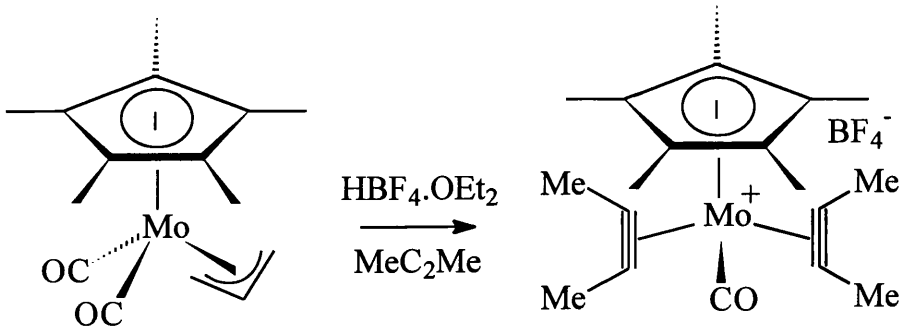

(**50**) (**48**) eq.3.2

The conversion of the carbonyl complex to the MeCN complex (**51**) was achieved in the same manner as the Cp analogue (**19**) by refluxing in MeCN (eq.3.3).

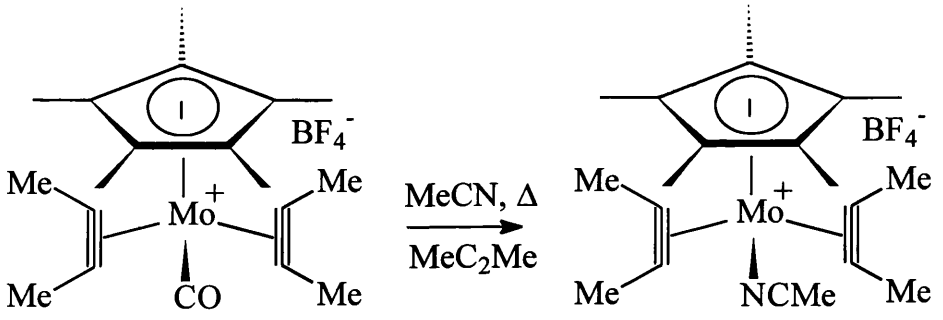

(**48**) (**51**) eq.3.3

Complex (**48**) proved to less reactive than the Cp analogue (**19**) as it took 21 hrs refluxing in MeCN before completion, compared to the 10 hrs or so needed by the Cp complex.

The next stage was again analogous to the Cp chemistry. The same conditions, refluxing THF and LiBr were used to synthesise the neutral complex (**52**) (eq.3.4).

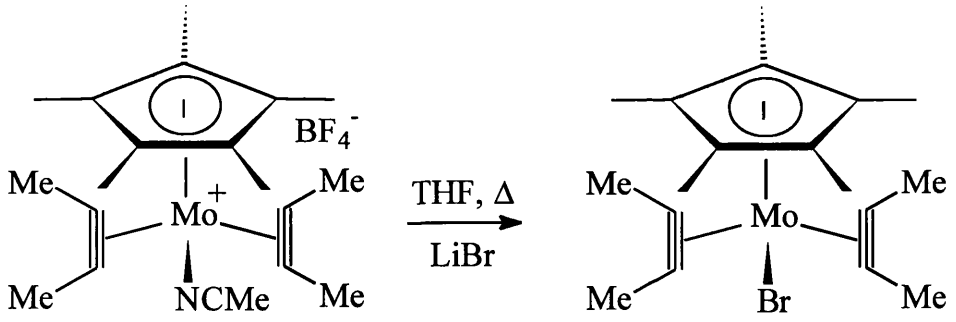

(51) **(52)** eq.3.4

This gave the desired product but in a lower yield than was obtained for the Cp analogue.

Unfortunately, on protonation with $HBF_4.OEt_2$ an analogous aqua η^4(5e)-butadienyl complex was not obtained. The reaction was not specific giving several different compounds on reaction.

3.2 Reduction of [BrMo(η^2-$MeC_2Me)_2$(η-C_5Me_5)].

Previously some examples of bis-alkyne complexes have been reduced to give the dimeric compounds (**53**),[81,82] (**55**)[83,84] and (**57**)[85] which are shown in Figure 3.1.

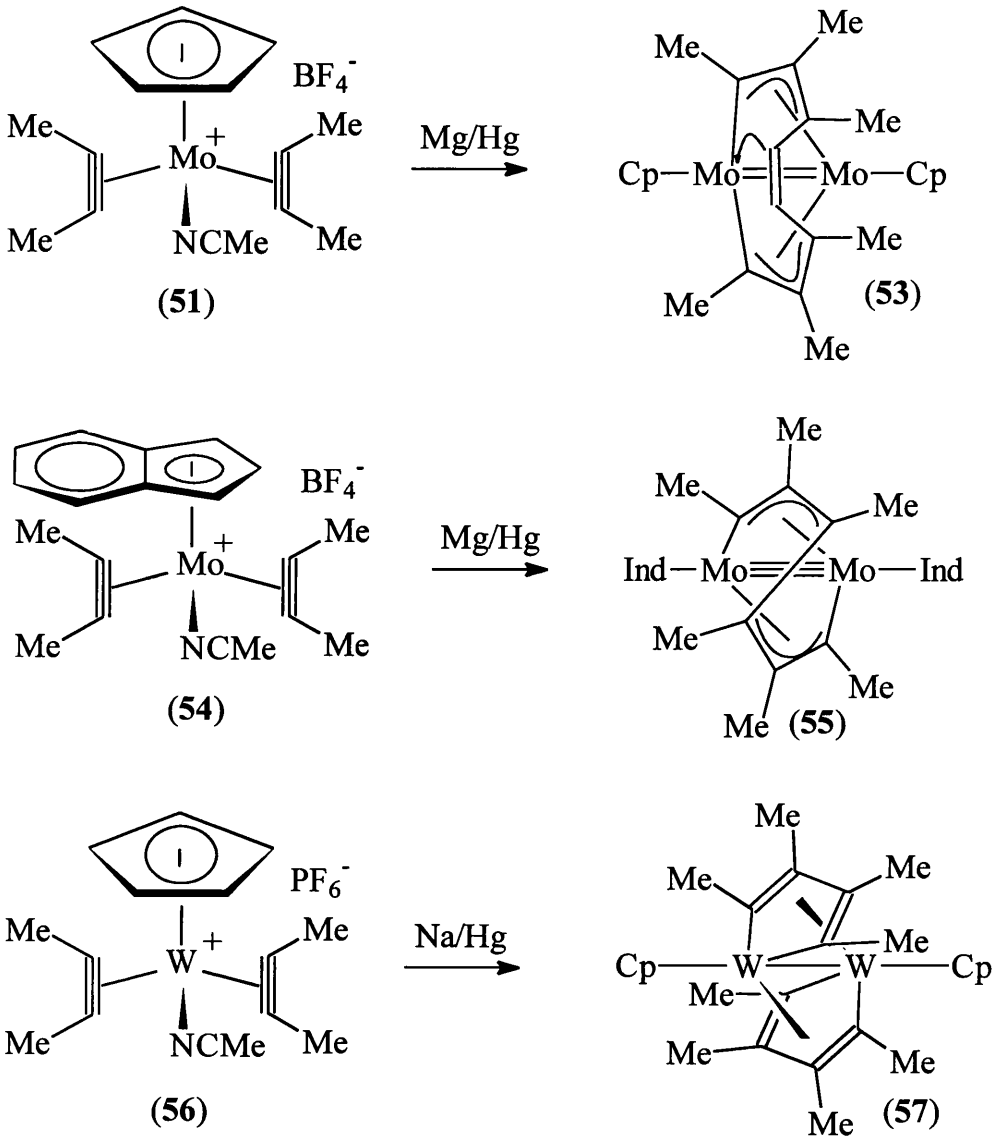

Figure 3.1. Reduction of bis-alkyne complexes of tungsten and molybdenum.

Later studies on the two molybdenum systems showed that improved yields were obtained when the halide analogues were used, and so a reduction of (**52**) was attempted using Mg/Hg amalgam.

Reaction of (**52**) with Mg/Hg amalgam afforded upon work-up, a low yield green compound (**58**). The ^{1}H NMR spectrum showed three singlets in the ratio 2:2:5. This indicated that there were four methyl groups to one Cp* ligand. The $^{13}C\{^{1}H\}$ NMR showed two methyl signals and two other resonances at 182.2 and 108.6 ppm, in addition to the Cp* resonance. The first explanation that could be envisaged for these observations, is that a reductive dimerisation has occurred to

give metallocyclopentene units as in the case of (**57**). Unfortunately there was no $^{13}C\{^1H\}$NMR data reported for complex (**57**), but some other related complexes have been described by Green[84] (molybdenum) and Stone[86] (platinum). These complexes have similar $^{13}C\{^1H\}$NMR with a value of between 90.0 and 140.0 ppm for (C_β) and a higher field resonance for the (C_α) of between 110.0 and 200.0 ppm. This could indicate the formation of a complex similar to (**57**) as shown in eq.3.5, but this complex obviously needs to be characterised by X-ray crystallography to be certain of its actual structure.

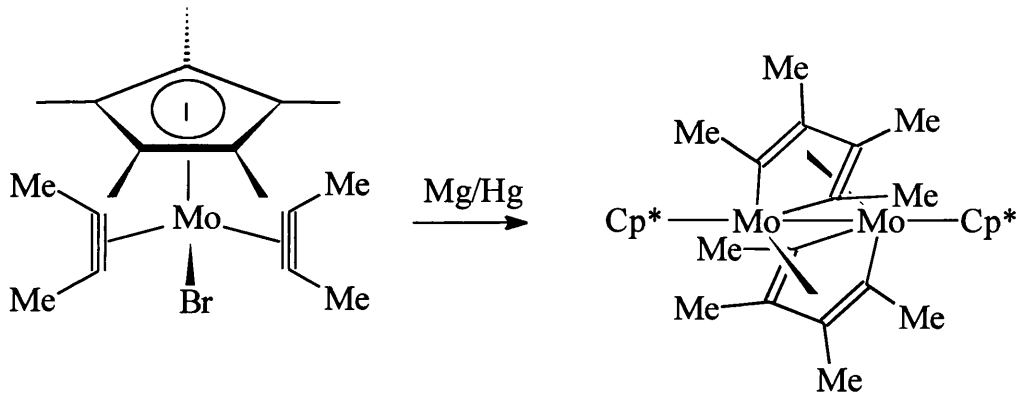

(**50**) (**58**) eq.3.5

3.3 Reaction of [Mo(η^2-RC_2R)$_2$(CO)(η-C_5Me_5)][BF_4] with $P(OMe)_3$, PMe_3 and K[$HBBu^s_3$].

The reactivity of (**48**) and (**49**) towards phosphorus containing ligands was also investigated. Complex (**48**) was stirred at room temperature with $P(OMe)_3$. No reaction occurred. It was only upon refluxing in THF that the required substitution took place as the colour of the solution changed from yellow to purple to give complex (**59**) in good yield (79%), which was identified by ^1H, $^{13}C\{^1H\}$ and $^{31}P\{^1H\}$ NMR spectroscopy (eq.3.6).

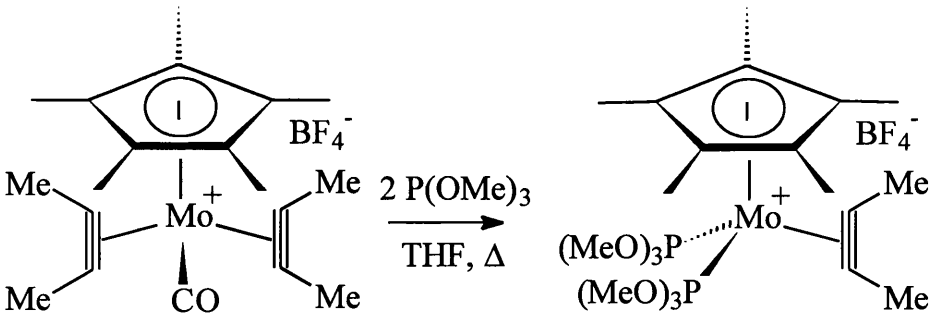

(**48**) (**59**) eq.3.6

Again the less reactive nature of these Cp* complexes is highlighted as more forcing conditions were required to displace the alkyne and carbonyl ligands. A similar reaction with complex (**49**) was attempted using the same conditions, i.e. a short reflux was required to displace the alkyne and carbonyl ligands, but interestingly the colour change was orange to green resulting in the dark green complex (**60**) in good yield (89%), which was identified by ^{1}H, $^{13}C\{^{1}H\}$ and $^{31}P\{^{1}H\}$ NMR spectroscopies (eq.3.7).

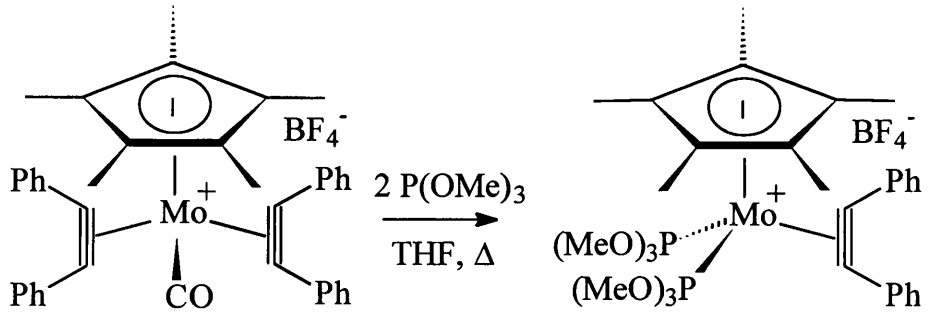

(**49**) (**60**) eq.3.7

In the Cp case complex (**60**) was purple and not green.

Complex (**49**) was also found to react with PMe_3, at room temperature, giving the mono carbonyl complex (**61**) in good yield (89%), which was identified by ^{1}H, $^{13}C\{^{1}H\}$ and $^{31}P\{^{1}H\}$ NMR and IR spectroscopy (eq.3.8).

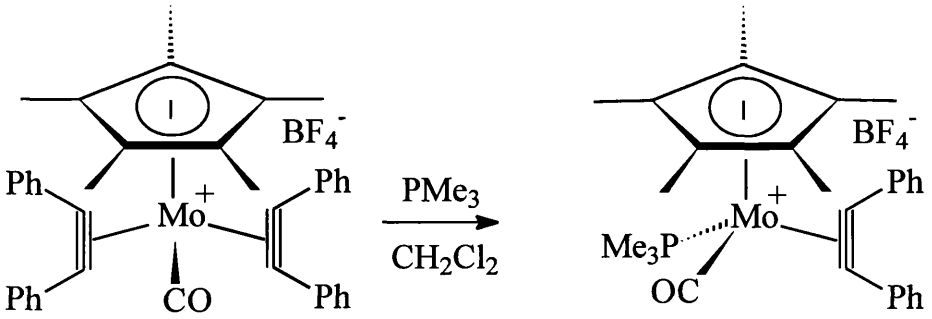

(**49**) (**61**) eq.3.8

Complex (**49**) did not react with PPh_3, even after refluxing in THF.

Investigation of the reactivity of complex (**48**) towards $K[HBBu^s_3]$ was prompted by earlier work on the Cp analogue, which showed a coupling reaction when treated with $K[HBBu^s_3]$ and CO.[87] Complex (**48**) was reacted with $K[HBBu^s_3]$ at low temperature causing a colour change from yellow to orange. An IR spectrum of the reaction mixture showed that the terminal carbonyl band had shifted from $2037cm^{-1}$ to $1898cm^{-1}$. On warming, the solution changed colour to black, and only decomposition products were obtained. The reaction was repeated in CH_2Cl_2, but this time once the $1898cm^{-1}$ band was obtained the complex was further reacted with $HBF_4.OEt_2$. After warming to room temperature a yellow solution was obtained which proved to be the starting material (**48**). There are three possible explanations for this reaction. These are attack on the alkyne ligand to give an η^1-vinyl ligand (see Chapter 1), attack on the CO ligand to give an aldehyde or direct attack on the metal centre to give a metal hydride (Figure 3.2).

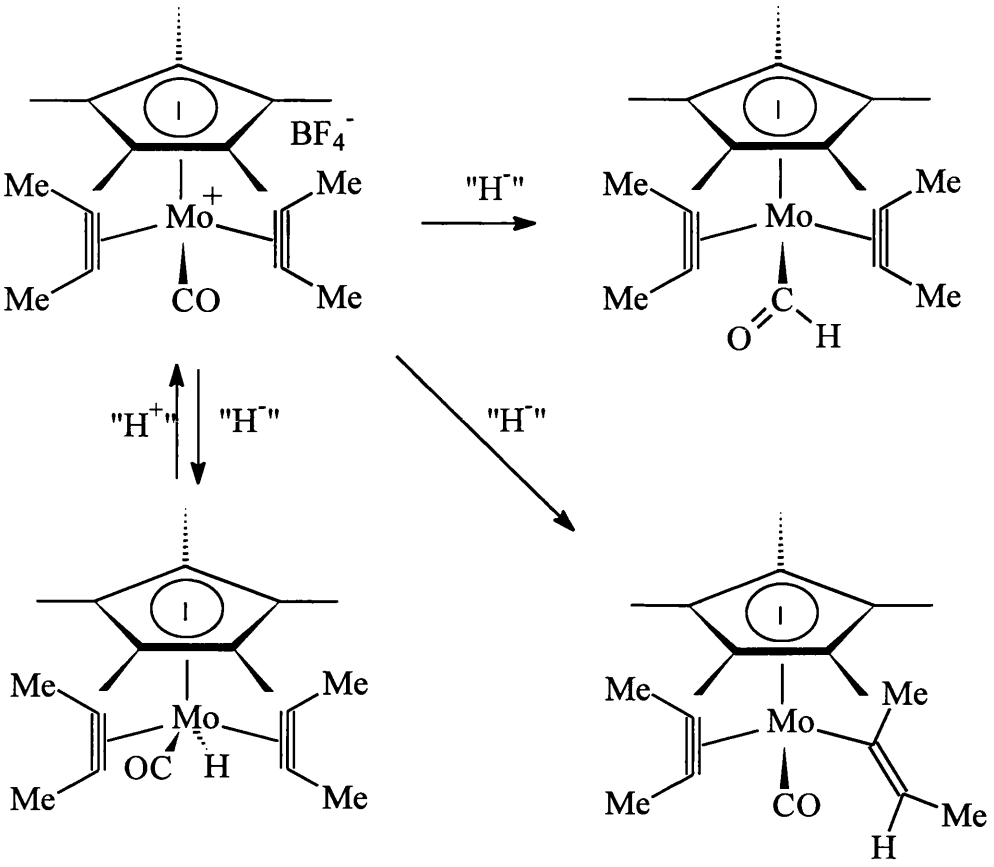

Figure 3.2. Possible products from reaction of (**48**) with K[HBBu$^s_3$].

The aldehyde product is unlikely as the IR band would be at a lower frequency than was observed. The η^1-vinyl could also be ruled out as further reaction with H^+ would more likely produce a carbene complex. It is therefore suggested that some form of unstable hydride complex is formed. Unfortunately, owing to time constraints, this work could not be investigated further, but merits more attention in the future.

3.4 Synthesis of Bis-Alkyne Pentamethylcyclopentadienyl Complexes of Tungsten.

The chemistry of tungsten Cp* alkyne complexes was also investigated. The complex $[W(CO)_3(MeCN)(\eta\text{-}C_5Me_5)][BF_4]$ (**62**) was prepared by literature methods.[22] Reaction of (**62**) with Me_3NO in MeCN, gave complex (**63**) in good yield (75%), which was identified by ^1H, $^{13}C\{^1H\}$ NMR and IR spectroscopy (eq.3.9).

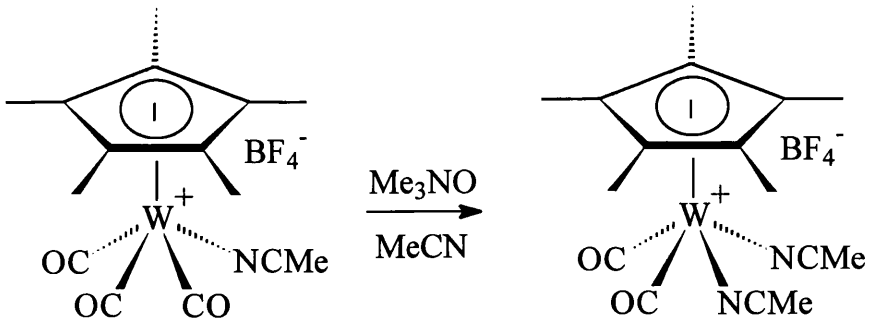

(**62**) (**63**) eq.3.9

Using known methods[80] the bis-acetonitrile complex (**63**) was converted to the allyl complex (**64**), on refluxing with allyltrimethylsilane (eq.3.10).

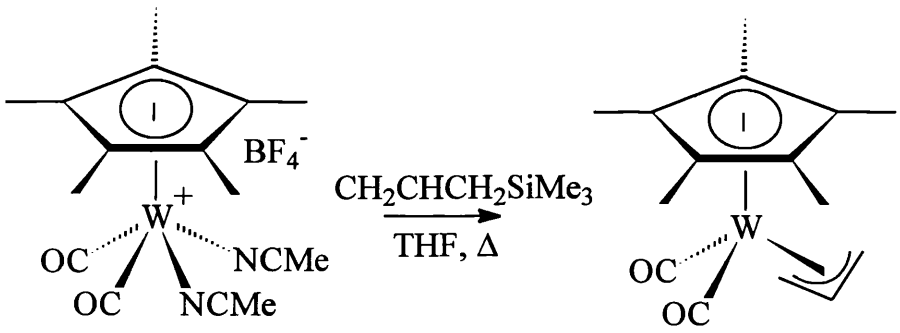

(**63**) (**64**) eq.3.10

Complex (**64**) had been prepared previously by Alt *et al*[88] by a photo-induced coupling reaction of the metal hydride and 1-propyne, and comparison of the IR spectrum confirmed that (**64**) had been synthesised. This synthesis using the silane reagent, afforded complex (**64**) in low yield (16%). Protonation of (**64**) at low temperature (-78°C) with $HBF_4.OEt_2$ and subsequent addition of 2-butyne gave the bis-alkyne complex (**65**) in high yield (87%) and was characterised by ^1H, $^{13}C\{^1H\}$ NMR and IR spectroscopy (eq.3.11).

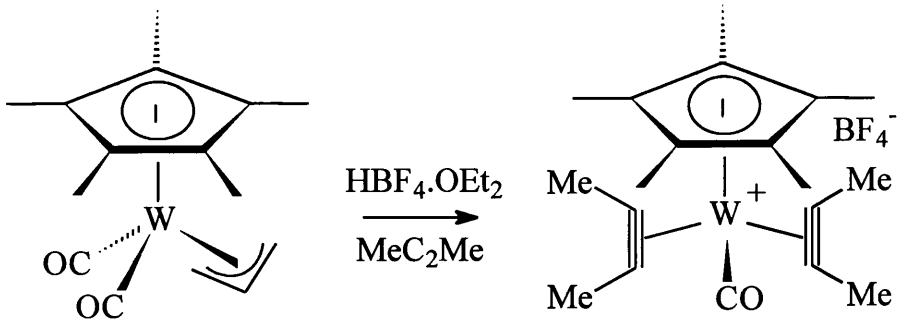

(**64**) (**65**) eq.3.11

This method of synthesis for the bis-alkyne complex was obviously unsatisfactory, because of the low yield of (**64**). After further investigation it was found that a long reflux, in THF, of (**63**) with an excess of alkyne, led to an alternative, higher overall yield synthesis of the bis alkyne complexes (**65**) (83%) and (**66**) (97%). Both these complexes were identified by ^{1}H, $^{13}C\{^{1}H\}$ NMR and IR spectroscopy (eq.3.12).

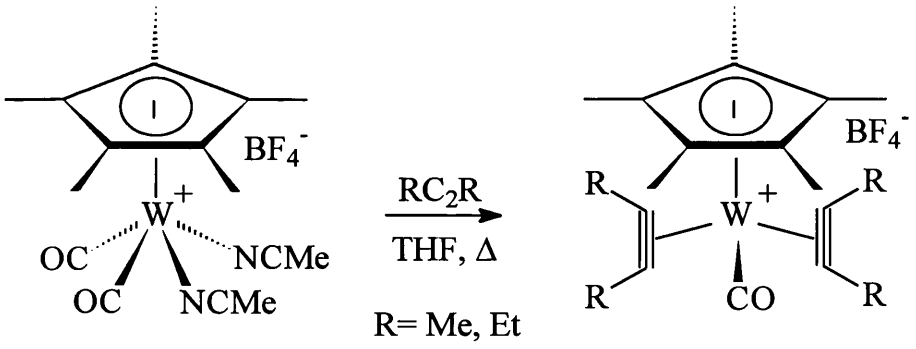

(**63**) (**65** R=Me) (**66** R=Et) eq.3.12

There is a report of a Cp analogue of (**65**) being converted to the MeCN complex *via* thermal decarbonylation.[89] Refluxing (**65**) in MeCN for 40 hrs left (**65**) unchanged. Reaction of (**65**) with Me_3NO in MeCN overnight did, however, give the acetonitrile complex (**67**) in good yield (75%), which was identified by ^{1}H, $^{13}C\{^{1}H\}$ NMR spectroscopy (eq.3.13).

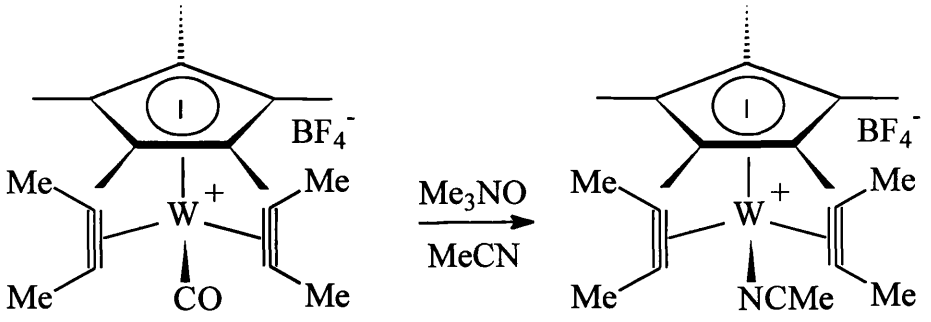

(**65**) (**67**) eq.3.13

All attempts to obtain a neutral halo complex from (**67**), the tungsten analogue of (**52**), failed.

3.5 Synthesis of a Heptamethylindenyl Complex of Molybdenum.

Recently the synthesis of heptamethylindene was reported [90,91] and some transition metal complexes containing it as an η^5 spectator ligand have been structurally identified[92] (Figure 3.3)

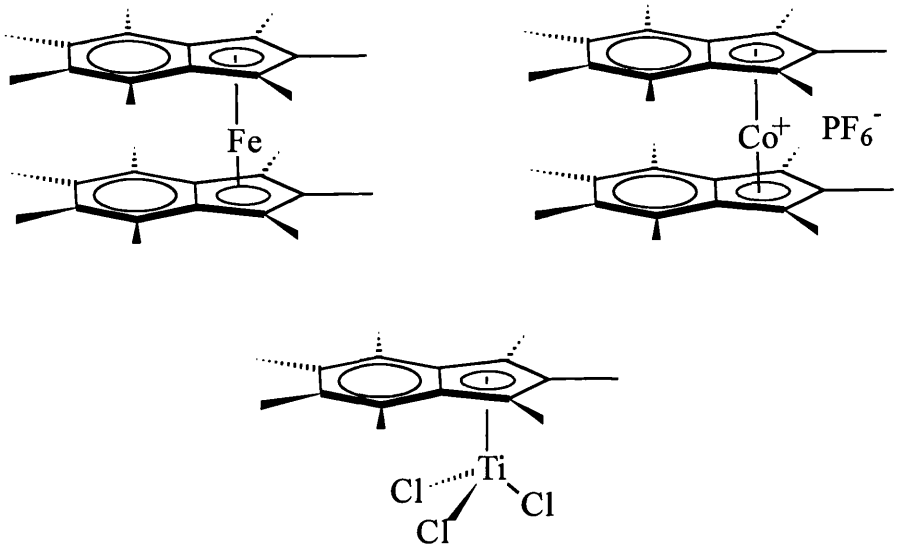

Figure 3.3. Transition metal complexes containing the heptamethylindenyl ligand.

A synthesis of a molybdenum Ind* complex was attempted, using the standard methods for the synthesis of Cp, Cp* and Ind complexes of molybdenum. LiInd* was refluxed with $Mo(CO)_6$ to give the anion $[Mo(CO)_3(\eta^5\text{-}C_9Me_7)][Li]$ (**68**),

which was then reacted with allylchloride to give the allyl complex (**69**) in good yield (75%) (eq.3.14).

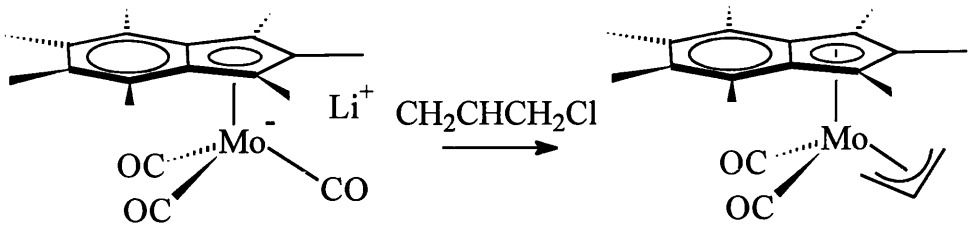

(**68**) (**69**) eq.3.14

A short lived intermediate was observed by IR (2002cm^{-1} and 1923cm^{-1}) which rearranged to give (**69**) (1933cm^{-1} and 1846cm^{-1}). This intermediate was probably a η^1-allyl complex (Figure 3.4).

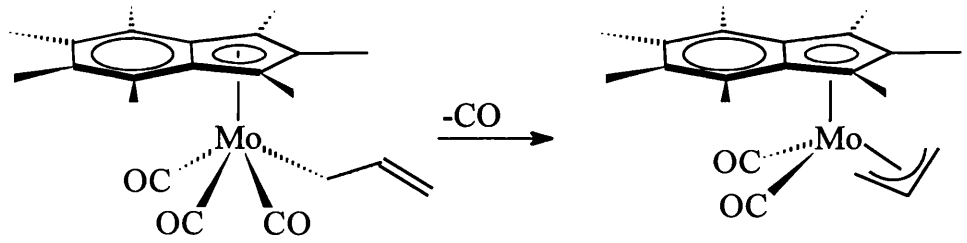

Figure 3.4. Rearrangement of an η^1-allyl to an η^3(3e)-allyl to give (**69**).

A single crystal suitable for X-ray diffraction was obtained and the structure was found to be that in Figure 3.5. Selected bond lengths and angles are shown in Table 3.1.

Table 3.1. Selected bond lengths (Å) and bond angles (°) for [Mo(η^3-C_3H_5)$(CO)_2$($\eta^5C_9Me_7$)] (**69**).

Bond	Bond Length (Å)
Mo-C31	1.947(6)
Mo-C41	1.938(6)
Mo-C21	2.337(6)
Mo-C22	2.209(6)
Mo-C23	2.322(6)
C21-C22	1.359(10)
C22-C23	1.337(11)

Bond Angle	Angle(°)
C31-Mo-C41	78.5(2)
C21-C22-C23	127.9(9)
Mo-C31-O31	177.7(6)
Mo-C41-O41	176.9(6)

With a complex such as (**69**), protonation ($HBF_4.OEt_2$) and subsequent addition of alkyne could open the way to investigate the chemistry of bis-alkyne complexes containing the heptamethylindenyl ligand in the future.

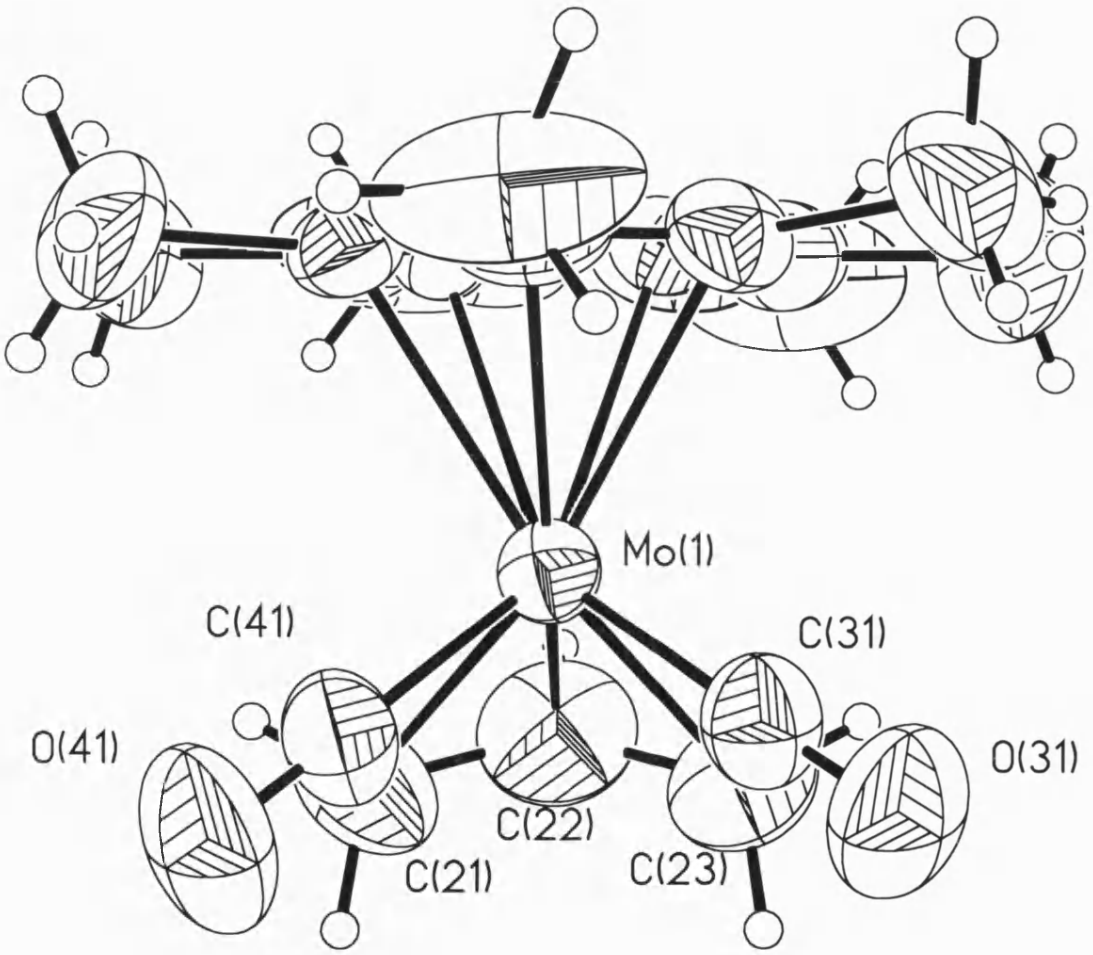

Figure 3.5. ORTEP representation of $[Mo(\eta^3\text{-}C_3H_5)(CO)_2(\eta^5\text{-}C_9Me_7)]$ (**69**).

3.6 Conclusions.

The area of Cp* three- and four-electron donor alkyne complexes of tungsten and molybdenum has proved viable. Future work can now be carried out on these systems to determine their reactivity to a variety of substrates.

The synthesis of Ind* alkyne complexes could now be attempted starting from the allyl complex, and is an area worthy of further investigation.

4. Experimental Section

General Practical Details.

All experiments were performed in an atmosphere of dry, oxygen free nitrogen using standard Schlenk tube techniques. Solvents were freshly distilled under a nitrogen atmosphere from potassium benzophenone ketal (THF), sodium metal (toluene), sodium / potassium benzophenone ketal (diethyl ether, hexane, pentane) and CaH_2 (MeCN, CH_2Cl_2).

Chromatography columns were packed with aluminium oxide Brockmann activity III, obtained from the Aldrich Chemical Co.

Unless otherwise stated all chemicals were reagent grade and used as received. Deuterated solvents for NMR spectroscopy were degassed and dried before use.

Characterisations.

Microanalyses for C, H and N were carried out in the analytical depatment of the School of Chemistry, by Mr A. Carver.

IR spectra were all recorded in NaCl solution cells on a Nicolet 510P FT-IR spectrometer.

Mass Spectra were recorded in *m*-NBA by the Mass Spectrum service at the University of Bath.

NMR spectra were recorded using a Jeol JNM GX 270 (270MHz) or a Jeol EX400 (400MHz). Spectra were recorded at 20°C, unless otherwise stated, and were referenced internally to the deuterated solvent (^{13}C and ^{1}H), or externally to 85% H_3PO_4 (^{31}P), $CFCl_3$ (^{19}F) and $BF_3.OEt_2$ (^{11}B).

Reaction of $[BrMo(\eta^2\text{-}EtC_2Et)_2(\eta\text{–}C_5H_5)]$ with $HBF_4.OEt_2$.

$[BrMo(\eta^2\text{-}EtC_2Et)_2(\eta\text{–}C_5H_5)]$ (470mg, 1.16mmol) was dissolved in CH_2Cl_2 (15mL) and cooled to -78°C. $HBF_4.OEt_2$ (172μL, 1.16mmol) was added dropwise to the solution, causing a colour change from yellow to purple. The solution was allowed to warm to ambient temperature over 2hrs. The volatiles were removed *in vacuo* and the residue was dissolved in CH_2Cl_2 (10mL), and then precipitated with Et_2O (50mL) to give a pink powder $[BrMo{=}C(Et)\text{-}\eta^3\text{-}\{C(Et)C(Et)CHEt\}(OH_2)(\eta\text{–}C_5H_5)][BF_4]$ (**21b**). Crystals suitable for X-ray crystallography were obtained by CH_2Cl_2/pentane layer diffusion at room temperature, and the molecular structure determined. (Yield= 429mg, 75%).

^{1}H NMR (270.1MHz, CD_2Cl_2).

δ 5.98 [s, 5H, C_5H_5], 4.12 [br.s, 2H, H_2O] 3.12-2.26 [5x um, 9H, 4xCH_2 and C*H*Et], 1.47 [t, 3H, CH_3, J_{HH} = 7.7Hz], 1.46 [t, 3H, CH_3, J_{HH} = 7.7Hz], 1.21 [t, 3H, CH_3, J_{HH} = 7.2Hz], 0.93 [t, 3H, CH_3, J_{HH} = 7.5Hz].

^{13}C{^{1}H} NMR (67.8MHz, CD_2Cl_2).

δ 298.4 [Et*C*=Mo], 147.8 [*C*Et], 117.9 [*C*Et], 102.8 [C_5H_5], 79.3 [*C*Et], 37.2 [CH_2], 23.3 [CH_2], 23.0 [CH_2], 21.1 [CH_2], 16.9 [CH_3], 14.4 [CH_3], 13.8 [CH_3], 12.1 [CH_3].

^{11}B{^{1}H} NMR (128.2MHz, CD_2Cl_2).

δ -3.09 [BF_4].

^{19}F NMR (376.1MHz, CD_2Cl_2).

δ -150.77 [br.s. BF_4] (the ^{10}B isotopomer could be seen as a shoulder on the main peak).

FAB Mass Spectrum.

FAB (+) $[M\text{-}(H_2O)]^+$ 406.9.

FAB (-) $[BF_4]^-$ 87.0.

Reaction of $[Mo(CO)_3(\eta-C_5H_5)]_2$ (18) with $Ag[BF_4]$ and $PhCH_2C_2CH_2Ph$.

$[Mo(CO)_3(\eta-C_5H_5)]_2$ (**18**) (3.010g, 6.140mmol) and $Ag[BF_4]$ (2.391g, 12.28mmol) were placed in a Schlenk tube. $PhCH_2C_2CH_2Ph$ (≈6g, ≈30mmol) was dissolved in CH_2Cl_2 (50mL) and transferred to the Schlenk tube *via* a cannula. Effervescence was noted. The reaction was stirred for 60hrs. The volatiles were then removed *in vacuo* and the product precipitated from CH_2Cl_2 (20mL) with Et_2O (150mL) several times to give a yellow powder $[Mo(\eta^2\text{-}PhCH_2C_2CH_2Ph)_2(CO)(\eta-C_5H_5)][BF_4]$ (**24**). (Yield=2.658g, 31%).

^{1}H NMR (270.1MHz, CD_2Cl_2).

δ 7.32-6.71 [m, 20H, *Ph*CH_2C≡], 5.86 [s, 5H, C_5H_5], 4.31 and 3.87 [AB, 4H, PhCH_2C≡, $^2J_{HH}$ = 16.4Hz], 4.18 and 3.87 [AB, 4H, PhCH_2C≡, $^2J_{HH}$ = 16.2Hz].

^{13}C{^{1}H} NMR (67.8MHz, CD_2Cl_2).

δ 219.6 [*C*O], 166.3 [*C*≡C], 150.2 [C≡*C*], 136.5-127.6 [*Ph*CH_2C≡], 101.3 [C_5H_5], 40.9 [Ph*C*H_2C≡], 36.7 [Ph*C*H_2C≡].

IR

ν=CO (CH_2Cl_2). 2049cm^{-1}.

Microanalysis.

$C_{38}H_{33}BF_4MoO$	requires:	C=66.30%	H=4.83%
	found:	C=66.10%	H=4.81%

FAB Mass Spectrum.

FAB (+) $[M]^+$ 602.3, $[M\text{-}CO]^+$ 570.3, $[M\text{-}CO\text{-}PhCH_2C_2CH_2Ph]^+$ 366.3.

FAB (-) $[BF_4]^-$ 87.0.

Reaction of $[Mo(\eta^2\text{-}PhCH_2C_2CH_2Ph)_2(CO)(\eta\text{-}C_5H_5)][BF_4]$ (24) with MeCN.

$[Mo(\eta^2\text{-}PhCH_2C_2CH_2Ph)_2(CO)(\eta\text{-}C_5H_5)][BF_4]$ (**24**) (2.658g, 3.860mmol) was dissolved in MeCN (50mL) and heated at reflux temperature for 12 hrs. The reaction was monitored by IR spectroscopy until completion. The volatiles were then removed *in vacuo* and the product precipitated from CH_2Cl_2 (10 mL) with Et_2O (150mL) several times to give a pale yellow powder $[Mo(\eta^2\text{-}PhCH_2C_2CH_2Ph)_2(NCMe)(\eta\text{-}C_5H_5)][BF_4]$ (**25**). (Yield=2.337g, 86%)

^{1}H NMR (270.1MHz, CD_2Cl_2).

δ 7.29-6.74 [m, 20H, *Ph*CH_2C≡], 5.58 [s, 5H, C_5H_5], 4.42 and 4.14 [AB, 4H, PhCH_2C≡, $^2J_{HH}$ = 16.9Hz], 3.98 and 3.89 [AB, 4H, PhCH_2C≡, $^2J_{HH}$ = 16.2Hz].

^{13}C{^{1}H} NMR (67.8MHz, CD_2Cl_2).

δ 183.2 [*C*≡C], 166.1 [C≡*C*], 139.8 [Me*C*N] 138.1-126.8 [*Ph*CH_2C≡], 101.8 [C_5H_5], 42.5 [Ph*C*H_2C≡], 34.9 [Ph*C*H_2C≡], 4.5 [*Me*CN].

Microanalysis.

$C_{39}H_{36}BF_4MoN$	requires:	C=66.78%	H=5.17%	N=2.00%
	found:	C=66.10%	H=5.15%	N=1.87%

FAB Mass Spectrum.

FAB (+) $[M]^+$ 616.2, $[M\text{-}MeCN]^+$ 573.2, $[M\text{-}MeCN\text{-}PhCH_2C_2CH_2Ph]^+$ 365.0.

FAB (-) $[BF_4]^-$ 87.0.

Reaction of [Mo(η^2-$PhCH_2C_2CH_2Ph$)$_2$(NCMe)(η-C_5H_5)][BF_4] (25) with LiBr.

[Mo(η^2-$PhCH_2C_2CH_2Ph$)$_2$(NCMe)(η-C_5H_5)][BF_4] (**25**) (2.337g, 3.330mmol) and LiBr (435mg, 5.00mmol) were dissolved in THF (80mL) and refluxed for 2hrs. The volatiles were then removed *in vacuo* and the residue chromatographed on alumina (2x10cm-eluting with hexane) giving a yellow band. The volatiles were removed *in vacuo* to give a bright yellow powder [BrMo(η^2-$PhCH_2C_2CH_2Ph$)$_2$(η-C_5H_5)] (**26**). (Yield=878mg, 40%).

^{1}H NMR (399.7MHz, CD_2Cl_2, -70°C).

δ 7.18-6.81 [m, 20H, *Ph*$CH_2C\equiv$], 5.36 [s, 5H, C_5H_5], 4.18 and 3.55 [AB, 4H, $PhCH_2C\equiv$, $^2J_{HH}$ = 16.7Hz], 4.05 and 4.00 [AB, 4H, $PhCH_2C\equiv$, $^2J_{HH}$ = 15.1Hz].

^{13}C{^{1}H} NMR (67.8MHz, CD_2Cl_2).

δ 181.1 [*C*≡C], 170.4 [C≡*C*], 140.2-125.8 [*Ph*$CH_2C\equiv$], 101.7 [C_5H_5], 41.7 [$PhCH_2C\equiv$], 36.2 [$PhCH_2C\equiv$].

Microanalysis.

$C_{37}H_{33}BrMo$	requires:	C=68.00%	H=5.09%
	found:	C=68.10%	H=5.13%

FAB Mass Spectrum.

FAB (+) $[M]^+$ 654.1, $[M-Br]^+$ 575.2, $[M-PhCH_2C_2CH_2Ph]^+$ 448.0.

Reaction of [BrMo=C(Et)-η^3-{C(Et)C(Et)CHEt}(OH_2)(η-C_5H_5)][BF_4] (21b) with MeCN and [Br_2Mo=C(Et)-η^3-{C(Et)C(Et)CHEt}(η-C_5H_5)] (30) with $AgBF_4$ and MeCN.

(A) [BrMo=C(Et)-η^3-{C(Et)C(Et)CHEt}(OH_2)(η-C_5H_5)][BF_4] (**21b**) (141mg, 0.29mmol) was dissolved in MeCN (10mL) and stirred for 1hr. The volatiles were removed *in vacuo* and the residue was dissolved in CH_2Cl_2 (10mL), and then precipitated with Et_2O (50mL) to give a bright orange powder [BrMo=C(Et)-η^3-{C(Et)C(Et)CH(Et)}(NCMe)(η-C_5H_5)][BF_4] (**27**). (Yield= 136mg, 89%). Crystals suitable for X-ray crystallography were obtained by MeCN/Et_2O layer diffusion at room temperature, and the molecular structure determined.

(B) [Br_2Mo=C(Et)-η^3-{C(Et)C(Et)CHEt}(η-C_5H_5)] (**30**) (96mg, 0.20mmol) and $AgBF_4$ (38mg, 0.20mmol) were dissolved in MeCN (10mL) and stirred for 1hr. The volatiles were removed *in vacuo* and the residue was dissolved in CH_2Cl_2 (10mL), and then precipitated with Et_2O (50mL) to give a bright orange powder [BrMo=C(Et)-η^3-{C(Et)C(Et)CH(Et)}(NCMe)(η-C_5H_5)][BF_4] (**27**). (Yield= 43mg, 40%).

^{1}H NMR (270.1MHz, CD_2Cl_2).

δ 6.04 [s, 5H, C_5H_5], 3.18-2.26 [5x um, 9H, 4xCH_2 and C*H*Et], 2.37 [s, 3H, *Me*CN], 1.51 [t, 3H, CH_3, J_{HH} = 7.7Hz], 1.49 [t, 3H, CH_3, J_{HH} = 7.7Hz], 1.27 [t, 3H, CH_3, J_{HH} = 7.5Hz], 1.02 [t, 3H, CH_3, J_{HH} = 7.5Hz].

^{13}C{^{1}H} NMR (67.8MHz, CD_2Cl_2).

δ 297.4 [Et*C*=Mo], 140.2 [*C*Et], 134.1 [Me*C*N], 119.3 [*C*Et], 102.5 [C_5H_5], 79.5 [*C*Et], 37.6 [CH_2], 24.4 [CH_2], 23.4 [CH_2], 20.8 [CH_2], 16.7 [CH_3], 14.3 [CH_3], 14.2 [CH_3], 12.0 [CH_3], 4.1 [*Me*CN].

FAB Mass Spectrum.

FAB (+) $[M\text{-}MeCN]^+$ 407.0.

FAB (-) $[BF_4]^-$ 87.

Reaction of [BrMo=C(Et)-η^3-{C(Et)C(Et)CH(Et)}(NCMe)(η-C_5H_5)][BF_4] (27) with $P(OMe)_3$.

[BrMo=C(Et)-η^3-{C(Et)C(Et)CH(Et)}(NCMe)(η-C_5H_5)][BF_4] (**27**) (57mg, 0.11mmol) was dissolved in CH_2Cl_2 (10ml). To this was added $P(OMe)_3$ (24μl, 0.22mmol) and the solution stirred for 2 hrs. The volume of the solution was then reduced to *ca.* 3ml and the pink product, [BrMo=C(Et)-η^3-{C(Et)C(Et)CH(Et)}{$P(OMe)_3$}(η-C_5H_5)][BF_4] (**28**), precipitated on addition of Et_2O (50ml). (Yield=60mg, 88%).

^{1}H NMR (399.7MHz, CD_2Cl_2).

δ 5.84 [d, 5H, C_5H_5, J_{PH} = 1.6Hz], 3.83 [d, 9H, P(O*Me*)$_3$, J_{PH} = 10.2Hz], 3.43-2.08 [5x um, 9H, 4xCH_2 and C*H*Et] 1.48 [t, 3H, CH_3, J_{HH} = 7.7Hz], 1.43 [t, 3H, CH_3, J_{HH} = 7.7Hz], 1.21 [t, 3H, CH_3, J_{HH} = 7.4Hz], 0.90 [t, 3H, CH_3, J_{HH} = 7.5Hz].

^{13}C{^{1}H} NMR (67.8MHz, CD_2Cl_2).

δ 307.2 [d, Et*C*=Mo, J_{PC} = 23.7Hz], 135.0 [*C*Et], 110.6 [*C*Et], 100.2 [C_5H_5], 78.9 [*C*HEt], 56.6 [d, P(O*Me*)$_3$, J_{PC} = 9.5Hz], 37.4 [CH_2C=Mo], 24.7 [CH_2], 23.5 [CH_2], 23.1 [CH_2], 15.8 [CH_3], 15.6 [CH_3], 14.2 [CH_3], 11.0 [d, CH_3, J_{PC} = 4.8Hz].

^{31}P{^{1}H} NMR (161.7MHz, CD_2Cl_2).

δ 118.22 [*P*(OMe)$_3$].

Microanalysis.

$C_{20}H_{35}BBrF_4MoO_3P$	requires:	C=38.93%	H=5.72%
	found:	C=38.80%	H=5.75%

Reaction of [BrMo=C(Et)-η^3-{C(Et)C(Et)CH(Et)}(NCMe)(η-C_5H_5)][BF_4] (27) with PMe_3.

[BrMo=C(Et)-η^3-{C(Et)C(Et)CH(Et)}(NCMe)(η-C_5H_5)][BF_4] (**27**) (104mg, 0.2 mmol) was dissolved in CH_2Cl_2 (10mL). To this was added PMe_3 (200μL, 0.2 mmol-1.0 mol soln. THF) and the solution stirred for 2 hrs. The volume of the solution was then reduced to *ca.* 5mL and the pink product [BrMo=C(Et)-η^3-{C(Et)C(Et)CH(Et)}(PMe_3)(η-C_5H_5)][BF_4] (**29**) precipitated on addition of Et_2O. (Yield= 98mg, 86%). Crystals suitable for X-ray crystallography were obtained by CH_2Cl_2/Et_2O layer diffusion at room temperature, and the molecular structure determined.

^{1}H NMR (399.1MHz, CD_2Cl_2).

δ 5.82 [d, 5H, C_5H_5, J_{PH} = 1.6Hz], 3.38-2.03 [5x um, 9H, 4xCH_2 and C*H*Et], 1.52 [d, 9H, PMe_3, J_{PH} = 10.2Hz], 1.53 [t, 3H, CH_3, J_{HH} = 7.3Hz], 1.42 [t, 3H, CH_3, J_{HH} = 7.6Hz], 1.22 [t, 3H, CH_3, J_{HH} = 7.5Hz], 0.87 [t, 3H, CH_3, J_{HH} = 7.5Hz].

^{13}C{^{1}H} NMR (67.8MHz, CD_2Cl_2).

δ 299.1 [d, Et*C*=Mo, J_{PC}=17.4Hz], 132.7 [*C*Et], 111.7 [*C*Et], 100.0 [C_5H_5], 77.5 [*C*HEt], 37.5 [CH_2C=Mo], 24.7 [CH_2], 24.1 [CH_2], 24.0 [CH_2], 17.5 [d, PMe_3, J_{PC}=31.7Hz], 16.1 [CH_3], 16.0 [CH_3], 14.5 [CH_3], 11.4.[d, CH_3, J_{PC}=3.2Hz].

^{31}P{^{1}H} NMR (161.7MHz, CD_2Cl_2).

δ -5.25 [*P*Me_3]

Microanalysis.

$C_{20}H_{35}BBrF_4MoP$	requires:	C=42.2%	H=6.20%
	found:	C=41.8%	H=6.31%

FAB Mass Spectrum.

FAB(+) $[M]^+$ 483.1, $[M\text{-}PMe_3]^+$ 407.0.

FAB(-) $[BF_4]^-$ 87.0.

Reaction of [BrMo=C(Et)-η^3-{C(Et)C(Et)CH(Et)}(OH_2)(η-C_5H_5)][BF_4] (21a) with PMe_3.

[BrMo=C(Et)-η^3-{C(Et)C(Et)CH(Et)}(OH_2)(η-C_5H_5)][BF_4] (**21a**) (150mg, 0.26 mmol) was dissolved in CH_2Cl_2 (10mL). To this was added PMe_3 (260μL, 0.26 mmol-1.0 mol soln. THF) and the solution stirred for 2 hrs. The volume of the solution was then reduced to *ca.* 5mL and the pink product [BrMo=C(Et)-η^3-{C(Et)C(Et)CH(Et)}(PMe_3)(η-C_5H_5)][BF_4] (**29**) precipitated on addition of Et_2O. The product was found to consist of two isomers (**29a**-Major) and (**29b**-Minor) (6:1).

^{1}H NMR (270.1MHz, CD_2Cl_2).

δ (Major) 5.80 [d, 5H, C_5H_5, J_{PH} = 1.7Hz], 3.29-2.11 [5x um, 9H, 4xCH_2 and C*H*Et] 1.49 [d, 9H, PMe_3, J_{PH} = 10.3Hz], 1.41 [t, 3H, CH_3, J_{HH} = 7.8Hz], 1.39 [t, 3H, CH_3, J_{HH} = 7.9Hz], 1.20 [t, 3H, CH_3, J_{HH} = 7.5Hz], 0.87 [t, 3H, CH_3, J_{HH} = 7.7Hz].

δ (Minor) most signals were obscured

^{13}C{^{1}H} NMR (67.8MHz, CD_2Cl_2).

δ (Major) 299.1 [d, Et*C*=Mo, J_{PC} = 17.4Hz], 132.7 [*C*Et], 111.7 [*C*Et], 100.0 [C_5H_5], 77.5 [*C*HEt], 37.5 [CH_2C=Mo], 24.7-21.6 [3xCH_2], 17.5 [d, PMe_3, J_{PC} = 31.7Hz], 16.1-13.5 [3xCH_3], 11.4 [d, CH_3, J_{PC} = 3.2Hz].

δ (Major) 297.8 [d, Et*C*=Mo, J_{PC} = 16.3Hz], 135.4 [*C*Et], 117.8 [*C*Et], 100.6 [C_5H_5], 82.1 [*C*HEt], 36.0 [CH_2C=Mo], 24.7-21.6 [3xCH_2], 16.1-13.5 [3xCH_3], 14.9 [d, PMe_3, J_{PC} = 28.5Hz], 12.5 [d, CH_3, J_{PC} = 3.9Hz].

^{31}P{^{1}H} NMR (109.3MHz, CD_2Cl_2).

δ (Major) -5.95 [*P*Me_3].

δ (Minor) -3.40 [*P*Me_3].

Microanalysis.

$C_{20}H_{35}BBrF_4MoP$	requires:	C=42.20%	H=6.20%
	found:	C=41.80%	H=6.31%

Reaction of [BrMo=C(Et)-η^3-{C(Et)C(Et)CHEt}(NCMe)(η–C_5H_5)][BF_4] (27) with LiI.

[BrMo=C(Et)-η^3-{C(Et)C(Et)CHEt}(NCMe)(η–C_5H_5)][BF_4] (**27**) (443mg, 0.83mmol) was dissolved in THF (10mL) and CH_2Cl_2 (10mL). To this solution was added LiI (167mg, 1.24mmol). The solution was then stirred for 3hrs. The volatiles were removed *in vacuo* and the product extracted with CH_2Cl_2 (2x3mL) and filtered through Celite. The volume of solvent was reduced to *ca.* 3mL and product precipitated by addition of hexane (50mL). The product was washed further with hexane (2x10mL) to give a dark purple powder. The product was in fact two compounds: [I_2Mo=C(Et)-η^3-{C(Et)C(Et)CHEt}(η–C_5H_5)] (**31**) and [BrIMo=C(Et)-η^3-{C(Et)C(Et)CHEt}(η–C_5H_5)] (**32**). (Yield= 391mg).

^{1}H NMR (270.1MHz, CD_2Cl_2).

δ (Major[I_2]) 5.79 [s, 5H, C_5H_5], 3.27-2.19 [5x um, 9H, 4xCH_2 and C*H*Et], 1.39 [t, 3H CH_3, J_{HH} = 7.7Hz], 1.38 [t, 3H, CH_3, J_{HH} = 7.7Hz], 1.10 [t, 3H, CH_3, J_{HH} = 7.4Hz], 0.94 [t, 3H, CH_3, J_{HH} = 7.3Hz].

δ (Minor[BrI]) 5.77 [s, 5H, C_5H_5], 3.27-2.19 [5x um, 9H, 4xCH_2 and C*H*Et], 1.12 [t, 3H, CH_3, J_{HH} = 7.3Hz], 0.93 [t, 3H, CH_3, J_{HH} = 7.6Hz].

^{13}C{^{1}H} NMR (67.8MHz, CD_2Cl_2).

δ (Major[I_2]) 295.4 [Et*C*=Mo], 135.2 [*C*Et], 109.8 [*C*Et], 99.5 [C_5H_5], 70.7 [*C*Et], 37.4 [CH_2], 27.9-23.4 [3xCH_2],16.4-10.8 [4xCH_3].

δ (Minor[BrI]) 296.8 [Et*C*=Mo], 133.9 [*C*Et], 112.9 [*C*Et], 100.3 [C_5H_5], 74.0 [*C*Et], 36.7 [CH_2], 27.9-23.4 [3xCH_2],16.4-10.8 [4xCH_3].

FAB Mass Spectrum.

FAB (+) $[M(I_2)]^+$ 579.0, $[M(I_2)\text{-}I]^+$454.8.

Reaction of [IMo=C(Et)-η^3-{C(Et)C(Et)CHEt}(OH_2)(η–C_5H_5)][BF_4] with MeCN.

[IMo=C(Et)-η^3-{C(Et)C(Et)CHEt}(OH_2)(η–C_5H_5)][BF_4] (382mg, 0.68mmol) was dissolved in MeCN (20mL) and stirred for 2hrs. The volatiles were removed *in vacuo* and the product was precipitated from MeCN (2mL) with Et_2O (70mL). Upon drying this gave a dark red/brown powder [IMo=C(Et)-η^3-{C(Et)C(Et)CHEt}(NCMe)(η–C_5H_5)][BF_4] (**35**). (Yield=368mg, 93%).

^{1}H NMR (270MHz, CD_3NO_2).

δ 6.02 [s, 5H, C_5H_5], 3.3-2.0 [5x um, 9H, 4xCH_2 and C*H*Et], 2.47 [s, 3H, *Me*CN], 1.54 [t, 3H, CH_3, J_{HH} = 7.7Hz], 1.47 [t, 3H, CH_3, J_{HH} = 7.7Hz], 1.21 [t, 3H, CH_3, J_{HH} = 7.4Hz], 0.96 [t, 3H, CH_3, J_{HH} = 7.5Hz].

^{13}C{^{1}H} NMR (67.8MHz, CD_3NO_2).

δ 301.3 [Et*C*=Mo], 137.0 [*C*Et], 133.2 [Me*C*N], 118.8 [*C*Et], 101.9 [C_5H_5], 75.8 [*C*Et], 38.2 [CH_2], 24.7 [CH_2], 24.3 [CH_2], 24.1 [CH_2], 16.4 [CH_3], 15.7 [CH_3], 14.4 [CH_3], 11.4 [CH_3], 3.66 [*Me*CN].

Microanalysis.

$C_{19}H_{29}BF_4IMoN$	requires:	C=39.27%	H=5.03%	N=2.41%
	found:	C=39.30%	H=5.07%	N=2.42%

FAB Mass Spectrum.

FAB (+) $[M]^+$ 494.0, $[M\text{-}MeCN]^+$ 454.9.

FAB (-) $[BF_4]^-$ 87.0.

Reaction of [IMo=C(Et)-η^3-{C(Et)C(Et)CHEt}(NCMe)(η-C_5H_5)][BF_4] (35) with LiCl.

[IMo=C(Et)-η^3-{C(Et)C(Et)CHEt}(NCMe)(η-C_5H_5)][BF_4] (**35**) (194mg, 0.33mmol) and LiCl (15mg, 0.35mmol) were suspended in THF (5mL) and CH_2Cl_2 (5mL). The solution was stirred for 2hrs. After this time the volatiles were removed *in vacuo* and the residue extracted with CH_2Cl_2 (2x3mL) and then filtered through Celite. The volume of the filtrate was reduced to *ca.* 2mL and the product was precipitated with hexane (70mL). Upon drying this gave a dark red powder [ClIMo=C(Et)-η^3-{C(Et)C(Et)CHEt}(η-C_5H_5)] (**36**). (Yield=158mg, 97%).

^{1}H NMR (270MHz, CD_2Cl_2).

δ 5.76 [s, 5H, C_5H_5], 3.16-2.22 [5x um, 9H, 4xCH_2 and C*H*Et], 1.39 [t, 3H, CH_3, J_{HH} = 7.7Hz], 1.38 [t, 3H, CH_3, J_{HH} = 7.7Hz], 1.14 [t, 3H, CH_3, J_{HH} = 7.5Hz], 0.92 [t, 3H, CH_3, J_{HH} = 7.5Hz].

^{13}C{^{1}H} NMR (67.8MHz, CD_2Cl_2).

δ 297.8 [Et*C*=Mo], 135.8 [*C*Et], 114.6 [*C*Et], 100.6 [C_5H_5], 76.0 [*C*Et], 36.2 [CH_2], 23.8 [CH_2], 23.6 [CH_2], 23.3 [CH_2],16.4 [CH_3], 16.1 [CH_3], 13.9 [CH_3], 11.8 [CH_3].

FAB Mass Spectrum.

FAB (+) $[M]^+$ 494.0, $[M\text{-}Cl]^+$ 454.9.

Reaction of [ClMo=C(Me)-η^3-{C(Me)C(Me)CH(Me)}(OH_2)(η-C_5H_5)][BF_4] (21a) with LiBr.

[ClMo=C(Et)-η^3-{C(Me)C(Me)CH(Me)}(OH_2)(η-C_5H_5)][BF_4] (**21a**) (240mg, 0.6mmol) and LiBr (80mg, 0.9mmol) were placed in a Schlenk tube then dissolved in THF (5mL) and CH_2Cl_2 (5mL). The solution was stirred for 1hr. The volatiles were removed *in vacuo* and the residue was extracted with CH_2Cl_2 (2x5mL) then filtered through Celite. The solution was concentrated to *ca.* 3mL and a purple product precipitated with pentane (50mL). Spectroscopic measurements showed this to be a mixture of two compounds [Br_2Mo=C(Et)-η^3-{C(Me)C(Me)CH(Me)}(η-C_5H_5)] (**37**) and [BrClMo=C(Et)-η^3-{C(Me)C(Me)CH(Me)}(η-C_5H_5)] (**38**). (Yield= 216mg).

^{1}H NMR (270.1MHz, CD_2Cl_2).

δ [Major(Br_2)] 5.72 [br.s, 5H, C_5H_5], 2.61 [br.s, 3H, CH_3C=Mo], 2.25 [br.s, 6H, 2xCH_3C], 2.03 [br.um, 4H, HCCH_3 and HCCH_3] .

δ [Minor(BrCl)] 5.72 [br.s, 5H, C_5H_5], 2.69 [br.s, 3H, CH_3C=Mo], 2.23 [br.s, 6H, 2xCH_3C], 2.03[br.um, 4H, HCCH_3 and HCCH_3] .

^{13}C{^{1}H} NMR (67.8MHz, CD_2Cl_2).

δ [Major(Br_2)] 292.2 [CH_3C=Mo], 131.9 [*C*Me], 110.7 [*C*Me], 101.4 [C_5H_5], 67.8 [*C*(H)Me], 27.9-11.8 [4xCH_3].

δ [Minor(BrCl)] 293.1 [CH_3C=Mo], 133.0 [*C*Me], 113.0 [*C*Me], 101.7 [C_5H_5], 69.7 [*C*(H)Me], 27.9-11.8 [4xCH_3].

FAB Mass Spectrum.

FAB(+) $[M(Br_2)]^+$ 430.

FAB(+) $[M(BrCl)]^+$ 386, $[M(BrCl)-Br]^+$ 351.

Reaction of $[Cl_2Mo{=}C(Me)\text{-}\eta^3\text{-}\{C(Me)C(Me)CHMe\}(\eta\text{-}C_5H_5)]$ (25) with $Ag[SO_3CF_3]$.

$[Cl_2Mo{=}C(Me)\text{-}\eta^3\text{-}\{C(Me)C(Me)CHMe\}(\eta\text{-}C_5H_5)]$ (**25**) (149mg, 0.44mmol) and $Ag[SO_3CF_3]$ (112mg, 0.44mmol) were dissolved in CH_2Cl_2 (5mL) and THF (5mL). The solution was stirred for 2hrs. The volatiles were removed *in vacuo* and the residue extracted with CH_2Cl_2 (2x3mL) and filtered through Celite. The red product $[ClMo{=}C(Me)\text{-}\eta^3\text{-}\{C(Me)C(Me)CHMe\}(\eta\text{-}C_5H_5)][CF_3SO_3]$ (**39**) was precipitated from CH_2Cl_2 (3mL) with Et_2O (50mL). (Yield=178mg, 89%).

^{1}H NMR (399.7MHz, CD_3NO_2).

δ 6.01 [s, 5H, C_5H_5], 2.90 [s, 3H, CH_3C=Mo], 2.21 [br.s, 4H, CH_3C and CHMe], 2.07 [s, 3H, $CHCH_3$], 2.06 [s, 3H, CH_3C].

$^{13}C\{^1H\}$ NMR (67.8MHz, CD_3NO_2).

δ 135.6 [Me*C*], 123.4 [q, CF_3], 104.6 [C_5H_5], 74.1 [*C*HMe], 28.4 [*Me*C=Mo], 16.5 [*Me*C], 16.3 [*Me*C], 11.5 [*Me*C].

Reaction of $[ClMo{=}C(Me)\text{-}\eta^3\text{-}\{C(Me)C(Me)CHMe\}\{P(OMe)_3\}(\eta\text{-}C_5H_5)][BF_4]$ (26) with $Li[N(SiMe_3)_3]$.

$[ClMo{=}C(Me)\text{-}\eta^3\text{-}\{C(Me)C(Me)CHMe\}\{P(OMe)_3\}(\eta\text{-}C_5H_5)][BF_4]$ (**26**) (215mg, 0.42mmol) was suspended in THF (15mL) and cooled to -78°C. $Li[N(SiMe_3)_3]$ (420μl, 0.42mmol-1.0mol. soln.) was added dropwise, causing a colour change from orange to purple. The solution was allowed to warm upto ambient temperature over 2 hrs. The volatiles were removed *in vacuo* and the product extracted with pentane (3x10mL) and filtered through Celite. The solvent was removed *in vacuo* to leave a purple oil $[ClMo\{\eta^4\text{-}CHMe{=}C(Me).C(Me){=}C{=}CH_2\}\{P(OMe)_3\}(\eta\text{-}C_5H_5)]$ (**41**). Crystals suitable for X-ray crystallography were obtained from a pentane solution cooled to -30°C, and the molecular structure determined. (Yield = 94mg, 52%)

^{1}H NMR (270.1MHz, C_6D_6).

δ.5.39 [dd, 1H, =CH*H*, J_{PH} = 3.3Hz, J_{HH} = 0.9Hz], 4.55 [d, 5H, C_5H_5, J_{PH} = 1.4Hz], 3.69 [dd, 1H, =C*H*H, J_{PH} = 2.0Hz, J_{HH} = 0.9Hz], 3.33 [d, 9H, P(O*Me*)$_3$, J_{PH} = 10.4Hz], 2.39 [dd, 3H, Me(H)C=C*Me*, J_{PH} = 2.0Hz, J_{HH} = 0.9Hz], 2.07 [dqq, 1H, =C*H*Me, $^{3}J_{HH}$ = 6.2Hz, J_{PH} = 2.5Hz, $^{4}J_{HH}$ = 1.0Hz], 1.91 [s, 3H, *Me*C], 1.86 [d, 3H, =CH*Me*, J_{HH} = 6.1Hz].

^{13}C{^{1}H} NMR (67.8MHz, C_6D_6).

δ 196.5 [d, =*C*=CH$_2$, J_{PC} = 10.5Hz], 129.1 [Me*C*], 103.6 [Me*C*], 93.0 [C_5H_5], 91.7 [=*C*H$_2$], 65.2 [*C*HMe], 52.6 [d, P(O*Me*)$_3$, J_{PC} = 6.1Hz], 17.8 [*C*H$_3$], 15.9 [*C*H$_3$], 14.3 [*C*H$_3$].

^{31}P{^{1}H} NMR (109.3MHz, C_6D_6).

δ 169.97 [*P*(OMe)$_3$].

Microanalysis.

$C_{16}H_{26}ClMoO_3P$	requires:	C=44.8%	H=6.11%
	found:	C=44.4%	H=6.20%

FAB Mass Spectrum.

FAB (+) $[M]^+$ 429, $[M\text{-}Cl]^+$ 394, $[M\text{-}P(OMe)_3]^+$ 305.

Reaction of [BrMo=C(Et)-η^3-{C(Et)C(Et)CHEt}{P(OMe)$_3$}(η-C_5H_5)][BF_4] (44) with Li[N(SiMe$_3$)$_3$].

[BrMo=C(Et)-η^3-{C(Et)C(Et)CHEt}{P(OMe)$_3$}(η-C_5H_5)][BF_4] (**44**) (213mg, 0.35mmol) was suspended in THF (15mL) and cooled to -78°C. Li[N(SiMe$_3$)$_3$] (350µl, 0.35mmol-1.0mol. soln.) was added dropwise, causing a colour change from orange to purple. The solution was allowed to warm up to ambient temperature over 2 hrs. The volatiles were removed *in vacuo* and the product extracted with pentane (3x10mL) and filtered through Celite. The solvent was removed *in vacuo* to leave a purple oil [BrMo{η^4-CHEt=C(Et).C(Et)=C=CHMe}{P(OMe)$_3$}(η-C_5H_5)] (**45a**) and (**45b**) (7:3).

^{1}H NMR (270.1MHz, C_6D_6).

δ (Major) 4.55 [d, 5H, C_5H_5, J_{PH} = 1.3Hz], 3.72 [dq, 1H, =C*H*Me, J_{PH} = 2.6Hz, J_{HH} = 6.5Hz], 3.32 [d, 9H, P(O*Me*)$_3$, J_{PH} = 10.6Hz], 2.95 [m, 2H, CH_2] 2.63 [m, 2H, CH_2] 2.43 [m, 2H, CH_2] 2.24 [dt, 1H C*H*CH$_2$, J_{PH} = 3.3Hz, J_{HH} = 7.6Hz], 1.89 [dd, 3H, CH*Me*, J_{PH} = 1.6Hz, J_{HH} = 6.5Hz], 1.51 [t, 3H, CH_3, J_{HH} = 7.5Hz], 1.28 [t, 3H, CH_3, J_{HH} = 7.7Hz], 1.00 [t, 3H, CH_3, J_{HH} = 7.7Hz].
δ (Major) 6.34 [dq, 1H, =C*H*Me, J_{PH} = 4.1Hz, J_{HH} = 6.7Hz], 4.88 [d, 5H, C_5H_5, J_{PH} = 1.5Hz], 3.36 [d, 9H, P(O*Me*)$_3$, J_{PH} = 10.3Hz], 3.16 [m, 2H, CH_2] 2.57 [m, 2H, CH_2] 2.19 [m, 2H, CH_2] 2.04 [dt, 1H C*H*CH$_2$, J_{PH} = 2.9Hz, J_{HH} = 7.6Hz], 1.48 [dd, 3H, CH*Me*, J_{PH} = 2.0Hz, J_{HH} = 6.7Hz], 1.45 [t, 3H, CH_3, J_{HH} = 7.5Hz], 1.26 [t, 3H, CH_3, J_{HH} = 7.7Hz], 1.03 [t, 3H, CH_3, J_{HH} = 7.7Hz].

^{13}C{^{1}H} NMR (67.8MHz, C_6D_6).

δ (Major) 183.6 [d, =*C*=CHMe, J_{PC} = 11.7Hz], 132.5 [Et*C*], 105.8 [Et*C*], 102.3 [=C=*C*HMe], 93.7 [C_5H_5], 72.6 [*C*HEt], 53.3 [d, P(O*Me*)$_3$, J_{PC} = 6.6Hz], 27.4-15.2 [3xCH$_2$ and 3xCH$_3$ and CH*Me*].
δ (Minor) 183.9 [d, =*C*=CHMe, J_{PC} = 11.0Hz], 133.4 [Et*C*], 107.9 [Et*C*], 106.7 [=C=*C*HMe], 90.9 [C_5H_5], 72.7 [*C*HEt], 53.5 [d, P(O*Me*)$_3$, J_{PC} = 6.4Hz], 27.4-15.2 [3xCH$_2$ and 3xCH$_3$ and CH*Me*].

$^{31}P\{^{1}H\}$ NMR (109.3MHz, C_6D_6).

δ (Major) 169.60 [*P*$(OMe)_3$].
δ (Minor) 167.50 [*P*$(OMe)_3$].

Reaction of $[I_2Mo{=}C(Et)\text{-}\eta^3\text{-}\{C(Et)C(Et)CH(Et)\}(\eta\text{-}C_5H_5)]$ (31) with $Li[N(SiMe_3)_3]$ and CO.

$[I_2Mo{=}C(Et)\text{-}\eta^3\text{-}\{C(Et)C(Et)CH(Et)\}(\eta\text{-}C_5H_5)]$ (**31**) (379mg, 0.65 mmol) was dissolved in THF (40mL) and cooled to -78°C. $Li[N(SiMe_3)_3]$ (653μL, 0.65mmol-1.0 mol. soln. THF) was added dropwise causing a colour change from purple to green. CO was then bubbled through the solution as it warmed up to ambient temperature over 3 hrs. The volatiles were removed *in vacuo* to leave a brown oil which was extracted with pentane (3x5mL), and filtered through Celite. Cooling of the pentane solution to -78°C caused an orange precipitate. The supernatant liquid was removed to give an orange powder $[BrMo\{\eta^4\text{-}CHEt{=}C(Et).C(Et){=}C{=}CHMe\}(CO)(\eta{-}C_5H_5)]$ (**46a**) and (**46b**). (Yield=52mg, 16%).

^{1}H NMR (270.1MHz, C_6D_6).

δ (Major) 6.12 [q, 1H, =C(*H*)Me, J_{HH} = 6.7Hz], 4.49 [s, 5H, C_5H_5], 1.63 [d, =C(H)*Me*, J_{HH} = 6.8Hz].
δ (Minor) 5.12 [q, 1H, =C(*H*)Me, J_{HH} = 6.6Hz], 4.55 [s, 5H, C_5H_5], 1.92 [d, =C(H)*Me*, J_{HH} = 6.6Hz].

$^{13}C\{^{1}H\}$ NMR (67.8MHz, C_6D_6).

δ (Major) 229.0 [*C*O], 168.0 [=*C*=C(H)Me], 118.7 [*C*Et], 118.1 [*C*Et], 99.5 [=*C*HMe], 92.8 [C_5H_5], 67.8 [=*C*HEt], 29.2-13.6 [3xCH_2 and 3xCH_3 and =CH*Me*].
δ (Minor) 238.0 [*C*O], 176.0 [=*C*=C(H)Me], 121.9 [*C*Et], 115.3 [*C*Et], 106.6 [=*C*HMe], 93.4 [C_5H_5], 74.2 [=*C*HEt], 29.2-13.6 [3xCH_2 and 3xCH_3 and =CH*Me*].

Reaction of $[Mo(\eta^3\text{-}C_3H_5)(CO)_2(\eta\text{-}C_5Me_5)]$ (50) and $[Mo(CH_3)(CO)_3(\eta\text{-}C_5Me_5)]$ (47) with $HBF_4.OEt_2$ and 2-butyne.

(A) $[Mo(\eta^3\text{-}C_3H_5)(CO)_2(\eta\text{-}C_5Me_5)]$ (**50**) (2.701g, 8.2mmol) was dissolved in CH_2Cl_2 (30mL) and cooled to -78°C. $HBF_4.OEt_2$ (1.55mL, 9.00mmol) was added dropwise. The solution was allowed to warm up slightly, producing a colour change from yellow to purple. 2-butyne (2mL, 25mmol) was added. The solution was then stirred at ambient temperature for 2hrs, and a colour change from purple to yellow was observed. The volatiles were removed *in vacuo* and the yellow product, $[Mo(\eta^2\text{-}MeC_2Me)_2(CO)(\eta\text{-}C_5Me_5)][BF_4]$ (**48**), precipitated from CH_2Cl_2 (10mL) by addition of Et_2O (200mL) and washed further with Et_2O (3x30mL). (Yield=3.604g, 96%)

(B) $[Mo(CH_3)(CO)_3(\eta\text{-}C_5Me_5)]$ (**47**) (3.103g, 9.4mmol) was dissolved in CH_2Cl_2 and cooled to -78°C. $HBF_4.OEt_2$ (1.79mL, 10 mmol) was added dropwise causing a colour change from yellow to deep purple. The solution was allowed to warm up slightly, before recooling to -78°C. 2-butyne (2.5mL, 30mmol) was added and the solution allowed to warm up to room temperature. A colour change from purple to orange was observed as the solution was stirred over 1.5 hrs. The volatiles were removed *in vacuo* and the yellow product $[Mo(\eta^2\text{-}MeC_2Me)_2(CO)(\eta\text{-}C_5Me_5)][BF_4]$ (**48**) precipitated from CH_2Cl_2 (10mL) by addition of Et_2O (200mL) and washed further with Et_2O (3x30mL). (Yield=4.121g, 96%)

^{1}H NMR (270.1MHz, CD_2Cl_2).

δ 2.88 [s, 6H, 2x*Me*C≡], 2.67 [s, 6H, 2x≡C*Me*], 1.94 [s, 15H, C_5Me_5].

$^{13}C\{^1H\}$-NMR (67.8MHz, CD_2Cl_2).

δ 224.4 [*C*O], 169.4 [C≡*C*], 146.4 [*C*≡C], 112.3 [C_5Me_5], 15.5 [*Me*C_2*Me*], 10.4 [C_5Me_5].

IR

ν=CO (CH_2Cl_2) 2037cm^{-1}.

Microanalysis.

$C_{19}H_{27}BF_4MoO$	requires:	C=50.14%	H=5.98%
	found:	C=49.50%	H=6.00%

FAB Mass Spectrum.

FAB (+) $[M]^+$ 369, $[M\text{-}CO]^+$ 339.

FAB (-) $[BF_4]^-$ 87.

Reaction of $[Mo(CH_3)(CO)_3(\eta\text{-}C_5Me_5)][BF_4]$ (47) with $HBF_4.OEt_2$ and PhC_2Ph.

$[Mo(CH_3)(CO)_3(\eta\text{-}C_5Me_5)]$ (567mg, 1.72mmol) (**47**) was dissolved in CH_2Cl_2 (10mL) and cooled to -78°C. $HBF_4.OEt_2$ (327μL, 1.89mmol) was added dropwise causing a colour change from yellow to deep purple. The solution was allowed to warm up slightly, before recooling to -78°C. PhC_2Ph (920mg, 5.16mmol) was added and the solution allowed to warm up to room temperature A colour change from purple to orange was observed as the solution was stirred over 1.5 hrs. The volatiles were removed *in vacuo* and the orange product, $[Mo(\eta^2\text{-}PhC_2Ph)_2(CO)(\eta\text{-}C_5Me_5)][BF_4]$ (**49**), precipitated from CH_2Cl_2 (5mL) by addition of Et_2O (100mL) and washed further with Et_2O (3x20mL). (Yield=1.146g, 95%).

^1H NMR (270 MHz, CD_2Cl_2).

δ 7.62-7.20 [m, 20H, *Ph*C≡], 1.96 [s, 15H, C_5Me_5].

$^{13}C\{^1H\}$ NMR (67.8MHz, CD_2Cl_2).

δ 222.2 [*C*O], 173.3 [Ph*C*≡], 156.6 [Ph*C*≡], 133.9-127.1 [*Ph*C≡], 114.3 [C_5Me_5], 11.3 [C_5Me_5].

IR.

ν=CO (CH_2Cl_2) 2060cm^{-1}.

Microanalysis.

$C_{39}H_{35}BF_4MoO$	requires:	C=66.68%	H=5.02%
	found:	C=66.10%	H=4.95%

FAB Mass Spectrum.

FAB (+) $[M]^+$ 617, $[M\text{-}CO]^+$ 589, $[M\text{-}PhC_2Ph]^+$ 409.

FAB (-) $[BF_4]^-$ 87.

Reaction of $[Mo(\eta^2\text{-}MeC_2Me)_2(CO)(\eta\text{-}C_5Me_5)][BF_4]$ (48) with MeCN.

$[Mo(\eta^2\text{-}MeC_2Me)_2(CO)(\eta\text{-}C_5Me_5)]$ (**48**) (227mg, 0.5mmol) was dissolved in MeCN (20mL) and heated at reflux temperature for 21 hrs The volatiles were removed *in vacuo* and the yellow product, $[Mo(\eta^2\text{-}MeC_2Me)_2(NCMe)(\eta\text{-}C_5Me_5)][BF_4]$ (**51**) precipitated from CH_2Cl_2 (5mL) by addition of Et_2O (100mL) and washed further with Et_2O (3x30mL). (Yield=204mg, 87%)

^{1}H NMR (270.1MHz, CD_2Cl_2).

δ 2.99 [s, 3H, *Me*CN], 2.87 [s, 6H, 2x*Me*C≡], 2.33 [s, 6H, 2x≡C*Me*], 1.76 [s, 15H, C_5Me_5].

^{13}C{^{1}H}-NMR (67.8MHz, CD_2Cl_2).

δ 185.2 [*C*≡C], 162.5 [C≡*C*], 137.9 [Me*C*N], 110.4 [C_5Me_5], 16.8 [*Me*C≡], 12.6 [≡C*Me*], 10.2 [C_5Me_5], 4.6 [*Me*CN].

Microanalysis.

$C_{20}H_{30}BF_4MoN$	requires:	C=51.31%	H=6.46%	N=2.99%
	found:	C=51.00%	H=6.50%	N=2.94%

FAB Mass Spectrum.

FAB (+) $[M]^+$ 382, $[M\text{-}MeCN]^+$ 339, $[M\text{-}MeC_2Me]^+$ 325, $[M\text{-}MeCN\text{-}MeC_2Me]^+$ 285.

FAB (-) $[BF_4]^-$ 87.

Reaction of $[Mo(\eta^2\text{-}MeC_2Me)_2(NCMe)(\eta\text{–}C_5Me_5)][BF_4]$ (51) with LiBr.

$[Mo(\eta^2\text{-}MeC_2Me)_2(NCMe)(\eta\text{–}C_5Me_5)][BF_4]$ (**51**) (107mg, 0.25mmol) and LiBr (35mg, 0.38mmol) were suspended in THF (20mL) and refluxed for 2hrs. The volatiles were removed *in vacuo* and the residue chromatographed on alumina (1x5cm-eluting with hexane) giving a yellow band. The volatiles were removed *in vacuo* to give a bright yellow powder $[BrMo(\eta^2\text{-}MeC_2Me)_2(\eta\text{-}C_5Me_5)]$ (**52**). (Yield= 28mg, 26%).

^{1}H NMR (270.1MHz, CD_2Cl_2).

δ 2.87 [br.s, 6H, $CH_3C\equiv$], 2.39 [br.s, 6H, $CH_3C\equiv$], 1.73 [s, 15H, C_5Me_5].

$^{13}C\{^1H\}$ NMR (67.8MHz, CD_2Cl_2).

δ 183.1 [$C\equiv$], 168.4 [$C\equiv$], 108.4 [C_5Me_5], 16.6 [$CH_3C\equiv$], 14.3 [$CH_3C\equiv$], 10.7 [C_5Me_5].

FAB Mass Spectrum.

FAB (+) $[M]^+$ 421.0, $[M\text{-}(MeC_2Me)]^+$ 365.9, $[M\text{-}2(MeC_2Me)]^+$ 310.9.

Reaction of [BrMo(η^2-MeC_2Me)$_2$(η–C_5Me_5)] (52) with Mg/Hg amalgam.

[BrMo(η^2-MeC_2Me)$_2$(η–C_5Me_5)] (**52**) (261mg, 0.623mmol) was dissolved in THF (25mL). This solution was added to a Mg/Hg amalgum (66mg Mg in 7mL Hg), and stirred for 4hrs. This caused a colour change from orange to green. The THF layer was removed, *via* a cannula, from the amalgum, which was also washed with THF (2x5mL). The THF extracts were combined and the volatiles removed *in vacuo*. The residue was re-dissolved in hexane/ether (1:1) (10mL) and chromatographed on alumina using hexane/ether (9:1) giving a lime green band. The solvent was removed *in vacuo* to give a green product (**58**).

^{1}H NMR (270.1MHz, CD_2Cl_2).

δ 2.78 [s, 6H, 2x*Me*], 1.93[s, 6H, 2x*Me*], 1.65 [s, 15H, C_5*Me*$_5$].

^{13}C{^{1}H} NMR (67.8MHz, CD_2Cl_2).

δ 182.2 [C_α], 108.6 [C_5Me_5], 102.3 [C_β], 17.7 [C*Me*], 12.4 [C*Me*], 11.3 [C_5*Me*$_5$].

Reaction of [Mo(η^2-MeC_2Me)$_2$(CO)(η–C_5Me_5)][BF_4] (48) with P(OMe)$_3$.

[Mo(η^2-MeC_2Me)$_2$(CO)(η–C_5Me_5)][BF_4] (**48**) (504mg, 1.1mmol) was suspended in THF (30mL). To this solution was added P(OMe)$_3$ (261μL, 2.2mmol). The solution was then heated to reflux temperature for 2hrs, during which the colour of the solution changed from yellow to purple. The volatiles were removed *in vacuo* and the product was disolved in CH_2Cl_2 (4mL) and precipitated using pentane/Et_2O (70mL), which was repeated several times. Upon drying this gave a dark purple powder [Mo(η^2-MeC_2Me){P(OMe)$_3$}$_2$(η–C_5Me_5)][BF_4] (**59**). (Yield= 537mg, 79%).

^{1}H NMR (270MHz, CD_3NO_2).

δ 3.60 [vt, 18H, P(OMe)$_3$, *N* = 11.2Hz], 2.88 [s, 6H, 2x*Me*C≡], 1.96 [s, 15H, C_5*Me*$_5$].

$^{13}C\{^1H\}$NMR (67.8MHz, CD_3NO_2).

δ 222.4 [t, *C*≡*C*, J_{PC} = 14.9Hz], 110.0 [C_5Me_5], 53.8 [d, P(O*Me*)$_3$, J_{PC} = 5.5Hz], 19.4 [*Me*C≡], 11.1 [C_5Me_5].

$^{31}P\{^1H\}$NMR (109.3MHz, CD_3NO_2).

δ 180.70 [*P*(OMe)$_3$].

FAB Mass Spectrum.

FAB (+) $[M]^+$ 535.1, $[M\text{-}P(OMe)_3]^+$ 409.0, $[M\text{-}2xP(OMe)_3]^+$ 285.0.

FAB (-) $[BF_4]^-$ 87.1.

Reaction of [Mo(η^2-PhC$_2$Ph)$_2$(CO)(η–C$_5$Me$_5$)][BF$_4$] (49) with P(OMe)$_3$.

[Mo(η^2-PhC$_2$Ph)$_2$(CO)(η–C$_5$Me$_5$)][BF$_4$] (**49**) (1.124g, 1.6mmol) was suspended in THF (30mL). To this solution was added P(OMe)$_3$ (377μL, 3.2mmol). The solution was then heated at reflux temperature for 2hrs, during which the colour of the solution changed from yellow to green. The volatiles were removed *in vacuo* and the product was disolved in CH_2Cl_2 (4mL) and precipitated using pentane/Et_2O (70mL), which was repeated several times. Upon drying this gave a dark green powder [Mo(η^2-PhC$_2$Ph){P(OMe)$_3$}$_2$(η–C$_5$Me$_5$)][BF$_4$] (**60**). (Yield=1.061g, 89%).

^{1}H NMR (270.1MHz, CD_2Cl_2).

δ 7.42-7.11 [m, 10H, *Ph*C≡], 3.61 [vt, 18H, P(O*Me*)$_3$, *N* = 11.0Hz], 1.85 [s, 15H, C_5Me_5].

$^{13}C\{^1H\}$ NMR (67.8MHz, CD_2Cl_2).

δ 226.2 [t, *C*≡*C*, J_{PC} = 14.9Hz], 140.6-126.6 [*Ph*C≡], 109.1 [C_5Me_5], 53.8 [br.s*, P(O*Me*)$_3$], 11.1 [C_5Me_5]. (* = signal obscured by solvent peak.)

$^{31}P\{^{1}H\}$ NMR (109.3MHz, CD_2Cl_2).

δ 173.44 [*P*$(OMe)_3$].

FAB Mass Spectrum.

FAB (+) $[M]^+$ 659.1, $[M\text{-}P(OMe)_3]^+$ 535.1, $[M\text{-}2xP(OMe)_3]^+$ 411.0.

FAB (-) $[BF_4]^-$ 87.1.

Reaction of $[Mo(\eta^2\text{-}PhC_2Ph)_2(CO)(\eta\text{–}C_5Me_5)][BF_4]$ (49)with PMe_3.

$[Mo(\eta^2\text{-}PhC_2Ph)_2(CO)(\eta\text{–}C_5Me_5)][BF_4]$ (**49**) (151mg, 0.22mmol) was dissolved in CH_2Cl_2 (10mL). To this solution was added PMe_3 (430μL, 0.44mmol-1.0M soln. in THF). This caused an instant colour change from yellow to green. After 1hr stirring, the volatiles were removed *in vacuo* and the product was disolved in CH_2Cl_2 (4mL) and precipitated using pentane/Et_2O (70mL), which was repeated several times. Upon drying this gave a light green powder $[Mo(\eta^2\text{-}PhC_2Ph)(CO)(PMe_3)(\eta\text{–}C_5Me_5)][BF_4]$ (**61**). (Yield=1.061g, 89%).

^{1}H NMR (270.1MHz, CD_2Cl_2).

δ 7.55-7.26 [m, 10H, *Ph*C≡], 1.61 [s, 15H, C_5*Me*$_5$], 1.17 [d, 9H, P*Me*$_3$, J_{PH} = 13.2Hz].

$^{13}C\{^{1}H\}$ NMR (67.8MHz, CD_2Cl_2).

δ 239.7 [*C*O], 219.0 [*C*≡*C*], 149.2-127.0 [*Ph*C≡], 108.8 [C_5Me_5], 19.5 [d, P*Me*$_3$, J_{PC} = 32.6Hz], 10.8 [C_5*Me*$_5$].

$^{31}P\{^{1}H\}$ NMR (109.3MHz, CD_2Cl_2).

δ 9.87 [*P*Me_3].

IR.

ν_{CO} (CH_2Cl_2) 1923cm^{-1}.

Reaction of $[W(CO)_3(NCMe)(\eta-C_5Me_5)][BF_4]$ (62) with Me_3NO and MeCN.

$[W(CO)_3(NCMe)(\eta-C_5Me_5)][BF_4]$ (**62**) (8.712g, 16.31mmol) was dissolved in MeCN (30mL). Me_3NO (1.248g, 16.31mmol) was added slowly to the solution and was stirred for 2 hrs. The volatiles were removed *in vacuo* and the product precipitated from CH_2Cl_2 (20 mL) with Et_2O (150mL) several times to give a bright orange powder $[W(CO)_2(NCMe)_2(\eta-C_5Me_5)][BF_4]$ (**63**). (Yield=6.641g, 75%)

^{1}H NMR (270.1MHz, CD_2Cl_2).

δ 2.74 [s, 6H, *Me*CN], 2.03 [s, 15H, C_5Me_5].

$^{13}C\{^1H\}$ NMR (67.8MHz, CD_2Cl_2).

δ 245.9 [*C*O], 142.0 [Me*C*N], 10.5 [C_5Me_5] 5.0 [*Me*CN].

IR.

$\nu_{CO}(CH_2Cl_2)$ 1963cm^{-1} and 1873cm^{-1}.

Microanalysis.

$C_{16}H_{21}BF_4N_2O_2W$	requires:	C=35.13%	H=3.87%	N=5.12%
	found:	C=34.90%	H=3.89%	N=4.87%

FAB Mass Spectrum.

FAB (+) $[M]^+$ 457, $[M\text{-}CO]^+$ 435, $[M\text{-}MeCN]^+$ 416.

FAB (-) $[BF_4]^-$ 87.

Reaction of $[W(CO)_2(NCMe)_2(\eta\text{-}C_5Me_5)][BF_4]$ (63) with $CH_2CHCH_2SiMe_3$.

$[W(CO)_2(NCMe)_2(\eta\text{-}C_5Me_5)][BF_4]$ (**63**) (745mg, 1.36mmol) was suspended in THF (50mL). To this was added $CH_2CHCH_2SiMe_3$ (0.5mL, ›2.04mmol) and the solution was then heated at reflux temperature for 1.5hrs The volatiles were removed *in vacuo* and the yellow product chromatographed twice on alumina (2x10cm) eluting with hexane, to give a yellow product $[W(\eta^3\text{-}C_3H_5)(CO)_2(\eta\text{-}C_5Me_5)]$ (**64**). (Yield=94mg, 16%). The product was characterised by comparison of the IR data of the complex, which had been synthesised previously by another route.

IR.

ν_{CO} (Pentane) 1950cm^{-1}, 1942cm^{-1}, 1880cm^{-1} and 1865cm^{-1}.

Reaction of $[W(\eta^3\text{-}C_3H_5)(CO)_2(\eta\text{-}C_5Me_5)]$ (64) with $HBF_4.OEt_2$ and 2-butyne, and $[W(CO)_2(NCMe)_2(\eta\text{-}C_5Me_5)]$ (63) with 2-butyne.

(A) $[W(\eta^3\text{-}C_3H_5)(CO)_2(\eta\text{-}C_5Me_5)]$ (**64**) (84mg, 0.2mmol) was dissolved in CH_2Cl_2 (30mL) and cooled to -78°C. $HBF_4.OEt_2$ (35µL, 0.2mmol) was added dropwise. The solution was allowed to warm up slightly, producing a colour change from yellow to purple. 2-butyne (47µL, ›0.6mmol) was added. The solution was then stirred at ambient temperature for 2hrs, causing the colour to change back to yellow. The volatiles were removed *in vacuo* and the yellow product, $[W(\eta^2\text{-}MeC_2Me)_2(CO)(\eta\text{-}C_5Me_5)][BF_4]$ (**65**), precipitated from CH_2Cl_2 (1mL) by addition of Et_2O (50mL) and washed further with Et_2O (3x100mL). (Yield=94mg, 87%).
(B) $[W(CO)_2(NCMe)_2(\eta\text{-}C_5Me_5)]$ (**63**) (428mg, 0.78mmol) was suspended in THF (50mL) with 2-butyne (180µL, ›2.34mmol) and refluxed for 10 hrs. The volatiles were removed *in vacuo* and the yellow product, $[W(\eta^2\text{-}MeC_2Me)_2(CO)(\eta\text{-}C_5Me_5)][BF_4]$ (**65**), precipitated from CH_2Cl_2 (10mL) by addition of Et_2O (100mL) and washed further with Et_2O (3x30mL). (Yield=350mg, 83%).

^{1}H NMR (270.1MHz, CD_2Cl_2).

δ 2.88 [s, 6H, 2x*Me*C≡], 2.75 [s, 6H, 2x≡C*Me*], 2.04 [s, 15H, C_5Me_5].

$^{13}C\{^1H\}$NMR (67.8MHz, CD_2Cl_2).

δ 213.1 [*C*O], 167.4 [*C*≡C], 145.1 [C≡*C*], 110.6 [C_5Me_5], 15.3 [4x*Me*C≡], 10.2 [C_5Me_5].

IR.

ν_{CO} (CH_2Cl_2) 2044cm^{-1}.

Microanalysis.

$C_{19}H_{27}BF_4OW$	requires:	C=42.10%	H=5.02%
	found:	C=41.50%	H=5.01%

FAB Mass Spectrum.

FAB (+) $[M]^+$ 455, $[M\text{-}CO]^+$ 425.
FAB (-) $[BF_4]^-$ 87.

Reaction of $[W(CO)_2(NCMe)_2(\eta\text{-}C_5Me_5)][BF_4]$ (63) with 3-hexyne.

$[W(CO)_2(NCMe)_2(\eta\text{-}C_5Me_5)][BF_4]$ (**63**) (745mg, 1.36mmol) was suspended in THF (50mL) with 3-hexyne (0.5mL, ›4.08mmol) and heated at reflux temperature for 10 hrs. The volatiles were removed *in vacuo* and the yellow product, $[W(\eta^2\text{-}EtC_2Et)_2(CO)(\eta\text{-}C_5Me_5)][BF_4]$ (**66**), precipitated from CH_2Cl_2 (10mL) by addition of Et_2O (100mL) and washed further with Et_2O (3x30mL). (Yield=793mg, 97%)

^{1}H NMR (399.7MHz, CD_2Cl_2).

δ 3.48 and 3.33 [ABM, 4H, C^1H_2, $^2J_{HH}$ = 15.8Hz, $^3J_{HH}$ = 7.3Hz], 3.26 and 3.12 [ABM, 4H, C^2H_2, $^2J_{HH}$ = 15.8Hz, $^3J_{HH}$ = 7.3Hz], 2.02 [s, 15H, C_5Me_5], 1.20 [t, 6H, 2xCH_3, J_{HH} = 7.5Hz], 1.06 [t, 6H, 2xCH_3, J_{HH} = 7.5Hz].

$^{13}C\{^1H\}$-NMR (67.8MHz, CD_2Cl_2).

δ 214.1[*C*O], 170.2 [*C*≡C], 149.9 [C≡*C*], 110.8 [C_5Me_5], 26.1 [CH_2], 25.1 [CH_2], 14.4 [CH_3], 13.7 [CH_3], 10.5 [C_5Me_5].

IR.

ν_{CO} (CH_2Cl_2) 2029cm^{-1}.

FAB Mass Spectrum.

FAB (+) $[M]^+$ 511.

FAB (-) $[BF_4]^-$ 87.

Reaction of $[W(\eta^2\text{-}MeC_2Me)_2(CO)(\eta\text{-}C_5Me_5)][BF_4]$ (65) with Me_3NO and MeCN.

$[W(\eta^2\text{-}MeC_2Me)_2(CO)(\eta\text{-}C_5Me_5)][BF_4]$ (**65**) (498mg, 0.92mmol) was dissolved in MeCN (30mL) with Me_3NO (69mg, 0.92mmol) and stirred for 16 hrs. The volatiles were removed *in vacuo* and the yellow product, $[W(\eta^2\text{-}MeC_2Me)_2(NCMe)(\eta\text{-}C_5Me_5)][BF_4]$ (**67**) precipitated from CH_2Cl_2 (5mL) by addition of Et_2O (100mL) and washed further with Et_2O (3x10mL). (Yield=384mg, 75%).

^1H NMR (270.1MHz, CD_2Cl_2).

δ 3.10 [s, 3H, *Me*CN], 2.83 [s, 6H, *Me*C≡], 2.41 [s,6H, *Me*C≡], 1.84 [s, 15H, C_5Me_5].

$^{13}C\{^1H\}$-NMR (67.8MHz, CD_2Cl_2).

δ 185.6 [*C*≡C], 164.5 [C≡*C*], 136.4 [Me*C*N], 109.7 [C_5Me_5], 17.4 [C*Me*], 12.8 [*Me*C], 10.0 [C_5Me_5], 4.5 [*Me*CN].

FAB Mass Spectrum.

FAB (+) $[M]^+$ 468, $[M\text{-}MeCN]^+$ 425.

FAB (-) $[BF_4]^-$ 87.

Preparation of [Mo(η^3-C_3H_5)(CO)$_2$(η^5-C_9Me_7)] (69).

To a solution of C_9Me_7H (0.5g, 2.33mmol) in THF (25mL), Bu^nLi (1.5mL of 1.6M solution, 2.40mmol) was added at 0°C, and allowed to warm up to room temperature over 1hr. To this was added $Mo(CO)_6$ (0.61g, 2.31mmol). This solution was then heated at reflux temperature overnight (16hrs). After cooling, a solution of CH_2=$CHCH_2Cl$ (0.19 mL, 0.182 g, 2.38mmol) in THF (10mL) was added slowly with stirring, during which the colour of the reaction mixture lightened slightly. IR spectroscopy of the solution showed two peaks, at 2002 and 1923 cm^{-1}. After 3 hours the volatiles was removed *in vacuo*, and the resulting yellow-brown product chromatographed on alumina (2x10cm-eluting hexane). A yellow band was collected, the volatiles removed *in vacuo*, and crystallised from pentane at -30°C to give the yellow complex [Mo(η^3-C_3H_5)(CO)$_2$(η^5-C_9Me_7)] (**69**). (Yield, 0.70g, 75%). A single crystal suitable for X-ray structure determination was obtained by cooling a pentane solution of (**69**) at -30°C.

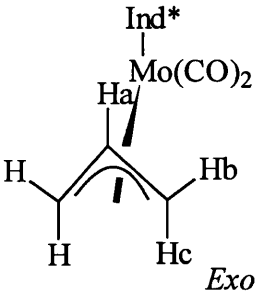

Exo

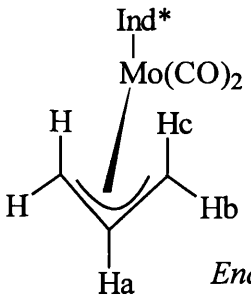

Endo

^{1}H NMR (270.1MHz, CD_2Cl_2).

δ [*exo* isomer] 2.64 [s, 6H, C_9Me_7], 2.36 [s, 6H, C_9Me_7], 2.19 [s, 6H, C_9Me_7], 2.17 [um, 2H, H_b], 2.13 [s, 3H, C_9Me_7], 1.80 [2H, H_c, $^3J_{ac}$.11.1Hz], 0.29 [um, 1H, H_a].

δ [*endo* isomer] 3.34 [um, 2H, H_b], 2.67 [s, 6H, C_9Me_7], 2.60 [um, 1H, H_a], 2.37 [s, 6H, C_9Me_7], 2.32 [s, 6H, C_9Me_7], 2.22 [s, 3H, C_9Me_7], -0.94[um, 2H, H_c].

^{13}C{^{1}H}-NMR (67.8MHz, CD_2Cl_2).

δ [only *exo* isomer observed] 240.7 [*C*O], 132.1-90.5 [C≡*C*], 136.4 [Me*C*N], 109.7 [C_5Me_5], 17.4 [C*Me*], 12.8 [*Me*C], 10.0 [C_5Me_5], 4.5 [*Me*CN].

IR.

ν_{CO} (CH_2Cl_2) 1933cm^{-1} and 1846cm^{-1}.

Microanalysis.

$C_{21}H_{26}MoO_2$	requires:	C=62.1%	H=6.45%
	found:	C=61.7%	H=6.45%

FAB Mass Spectrum.

FAB (+) $[M]^+$ 408, $[M\text{-}CO]^+$ 380, $[M\text{-}C_3H_5]^+$ 365, $[M\text{-}2CO]^+$ 352.

5. References

1 F. R. Hartley, *Angew. Chem. Int. Ed. Engl.*, **1972**, *11*, 596.

2 R.Ugo, G. Lamonica, F. Carloti, S. Cenini and F. Conti, *Inorg. Chim. Acta*, **1970**, *4*, 390.

3 M. H. Chisholm and H. C. Clark, *Acc. Chem. Res.*, **1973**, *6*, 202.

4 G. Wilkinson and F. G. A. Stone, Eds., "Comprehensive Organometallic Chemistry", Pergamon Press, Oxford, **1982**, *5*, 440.

5 D. P. Tate and J. M. Augl, *J. Am. Chem. Soc.*, **1963**, *85*, 2174.

6 D. P. Tate, J. M. Augl, W. M. Richey, B. L. Ros, and J. G. Grasselli, *J. Am. Chem. Soc.*, **1964**, *86*, 3261.

7 R. M. Laine, R. F. Moriarty and R. Bau, *J. Am. Chem. Soc.*, **1972**, *94*, 1402.

8 R. B. King, *Inorg. Chem.*, **1968**, *7*, 1044.

9 J. L. Thomas, *Inorg. Chem.*, **1978**, *17*, 1507.

10 M. J. S. Dewar, *Bull. Soc. Chim.*, **1951**, *18*, C71.

11 J. Chatt and L. A. Duncanson, *J. Chem. Soc. (B).*, **1953**, 2939.

12 J. L. Templeton and B. C. Ward, *J. Am. Chem. Soc.*, **1980**, *102*, 3288.

13 J. L. Templeton, *Adv. Organomet. Chem.*, **1989**, *29*, 1.

14 K. Sünkel, U. Nagel and W. Beck, *J. Organomet. Chem.*, **1981**, *222*, 251.

15 L. Ricard, R. Weiss, W. E. Newton, G. J. J. Chen and J. W. McDonald, *J. Am. Chem. Soc.*, **1978**, *100*, 1318.

16 J. L. Templeton, R. S. Hernick and J. L. Morrow, *Organometallics*, **1984**, *3*, 535.

17 B. C. Ward and J. L. Templeton, *J. Am. Chem. Soc.*, **1980**, *102*, 1532.

18 S. R. Allen, P. K. Baker, S. G. Barnes, M. Green, L. Trollope, L. Manojlovic and K. W. Muir, *J. Chem. Soc. Dalton Trans.*, **1981**, 873.

19 P. B. Winston, S. J. N. Burgmeyer and J. L. Templeton, *Organometallics*, **1983**, *2*, 167.

20 P. B. Winston, S. J. N. Burgmeyer, T. L. Tonker and J. L. Templeton, *Organometallics*, **1986**, *5*, 1707.

21 M. Botrill and M. Green, *J. Chem. Soc. Dalton Trans.*, **1977**, 2365.

22 S.A. Benynes, A. Binelli, M. Green and M. J. Grimshire, *J. Chem. Soc. Dalton Trans.*, **1991**, 895.

23 W. Beck, K. Schloter, K. Sünkel and G. Urban, *Inorg. Synth.*, **1990**, *28*, 5.

24 W. A. Hermann, R. A. Fischer and E. Herdtweck, *Angew. Chem. Int. Ed. Engl.*, **1987**, *26*, 1263.

25 A. N. Nesmeyanov, K. A. Anisimov, N. E. Kolobova and A. A. Pasynski, *Dokl. Chem.(Engl. Trans.).*, **1968**, *182*, 78.

26 M. Cooke, M. Green and T. A. Tuc, *J. Chem. Soc. (A).*, **1971**, 1200.

27 A. Dobson, D. S. Moore and S. D. Robinson, *J. Organomet. Chem.*, **1979**, *177*, C8.

28 T. Yasuda, Y. Kai, N. Yasuoka and N. Kasai, *Bull. Chem. Soc. Jpn.*, **1977**, *50*, 2888.

29 G. Wilkinson and F. G. A. Stone, Eds., "Comprehensive Organometallic Chemistry", Pergamon Press, Oxford, **1982**, *6*, 570.

30 P. K. Maples, M. Green and F. G. A. Stone, *J. Chem. Soc. Dalton Trans.*, **1973**, 2009.

31 D. L. Reger and P. J. McElligott, *J. Am. Chem. Soc.*, **1980**, *102*, 5924.

32 D. L. Reger, K. A. Belmere, E. Mintz and P. J. McElligott, *Organometallics*, **1984**, *3*, 134.

33 M. Bottrill and M. Green, *J. Am. Chem. Soc.*, **1977**, *99*, 5795.

34 S. R. Allen, R. G. Beevor, M. Green, N. C. Norman, A. G. Orpen and I. D. Williams, *J. Chem. Soc. Dalton Trans.*, **1985**, 435.

35 S. R. Allen, M. Green, N. C. Norman, K. E. Paddick and A. G. Orpen, *J. Chem. Soc. Dalton Trans.*, **1983**, 1625.

36 F. R. Kreissel, P. Friedrich and G. Huttner, *Angew. Chem. Int. Ed. Engl.*, **1977**, *16*, 162.

37 K. Erbl, F. R. Kreissel and W. Uedelhoven, *Chem. Ber.*, **1977**, *110*, 3782.

38 K. Erbl, F. R. Kreissel and W. Uedelhoven, *Chem. Ber.*, **1979**, *112*, 3376.

39 E. O. Fischer, A. C. Fillipou, H. G. Alt and K. J. Ackermann, *J. Organomet. Chem.*, **1983**, *254*, C21.

40 S. R. Allen, P. K. Baker, S. G. Barnes, M. Bottrill, M. Green, A. G. Orpen and I. D. Williams, *J. Chem. Soc. Dalton Trans.*, **1983**, 927.

41 M. Green, *J. Organomet. Chem.*, **1986**, *300*, 93.

42 S. R. Allen, R. G. Beevor, M. Green, A. G. Orpen, K. E. Paddick and I. D. Williams, *J. Chem. Soc. Dalton Trans.*, **1987**, 591.

43 W. Clegg, M. Green, C. A. Hall, D. C. R. Hockless, N. C. Norman and C. M. Woolhouse, *J. Chem. Soc. Chem. Commun.*, **1990**, 1330.

44 R. R. Schrock, *Acc. Chem. Res.*, **1979**, *12*, 98.

45 R. R. Schrock, *J. Am. Chem. Soc.*, **1974**, *96*, 6796.

46 R. R. Schrock, *J. Am. Chem. Soc.*, **1976**, *98*, 5399.

47 D. C. Brower, K. R. Birdwhistell and J. L. Templeton, *Organometallics*, **1986**, *5*, 94.

48 B. E. R. Schilling, R. Hoffmann and D. L. Lichtenberger, *J. Am. Chem. Soc.*, **1979**, *101*, 585.

49 N. M. Kostiz and R. F. Fenske, *Organometallics*, **1982**, *1*, 974.

50 T. Blackmore, M. I. Bruce, F. G. A. Stone, R. E. Davis and A. Garza: *J. Chem. Soc., Chem, Commun.*, **1971**, 852.

51 T. Blackmore, M. I. Bruce and F. G. A. Stone: *J. Chem. Soc., Dalton. Trans.*, **1974**, 106.

52 M.Crocker, M. Green, A. G. Orpen, H. P. Neumann and C. J. Schaverien, *J. Chem. Soc., Chem, Commun.*, **1984**, 1351.

53 M. W. Schoonover and R. Eisenburg, *J. Am. Chem. Soc.*, **1977**, *99*, 8371.

54 M. W. Schoonover, C. P. Kubiak and R. Eisenburg, *Inorg. Chem*, **1978**, *17*, 3050.

55 J. R. Morrow, T. L. Tonker and J. L. Templeton, *J. Am. Chem. Soc.*, **1985**, *107*, 5004.

56 L. Carlton, J. L. Davidson, P. Ewing, L. Manojlovic-Muir and K. W. Muir, *J. Chem. Soc., Chem, Commun.*, **1985**, 1474.

57 N. M. Agh-Atabay, J. L. Davidson and K. W. Muir, *J. Chem. Soc., Chem, Commun.*, **1990**, 1399.

58 L. Carlton, N. M. Agh-Atabay and J. L. Davidson, *J. Organomet. Chem.*, **1991**, *413*, 205.

59 N. M. Agh-Atabay and J. L. Davidson, *J. Chem. Soc., Dalton. Trans.*, **1992**, 3531.

60 S. J. Dossett, M. Green, M. F. Mahon and J. M. McInnes, *J. Chem. Soc., Chem, Commun.*, **1995**, 767.

61 R. J. Deeth, S. J. Dossett, M. Green, M. F. Mahon and S. J. Rumble, *J. Chem. Soc., Chem, Commun.*, **1995**, 593.

62 F. Biasotto, M. Etienne and F. Dahan, *Organometallics*, **1995**, *14*, 1870.

63 G. C. Conole, M. Green, M. McPartlin, C. Reeve and C. M. Woolhouse, *J. Chem. Soc., Chem, Commun.*, **1988**, 1310.

64 C. M. Woolhouse, Ph. D. Thesis, University of Bristol, **1989**.

65 A. Fries, Dissertation Universität Würzburg, **1993**.

66 C. B. M. Nation, Ph. D. Thesis, King's College, University of London, **1991**.

67 S. R. Allen, R. G. Beevor, M. Green, N. C. Norman, A. G. Orpen and I. D. Williams, *J. Chem. Soc., Dalton. Trans.*, **1985**, 435.

68 R. V. Honeychuck and W. H. Hersh, *Inorg. Chem.*, **1989**, *28*, 2869.

69 M. Green, H. P. Kirsch, F. G. A. Stone and A. J. Welch, *J. Chem. Soc., Dalton. Trans.*, **1977**, 1755.

70 K. H. Dötz, *Angew. Chem. Int. Ed. Engl.*, **1984**, *23*, 587.

71 P. Hofmann and M Hämmerle, *Angew. Chem. Int. Ed. Engl.*, **1989**, *28*, 908.

72 CAChe system, a comprehensive package of molecular modelling and computational tools developed by CAChe Scientific Inc., Beaverton OR 97006, USA.

73 PLUTON, Molecular graphics program, A. L. Spek, Utrecht Universiteit, The Netherlands, **1994**.

74 W. A. Herrmann, R. A. Fischer and E. Herdtweck, *Organometallics*, **1989**, *8*, 2821.

75 C. A. Tolman, *Chem. Revs.*, **1977**, *77*, 313.

76 A. G. Orpen and N. G. Connelly, *J. Chem. Soc., Chem, Commun.*, **1985**, 1310.

77 Ch. Elschenbroich and A. Salzer, "Organometallics- A Concise Introduction", VCH Publishers (UK) Ltd., Cambridge, **1989**.

78 M. Green, M. F. Mahon, K. C. Molloy, C. B. M. Nation and C. M. Woolhouse, *J. Chem. Soc., Chem, Commun.*, **1991**, 1587.

79 R. B. King and M. B. Bisnette, *J. Organomet. Chem.*, **1967**, *8*, 287.

80 C. Butters, Ph. D. Thesis, University of Bath, **1995**.

81 M. Green, N. C. Norman and A. G. Orpen, *J. Am. Chem. Soc.*, **1981**, *103*, 1269.

82 M. Green, N. C. Norman, A. G. Orpen and C. J. Schaverien, *J. Chem. Soc., Dalton Trans.*, **1984**, 2455.

83 L. Brammer, M. Green, A. G. Orpen, K. E. Paddick and D. R. Saunders, *J. Chem. Soc., Dalton Trans.*, **1986**, 657.

84 M. Green, P. A. Kale and R. J. Mercer, *J. Chem. Soc., Chem. Commun.*, **1987**, 376.

85 N. G. Connelly, T. Escher, A. J. Martin, B. Metz and A. G. Orpen, *J. Organomet. Chem.*, In Press.

86 N. Carr, D. F. Mullica, E. L. Sappenfield and F. G. A. Stone, *Inorg. Chem.*, **1994**, *33*, 1666.

87 S. R. Allen, M. Green, N. C. Norman, K. E. Paddick and A. G. Orpen, *J. Chem. Soc., Dalton Trans.*, **1983**, 1625.

88 H. G. Alt, H. E. Engelhardt, B. Wrackmeyer and R. D. Rogers, *J. Organomet. Chem.*, **1989**, *379*, 289.

89 P. L. Watson and R. G. Bergman, *J. Am. Chem. Soc.*, **1980**, *102*, 2698.

90 T. K. Miyamoto, M. Tsutsui and L. B. Chen, *Chem Lett.*, **1981**, 729.

91 D. O'Hare, J. C. Green, T. Marder, S. Collins, G. Stringer, A. K. Kakkar, N. Kaltsoyannis, A. Kuhn, R. Lewis, C. Mehnert, P. Scott, M. Kurmoo and S. Pugh, *Organometallics*, **1992**, *11*, 48.

92 D. O'Hare, V. Murphy, G. M. Diamond, P. Arnold and P. Mountford, *Organometallics*, **1994**, *13*, 4689.

93 G. M. Sheldrick, SHELX86, a computer program for crystal structure determination, University of Göttingen, **1986**.

94 G. M. Sheldrick, SHELX93, a computer program for crystal structure determination, University of Göttingen, **1993**.

95 N. Walker and D. Stewart, *Acta. Cryst.*, **1983**, *A39*, 158.

96 G. M. Sheldrick, *Acta. Cryst.*, **1990**, *A46*, 467.

97 G. M. Sheldrick, *Acta. Cryst.*, **1995**, in preparation.

98 G. M. Sheldrick, SHELX76, a computer program for crystal structure determination, University of Göttingen, **1976**.

6. Appendices

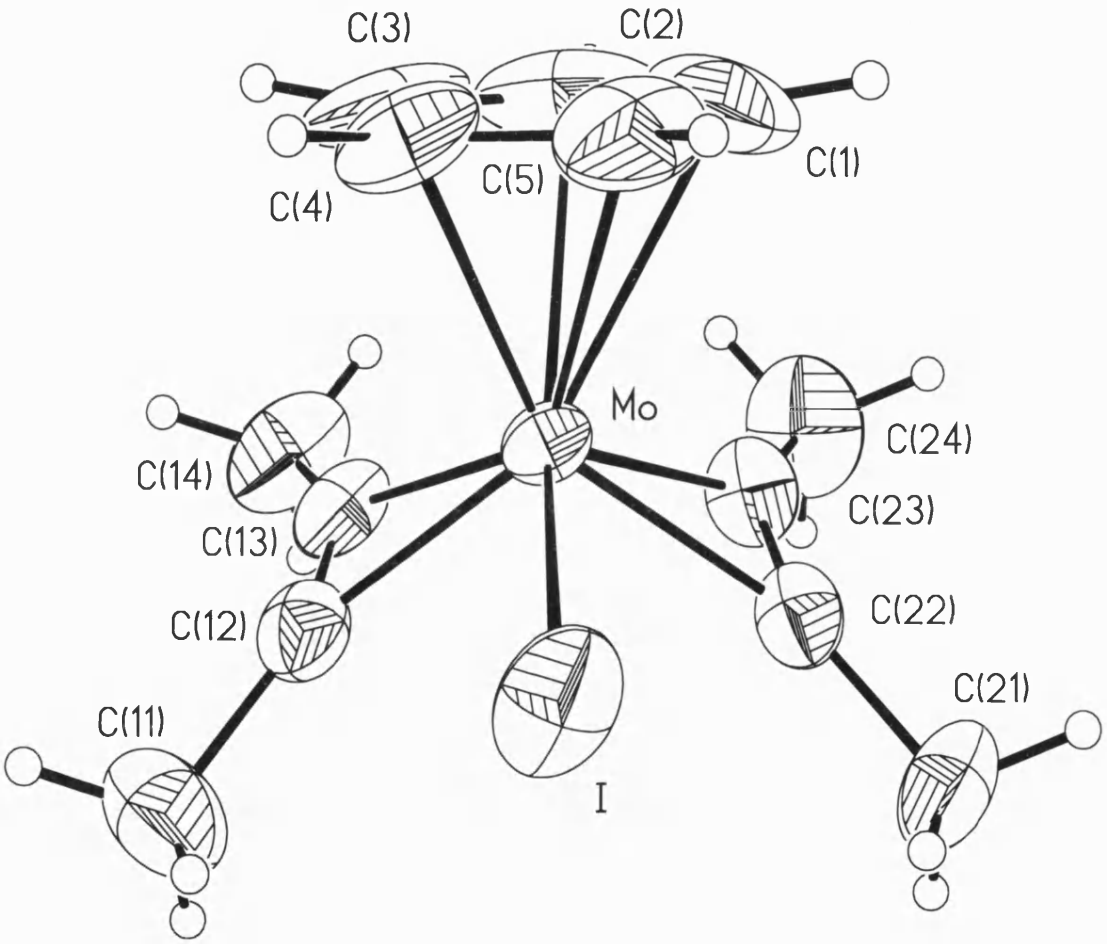

Figure 6.1. ORTEP representation of [IMo(η^2-MeC$_2$Me)$_2$(η-C$_5$H$_5$)] (**15**).

$[IMo(MeC{\equiv}CMe)_2(\eta\text{-}C_5H_5)]$ (15).

Large orange-brown *crystals* of (**15**) were obtained by slow diffusion of hexane into a CH_2Cl_2 solution at room temperature. A crystal of approximate dimensions 0.5 x 0.4 x 0.3 mm was chosen for data collection. Data were measured at 293(2)K on a Siemens P4 automatic four-circle diffractometer operating in the ω-scan mode, with graphite-monochromated Mo K_α X-radiation ($\bar{\lambda}$ = 0.71073Å).

Crystal Data — $C_{13}H_{17}IMo$. M_r = 396.11, monoclinic, $P2_1/n$, a = 8.4912(6), b = 13.6481(15), c = 12.2449(21)Å, β = 103.035(9)°, U = 1382.5(3)Å^2, Z = 4, D_c = 1.903gcm^{-3}, μ = 3.151mm^{-1}, F(000) = 760. Cell parameters from 28 centred reflections in the range $5 \leq \theta \leq 13°$

Data Collection and Processing — One quadrant of diffracted data were measured for $2.27 \leq \theta \leq 25.00°$ ($-1 \leq h \leq 10$, $-1 \leq k \leq 16$, $-14 \leq l \leq 14$). Three standard reflections were redetermined after every 97 reflections measured, and revealed negligible crystal decay or movement. A total of 3243 data were measured, of which 2442 were unique. A semi-empirical absorption correction (psi scans) was applied (T_{min} 0.2734, T_{max} 0.4810).

Structure Solution and Refinement — The structure was solved (Mo, I, all C atoms) without difficulty by direct methods (*SHELXS*-86)[93], and refined (*SHELXL*-93)[94] by full-matrix least-squares on F^2. Although many of the H atoms were readily located from difference Fourier syntheses, all were set riding in calculated positions [C—H 0.98Å (C_5H_5), 0.96Å (CH_3)] with isotropic thermal parameters calculated as 1.2 (C_5H_5) or 1.5 (CH_3) times the corresponding (equivalent) isotropic thermal parameter for the parent C atom. Following isotropic convergence, all non-H atoms were successfully allowed anisotropic thermal motion. The structure converged to a conventional [*i.e.*, based on 1891 data with $F_o > 4\sigma(F_o)$] R_1 = 0.0398 (0.0596 for all data) and wR_2 = 0.0955. Goodness of fit = 1.046. An extinction coefficient was refined to 0.0068(5). The maximum and minimum residual electron densities in the final difference map were 0.70 (near I) and -1.22e/Å^{-3} respectively.

Table 6.1. Atomic coordinates (x 10^4) and equivalent isotropic displacement parameters ($Å^2$ x 10^3) for (**15**). U(eq) is defined as one third of the trace of the orthogonalized Uij tensor.

	x	y	z	U(eq)
Mo	232(1)	7176(1)	3563(1)	32(1)
I	-2367(1)	7932(1)	4396(1)	64(1)
C(1)	2510(13)	8261(8)	3998(11)	97(3)
C(2)	2556(13)	7761(7)	3020(13)	97(4)
C(3)	1268(13)	8056(6)	2201(8)	79(3)
C(4)	329(10)	8705(5)	2669(7)	65(2)
C(5)	1143(13)	8823(6)	3782(7)	76(3)
C(11)	-3323(8)	6147(6)	2162(7)	73(2)
C(12)	-1564(8)	6391(5)	2510(5)	44(2)
C(13)	-216(9)	6161(5)	2302(5)	44(2)
C(14)	602(11)	5529(5)	1603(6)	67(2)
C(21)	293(10)	6199(6)	6135(5)	61(2)
C(22)	754(7)	6424(4)	5065(5)	41(1)
C(23)	1800(7)	6205(5)	4499(5)	43(2)
C(24)	3284(9)	5621(6)	4517(7)	75(2)

Table 6.2. Bond lengths (Å) and angles (°) for (**15**).

Mo-C(23)	2.038(6)
Mo-C(13)	2.046(6)
Mo-C(12)	2.061(6)
Mo-C(22)	2.065(6)
Mo-C(2)	2.359(8)
Mo-C(4)	2.367(6)
Mo-C(5)	2.373(7)
Mo-C(3)	2.379(7)
Mo-C(1)	2.399(8)
Mo-I	2.8266(7)
C(1)-C(5)	1.367(13)
C(1)-C(2)	1.39(2)
C(2)-C(3)	1.367(14)
C(3)-C(4)	1.398(11)
C(4)-C(5)	1.392(11)
C(11)-C(12)	1.496(9)
C(12)-C(13)	1.267(9)
C(13)-C(14)	1.492(9)
C(21)-C(22)	1.482(8)
C(22)-C(23)	1.279(8)
C(23)-C(24)	1.487(9)

C(23)-Mo-C(13)	88.3(3)
C(23)-Mo-C(12)	108.1(3)
C(13)-Mo-C(12)	35.9(3)
C(23)-Mo-C(22)	36.3(2)
C(13)-Mo-C(22)	107.6(2)
C(12)-Mo-C(22)	106.2(2)

C(23)-Mo-C(2)	84.1(3)
C(13)-Mo-C(2)	92.4(4)
C(12)-Mo-C(2)	123.2(4)
C(22)-Mo-C(2)	113.2(4)
C(23)-Mo-C(4)	138.3(3)
C(13)-Mo-C(4)	105.5(3)
C(12)-Mo-C(4)	105.5(3)
C(22)-Mo-C(4)	145.8(3)
C(2)-Mo-C(4)	56.8(3)
C(23)-Mo-C(5)	113.4(3)
C(13)-Mo-C(5)	136.6(3)
C(12)-Mo-C(5)	137.7(3)
C(22)-Mo-C(5)	111.8(3)
C(2)-Mo-C(5)	55.9(3)
C(4)-Mo-C(5)	34.1(3)
C(23)-Mo-C(3)	115.1(3)
C(13)-Mo-C(3)	81.2(3)
C(12)-Mo-C(3)	99.3(3)
C(22)-Mo-C(3)	146.8(3)
C(2)-Mo-C(3)	33.5(3)
C(4)-Mo-C(3)	34.3(3)
C(5)-Mo-C(3)	55.8(3)
C(23)-Mo-C(1)	83.4(3)
C(13)-Mo-C(1)	126.1(4)
C(12)-Mo-C(1)	154.9(3)
C(22)-Mo-C(1)	96.2(3)
C(2)-Mo-C(1)	33.9(4)
C(4)-Mo-C(1)	56.5(3)
C(5)-Mo-C(1)	33.3(3)
C(3)-Mo-C(1)	55.7(4)
C(23)-Mo-I	119.9(2)
C(13)-Mo-I	119.5(2)

C(12)-Mo-I	83.6(2)
C(22)-Mo-I	83.6(2)
C(2)-Mo-I	138.5(3)
C(4)-Mo-I	87.5(2)
C(5)-Mo-I	82.8(2)
C(3)-Mo-I	120.7(2)
C(1)-Mo-I	110.5(4)
C(5)-C(1)-C(2)	107.3(10)
C(5)-C(1)-Mo	72.3(5)
C(2)-C(1)-Mo	71.5(5)
C(3)-C(2)-C(1)	108.4(9)
C(3)-C(2)-Mo	74.0(5)
C(1)-C(2)-Mo	74.6(5)
C(2)-C(3)-C(4)	108.8(8)
C(2)-C(3)-Mo	72.4(5)
C(4)-C(3)-Mo	72.4(4)
C(5)-C(4)-C(3)	105.7(8)
C(5)-C(4)-Mo	73.2(4)
C(3)-C(4)-Mo	73.3(4)
C(1)-C(5)-C(4)	109.7(9)
C(1)-C(5)-Mo	74.4(5)
C(4)-C(5)-Mo	72.7(4)
C(13)-C(12)-C(11)	141.0(7)
C(13)-C(12)-Mo	71.4(4)
C(11)-C(12)-Mo	147.6(5)
C(12)-C(13)-C(14)	144.8(7)
C(12)-C(13)-Mo	72.7(4)
C(14)-C(13)-Mo	142.5(6)
C(23)-C(22)-C(21)	141.7(6)
C(23)-C(22)-Mo	70.7(4)
C(21)-C(22)-Mo	147.6(5)
C(22)-C(23)-C(24)	143.8(7)

C(22)-C(23)-Mo	73.0(4)
C(24)-C(23)-Mo	143.2(5)

Table 6.3. Anisotropic displacement parameters ($Å^2$ x 10^3) for (**15**).

The anisotropic displacement factor exponent takes the form:

$-2\pi^2 [h^2 a^{*2} U11 + ... + 2 h k a^* b^* U12]$

	U11	U22	U33	U23	U13	U12
Mo	34(1)	30(1)	34(1)	2(1)	15(1)	3(1)
I	56(1)	90(1)	53(1)	5(1)	27(1)	31(1)
C(1)	74(7)	75(7)	129(9)	29(7)	-4(6)	-42(6)
C(2)	69(6)	70(7)	172(12)	33(8)	70(8)	-2(5)
C(3)	126(8)	56(5)	82(6)	-1(5)	79(7)	-29(5)
C(4)	89(6)	38(4)	75(5)	28(4)	29(5)	4(4)
C(5)	128(8)	34(4)	74(6)	-11(4)	41(6)	-28(5)
C(11)	59(5)	59(5)	92(6)	2(5)	-2(4)	-10(4)
C(12)	56(4)	35(3)	40(3)	6(3)	7(3)	-1(3)
C(13)	70(4)	33(3)	33(3)	3(3)	19(3)	1(3)
C(14)	114(7)	43(4)	55(4)	-9(3)	41(4)	6(4)
C(21)	91(6)	55(5)	38(3)	7(3)	14(4)	2(4)
C(22)	44(3)	32(3)	41(3)	1(3)	0(3)	4(3)
C(23)	43(3)	37(4)	48(4)	-2(3)	4(3)	12(3)
C(24)	57(5)	79(6)	85(6)	0(5)	8(4)	34(5)

Table 6.4. Hydrogen coordinates (x 10^4) and isotropic displacement parameters ($Å^2$ x 10^3) for(**15**).

	x	y	z	U(eq)
H(1A)	3356(13)	8263(8)	4691(11)	116
H(2A)	3456(13)	7356(7)	2903(13)	116
H(3A)	1088(13)	7888(6)	1404(8)	95
H(4A)	-596(10)	9089(5)	2264(7)	79
H(5A)	850(13)	9296(6)	4305(7)	91
H(11A)	-3915(8)	6539(6)	2583(7)	110
H(11B)	-3479(8)	5466(6)	2303(7)	110
H(11C)	-3706(8)	6280(6)	1377(7)	110
H(14A)	1744(11)	5651(5)	1796(6)	101
H(14B)	186(11)	5676(5)	825(6)	101
H(14C)	402(11)	4852(5)	1739(6)	101
H(21A)	-644(10)	6575(6)	6185(5)	92
H(21B)	1171(10)	6365(6)	6751(5)	92
H(21C)	55(10)	5514(6)	6163(5)	92
H(24A)	3622(9)	5719(6)	3827(7)	112
H(24B)	3060(9)	4939(6)	4599(7)	112
H(24C)	4129(9)	5829(6)	5134(7)	112

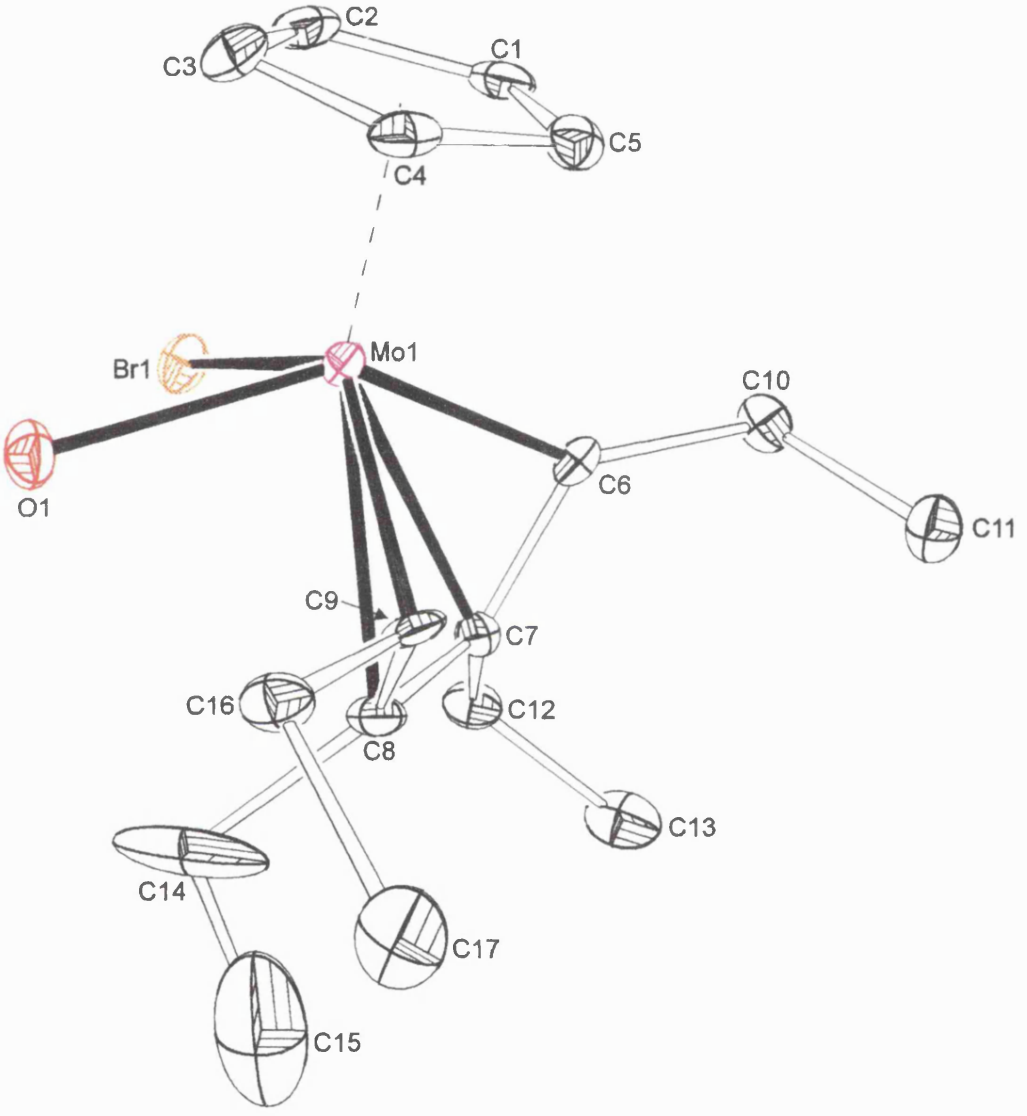

Figure 6.2. ORTEX representation of [BrMo=C(Et)-η^3-{C(Et)C(Et)CHEt}(OH_2)(η-C_5H_5)][BF_4]. Hydrogen atoms omitted for clarity.

[BrMo=C{Et}-η^3-{C(Et)C(Et)CHEt}(OH_2)(η-C_5H_5)][BF_4] (21b).

A crystal of approximate dimensions 0.4 x 0.3 x 0.3 mm was used for data collection

Crystal Data: $C_{17}H_{28}BBrF_4OMo$, M=511.05, Triclinic, a=10.107(2), b=12.701(2), c=15.740(3)Å, α=99.01(2), β=99.21(1), γ=90.01(2)°, U=1969.2(6)Å^3, space group P-1(no.2), Z=4, D_c=1.724gcm^{-3}, μ(Mo-K_α)=2.734 mm^{-1}, F(000)=1024. Crystallographic measurements were made at 170(2) K on a CAD4 automatic four-circle diffractometer in the range 2.04<θ<23.94. Data (6949 reflections) were corrected for Lorentz and polarisation and also for absorption.[95] (Max. and Min absorption corrections; 1.114, 0.802 respectively). The asymmetric unit was seen to consist of 2 molecules of the molybdenum salt.

In the final least squares cycles all atoms were allowed to vibrate anisotropically. The relatively large thermal vibrational parameters associated with C15 seemed to indicate that this carbon was positionally disordered between two sites. However, attempts to refine a model to accommodate such disorder were unsuccessful and therefore abandoned when the refinement became unstable. Hydrogen atoms were included at calculated positions where relevant, exept in the cases of C9 and C9A and the bound water molecules containing O1 and O2.

Analysis of the supramolecular structure revealed that there is considerable interaction between the fluoroborate anions and the ligated water molecules contained in the cations. In particular, O1 in the asymmetric unit, as presented, interacts with fluorines F1 and F7 of the anions generated *via* the operators -1-x, y, z and 1-x, 1-y, 2-z respectively. [O1...F1, 2.68(1)Å; O1...F3, 2.78(1)Å]. Similarly, O2 interacts with F3 in the same asymmetric unit, and with F6 of the anion generated *via* the 2-x, 1-y, 2-z transformation. [O2...F3, 2.78(1)Å; O2...F6, 2.81(1)Å]. Although the water hydrogen atoms could not be located reliably in this molecule, it is reasonable to suggest that the above contacts are in fact, indicative of hydrogen bonding.

The solution of the structure (SHELX86)[96] and refinement (SHELX93)[97] converged to a conventional [i.e. based on 4187 with Fo>4σ(Fo)] R1=0.0698 and wR$_2$=0.1599. Goodness of fit=1.066. The max. and min. residual densities were 4.597 and -2.780Å^{-3} respectively. The asymmetric unit is shown in Figure 6.2, along with the labelling scheme used and was produced using ORTEX.

Table 6.5. Atomic coordinates (x 10^4) and equivalent isotropic displacement parameters ($Å^2$ x 10^3) for (**21b**).U(eq) is defined as one third of the trace of the orthogonalized Uij tensor.

Atom	x	y	z	U(eq)
Mo(1)	1534(1)	2050(1)	4368(1)	20(1)
Br(1)	1877(1)	61(1)	4480(1)	33(1)
B(1)	12359(17)	1164(14)	7912(10)	52(4)
O(1)	1820(7)	2083(6)	5804(4)	33(2)
F(1)	12258(10)	829(6)	7035(5)	70(3)
F(2)	13619(10)	1348(12)	8252(10)	153(6)
F(3)	11629(10)	2039(7)	8071(6)	78(3)
F(4)	11889(12)	311(9)	8246(8)	107(4)
C(1)	-244(10)	1816(9)	3249(7)	33(3)
C(2)	-728(10)	1488(10)	3971(8)	36(3)
C(3)	-675(11)	2371(9)	4617(8)	36(3)
C(4)	-146(10)	3260(8)	4333(7)	28(2)
C(5)	86(10)	2923(8)	3482(7)	27(2)
C(6)	2497(10)	2097(7)	3407(6)	20(2)
C(7)	3706(10)	1994(8)	4027(6)	23(2)
C(8)	3827(10)	2687(8)	4826(7)	26(2)
C(9)	2878(9)	3544(8)	4875(7)	25(2)
C(10)	2425(11)	2176(8)	2482(6)	28(2)
C(11)	3008(12)	3238(9)	2336(7)	36(3)
C(12)	4681(10)	1125(8)	3807(7)	31(3)
C(13)	5716(12)	1481(11)	3308(8)	47(3)
C(14)	4739(14)	2299(19)	5665(12)	114(10)
C(15)	5970(32)	2628(16)	5664(14)	139(12)
C(16)	2821(10)	4304(8)	5709(7)	27(2)
C(17)	3790(14)	5274(9)	5792(8)	47(3)
Mo(2)	8177(1)	1991(1)	9253(1)	35(1)
Br(2)	10493(1)	1959(1)	10213(1)	34(1)
F(5)	10605(9)	5285(8)	12445(5)	78(3)

F(6)	11201(10)	6861(7)	13076(7)	83(3)
F(7)	9340(11)	6211(9)	13330(7)	103(4)
F(8)	11170(12)	5488(7)	13876(6)	93(3)
O(2)	9482(9)	3064(6)	8713(5)	46(2)
B(2)	10680(16)	5961(11)	13230(10)	46(4)
C(1A)	7772(12)	189(10)	9082(10)	55(4)
C(2A)	8812(13)	346(9)	8600(9)	45(3)
C(3A)	8286(16)	890(11)	7931(9)	56(4)
C(4A)	6933(13)	1089(9)	7996(8)	41(3)
C(5A)	6617(14)	656(10)	8706(8)	45(3)
C(6A)	7163(12)	2026(9)	10184(8)	38(3)
C(7A)	7627(11)	3094(9)	10446(7)	36(3)
C(8A)	7452(11)	3744(9)	9789(8)	37(3)
C(9A)	6692(13)	3261(10)	8981(8)	44(3)
C(10A)	6312(14)	1386(10)	10665(9)	50(3)
C(11A)	4896(13)	1816(12)	10606(9)	55(4)
C(12A)	8382(13)	3428(12)	11361(8)	57(4)
C(13A)	7468(15)	3955(14)	11993(9)	71(5)
C(14A)	8102(12)	4843(10)	9920(10)	53(4)
C(15A)	7112(15)	5709(10)	10132(11)	64(4)
C(16A)	6498(13)	3770(11)	8161(8)	45(3)
C(17A)	5197(13)	4260(13)	7987(9)	60(4)

Table 6.6. Bond lengths [Å] and angles [°] for (**21b**).

Mo(1)-C(6)	1.933(9)
Mo(1)-O(1)	2.225(7)
Mo(1)-C(5)	2.269(10)
Mo(1)-C(1)	2.289(10)
Mo(1)-C(4)	2.291(10)
Mo(1)-C(9)	2.294(10)
Mo(1)-C(7)	2.341(10)

Mo(1)-C(2)	2.351(10)
Mo(1)-C(3)	2.353(10)
Mo(1)-C(8)	2.414(10)
Mo(1)-Br(1)	2.5786(14)
B(1)-F(2)	1.31(2)
B(1)-F(3)#1	1.35(2)
B(1)-F(3)	1.35(2)
B(1)-F(1)	1.37(2)
B(1)-F(4)	1.39(2)
C(1)-C(5)	1.42(2)
C(1)-C(2)	1.42(2)
C(2)-C(3)	1.39(2)
C(3)-C(4)	1.41(2)
C(4)-C(5)	1.40(2)
C(6)-C(7)	1.457(14)
C(6)-C(10)	1.465(14)
C(7)-C(8)	1.405(14)
C(7)-C(12)	1.517(14)
C(8)-C(9)	1.452(14)
C(8)-C(14)	1.63(2)
C(9)-C(16)	1.512(14)
C(10)-C(11)	1.536(14)
C(12)-C(13)	1.51(2)
C(14)-C(15)	1.31(3)
C(16)-C(17)	1.55(2)
Mo(2)-C(6A)	1.913(13)
Mo(2)-O(2)	2.245(8)
Mo(2)-C(9A)	2.247(12)
Mo(2)-C(5A)	2.283(13)
Mo(2)-C(1A)	2.292(13)
Mo(2)-C(4A)	2.302(11)
Mo(2)-C(7A)	2.303(11)

Mo(2)-C(2A)	2.318(11)
Mo(2)-C(3A)	2.337(12)
Mo(2)-C(8A)	2.411(11)
Mo(2)-Br(2)	2.579(2)
F(5)-B(2)	1.38(2)
F(6)-B(2)	1.33(2)
F(7)-B(2)	1.42(2)
F(8)-B(2)	1.29(2)
C(1A)-C(5A)	1.40(2)
C(1A)-C(2A)	1.42(2)
C(2A)-C(3A)	1.39(2)
C(3A)-C(4A)	1.41(2)
C(4A)-C(5A)	1.40(2)
C(6A)-C(7A)	1.41(2)
C(6A)-C(10A)	1.54(2)
C(7A)-C(8A)	1.41(2)
C(7A)-C(12A)	1.52(2)
C(8A)-C(9A)	1.42(2)
C(8A)-C(14A)	1.51(2)
C(9A)-C(16A)	1.52(2)
C(10A)-C(11A)	1.53(2)
C(12A)-C(13A)	1.54(2)
C(14A)-C(15A)	1.52(2)
C(16A)-C(17A)	1.46(2)

C(6)-Mo(1)-O(1)	142.8(4)
C(6)-Mo(1)-C(5)	78.3(4)
O(1)-Mo(1)-C(5)	131.0(3)
C(6)-Mo(1)-C(1)	81.1(4)
O(1)-Mo(1)-C(1)	136.0(3)
C(5)-Mo(1)-C(1)	36.4(4)
C(6)-Mo(1)-C(4)	110.0(4)

O(1)-Mo(1)-C(4)	95.4(3)
C(5)-Mo(1)-C(4)	35.7(4)
C(1)-Mo(1)-C(4)	60.0(4)
C(6)-Mo(1)-C(9)	78.6(4)
O(1)-Mo(1)-C(9)	77.9(3)
C(5)-Mo(1)-C(9)	92.5(4)
C(1)-Mo(1)-C(9)	128.0(4)
C(4)-Mo(1)-C(9)	83.2(4)
C(6)-Mo(1)-C(7)	38.4(4)
O(1)-Mo(1)-C(7)	104.7(3)
C(5)-Mo(1)-C(7)	113.3(4)
C(1)-Mo(1)-C(7)	118.5(4)
C(4)-Mo(1)-C(7)	135.2(4)
C(9)-Mo(1)-C(7)	63.2(3)
C(6)-Mo(1)-C(2)	115.3(4)
O(1)-Mo(1)-C(2)	100.9(3)
C(5)-Mo(1)-C(2)	59.3(4)
C(1)-Mo(1)-C(2)	35.7(4)
C(4)-Mo(1)-C(2)	59.0(4)
C(9)-Mo(1)-C(2)	142.1(4)
C(7)-Mo(1)-C(2)	148.2(4)
C(6)-Mo(1)-C(3)	135.6(4)
O(1)-Mo(1)-C(3)	80.1(3)
C(5)-Mo(1)-C(3)	58.5(4)
C(1)-Mo(1)-C(3)	58.5(4)
C(4)-Mo(1)-C(3)	35.4(4)
C(9)-Mo(1)-C(3)	110.8(4)
C(7)-Mo(1)-C(3)	170.5(4)
C(2)-Mo(1)-C(3)	34.3(4)
C(6)-Mo(1)-C(8)	66.7(4)
O(1)-Mo(1)-C(8)	77.4(3)
C(5)-Mo(1)-C(8)	120.3(4)

C(1)-Mo(1)-C(8)	145.5(4)
C(4)-Mo(1)-C(8)	119.0(4)
C(9)-Mo(1)-C(8)	35.8(3)
C(7)-Mo(1)-C(8)	34.3(3)
C(2)-Mo(1)-C(8)	177.4(4)
C(3)-Mo(1)-C(8)	143.2(4)
C(6)-Mo(1)-Br(1)	97.2(3)
O(1)-Mo(1)-Br(1)	78.5(2)
C(5)-Mo(1)-Br(1)	133.4(3)
C(1)-Mo(1)-Br(1)	97.0(3)
C(4)-Mo(1)-Br(1)	139.6(3)
C(9)-Mo(1)-Br(1)	132.6(3)
C(7)-Mo(1)-Br(1)	84.3(2)
C(2)-Mo(1)-Br(1)	82.7(3)
C(3)-Mo(1)-Br(1)	104.8(3)
C(8)-Mo(1)-Br(1)	98.8(3)
F(2)-B(1)-F(3)#1	111(2)
F(2)-B(1)-F(3)	111(2)
F(3)#1-B(1)-F(3)	0.0(14)
F(2)-B(1)-F(1)	109.3(14)
F(3)#1-B(1)-F(1)	110.5(12)
F(3)-B(1)-F(1)	110.5(12)
F(2)-B(1)-F(4)	108(2)
F(3)-B(1)-F(4)	111.6(13)
F(1)-B(1)-F(4)	105.6(13)
C(5)-C(1)-C(2)	106.9(10)
C(5)-C(1)-Mo(1)	71.0(6)
C(2)-C(1)-Mo(1)	74.5(6)
C(3)-C(2)-C(1)	107.6(10)
C(3)-C(2)-Mo(1)	72.9(6)
C(1)-C(2)-Mo(1)	69.8(6)
C(2)-C(3)-C(4)	109.6(10)

C(2)-C(3)-Mo(1)	72.8(6)
C(4)-C(3)-Mo(1)	69.9(6)
C(5)-C(4)-C(3)	107.1(9)
C(5)-C(4)-Mo(1)	71.3(6)
C(3)-C(4)-Mo(1)	74.7(6)
C(4)-C(5)-C(1)	108.7(10)
C(4)-C(5)-Mo(1)	73.0(6)
C(1)-C(5)-Mo(1)	72.6(6)
C(7)-C(6)-C(10)	126.5(9)
C(7)-C(6)-Mo(1)	86.1(6)
C(10)-C(6)-Mo(1)	147.3(8)
C(8)-C(7)-C(6)	115.7(9)
C(8)-C(7)-C(12)	124.7(9)
C(6)-C(7)-C(12)	119.5(8)
C(8)-C(7)-Mo(1)	75.7(6)
C(6)-C(7)-Mo(1)	55.5(5)
C(12)-C(7)-Mo(1)	135.6(7)
C(7)-C(8)-C(9)	116.3(9)
C(7)-C(8)-C(14)	117.1(10)
C(9)-C(8)-C(14)	124.7(9)
C(7)-C(8)-Mo(1)	70.0(6)
C(9)-C(8)-Mo(1)	67.6(5)
C(14)-C(8)-Mo(1)	120.3(10)
C(8)-C(9)-C(16)	122.3(9)
C(8)-C(9)-Mo(1)	76.6(6)
C(16)-C(9)-Mo(1)	125.5(7)
C(6)-C(10)-C(11)	112.9(8)
C(13)-C(12)-C(7)	112.4(9)
C(15)-C(14)-C(8)	106(2)
C(9)-C(16)-C(17)	110.6(9)
C(6A)-Mo(2)-O(2)	140.1(4)
C(6A)-Mo(2)-C(9A)	78.0(5)

O(2)-Mo(2)-C(9A)	81.2(4)
C(6A)-Mo(2)-C(5A)	78.0(5)
O(2)-Mo(2)-C(5A)	136.8(4)
C(9A)-Mo(2)-C(5A)	92.4(5)
C(6A)-Mo(2)-C(1A)	83.4(5)
O(2)-Mo(2)-C(1A)	135.6(4)
C(9A)-Mo(2)-C(1A)	127.6(5)
C(5A)-Mo(2)-C(1A)	35.6(5)
C(6A)-Mo(2)-C(4A)	108.7(5)
O(2)-Mo(2)-C(4A)	101.4(4)
C(9A)-Mo(2)-C(4A)	81.7(5)
C(5A)-Mo(2)-C(4A)	35.6(4)
C(1A)-Mo(2)-C(4A)	58.9(5)
C(6A)-Mo(2)-C(7A)	37.7(5)
O(2)-Mo(2)-C(7A)	102.4(4)
C(9A)-Mo(2)-C(7A)	63.3(4)
C(5A)-Mo(2)-C(7A)	112.7(4)
C(1A)-Mo(2)-C(7A)	120.2(5)
C(4A)-Mo(2)-C(7A)	133.5(4)
C(6A)-Mo(2)-C(2A)	118.1(5)
O(2)-Mo(2)-C(2A)	99.7(4)
C(9A)-Mo(2)-C(2A)	139.8(5)
C(5A)-Mo(2)-C(2A)	59.4(5)
C(1A)-Mo(2)-C(2A)	35.9(5)
C(4A)-Mo(2)-C(2A)	58.5(4)
C(7A)-Mo(2)-C(2A)	150.7(5)
C(6A)-Mo(2)-C(3A)	136.7(5)
O(2)-Mo(2)-C(3A)	82.1(4)
C(9A)-Mo(2)-C(3A)	107.6(5)
C(5A)-Mo(2)-C(3A)	59.1(5)
C(1A)-Mo(2)-C(3A)	58.7(5)
C(4A)-Mo(2)-C(3A)	35.3(5)

C(7A)-Mo(2)-C(3A)	168.7(5)
C(2A)-Mo(2)-C(3A)	34.6(5)
C(6A)-Mo(2)-C(8A)	66.0(5)
O(2)-Mo(2)-C(8A)	77.3(4)
C(9A)-Mo(2)-C(8A)	35.4(4)
C(5A)-Mo(2)-C(8A)	119.5(4)
C(1A)-Mo(2)-C(8A)	146.4(4)
C(4A)-Mo(2)-C(8A)	117.0(4)
C(7A)-Mo(2)-C(8A)	34.7(4)
C(2A)-Mo(2)-C(8A)	174.4(5)
C(3A)-Mo(2)-C(8A)	139.7(5)
C(6A)-Mo(2)-Br(2)	95.7(3)
O(2)-Mo(2)-Br(2)	75.8(2)
C(9A)-Mo(2)-Br(2)	134.9(3)
C(5A)-Mo(2)-Br(2)	130.5(3)
C(1A)-Mo(2)-Br(2)	95.1(4)
C(4A)-Mo(2)-Br(2)	140.5(3)
C(7A)-Mo(2)-Br(2)	84.3(3)
C(2A)-Mo(2)-Br(2)	82.7(3)
C(3A)-Mo(2)-Br(2)	106.9(4)
C(8A)-Mo(2)-Br(2)	101.1(3)
F(8)-B(2)-F(6)	123(2)
F(8)-B(2)-F(5)	111.3(11)
F(6)-B(2)-F(5)	103.6(11)
F(8)-B(2)-F(7)	106.8(11)
F(6)-B(2)-F(7)	104.4(11)
F(5)-B(2)-F(7)	106.3(13)
C(5A)-C(1A)-C(2A)	108.0(14)
C(5A)-C(1A)-Mo(2)	71.9(8)
C(2A)-C(1A)-Mo(2)	73.1(7)
C(3A)-C(2A)-C(1A)	107.9(13)
C(3A)-C(2A)-Mo(2)	73.4(7)

C(1A)-C(2A)-Mo(2)	71.0(7)
C(2A)-C(3A)-C(4A)	108.0(13)
C(2A)-C(3A)-Mo(2)	71.9(7)
C(4A)-C(3A)-Mo(2)	71.0(7)
C(5A)-C(4A)-C(3A)	108.5(12)
C(5A)-C(4A)-Mo(2)	71.4(7)
C(3A)-C(4A)-Mo(2)	73.7(7)
C(1A)-C(5A)-C(4A)	107.6(12)
C(1A)-C(5A)-Mo(2)	72.6(7)
C(4A)-C(5A)-Mo(2)	73.0(7)
C(7A)-C(6A)-C(10A)	126.8(11)
C(7A)-C(6A)-Mo(2)	86.3(8)
C(10A)-C(6A)-Mo(2)	146.7(9)
C(8A)-C(7A)-C(6A)	115.8(10)
C(8A)-C(7A)-C(12A)	125.0(12)
C(6A)-C(7A)-C(12A)	118.9(11)
C(8A)-C(7A)-Mo(2)	76.8(7)
C(6A)-C(7A)-Mo(2)	56.0(6)
C(12A)-C(7A)-Mo(2)	132.0(8)
C(7A)-C(8A)-C(9A)	115.0(10)
C(7A)-C(8A)-C(14A)	122.2(11)
C(9A)-C(8A)-C(14A)	122.8(11)
C(7A)-C(8A)-Mo(2)	68.5(6)
C(9A)-C(8A)-Mo(2)	66.0(6)
C(14A)-C(8A)-Mo(2)	132.8(8)
C(8A)-C(9A)-C(16A)	123.8(12)
C(8A)-C(9A)-Mo(2)	78.6(7)
C(16A)-C(9A)-Mo(2)	124.6(9)
C(11A)-C(10A)-C(6A)	109.9(10)
C(7A)-C(12A)-C(13A)	112.3(10)
C(8A)-C(14A)-C(15A)	111.3(10)
C(17A)-C(16A)-C(9A)	113.6(11)

Table 6.7. Anisotropic displacement parameters ($Å^2$ x 10^3) for (**21b**). The anisotropic displacement factor exponent takes the form:

$-2\pi^2 [h^2 a^* 2 U11 + ... + 2 h k a^* b^* U12]$

Atom	U11	U22	U33	U23	U13	U12
Mo(1)	18(1)	23(1)	21(1)	6(1)	6(1)	-1(1)
Br(1)	40(1)	25(1)	37(1)	10(1)	14(1)	1(1)
B(1)	60(11)	62(10)	33(8)	5(7)	7(7)	17(8)
O(1)	37(4)	42(4)	22(4)	7(3)	11(3)	8(4)
F(1)	123(8)	45(4)	42(5)	13(4)	8(5)	14(5)
F(2)	45(6)	192(14)	180(14)	-47(11)	-30(7)	22(7)
F(3)	95(7)	62(5)	83(6)	7(5)	40(5)	30(5)
F(4)	138(10)	96(8)	117(9)	55(7)	77(8)	41(7)
C(1)	15(5)	46(7)	32(6)	0(5)	-6(5)	1(5)
C(2)	17(6)	43(7)	47(7)	6(6)	2(5)	-8(5)
C(3)	23(6)	51(7)	40(7)	10(6)	17(5)	6(5)
C(4)	14(5)	28(6)	41(7)	5(5)	1(5)	3(4)
C(5)	26(6)	24(5)	31(6)	6(4)	0(5)	0(4)
C(6)	22(5)	13(5)	26(5)	1(4)	12(4)	0(4)
C(7)	22(5)	29(5)	19(5)	3(4)	3(4)	-1(4)
C(8)	16(5)	33(6)	25(6)	-2(5)	2(4)	-4(4)
C(9)	11(5)	33(6)	32(6)	1(5)	7(4)	-8(4)
C(10)	35(6)	29(6)	18(5)	-4(4)	6(5)	4(5)
C(11)	45(7)	31(6)	34(6)	8(5)	9(5)	-2(5)
C(12)	24(6)	31(6)	37(6)	1(5)	3(5)	6(5)
C(13)	30(7)	58(8)	47(8)	-10(6)	10(6)	13(6)
C(14)	24(8)	180(21)	92(13)	-118(14)	5(8)	-3(10)
C(15)	275(38)	66(13)	71(14)	-4(11)	25(19)	-41(18)
C(16)	25(6)	24(5)	28(6)	-4(4)	3(4)	-4(4)
C(17)	71(9)	33(7)	32(7)	-15(5)	16(6)	-10(6)
Mo(2)	34(1)	35(1)	31(1)	-2(1)	-3(1)	4(1)

Br(2)	30(1)	42(1)	29(1)	6(1)	-1(1)	3(1)
F(5)	83(6)	112(7)	43(5)	3(5)	28(4)	45(6)
F(6)	104(7)	54(5)	104(7)	16(5)	56(6)	-5(5)
F(7)	107(8)	112(8)	105(8)	11(6)	72(7)	39(7)
F(8)	174(11)	54(5)	52(5)	20(4)	12(6)	19(6)
O(2)	63(6)	39(5)	37(5)	9(4)	15(4)	5(4)
B(2)	66(10)	28(7)	60(10)	22(7)	47(8)	5(7)
C(1A)	33(7)	41(7)	83(11)	-17(7)	16(7)	-5(6)
C(2A)	38(7)	35(7)	54(8)	-17(6)	4(6)	3(5)
C(3A)	80(11)	45(8)	34(7)	-21(6)	9(7)	-11(7)
C(4A)	45(8)	38(7)	32(7)	-10(5)	-1(6)	3(6)
C(5A)	50(8)	39(7)	45(8)	-2(6)	7(6)	-2(6)
C(6A)	38(7)	38(7)	34(6)	6(5)	-7(5)	10(5)
C(7A)	27(6)	40(7)	37(7)	-4(5)	4(5)	12(5)
C(8A)	28(6)	31(6)	46(7)	-1(5)	-2(5)	2(5)
C(9A)	59(8)	41(7)	36(7)	21(6)	0(6)	15(6)
C(10A)	70(10)	44(8)	44(8)	13(6)	26(7)	-5(7)
C(11A)	51(9)	65(9)	54(9)	15(7)	25(7)	-5(7)
C(12A)	46(8)	74(10)	35(7)	-27(7)	0(6)	18(7)
C(13A)	62(10)	113(13)	29(7)	-10(8)	1(7)	33(9)
C(14A)	25(7)	47(8)	83(10)	-5(7)	12(7)	-12(6)
C(15A)	61(10)	27(7)	108(13)	2(7)	32(9)	-8(6)
C(16A)	48(8)	53(8)	48(8)	31(6)	24(6)	19(6)
C(17A)	46(8)	87(11)	56(9)	31(8)	15(7)	7(8)

Table 6.8. Hydrogen coordinates (x 10^4) and isotropic displacement parameters ($Å^2$ x 10^3) for (**21b**).

Atom	x	y	z	U(eq)
H(1)	-159(10)	1388(9)	2725(7)	39
H(2)	-1026(10)	805(10)	4003(8)	43
H(3)	-947(11)	2378(9)	5155(8)	44
H(4)	17(10)	3941(8)	4652(7)	34
H(5)	403(10)	3352(8)	3127(7)	32
H(10A)	1496(11)	2099(8)	2201(6)	34
H(10B)	2912(11)	1594(8)	2210(6)	34
H(11A)	2936(12)	3248(9)	1721(7)	54
H(11B)	3934(12)	3312(9)	2601(7)	54
H(11C)	2517(12)	3817(9)	2593(7)	54
H(12A)	5135(10)	913(8)	4343(7)	38
H(12B)	4186(10)	507(8)	3462(7)	38
H(13A)	6309(12)	907(11)	3184(8)	70
H(13B)	6222(12)	2083(11)	3652(8)	70
H(13C)	5273(12)	1677(11)	2772(8)	70
H(14A)	4431(14)	2610(19)	6200(12)	137
H(14B)	4693(14)	1529(19)	5616(12)	137
H(15A)	6554(32)	2418(16)	6148(14)	209
H(15B)	5998(32)	3391(16)	5713(14)	209
H(15C)	6257(32)	2317(16)	5130(14)	209
H(16A)	3066(10)	3934(8)	6204(7)	32
H(16B)	1913(10)	4550(8)	5714(7)	32
H(17A)	3740(14)	5747(9)	6325(8)	70
H(17B)	3539(14)	5645(9)	5307(8)	70
H(17C)	4690(14)	5031(9)	5797(8)	70
H(1A)	7847(12)	-162(10)	9563(10)	66
H(2A)	9690(13)	122(9)	8714(9)	54

H(3A)	8746(16)	1089(11)	7512(9)	67
H(4A)	6348(13)	1448(9)	7629(8)	49
H(5A)	5789(14)	675(10)	8894(8)	55
H(10C)	6274(14)	639(10)	10406(9)	60
H(10D)	6722(14)	1442(10)	11272(9)	60
H(11D)	4372(13)	1414(12)	10907(9)	82
H(11E)	4490(13)	1752(12)	10005(9)	82
H(11F)	4936(13)	2552(12)	10869(9)	82
H(12C)	9103(13)	3925(12)	11346(8)	68
H(12D)	8780(13)	2806(12)	11577(8)	68
H(13D)	7985(15)	4153(14)	12564(9)	107
H(13E)	6762(15)	3461(14)	12020(9)	107
H(13F)	7086(15)	4580(14)	11789(9)	107
H(14C)	8440(12)	4945(10)	9395(10)	64
H(14D)	8857(12)	4900(10)	10392(10)	64
H(15D)	7551(15)	6396(10)	10211(11)	97
H(15E)	6789(15)	5617(10)	10657(11)	97
H(15F)	6372(15)	5662(10)	9661(11)	97
H(16C)	7198(13)	4309(11)	8214(8)	54
H(16D)	6595(13)	3229(11)	7668(8)	54
H(17D)	5139(13)	4566(13)	7462(9)	90
H(17E)	5100(13)	4809(13)	8466(9)	90
H(17F)	4497(13)	3728(13)	7919(9)	90

Table 6.9. Oxygen - Fluorine interactions [Å].

O1 - F1_#1	2.680 (0.010)
O1 - F7_#4	2.741 (0.009)
O2 - F3_#2	2.778 (0.008)
O2 - F5_#3	2.978 (0.012)
O2 - F6_#3	2.806 (0.013)

Symmetry operators:

#1 *-1+x, y, z*

#2 *x, y, z*

#3 *2-x, 1-y, 2-z*

#4 *1-x, 1-y, 2-z*

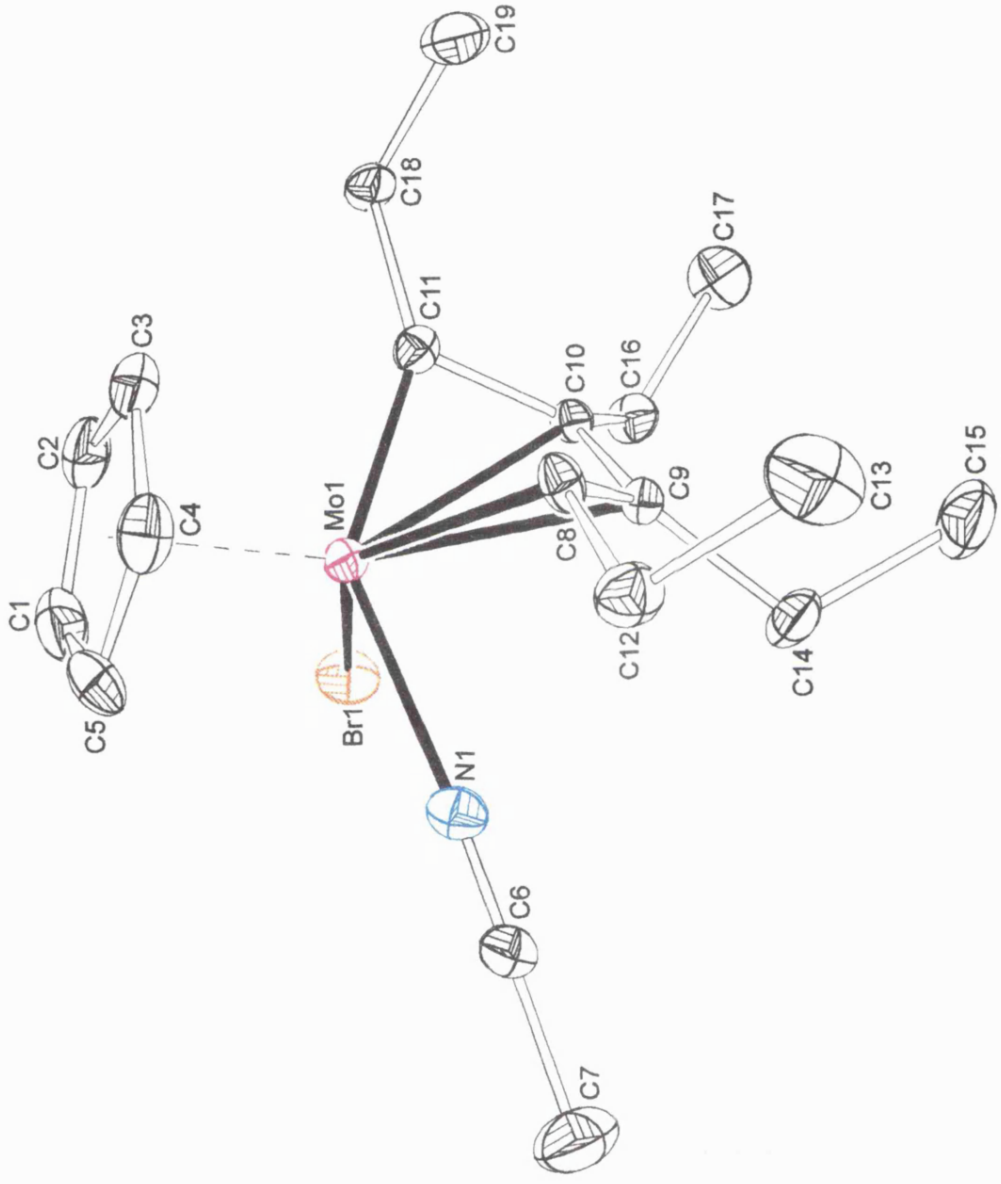

Figure 6.3. ORTEX representation of [BrMo=C(Et)-η^3-{C(Et)C(Et)CHEt}(NCMe)(η-C_5H_5)][BF_4]. Hydrogen atoms omitted for clarity.

[BrMo=C{Et}-η^3-{C(Et)C(Et)CHEt}(NCMe)(η-C_5H_5)][BF_4] (27).

A crystal of approximate dimensions 0.3 x 0.3 x 0.15 mm was used for data collection

Crystal Data: $C_{19}H_{29}BNBrF_4Mo$, M=534.1, monoclinic, a=8.2124(6), b=9.259(1), c=28.930(3)Å, β=96.892(1)°, U=2183.9Å^3, space group $P2_1/n$, Z=4, D_c=1.62gcm^{-3}, μ(Mo-K_α)=1.62 cm^{-1}, F(000)=1072. Crystallographic measurements were made at room temperature on a CAD4 automatic four-circle diffractometer in the range $2\leq\theta\leq24$. 6949 reflections were collected of which 2407 were unique with $I\geq2\sigma(I)$. Data were corrected for Lorentz and polarisation and also for absorption.[95] (Max. and Min. absorption corrections; 1.496, 0.907 respectively). The structure was solved by Patterson methods and refined using the SHELX[93,92] suite of programs. In the final least squares cycles all atoms were allowed to vibrate anisotropically. Hydrogen atoms were included at calculated positions except in the instance of H81(attached to C8) which was located in an advanced Difference Fourier and refined at a distance of 0.96Å from the parent atom. Final residuals after 12 cycles of least squares were R=0.0429, R_w=0.0417, for a weighting scheme of $w=2.9464/[\sigma^2(F) + 0.000352(F)^2]$. Max. final shift/esd was 0.005. The max. and min. residual densities were 0.37 and -0.26 eÅ^{-3} respectively. The asymmetric unit is shown in Figure 6.3, along with the labelling scheme used.

Table 6.10.

Fractional atomic co-ordinates ($x10^4$) and equivalent isotropic temperature factors ($Å^2 x10^3$) for (**27**).

	x	y	z	U
Mo(1)	151(1)	1871(1)	1175	27
Br(1)	-2330(1)	2781(1)	608	52
N(1)	-378(6)	3935(6)	1505(2)	38(2)
C(1)	-1851(9)	373(8)	1429(3)	57(3)
C(2)	-798(9)	-449(7)	1181(3)	50(3)
C(3)	768(9)	-406(7)	1446(3)	45(3)
C(4)	674(9)	459(7)	1843(3)	47(3)
C(5)	-951(10)	927(8)	1822(3)	51(3)
C(6)	-642(8)	4939(8)	1705(3)	40(3)
C(7)	-927(11)	6207(8)	1985(3)	74(4)
C(8)	2776(7)	2689(6)	1437(2)	29(2)
C(9)	2363(7)	3458(6)	1006(2)	30(2)
C(10)	1769(7)	2662(6)	615(2)	26(2)
C(11)	1407(7)	1165(6)	702(2)	29(2)
C(12)	3331(8)	3414(7)	1892(2)	41(2)
C(13)	5172(8)	3689(9)	1952(3)	60(3)
C(14)	2428(8)	5094(7)	983(3)	44(3)
C(15)	3935(10)	5619(8)	770(3)	64(3)
C(16)	1382(8)	3253(7)	129(2)	41(2)
C(17)	2780(9)	3040(9)	-169(2)	56(3)
C(18)	1942(7)	-105(6)	443(2)	35(2)
C(19)	3819(8)	-313(7)	532(3)	51(3)
B(1)	4853(11)	8370(10)	2023(4)	54(4)
F(1)	3578(8)	7517(7)	2072(3)	125(3)
F(2)	4489(7)	9734(6)	1961(3)	173(4)
F(3)	6183(7)	8184(7)	2324(2)	110(3)
F(4)	5350(10)	7943(9)	1598(2)	152(4)

Table 6.11

Anisotropic temperature factors (Å x10^3) for (**27**).

	U11	U22	U33	U23	U13	U12
Mo(1)	29	25	27	0	6	0
Br(1)	40	61(1)	51(1)	0	-4	11
N(1)	35(3)	41(3)	39(4)	-1(3)	5(3)	6(3)
C(1)	44(4)	60(5)	69(6)	13(5)	14(4)	-14(4)
C(2)	57(5)	37(4)	55(6)	1(4)	4(4)	-21(4)
C(3)	56(5)	29(4)	52(5)	9(4)	16(4)	-4(3)
C(4)	57(5)	40(4)	42(5)	14(4)	4(4)	-8(4)
C(5)	67(5)	58(5)	34(5)	6(4)	30(4)	-5(4)
C(6)	37(4)	38(4)	47(5)	0(4)	15(3)	4(3)
C(7)	93(6)	43(5)	88(8)	-18(5)	24(6)	11(5)
C(8)	26(3)	31(4)	30(4)	-2(3)	4(3)	-4(3)
C(9)	27(3)	24(3)	41(4)	-1(3)	7(3)	-2(2)
C(10)	33(3)	26(3)	22(4)	5(3)	8(3)	3(3)
C(11)	28(3)	27(3)	31(4)	0(3)	-2(3)	-1(3)
C(12)	44(4)	40(4)	39(4)	-10(3)	1(3)	0(3)
C(13)	46(4)	83(6)	49(5)	-11(5)	-1(4)	-2(4)
C(14)	57(4)	25(4)	49(5)	-4(3)	8(4)	-5(3)
C(15)	85(6)	39(4)	70(6)	2(4)	21(5)	-22(4)
C(16)	52(4)	36(4)	35(4)	6(3)	8(3)	7(3)
C(17)	75(5)	64(5)	30(4)	9(4)	20(4)	1(4)
C(18)	46(4)	29(3)	30(4)	-10(3)	12(3)	0(3)
C(19)	53(4)	43(4)	58(6)	-1(4)	11(4)	15(3)
B(1)	53(5)	44(6)	62(7)	15(5)	-3(5)	-1(4)
F(1)	119(5)	105(4)	159(7)	34(5)	52(5)	-10(4)
F(2)	102(5)	58(4)	334(12)	4(5)	-77(6)	25(3)
F(3)	111(4)	141(5)	68(4)	6(3)	-26(3)	54(4)
F(4)	207(8)	195(8)	56(4)	-11(5)	29(5)	-57(6)

The temperature factor exponent takes the form:

-2 (U .h .a* +...+2U .h.k.a*.b*)

Table 6.12

Hydrogen fractional atomic co-ordinates ($x10^4$) and isotropic temperature factors ($Å^2 x10^3$) for (**27**).

	x	y	z	U
H(11)	-3002(9)	518(8)	1339(3)	80(5)
H(21)	-1083(9)	-939(7)	890(3)	80(5)
H(31)	1733(9)	-887(7)	1368(3)	80(5)
H(41)	1554(9)	683(7)	2082(3)	80(5)
H(51)	-1375(10)	1542(8)	2047(3)	80(5)
H(71)	-1678(11)	6845(8)	1806(3)	80(5)
H(72)	92(11)	6699(8)	2072(3)	80(5)
H(73)	-1384(11)	5912(8)	2260(3)	80(5)
H(81)	3294(81)	1772(37)	1404(29)	80(5)
H(121)	2767(8)	4321(7)	1899(2)	80(5)
H(122)	3062(8)	2816(7)	2143(2)	80(5)
H(131)	5484(8)	4163(9)	2245(3)	80(5)
H(132)	5449(8)	4290(9)	1703(3)	80(5)
H(133)	5743(8)	2786(9)	1947(3)	80(5)
H(141)	1461(8)	5434(7)	796(3)	80(5)
H(142)	2459(8)	5477(7)	1292(3)	80(5)
H(151)	3934(10)	6656(8)	761(3)	80(5)
H(152)	3911(10)	5246(8)	460(3)	80(5)
H(153)	4909(10)	5288(8)	957(3)	80(5)
H(161)	423(8)	2773(7)	-20(2)	80(5)
H(162)	1166(8)	4269(7)	149(2)	80(5)
H(171)	2470(9)	3435(9)	-474(2)	80(5)
H(172)	3002(9)	2027(9)	-195(2)	80(5)
H(173)	3745(9)	3522(9)	-26(2)	80(5)
H(181)	1415(7)	-955(6)	544(2)	80(5)

H(182)	1625(7)	38(6)	116(2)	80(5)
H(191)	4125(8)	-1138(7)	361(3)	80(5)
H(192)	4144(8)	-461(7)	858(3)	80(5)
H(193)	4354(8)	532(7)	430(3)	80(5)

Table 6.13

Bond lengths (Å) for (**27**).

Br(1)-Mo(1)	2.598(4)	N(1)-Mo(1)	2.201(8)
C(1)-Mo(1)	2.335(9)	C(2)-Mo(1)	2.286(8)
C(3)-Mo(1)	2.285(8)	C(4)-Mo(1)	2.330(9)
C(5)-Mo(1)	2.344(9)	C(8)-Mo(1)	2.324(8)
C(9)-Mo(1)	2.431(8)	C(10)-Mo(1)	2.335(8)
C(11)-Mo(1)	1.925(8)	C(6)-N(1)	1.129(9)
C(2)-C(1)	1.410(11)	C(3)-C(1)	2.263(12)
C(4)-C(1)	2.268(13)	C(5)-C(1)	1.380(12)
C(3)-C(2)	1.416(11)	C(4)-C(2)	2.297(13)
C(5)-C(2)	2.266(13)	C(4)-C(3)	1.410(11)
C(5)-C(3)	2.251(12)	C(5)-C(4)	1.397(11)
C(7)-C(6)	1.462(11)	C(9)-C(8)	1.440(10)
C(12)-C(8)	1.500(11)	C(10)-C(9)	1.390(9)
C(14)-C(9)	1.517(10)	C(11)-C(10)	1.447(9)
C(16)-C(10)	1.507(11)	C(18)-C(11)	1.488(9)
C(13)-C(12)	1.523(11)	C(15)-C(14)	1.527(11)
C(17)-C(16)	1.529(11)	C(19)-C(18)	1.544(11)
F(1)-B(1)	1.332(11)	F(2)-B(1)	1.306(11)
F(3)-B(1)	1.324(11)	F(4)-B(1)	1.400(12)
H(11)-C(1)	0.960	H(21)-C(2)	0.960
H(31)-C(3)	0.960	H(41)-C(4)	0.960
H(51)-C(5)	0.960	H(71)-C(7)	0.959
H(72)-C(7)	0.960	H(73)-C(7)	0.960
H(81)-C(8)	0.960(2)	H(121)-C(12)	0.960

H(122)-C(12)	0.960	H(131)-C(13)	0.960
H(132)-C(13)	0.960	H(133)-C(13)	0.960
H(141)-C(14)	0.960	H(142)-C(14)	0.960
H(151)-C(15)	0.960	H(152)-C(15)	0.960
H(153)-C(15)	0.960	H(161)-C(16)	0.960
H(162)-C(16)	0.960	H(171)-C(17)	0.960
H(172)-C(17)	0.960	H(173)-C(17)	0.960
H(181)-C(18)	0.960	H(182)-C(18)	0.960
H(191)-C(19)	0.960	H(192)-C(19)	0.960
H(193)-C(19)	0.960		

Table 6.14

Bond angles (°) for (**27**).

N(1)-Mo(1)-Br(1)	79.2(2)	C(1)-Mo(1)-Br(1)	82.1(3)
C(1)-Mo(1)-N(1)	101.4(3)	C(2)-Mo(1)-Br(1)	93.9(3)
C(2)-Mo(1)-N(1)	136.7(2)	C(2)-Mo(1)-C(1)	35.5(2)
C(3)-Mo(1)-Br(1)	129.8(3)	C(3)-Mo(1)-N(1)	134.4(2)
C(3)-Mo(1)-C(1)	58.6(4)	C(3)-Mo(1)-C(2)	36.1(3)
C(4)-Mo(1)-Br(1)	139.3(2)	C(4)-Mo(1)-N(1)	98.9(3)
C(4)-Mo(1)-C(1)	58.2(4)	C(4)-Mo(1)-C(2)	59.7(4)
C(4)-Mo(1)-C(3)	35.6(2)	C(5)-Mo(1)-Br(1)	106.1(3)
C(5)-Mo(1)-N(1)	82.1(3)	C(5)-Mo(1)-C(1)	34.3(3)
C(5)-Mo(1)-C(2)	58.6(4)	C(5)-Mo(1)-C(3)	58.2(4)
C(5)-Mo(1)-C(4)	34.8(2)	C(8)-Mo(1)-Br(1)	136.6(2)
C(8)-Mo(1)-N(1)	78.4(3)	C(8)-Mo(1)-C(1)	138.7(3)
C(8)-Mo(1)-C(2)	127.4(3)	C(8)-Mo(1)-C(3)	91.7(3)
C(8)-Mo(1)-C(4)	80.9(3)	C(8)-Mo(1)-C(5)	107.0(4)
C(9)-Mo(1)-Br(1)	103.0(2)	C(9)-Mo(1)-N(1)	75.7(3)
C(9)-Mo(1)-C(1)	173.3(3)	C(9)-Mo(1)-C(2)	146.4(2)

C(9)-Mo(1)-C(3)	119.1(3)	C(9)-Mo(1)-C(4)	116.0(3)
C(9)-Mo(1)-C(5)	139.1(3)	C(9)-Mo(1)-C(8)	35.2(2)
C(10)-Mo(1)-Br(1)	85.9(2)	C(10)-Mo(1)-N(1)	100.8(3)
C(10)-Mo(1)-C(1)	152.3(3)	C(10)-Mo(1)-C(2)	121.5(3)
C(10)-Mo(1)-C(3)	114.0(3)	C(10)-Mo(1)-C(4)	133.5(2)
C(10)-Mo(1)-C(5)	168.0(2)	C(10)-Mo(1)-C(8)	62.7(3)
C(10)-Mo(1)-C(9)	33.8(2)	C(11)-Mo(1)-Br(1)	96.2(3)
C(11)-Mo(1)-N(1)	138.9(2)	C(11)-Mo(1)-C(1)	118.6(4)
C(11)-Mo(1)-C(2)	84.1(4)	C(11)-Mo(1)-C(3)	79.3(4)
C(11)-Mo(1)-C(4)	109.7(4)	C(11)-Mo(1)-C(5)	137.1(3)
C(11)-Mo(1)-C(8)	77.7(3)	C(11)-Mo(1)-C(9)	65.5(3)
C(11)-Mo(1)-C(10)	38.2(2)	C(3)-C(1)-C(2)	36.9(4)
C(4)-C(1)-C(2)	73.1(6)	C(4)-C(1)-C(3)	36.3(3)
C(5)-C(1)-C(2)	108.6(8)	C(5)-C(1)-C(3)	71.7(6)
C(5)-C(1)-C(4)	35.5(4)	C(3)-C(2)-C(1)	106.4(8)
C(4)-C(2)-C(1)	70.9(6)	C(4)-C(2)-C(3)	35.5(4)
C(5)-C(2)-C(1)	35.3(4)	C(5)-C(2)-C(3)	71.2(6)
C(5)-C(2)-C(4)	35.6(3)	C(2)-C(3)-C(1)	36.7(4)
C(4)-C(3)-C(1)	72.1(6)	C(4)-C(3)-C(2)	108.8(7)
C(5)-C(3)-C(1)	35.6(3)	C(5)-C(3)-C(2)	72.3(6)
C(5)-C(3)-C(4)	36.5(4)	C(2)-C(4)-C(1)	36.0(3)
C(3)-C(4)-C(1)	71.7(6)	C(3)-C(4)-C(2)	35.7(4)
C(5)-C(4)-C(1)	35.0(4)	C(5)-C(4)-C(2)	70.9(6)
C(5)-C(4)-C(3)	106.7(8)	C(2)-C(5)-C(1)	36.1(4)
C(3)-C(5)-C(1)	72.7(6)	C(3)-C(5)-C(2)	36.5(3)
C(4)-C(5)-C(1)	109.5(8)	C(4)-C(5)-C(2)	73.4(6)
C(4)-C(5)-C(3)	36.9(4)	C(7)-C(6)-N(1)	176.9(8)
C(12)-C(8)-C(9)	123.6(6)	C(10)-C(9)-C(8)	117.8(6)
C(14)-C(9)-C(8)	121.7(7)	C(14)-C(9)-C(10)	120.2(7)
C(11)-C(10)-C(9)	115.1(6)	C(16)-C(10)-C(9)	125.6(6)
C(16)-C(10)-C(11)	119.1(6)	C(10)-C(11)-Mo(1)	86.5(5)
C(18)-C(11)-Mo(1)	147.4(5)	C(18)-C(11)-C(10)	126.1(6)

C(13)-C(12)-C(8)	111.6(6)	C(15)-C(14)-C(9)	111.8(6)
C(17)-C(16)-C(10)	113.0(6)	C(19)-C(18)-C(11)	111.4(6)
F(2)-B(1)-F(1)	114.7(9)	F(3)-B(1)-F(1)	116.8(9)
F(3)-B(1)-F(2)	111.9(9)	F(4)-B(1)-F(1)	104.0(9)
F(4)-B(1)-F(2)	103.8(10)	F(4)-B(1)-F(3)	103.7(9)
C(2)-C(1)-H(11)	125.6(6)	C(3)-C(1)-H(11)	162.5(3)
C(4)-C(1)-H(11)	161.2(3)	C(5)-C(1)-H(11)	125.8(6)
H(21)-C(2)-C(1)	126.9(6)	C(3)-C(2)-H(21)	126.7(5)
C(4)-C(2)-H(21)	162.2(3)	C(5)-C(2)-H(21)	162.1(3)
H(31)-C(3)-C(1)	162.2(3)	H(31)-C(3)-C(2)	125.5(5)
C(4)-C(3)-H(31)	125.7(5)	C(5)-C(3)-H(31)	162.2(3)
H(41)-C(4)-C(1)	161.6(3)	H(41)-C(4)-C(2)	162.4(3)
H(41)-C(4)-C(3)	126.7(5)	C(5)-C(4)-H(41)	126.6(6)
H(51)-C(5)-C(1)	125.2(6)	H(51)-C(5)-C(2)	161.3(3)
H(51)-C(5)-C(3)	162.1(3)	H(51)-C(5)-C(4)	125.2(6)
H(71)-C(7)-C(6)	109.3(6)	H(72)-C(7)-C(6)	109.5(5)
H(72)-C(7)-H(71)	109.4	H(73)-C(7)-C(6)	109.7(5)
H(73)-C(7)-H(71)	109.4	H(73)-C(7)-H(72)	109.5

C(9)-C(8)-H(81)	114.3(52)	C(12)-C(8)-H(81)	113.1(51)
H(121)-C(12)-C(8)	108.3(4)	H(122)-C(12)-C(8)	109.4(5)
H(122)-C(12)-H(121)	109.5	C(13)-C(12)-H(121)	109.0(5)
C(13)-C(12)-H(122)	109.0(5)	H(131)-C(13)-C(12)	109.5(5)
H(132)-C(13)-C(12)	109.4(5)	H(132)-C(13)-H(131)	109.5
H(133)-C(13)-C(12)	109.5(5)	H(133)-C(13)-H(131)	109.5
H(133)-C(13)-H(132)	109.5	H(141)-C(14)-C(9)	108.8(4)
H(142)-C(14)-C(9)	108.9(5)	H(142)-C(14)-H(141)	109.5

C(15)-C(14)-H(141)	108.8(5)	C(15)-C(14)-H(142)	109.0(5)
H(151)-C(15)-C(14)	109.4(5)	H(152)-C(15)-C(14)	109.6(5)
H(152)-C(15)-H(151)	109.5	H(153)-C(15)-C(14)	109.4(5)

H(153)-C(15)-H(151)	109.5	H(153)-C(15)-H(152)	109.5
H(161)-C(16)-C(10)	108.6(4)	H(162)-C(16)-C(10)	108.6(4)
H(162)-C(16)-H(161)	109.5	C(17)-C(16)-H(161)	108.6(5)
C(17)-C(16)-H(162)	108.5(5)	H(171)-C(17)-C(16)	109.5(5)
H(172)-C(17)-C(16)	109.4(5)	H(172)-C(17)-H(171)	109.5
H(173)-C(17)-C(16)	109.5(5)	H(173)-C(17)-H(171)	109.5
H(173)-C(17)-H(172)	109.5	H(181)-C(18)-C(11)	108.9(4)
H(182)-C(18)-C(11)	109.0(4)	H(182)-C(18)-H(181)	109.5
C(19)-C(18)-H(181)	109.0(5)	C(19)-C(18)-H(182)	109.1(5)
H(191)-C(19)-C(18)	109.4(4)	H(192)-C(19)-C(18)	109.6(5)
H(192)-C(19)-H(191)	109.5	H(193)-C(19)-C(18)	109.4(5)
H(193)-C(19)-H(191)	109.5	H(193)-C(19)-H(192)	109.5

Table 6.15.

Selected non-bonded distances (Å) for (**27**).

Intramolecular:

H(11)-Mo(1)	2.965	H(21)-Mo(1)	2.877
H(31)-Mo(1)	2.890	H(41)-Mo(1)	2.948
H(51)-Mo(1)	2.963	C(6)-Mo(1)	3.328
H(81)-Mo(1)	2.588	C(12)-Mo(1)	3.444
C(14)-Mo(1)	3.600	C(16)-Mo(1)	3.545
C(18)-Mo(1)	3.278	N(1)-Br(1)	3.073
C(1)-Br(1)	3.246	H(11)-Br(1)	3.073
C(2)-Br(1)	3.574	C(10)-Br(1)	3.365
C(11)-Br(1)	3.395	C(16)-Br(1)	3.524
H(161)-Br(1)	3.066	C(5)-N(1)	2.987

C(7)-N(1)	2.590	C(8)-N(1)	2.863
C(9)-N(1)	2.849	C(12)-N(1)	3.153
H(121)-N(1)	2.719	C(14)-N(1)	3.094
H(21)-C(1)	2.129	H(51)-C(1)	2.087
C(2)-H(11)	2.118	C(5)-H(11)	2.092
H(31)-C(2)	2.123	C(11)-C(2)	2.834
C(18)-C(2)	3.298	H(181)-C(2)	2.780
C(3)-H(21)	2.134	H(181)-H(21)	2.389
H(41)-C(3)	2.128	C(11)-C(3)	2.700
C(18)-C(3)	3.177	H(181)-C(3)	2.772
C(4)-H(31)	2.119	C(11)-H(31)	2.695
C(18)-H(31)	2.796	H(181)-H(31)	2.367
H(51)-C(4)	2.102	C(8)-C(4)	3.018
C(5)-H(41)	2.115	H(122)-H(41)	2.327
H(71)-C(6)	1.996	H(72)-C(6)	1.998
H(73)-C(6)	2.001	H(121)-C(6)	2.847
H(72)-H(71)	1.566	H(73)-H(71)	1.566
H(73)-H(72)	1.568	C(10)-C(8)	2.424
C(11)-C(8)	2.683	H(121)-C(8)	2.019
H(122)-C(8)	2.032	C(13)-C(8)	2.500
H(132)-C(8)	2.685	H(133)-C(8)	2.695
C(14)-C(8)	2.583	H(142)-C(8)	2.623
C(9)-H(81)	2.033	C(10)-H(81)	2.603
C(11)-H(81)	2.466	C(12)-H(81)	2.074
H(122)-H(81)	2.377	C(13)-H(81)	2.732
C(11)-C(9)	2.394	C(12)-C(9)	2.591
H(121)-C(9)	2.686	H(141)-C(9)	2.040
H(142)-C(9)	2.042	C(15)-C(9)	2.520
H(152)-C(9)	2.709	H(153)-C(9)	2.709
C(16)-C(9)	2.577	H(162)-C(9)	2.664
C(14)-C(10)	2.522	H(141)-C(10)	2.638
C(15)-C(10)	3.267	H(161)-C(10)	2.029

H(162)-C(10)	2.028	C(17)-C(10)	2.531
H(172)-C(10)	2.725	H(173)-C(10)	2.724
C(18)-C(10)	2.617	H(182)-C(10)	2.821
C(19)-C(10)	3.252	C(16)-C(11)	2.547
H(161)-C(11)	2.614	H(181)-C(11)	2.016
H(182)-C(11)	2.017	C(19)-C(11)	2.505
H(192)-C(11)	2.698	H(193)-C(11)	2.698
H(131)-C(12)	2.053	H(132)-C(12)	2.052
H(133)-C(12)	2.053	C(14)-C(12)	3.068
H(142)-C(12)	2.621	H(122)-H(121)	1.568
C(13)-H(121)	2.048	H(131)-H(121)	2.337
H(132)-H(121)	2.339	C(14)-H(121)	2.727
H(142)-H(121)	2.045	C(13)-H(122)	2.047
H(131)-H(122)	2.336	H(133)-H(122)	2.339
H(132)-H(131)	1.568	H(133)-H(131)	1.568
H(133)-H(132)	1.568	H(153)-H(132)	2.341
H(151)-C(14)	2.056	H(152)-C(14)	2.058
H(153)-C(14)	2.056	C(16)-C(14)	3.041
H(162)-C(14)	2.623	H(142)-H(141)	1.568
C(15)-H(141)	2.049	H(151)-H(141)	2.338
H(152)-H(141)	2.343	C(16)-H(141)	2.788
H(162)-H(141)	2.148	C(15)-H(142)	2.052
H(151)-H(142)	2.340	H(153)-H(142)	2.343
H(152)-H(151)	1.568	H(153)-H(151)	1.568
H(153)-H(152)	1.568	C(16)-H(152)	2.856
C(17)-H(152)	2.818	H(173)-H(152)	2.120
H(171)-C(16)	2.059	H(172)-C(16)	2.058
H(173)-C(16)	2.058	C(18)-C(16)	3.257
H(162)-H(161)	1.568	C(17)-H(161)	2.048
H(171)-H(161)	2.336	H(172)-H(161)	2.340
C(17)-H(162)	2.047	H(171)-H(162)	2.336
H(173)-H(162)	2.340	H(172)-H(171)	1.568

H(173)-H(171)	1.568	H(173)-H(172)	1.568
H(182)-H(172)	2.393	H(193)-H(172)	2.437
H(191)-C(18)	2.071	H(192)-C(18)	2.073
H(193)-C(18)	2.071	H(182)-H(181)	1.568
C(19)-H(181)	2.066	H(191)-H(181)	2.355
H(192)-H(181)	2.359	C(19)-H(182)	2.067
H(191)-H(182)	2.356	H(193)-H(182)	2.359
H(192)-H(191)	1.568	H(193)-H(191)	1.568
H(193)-H(192)	1.568	F(2)-F(1)	2.221
F(3)-F(1)	2.262	F(4)-F(1)	2.153
F(3)-F(2)	2.179	F(4)-F(2)	2.129
F(4)-F(3)	2.143		

Intermolecular:

F(2)-H(31a)	2	F(2)-C(4a)	3.18
F(2)-H(41a)	2	F(3)-H(51b)	2.36
F(3)-H(71c)	2	F(4)-H(71c)	2.64
F(2)-H(81a)	2	H(191)-H(151d)	2.36
H(162)-H(162e)	2	F(4)-H(192a)	2.69

Key to symmetry operations relating designated atoms to reference atoms at (x,y,z):

(a) x,1.0+y,z

(b) 0.5-x,0.5+y,0.5-z

(c) 1.0+x,y,z

(d) x,-1.0+y,z

(e) -x,1.0-y,-z

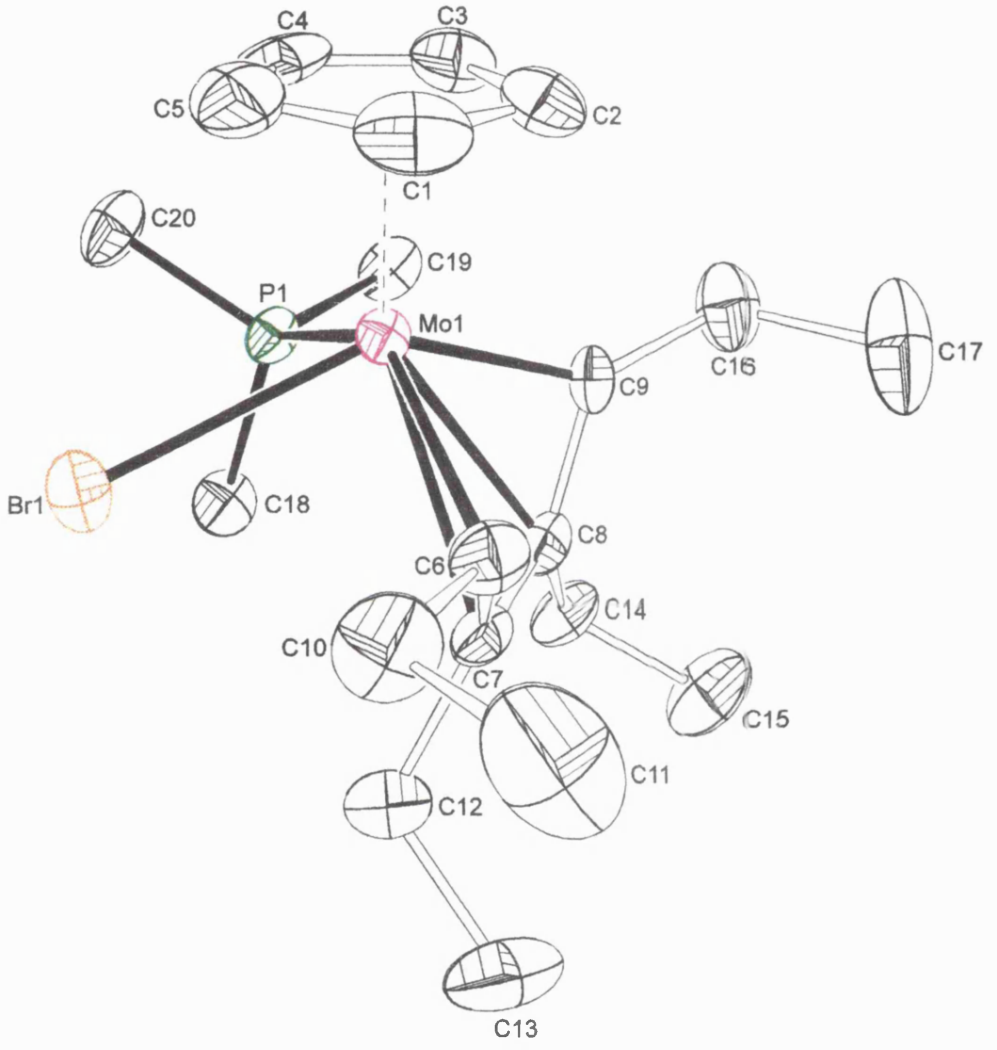

Figure 6.4. ORTEX representation of [BrMo=C(Et)-η^3-{C(Et)C(Et)CHEt}(PMe_3)(η-C_5H_5)][BF_4]. Hydrogen atoms omitted for clarity.

[BrMo=C{Et}-η^3-{C(Et)C(Et)CHEt}(PMe_3)(η-C_5H_5)][BF_4] (29).

A crystal of approximate dimensions 0.2 x 0.3 x 0.3 mm was used for data collection

Crystal Data: $C_{20}H_{35}BBrF_4PMo$, M=569.1, monoclinic, a=13.375(3), b=15.041(1), c=14.399(3)Å, β=104.43(2)°, U=2478.0Å^3, space group $P2_1/a$, Z=4, D_c=1.53gcm^{-3}, μ(Mo-K_α)=12.4 cm^{-1}, F(000)=1152. Crystallographic measurements were made at room temperature on a CAD4 automatic four-circle diffractometer in the range $2\leq\theta\leq24$. 4272 reflections were collected of which 2229 were unique with $I\geq2\sigma(I)$. Data were corrected for Lorentz and polarisation but not for absorption. The structure was solved by Patterson methods and refined using the SHELX[93,98] suite of programs. In the final least squares cycles all atoms were treated anisotropically. Hydrogen atoms were included at calculated positions except in the instance of H61(attached to C6) which was located in an advanced Difference Fourier and refined at a distance of 0.96Å from the parent atom. Final residuals after 10 cycles of least squares were R=0.0385, R_w=0.0419, for a weighting scheme of w=1.5618/[σ^2(F) + 0.001197(F)^2]. Max. final shift/esd was 0.952 (y co-ordinate of H61). The max. and min. residual densities were 0.33 and -0.18 eÅ^{-3} respectively. The asymmetric unit is shown in Figure 6.4, along with the labelling scheme used.

Table 6.16

Fractional atomic co-ordinates ($x10^3$) for (**29**).

	x	y	z
Mo(1)	3339.1(4)	338.7(4)	2133.1(4)
Br(1)	4742(1)	1352(1)	3155(1)
P(1)	2894(1)	2223(1)	1790(1)
C(1)	4220(9)	-1039(8)	1525(7)
C(2)	3264(8)	-988(7)	1068(6)
C(3)	3179(8)	-58(7)	587(6)
C(4)	4067(9)	470(8)	737(7)
C(5)	4729(8)	-133(10)	1302(7)
C(6)	3425(6)	-795(7)	3396(5)
C(7)	2782(6)	6(6)	3693(5)
C(8)	1987(6)	330(6)	3074(5)
C(9)	1949(5)	-58(5)	2139(5)
C(10)	4368(7)	-1161(8)	3928(7)
C(11)	4246(10)	-2215(8)	4343(9)
C(12)	3022(7)	541(8)	4616(6)
C(13)	2565(11)	-5(10)	5405(7)
C(14)	1142(6)	1035(7)	3364(6)
C(15)	290(7)	427(9)	3755(8)
C(16)	1048(6)	-436(7)	1559(7)
C(17)	731(8)	-1522(8)	1862(11)
C(18)	2706(7)	3026(6)	2794(6)
C(19)	1756(6)	2396(7)	1049(6)
C(20)	3802(7)	2967(7)	1179(7)
B(1)	2699(10)	-3885(10)	1687(9)
F(1)	3419(7)	-4363(10)	1215(9)
F(2)	3078(8)	-3292(7)	2329(5)
F(3)	2169(8)	-3321(5)	990(5)
F(4)	2109(7)	-4637(8)	1864(7)

Table 6.17

Anisotropic temperature factors (Å x10^2) for (**29**).

	U_{11}	U_{22}	U_{33}	U_{23}	U_{13}	U_{12}
Mo(1)	38.4(4)	31.1(3)	40.9(3)	-0.7(3)	4.2(2)	2.5(3)
Br(1)	57(1)	66(1)	74(1)	-2.8(5)	-6.2(4)	-11.4(4)
P(1)	48(1)	34(1)	57(1)	5(1)	13(1)	3(1)
C(1)	98(8)	64(7)	79(7)	-10(5)	20(6)	46(6)
C(2)	98(8)	61(6)	73(6)	-31(5)	20(6)	2(6)
C(3)	87(7)	61(6)	56(5)	-8(4)	9(5)	17(5)
C(4)	114(9)	58(6)	71(6)	-1(5)	60(6)	23(6)
C(5)	60(6)	112(9)	84(7)	-31(7)	22(5)	15(6)
C(6)	66(5)	50(5)	53(5)	13(4)	3(4)	4(4)
C(7)	54(5)	51(5)	45(4)	12(3)	11(4)	-8(4)
C(8)	50(4)	43(4)	59(5)	7(4)	16(4)	-6(4)
C(9)	38(4)	32(4)	62(5)	3(3)	0(3)	-5(3)
C(10)	74(6)	81(7)	88(7)	29(6)	-8(5)	17(5)
C(11)	175(13)	75(8)	130(11)	24(7)	-60(9)	13(8)
C(12)	85(6)	84(7)	52(5)	4(5)	10(4)	6(5)
C(13)	165(12)	147(12)	57(6)	22(7)	35(7)	5(9)
C(14)	56(5)	77(6)	72(6)	15(5)	31(4)	14(5)
C(15)	53(5)	129(10)	129(9)	39(8)	40(6)	18(6)
C(16)	52(5)	69(6)	114(8)	-4(6)	-5(5)	-4(5)
C(17)	69(7)	74(8)	247(17)	-15(9)	3(9)	-23(6)
C(18)	83(6)	42(5)	87(6)	-11(5)	20(5)	4(4)
C(19)	65(5)	59(5)	79(6)	22(5)	14(4)	16(4)
C(20)	72(6)	52(5)	112(7)	15(5)	34(5)	-4(5)
B(1)	89(9)	64(7)	77(8)	-10(7)	7(7)	-6(7)
F(1)	122(7)	244(13)	312(16)	-134(12)	-23(8)	9(8)
F(2)	230(9)	137(7)	117(6)	-37(5)	-40(6)	-38(6)
F(3)	264(10)	68(4)	108(5)	-4(4)	-27(6)	12(5)
F(4)	152(8)	195(10)	244(11)	124(8)	-63(7)	-95(7)

Table 6.18.

Hydrogen fractional atomic co-ordinates ($x10^3$) and isotropic temperature factors ($Å^2 x10^3$) for (**29**)

	x	y	z	U
H(11)	4481(9)	-1591(8)	1919(7)	110(6)
H(21)	2752(8)	-1508(7)	1085(6)	110(6)
H(31)	2599(8)	177(7)	212(6)	110(6)
H(41)	4208(9)	1143(8)	495(7)	110(6)
H(51)	5410(8)	41(10)	1501(7)	110(6)
H(61)	3083(64)	-1386(54)	3109(63)	110(6)
H(101)	4896(7)	-1190(8)	3512(7)	110(6)
H(102)	4543(7)	-677(8)	4419(7)	110(6)
H(111)	4864(10)	-2417(8)	4675(9)	110(6)
H(112)	4075(10)	-2707(8)	3857(9)	110(6)
H(113)	3723(10)	-2194(8)	4764(9)	110(6)
H(121)	2765(7)	1236(8)	4575(6)	110(6)
H(122)	3736(7)	561(8)	4744(6)	110(6)
H(131	2734(11)	360(10)	5976(7)	110(6)
H(132)	2821(11)	-699(10)	5455(7)	110(6)
H(133)	1849(11)	-25(10)	5287(7)	110(6)
H(141)	879(6)	1419(7)	2829(6)	110(6)
H(142)	1413(6)	1508(7)	3833(6)	110(6)
H(151)	-220(7)	899(9)	3927(8)	110(6)
H(152)	544(7)	45(9)	4294(8)	110(6)
H(153)	10(7)	-44(9)	3290(8)	110(6)
H(161)	503(6)	37(7)	1623(7)	110(6)
H(162)	1203(6)	-460(7)	919(7)	110(6)
H(171)	153(8)	-1742(8)	1477(11)	110(6)
H(172)	571(8)	-1503(8)	2501(11)	110(6)
H(173)	1271(8)	-2000(8)	1796(11)	110(6)
H(181)	2232(7)	2698(6)	3167(6)	110(6)

H(182)	2453(7)	3691(6)	2590(6)	110(6)
H(183)	3332(7)	3113(6)	3156(6)	110(6)
H(191)	1217(6)	2029(7)	1308(6)	110(6)
H(192)	1851(6)	2129(7)	440(6)	110(6)
H(193)	1595(6)	3120(7)	1006(6)	110(6)
H(201)	4447(7)	2928(7)	1518(7)	110(6)
H(202)	3591(7)	3677(7)	1132(7)	110(6)
H(203)	3847(7)	2686(7)	566(7)	110(6)

Table 6.19.

Bond lengths (Å) for (**29**).

Br(1)-Mo(1)	2.642(4)	P(1)-Mo(1)	2.542(5)
C(1)-Mo(1)	2.337(10)	C(2)-Mo(1)	2.295(10)
C(3)-Mo(1)	2.280(11)	C(4)-Mo(1)	2.303(10)
C(5)-Mo(1)	2.364(11)	C(6)-Mo(1)	2.331(10)
C(7)-Mo(1)	2.457(9)	C(8)-Mo(1)	2.341(9)
C(9)-Mo(1)	1.930(9)	C(18)-P(1)	1.811(10)
C(19)-P(1)	1.806(11)	C(20)-P(1)	1.825(10)
C(2)-C(1)	1.395(15)	C(5)-C(1)	1.403(16)
C(3)-C(2)	1.387(14)	C(4)-C(3)	1.373(15)
C(5)-C(4)	1.394(15)	C(7)-C(6)	1.429(12)
C(10)-C(6)	1.502(14)	C(8)-C(7)	1.400(12)
C(12)-C(7)	1.511(14)	C(9)-C(8)	1.434(11)
C(14)-C(8)	1.532(13)	C(16)-C(9)	1.496(12)
C(11)-C(10)	1.498(14)	C(13)-C(12)	1.504(14)
C(15)-C(14)	1.525(14)	C(17)-C(16)	1.537(15)
F(1)-B(1)	1.367(16)	F(2)-B(1)	1.276(14)
F(3)-B(1)	1.389(15)	F(4)-B(1)	1.289(15)
H(11)-C(1)	0.960	H(21)-C(2)	0.960

H(31)-C(3)	0.960	H(41)-C(4)	0.960
H(51)-C(5)	0.960	H(61)-C(6)	0.966(12)
H(101)-C(10)	0.960	H(102)-C(10)	0.960
H(111)-C(11)	0.960	H(112)-C(11)	0.960
H(113)-C(11)	0.960	H(121)-C(12)	0.960
H(122)-C(12)	0.960	H(131)-C(13)	0.960
H(132)-C(13)	0.960	H(133)-C(13)	0.960
H(141)-C(14)	0.960	H(142)-C(14)	0.960
H(151)-C(15)	0.960	H(152)-C(15)	0.960
H(153)-C(15)	0.960	H(161)-C(16)	0.960
H(162)-C(16)	0.960	H(171)-C(17)	0.960
H(172)-C(17)	0.960	H(173)-C(17)	0.960
H(181)-C(18)	0.960	H(182)-C(18)	0.960
H(183)-C(18)	0.960	H(191)-C(19)	0.960
H(192)-C(19)	0.960	H(193)-C(19)	0.960
H(201)-C(20)	0.960	H(202)-C(20)	0.960
H(203)-C(20)	0.960		

Table 6.20.

Bond angles (°) for (**29**)

P(1)-Mo(1)-Br(1)	77.4(2)	C(1)-Mo(1)-Br(1)	103.2(4)
C(1)-Mo(1)-P(1)	140.4(3)	C(2)-Mo(1)-Br(1)	137.3(3)
C(2)-Mo(1)-P(1)	125.8(4)	C(2)-Mo(1)-C(1)	35.1(3)
C(3)-Mo(1)-Br(1)	131.8(3)	C(3)-Mo(1)-P(1)	91.2(3)
C(3)-Mo(1)-C(1)	58.5(4)	C(3)-Mo(1)-C(2)	35.3(3)
C(4)-Mo(1)-Br(1)	96.9(4)	C(4)-Mo(1)-P(1)	82.4(3)
C(4)-Mo(1)-C(1)	58.1(4)	C(4)-Mo(1)-C(2)	58.2(5)
C(4)-Mo(1)-C(3)	34.8(4)	C(5)-Mo(1)-Br(1)	81.8(4)
C(5)-Mo(1)-P(1)	109.2(4)	C(5)-Mo(1)-C(1)	34.7(4)
C(5)-Mo(1)-C(2)	57.8(5)	C(5)-Mo(1)-C(3)	57.8(5)

C(5)-Mo(1)-C(4)	34.7(4)	C(6)-Mo(1)-Br(1)	83.3(3)
C(6)-Mo(1)-P(1)	138.5(2)	C(6)-Mo(1)-C(1)	79.6(4)
C(6)-Mo(1)-C(2)	92.9(4)	C(6)-Mo(1)-C(3)	128.2(4)
C(6)-Mo(1)-C(4)	136.7(3)	C(6)-Mo(1)-C(5)	103.9(5)
C(7)-Mo(1)-Br(1)	80.1(3)	C(7)-Mo(1)-P(1)	105.2(3)
C(7)-Mo(1)-C(1)	113.9(4)	C(7)-Mo(1)-C(2)	118.6(4)
C(7)-Mo(1)-C(3)	147.3(3)	C(7)-Mo(1)-C(4)	170.8(3)
C(7)-Mo(1)-C(5)	136.2(4)	C(7)-Mo(1)-C(6)	34.6(3)
C(8)-Mo(1)-Br(1)	103.1(3)	C(8)-Mo(1)-P(1)	86.4(3)
C(8)-Mo(1)-C(1)	130.3(4)	C(8)-Mo(1)-C(2)	112.7(4)
C(8)-Mo(1)-C(3)	123.0(4)	C(8)-Mo(1)-C(4)	154.3(4)
C(8)-Mo(1)-C(5)	164.4(4)	C(8)-Mo(1)-C(6)	62.6(4)
C(8)-Mo(1)-C(7)	33.8(3)	C(9)-Mo(1)-Br(1)	140.6(2)
C(9)-Mo(1)-P(1)	92.4(3)	C(9)-Mo(1)-C(1)	108.3(5)
C(9)-Mo(1)-C(2)	79.1(4)	C(9)-Mo(1)-C(3)	85.7(5)
C(9)-Mo(1)-C(4)	119.6(5)	C(9)-Mo(1)-C(5)	136.8(4)
C(9)-Mo(1)-C(6)	79.7(4)	C(9)-Mo(1)-C(7)	65.9(4)
C(9)-Mo(1)-C(8)	37.8(3)	C(19)-P(1)-C(18)	103.8(5)
C(20)-P(1)-C(18)	102.8(5)	C(20)-P(1)-C(19)	102.3(5)
C(5)-C(1)-C(2)	107.3(10)	C(3)-C(2)-C(1)	108.3(11)
C(4)-C(3)-C(2)	108.2(10)	C(5)-C(4)-C(3)	108.7(10)
C(4)-C(5)-C(1)	107.5(11)	C(10)-C(6)-C(7)	125.1(9)
C(8)-C(7)-C(6)	118.1(8)	C(12)-C(7)-C(6)	120.0(8)
C(12)-C(7)-C(8)	121.6(8)	C(9)-C(8)-C(7)	117.7(8)
C(14)-C(8)-C(7)	123.0(8)	C(14)-C(8)-C(9)	119.2(8)
C(16)-C(9)-C(8)	127.5(8)	C(11)-C(10)-C(6)	112.2(9)
C(13)-C(12)-C(7)	112.3(10)	C(15)-C(14)-C(8)	112.4(9)
C(17)-C(16)-C(9)	111.5(9)	F(2)-B(1)-F(1)	111.9(13)
F(3)-B(1)-F(1)	102.6(12)	F(3)-B(1)-F(2)	111.3(12)
F(4)-B(1)-F(1)	102.9(13)	F(4)-B(1)-F(2)	121.7(13)
F(4)-B(1)-F(3)	104.5(12)	C(2)-C(1)-H(11)	126.4(7)
C(5)-C(1)-H(11)	126.3(8)	H(21)-C(2)-C(1)	125.8(7)

C(3)-C(2)-H(21)	125.8(8)	H(31)-C(3)-C(2)	125.9(8)
C(4)-C(3)-H(31)	125.8(7)	H(41)-C(4)-C(3)	125.7(7)
C(5)-C(4)-H(41)	125.6(8)	H(51)-C(5)-C(1)	126.3(8)
H(51)-C(5)-C(4)	126.3(8)	C(7)-C(6)-H(61)	115.0(63)
C(10)-C(6)-H(61)	108.8(62)	H(101)-C(10)-C(6)	108.8(6)
H(102)-C(10)-C(6)	108.7(7)	H(102)-C(10)-H(101)	109.5
C(11)-C(10)-H(101)	108.7(8)	C(11)-C(10)-H(102)	109.0(7)
H(111)-C(11)-C(10)	109.3(7)	H(112)-C(11)-C(10)	109.7(7)
H(112)-C(11)-H(111)	109.5	H(113)-C(11)-C(10)	109.5(8)
H(113)-C(11)-H(111)	109.5	H(113)-C(11)-H(112)	109.5
H(121)-C(12)-C(7)	108.7(6)	H(122)-C(12)-C(7)	108.8(6)
H(122)-C(12)-H(121)	109.5	C(13)-C(12)-H(121)	108.6(8)
C(13)-C(12)-H(122)	108.8(8)	H(131)-C(13)-C(12)	109.5(7)
H(132)-C(13)-C(12)	109.3(8)	H(132)-C(13)-H(131)	109.5
H(133)-C(13)-C(12)	109.5(8)	H(133)-C(13)-H(131)	109.5
H(133)-C(13)-H(132)	109.5	H(141)-C(14)-C(8)	108.7(5)
H(142)-C(14)-C(8)	108.8(6)	H(142)-C(14)-H(141)	109.5
C(15)-C(14)-H(141)	108.8(7)	C(15)-C(14)-H(142)	108.7(7)
H(151)-C(15)-C(14)	109.5(6)	H(152)-C(15)-C(14)	109.5(7)
H(152)-C(15)-H(151)	109.5	H(153)-C(15)-C(14)	109.4(7)
H(153)-C(15)-H(151)	109.5	H(153)-C(15)-H(152)	109.5
H(161)-C(16)-C(9)	109.0(6)	H(162)-C(16)-C(9)	108.9(6)
H(162)-C(16)-H(161)	109.5	C(17)-C(16)-H(161)	108.9(7)
C(17)-C(16)-H(162)	109.0(8)	H(171)-C(17)-C(16)	109.4(7)
H(172)-C(17)-C(16)	109.6(8)	H(172)-C(17)-H(171)	109.5
H(173)-C(17)-C(16)	109.4(7)	H(173)-C(17)-H(171)	109.5
H(173)-C(17)-H(172)	109.5	H(181)-C(18)-P(1)	109.4(4)
H(182)-C(18)-P(1)	109.5(4)	H(182)-C(18)-H(181)	109.5
H(183)-C(18)-P(1)	109.5(4)	H(183)-C(18)-H(181)	109.5
H(183)-C(18)-H(182)	109.5	H(191)-C(19)-P(1)	109.5(4)
H(192)-C(19)-P(1)	109.4(4)	H(192)-C(19)-H(191)	109.5
H(193)-C(19)-P(1)	109.5(4)	H(193)-C(19)-H(191)	109.5

H(193)-C(19)-H(192)	109.5	H(201)-C(20)-P(1)	109.4(4)
H(202)-C(20)-P(1)	109.5(4)	H(202)-C(20)-H(201)	109.5
H(203)-C(20)-P(1)	109.5(4)	H(203)-C(20)-H(201)	109.5
H(203)-C(20)-H(202)	109.5		

Table 6.21.

Selected non-bonded distances [Å] for (**29**).

Intramolecular:

H(11)-Mo(1)	2.948	H(21)-Mo(1)	2.900
H(31)-Mo(1)	2.871	H(41)-Mo(1)	2.901
H(51)-Mo(1)	3.003	H(61)-Mo(1)	2.663
C(10)-Mo(1)	3.432	H(102)-Mo(1)	3.391
C(12)-Mo(1)	3.642	C(14)-Mo(1)	3.656
C(16)-Mo(1)	3.270	H(162)-Mo(1)	3.397
C(18)-Mo(1)	3.710	C(19)-Mo(1)	3.671
C(20)-Mo(1)	3.726	P(1)-Br(1)	3.242
C(4)-Br(1)	3.710	C(5)-Br(1)	3.284
H(51)-Br(1)	3.107	C(6)-Br(1)	3.314
C(7)-Br(1)	3.284	C(10)-Br(1)	3.476
H(101)-Br(1)	3.323	H(102)-Br(1)	3.210
C(12)-Br(1)	3.396	H(122)-Br(1)	2.922
C(18)-Br(1)	3.484	H(183)-Br(1)	2.953
C(20)-Br(1)	3.672	H(201)-Br(1)	3.117
C(3)-P(1)	3.450	C(4)-P(1)	3.198
H(41)-P(1)	2.999	C(8)-P(1)	3.346
C(9)-P(1)	3.257	H(181)-P(1)	2.315
H(182)-P(1)	2.316	H(183)-P(1)	2.316
H(191)-P(1)	2.311	H(192)-P(1)	2.310
H(193)-P(1)	2.311	H(201)-P(1)	2.327
H(202)-P(1)	2.328	H(203)-P(1)	2.329
H(21)-C(1)	2.106	C(3)-C(1)	2.255

C(4)-C(1)	2.255	H(51)-C(1)	2.117
C(6)-C(1)	2.985	H(61)-C(1)	2.868
C(2)-H(11)	2.111	C(5)-H(11)	2.118
C(6)-H(11)	2.832	H(101)-H(11)	2.376
H(31)-C(2)	2.100	C(4)-C(2)	2.236
C(5)-C(2)	2.253	C(9)-C(2)	2.706
C(16)-C(2)	3.179	H(162)-C(2)	2.833
C(3)-H(21)	2.099	C(9)-H(21)	2.684
C(16)-H(21)	2.795	H(173)-H(21)	2.383
F(3)-H(21)	2.466	H(41)-C(3)	2.084
C(5)-C(3)	2.247	C(9)-C(3)	2.873
H(162)-C(3)	2.770	C(4)-H(31)	2.085
H(162)-H(31)	2.342	H(51)-C(4)	2.109
C(5)-H(41)	2.103	C(20)-H(41)	2.623
H(203)-H(41)	2.053	C(8)-C(6)	2.427
C(9)-C(6)	2.746	H(101)-C(6)	2.027
H(102)-C(6)	2.025	C(11)-C(6)	2.490
H(112)-C(6)	2.683	H(113)-C(6)	2.680
C(12)-C(6)	2.547	H(122)-C(6)	2.623
C(7)-H(61)	2.036	C(8)-H(61)	2.654
C(9)-H(61)	2.621	C(10)-H(61)	2.031
C(11)-H(61)	2.511	H(112)-H(61)	2.369
F(2)-H(61)	2.703	C(9)-C(7)	2.425
C(10)-C(7)	2.602	H(102)-C(7)	2.655
H(121)-C(7)	2.034	H(122)-C(7)	2.035
C(13)-C(7)	2.504	H(132)-C(7)	2.693
H(133)-C(7)	2.694	C(14)-C(7)	2.578
H(142)-C(7)	2.685	C(12)-C(8)	2.542
H(121)-C(8)	2.605	H(141)-C(8)	2.053
H(142)-C(8)	2.053	C(15)-C(8)	2.541
H(152)-C(8)	2.729	H(153)-C(8)	2.728
C(16)-C(8)	2.628	H(161)-C(8)	2.798

C(14)-C(9)	2.559	H(141)-C(9)	2.623
H(161)-C(9)	2.023	H(162)-C(9)	2.022
C(17)-C(9)	2.507	H(172)-C(9)	2.699
H(173)-C(9)	2.698	H(111)-C(10)	2.029
H(112)-C(10)	2.033	H(113)-C(10)	2.031
C(12)-C(10)	3.052	H(122)-C(10)	2.680
H(102)-H(101)	1.568	C(11)-H(101)	2.022
H(111)-H(101)	2.307	H(112)-H(101)	2.316
C(11)-H(102)	2.025	H(111)-H(102)	2.310
H(113)-H(102)	2.316	C(12)-H(102)	2.603
H(122)-H(102)	2.002	H(112)-H(111)	1.568
H(113)-H(111)	1.568	H(113)-H(112)	1.568
F(2)-H(112)	2.598	H(131)-C(12)	2.037
H(132)-C(12)	2.035	H(133)-C(12)	2.037
C(14)-C(12)	3.050	H(142)-C(12)	2.664
H(122)-H(121)	1.568	C(13)-H(121)	2.027
H(131)-H(121)	2.315	H(133)-H(121)	2.320
C(14)-H(121)	2.693	H(142)-H(121)	2.061
C(13)-H(122)	2.029	H(131)-H(122)	2.317
H(132)-H(122)	2.320	H(132)-H(131)	1.568
H(133)-H(131)	1.568	H(133)-H(132)	1.568
H(152)-H(133)	2.175	H(151)-C(14)	2.056
H(152)-C(14)	2.056	H(153)-C(14)	2.054
C(16)-C(14)	3.213	H(181)-C(14)	2.621
H(142)-H(141)	1.568	C(15)-H(141)	2.047
H(151)-H(141)	2.336	H(153)-H(141)	2.339
H(191)-H(141)	2.402	C(15)-H(142)	2.046
H(151)-H(142)	2.335	H(152)-H(142)	2.339
H(181)-H(142)	2.153	H(152)-H(151)	1.568
H(153)-H(151)	1.568	H(153)-H(152)	1.568
H(172)-H(153)	2.351	H(171)-C(16)	2.065
H(172)-C(16)	2.067	H(173)-C(16)	2.065

H(162)-H(161)	1.568	C(17)-H(161)	2.059
H(171)-H(161)	2.348	H(172)-H(161)	2.352
C(17)-H(162)	2.061	H(171)-H(162)	2.349
H(173)-H(162)	2.352	H(172)-H(171)	1.568
H(173)-H(171)	1.568	H(173)-H(172)	1.568
F(3)-H(173)	2.430	C(19)-C(18)	2.847
H(193)-C(18)	2.877	C(20)-C(18)	2.841
H(202)-C(18)	2.874	H(182)-H(181)	1.568
H(183)-H(181)	1.568	H(183)-H(182)	1.568
C(19)-H(182)	2.876	C(20)-C(19)	2.827
H(192)-H(191)	1.568	H(193)-H(191)	1.568
H(193)-H(192)	1.568	H(202)-H(201)	1.568
H(203)-H(201)	1.568	H(203)-H(202)	1.568
F(2)-F(1)	2.191	F(3)-F(1)	2.151
F(4)-F(1)	2.078	F(3)-F(2)	2.201
F(4)-F(2)	2.240	F(4)-F(3)	2.119

Intermolecular:

H(141)-Br(1a)	3.304	H(171)-H(11b)	2.435
F(3)-C(3c)	3.200	F(1)-H(31c)	2.452
F(3)-H(31c)	2.632	F(4)-H(51b)	2.352
F(1)-H(171d)	2.723	F(4)-H(182e)	2.427
H(201)-H(191f)	2.410	F(3)-H(192c)	2.588
F(1)-H(202e)	2.543		

Key to symmetry operations relating designated atoms to reference atoms at (x,y,z):

(a) -0.5+x,0.5-y,z

(b) -0.5+x,-0.5-y,z

(c) 0.5-x,-0.5+y,-z

(d) 0.5+x,-0.5-y,z

(e) x,-1.0+y,z

(f) 0.5+x,0.5-y,z

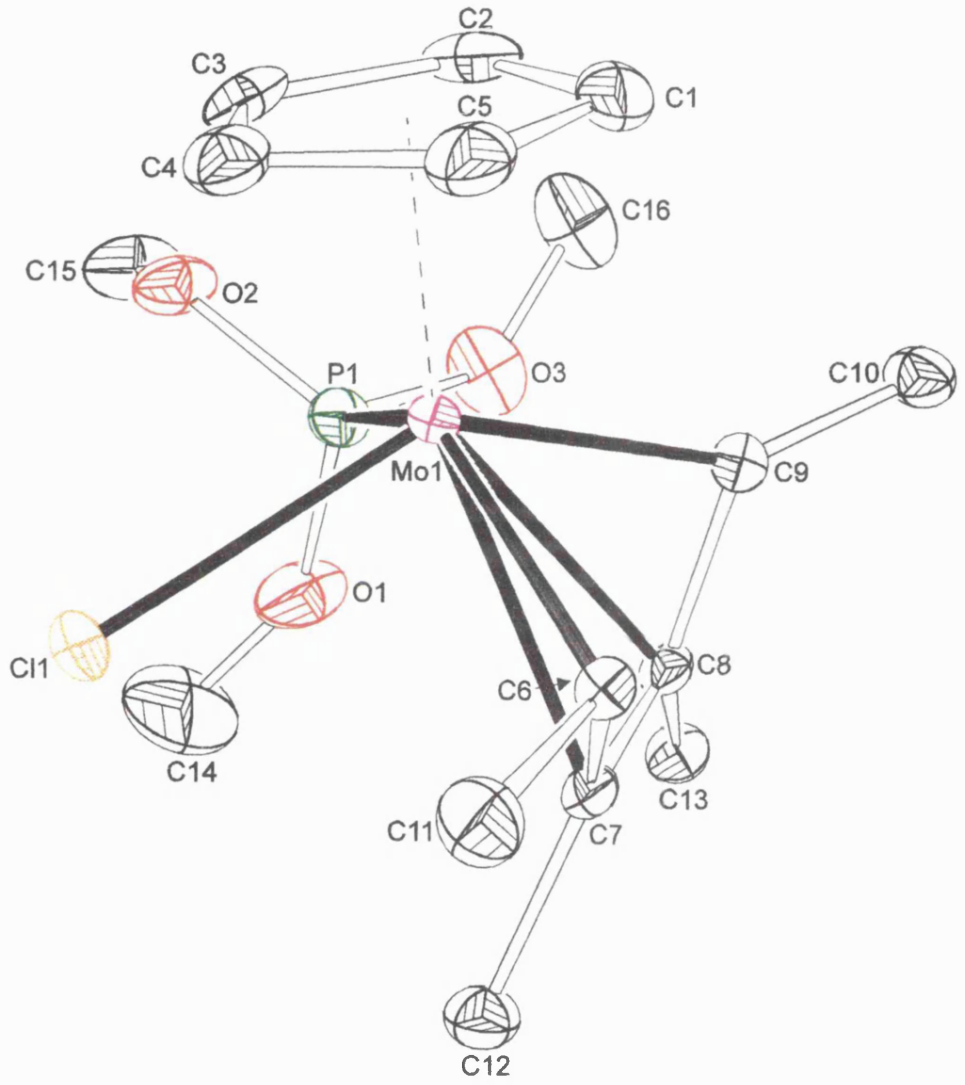

Figure 6.5. ORTEX representation of [ClMo{η^4-CHMe=C(Me).C(Me)=C=CH_2}{$P(OMe)_3$}(η-C_5H_5)] Hydrogen atoms omitted for clarity.

[ClMo{η^4-CHMe=C(Me).C(Me)=C=CH_2}{$P(OMe)_3$}(η-C_5H_5)](38).

A crystal of approximate dimensions 0.2 x 0.2 x 0.15 mm was used for data collection

Crystal Data: $C_{16}H_{26}ClMoO_3P$, M =428.7, monoclinic, a=14.311(5), b=8.801(3), c=14.873(4)Å, β=102.65(3)°, U=1827.8Å^3, space group $P2_1/c$, Z=4, D_c=1.56gcm^{-3}, μ(Mo-K_α)=9.4 cm^{-1}, F(000)=880. Crystallographic measurements were made at 170 K on a CAD4 automatic four-circle diffractometer in the range 2≤θ≤24. 3195 reflections were collected of which 2091 were unique with I≥2σ(I). Data were corrected for Lorentz and polarisation but not for absorption. The structure was solved by Patterson methods and refined using the SHELX[93,94] suite of programs. In the final least squares cycles all atoms were treated anisotropically. Hydrogen atoms were included at calculated positions except in the instance of H61, and H101 and H102 (attached to C6 and C10 respectively) which were located in an advanced Difference Fourier and positionally fixed during the final least squares run. Final residuals after 12 cycles of least squares were R=0.0495, R_w=0.0512, for a weighting scheme of w=2.3416/[σ^2(F) + 0.000941(F)^2]. Max. final shift/esd was 0.05. The max. and min. residual densities were 0.51 and -0.33 eÅ^{-3} respectively. The asymmetric unit is shown in Figure 6.5, along with the labelling scheme used.

Table 6.22.

Fractional atomic co-ordinates ($x10^4$) and equivalent isotropic temperature factors ($Å^2 x10^3$) for (**38**).

	x	y	z	U
Mo(1)	2801	1581(1)	1889	23
P(1)	1277(1)	417(3)	1994(1)	37(1)
Cl(1)	2246(1)	1025(2)	191(1)	35(1)
O(1)	964(5)	-1226(8)	1583(6)	83(3)
O(2)	398(4)	1490(7)	1617(5)	53(2)
O(3)	1135(5)	-175(9)	2980(5)	67(3)
C(1)	3417(7)	3568(9)	2834(6)	48(3)
C(2)	2419(7)	3536(9)	2703(6)	48(3)
C(3)	2003(6)	3795(8)	1746(6)	40(3)
C(4)	2788(6)	4043(9)	1319(6)	38(3)
C(5)	3626(6)	3909(9)	1982(6)	42(3)
C(6)	4296(5)	851(8)	1691(5)	25(2)
C(7)	3812(5)	-587(8)	1732(5)	28(2)
C(8)	3397(5)	-820(8)	2494(5)	27(2)
C(9)	3455(5)	444(8)	3111(5)	27(2)
C(10)	3778(6)	523(9)	4026(5)	37(3)
C(11)	4687(6)	1275(9)	866(5)	35(3)
C(12)	3724(6)	-1758(8)	965(5)	36(3)
C(13)	2977(5)	-2327(8)	2682(6)	35(3)
C(14)	741(13)	-1778(16)	772(11)	121(8)
C(15)	-576(6)	1033(12)	1696(9)	74(4)
C(16)	1224(7)	713(15)	3744(7)	76(5)

Table 6.23.

Anisotropic temperature factors (Å x10^3) for (**38**).

	U_{11}	U_{22}	U_{33}	U_{23}	U_{13}	U_{12}
Mo(1)	26	20	22	-4	2	2
P(1)	27(1)	39(1)	43(1)	-8(1)	4(1)	-3(1)
Cl(1)	37(1)	41(1)	22(1)	-5(1)	-3(1)	2(1)
O(1)	47(4)	57(5)	128(7)	-40(5)	-14(4)	3(3)
O(2)	30(3)	47(4)	81(4)	-17(3)	9(3)	7(3)
O(3)	60(4)	83(5)	63(4)	2(4)	22(3)	-25(4)
C(1)	69(6)	23(4)	44(5)	-5(4)	-6(4)	-2(4)
C(2)	85(7)	20(4)	50(5)	-3(4)	40(5)	5(4)
C(3)	38(4)	17(4)	66(6)	4(4)	10(4)	7(3)
C(4)	50(5)	21(4)	44(5)	2(4)	13(4)	1(4)
C(5)	44(5)	24(4)	55(5)	-4(4)	3(4)	0(4)
C(6)	24(4)	24(4)	26(4)	0(3)	5(3)	3(3)
C(7)	26(4)	23(4)	32(4)	-4(3)	1(3)	7(3)
C(8)	27(4)	18(4)	34(4)	0(3)	1(3)	3(3)
C(9)	26(4)	27(4)	27(4)	1(3)	5(3)	0(3)
C(10)	49(5)	34(5)	29(4)	1(3)	9(4)	2(4)
C(11)	38(4)	37(5)	31(4)	1(3)	10(3)	-1(4)
C(12)	38(4)	30(5)	39(4)	-10(4)	9(3)	1(3)
C(13)	40(4)	24(4)	43(5)	4(4)	10(4)	-1(4)
C(14)	167(16)	81(11)	109(12)	-51(9)	19(11)	-26(10)
C(15)	23(5)	70(7)	127(10)	-36(7)	9(5)	-3(5)
C(16)	58(6)	127(10)	54(6)	-16(7)	33(5)	-21(7)

The temperature factor exponent takes the form:

-2 (U .h .a* + ... +2U .h.k.a*.b*)

Table 6.24.

Hydrogen fractional atomic co-ordinates ($x10^4$) and isotropic temperature factors ($Å^2 x10^3$) for (**38**).

	x	y	z	U
H(11)	3929(7)	3366(9)	3473(6)	93(8)
H(21)	2026(7)	3346(9)	3235(6)	93(8)
H(31)	1251(6)	3800(8)	1418(6)	93(8)
H(41)	2737(6)	4296(9)	599(6)	93(8)
H(51)	4338(6)	4046(9)	1861(6)	93(8)
H(61)	4665	911	2425	93(8)
H(102)	3612	1761	4185	93(8)
H(101)	4186	-335	4408	93(8)
H(111)	4147(6)	1082(9)	245(5)	93(8)
H(112)	5309(6)	589(9)	850(5)	93(8)
H(113)	4886(6)	2461(9)	909(5)	93(8)
H(121)	4093(6)	-1354(8)	452(5)	93(8)
H(122)	2977(6)	-1933(8)	652(5)	93(8)
H(123)	4039(6)	-2817(8)	1248(5)	93(8)
H(131)	2700(5)	-2242(8)	3300(6)	93(8)
H(132)	3527(5)	-3189(8)	2775(6)	93(8)
H(133)	2404(5)	-2630(8)	2108(6)	93(8)
H(141)	578(13)	-2969(16)	821(11)	93(8)
H(142)	1329(13)	-1651(16)	430(11)	93(8)
H(143)	119(13)	-1194(16)	383(11)	93(8)
H(151)	-1078(6)	1910(12)	1402(9)	93(8)
H(152)	-593(6)	875(12)	2412(9)	93(8)
H(153)	-768(6)	-18(12)	1326(9)	93(8)
H(161)	1093(7)	38(15)	4310(7)	93(8)
H(162)	710(7)	1629(15)	3605(7)	93(8)
H(163)	1939(7)	1178(15)	3922(7)	93(8)

Table 6.25.

Bond lengths (Å) for (**38**).

P(1)-Mo(1)	2.446(4)	Cl(1)-Mo(1)	2.523(5)
C(1)-Mo(1)	2.294(10)	C(2)-Mo(1)	2.239(10)
C(3)-Mo(1)	2.244(9)	C(4)-Mo(1)	2.324(10)
C(5)-Mo(1)	2.353(10)	C(6)-Mo(1)	2.313(9)
C(7)-Mo(1)	2.437(9)	C(8)-Mo(1)	2.380(9)
C(9)-Mo(1)	2.106(9)	O(1)-P(1)	1.595(9)
O(2)-P(1)	1.575(8)	O(3)-P(1)	1.610(9)
C(14)-O(1)	1.273(16)	C(15)-O(2)	1.479(11)
C(16)-O(3)	1.362(13)	C(2)-C(1)	1.398(14)
C(5)-C(1)	1.397(13)	C(3)-C(2)	1.436(13)
C(4)-C(3)	1.423(12)	C(5)-C(4)	1.381(12)
C(7)-C(6)	1.450(11)	C(11)-C(6)	1.504(11)
C(8)-C(7)	1.404(11)	C(12)-C(7)	1.522(11)
C(9)-C(8)	1.433(11)	C(13)-C(8)	1.507(12)
C(10)-C(9)	1.341(11)	H(11)-C(1)	1.080
H(21)-C(2)	1.080	H(31)-C(3)	1.080
H(41)-C(4)	1.080	H(51)-C(5)	1.080
H(61)-C(6)	1.106(8)	H(102)-C(10)	1.151(9)
H(101)-C(10)	1.043(9)	H(111)-C(11)	1.080
H(112)-C(11)	1.080	H(113)-C(11)	1.080
H(121)-C(12)	1.080	H(122)-C(12)	1.080
H(123)-C(12)	1.080	H(131)-C(13)	1.080
H(132)-C(13)	1.080	H(133)-C(13)	1.080
H(141)-C(14)	1.080	H(142)-C(14)	1.080
H(143)-C(14)	1.080	H(151)-C(15)	1.080
H(152)-C(15)	1.080	H(153)-C(15)	1.080
H(161)-C(16)	1.080	H(162)-C(16)	1.080
H(163)-C(16)	1.080		

Table 6.26.

Bond angles (°) for (**38**).

Cl(1)-Mo(1)-P(1)	83.8(2)	C(1)-Mo(1)-P(1)	120.6(4)
C(1)-Mo(1)-Cl(1)	139.1(2)	C(2)-Mo(1)-P(1)	87.8(4)
C(2)-Mo(1)-Cl(1)	129.0(4)	C(2)-Mo(1)-C(1)	35.9(3)
C(3)-Mo(1)-P(1)	85.9(3)	C(3)-Mo(1)-Cl(1)	91.8(3)
C(3)-Mo(1)-C(1)	61.1(4)	C(3)-Mo(1)-C(2)	37.3(3)
C(4)-Mo(1)-P(1)	118.6(3)	C(4)-Mo(1)-Cl(1)	80.8(3)
C(4)-Mo(1)-C(1)	59.0(4)	C(4)-Mo(1)-C(2)	59.9(4)
C(4)-Mo(1)-C(3)	36.2(3)	C(5)-Mo(1)-P(1)	143.5(2)
C(5)-Mo(1)-Cl(1)	105.8(3)	C(5)-Mo(1)-C(1)	35.0(3)
C(5)-Mo(1)-C(2)	58.5(4)	C(5)-Mo(1)-C(3)	59.2(4)
C(5)-Mo(1)-C(4)	34.3(3)	C(6)-Mo(1)-P(1)	138.9(2)
C(6)-Mo(1)-Cl(1)	85.1(3)	C(6)-Mo(1)-C(1)	92.8(4)
C(6)-Mo(1)-C(2)	128.7(4)	C(6)-Mo(1)-C(3)	134.0(3)
C(6)-Mo(1)-C(4)	98.4(4)	C(6)-Mo(1)-C(5)	77.5(4)
C(7)-Mo(1)-P(1)	103.6(3)	C(7)-Mo(1)-Cl(1)	79.4(3)
C(7)-Mo(1)-C(1)	119.9(4)	C(7)-Mo(1)-C(2)	150.9(3)
C(7)-Mo(1)-C(3)	166.2(3)	C(7)-Mo(1)-C(4)	130.7(3)
C(7)-Mo(1)-C(5)	112.7(4)	C(7)-Mo(1)-C(6)	35.4(2)
C(8)-Mo(1)-P(1)	81.6(3)	C(8)-Mo(1)-Cl(1)	102.3(3)
C(8)-Mo(1)-C(1)	112.8(4)	C(8)-Mo(1)-C(2)	126.0(4)
C(8)-Mo(1)-C(3)	159.9(3)	C(8)-Mo(1)-C(4)	159.8(3)
C(8)-Mo(1)-C(5)	128.1(4)	C(8)-Mo(1)-C(6)	62.4(4)
C(8)-Mo(1)-C(7)	33.9(2)	C(9)-Mo(1)-P(1)	88.9(3)
C(9)-Mo(1)-Cl(1)	138.9(2)	C(9)-Mo(1)-C(1)	78.2(4)
C(9)-Mo(1)-C(2)	90.8(4)	C(9)-Mo(1)-C(3)	128.0(4)
C(9)-Mo(1)-C(4)	136.4(3)	C(9)-Mo(1)-C(5)	103.9(4)
C(9)-Mo(1)-C(6)	74.3(4)	C(9)-Mo(1)-C(7)	63.2(4)

C(9)-Mo(1)-C(8)	36.6(3)	O(2)-P(1)-O(1)	105.8(4)
O(3)-P(1)-O(1)	88.6(5)	O(3)-P(1)-O(2)	105.6(5)
C(14)-O(1)-P(1)	134.4(10)	C(15)-O(2)-P(1)	120.1(7)
C(16)-O(3)-P(1)	124.5(8)	C(5)-C(1)-C(2)	107.0(8)
C(3)-C(2)-C(1)	108.9(8)	C(4)-C(3)-C(2)	105.7(8)
C(5)-C(4)-C(3)	108.4(8)	C(4)-C(5)-C(1)	109.9(9)
C(11)-C(6)-C(7)	121.2(7)	C(8)-C(7)-C(6)	116.8(7)
C(12)-C(7)-C(6)	121.4(7)	C(12)-C(7)-C(8)	121.7(7)
C(9)-C(8)-C(7)	115.3(7)	C(13)-C(8)-C(7)	122.3(7)
C(13)-C(8)-C(9)	122.2(7)	C(10)-C(9)-C(8)	130.5(7)
C(2)-C(1)-H(11)	126.5(6)	C(5)-C(1)-H(11)	126.5(6)
H(21)-C(2)-C(1)	125.5(6)	C(3)-C(2)-H(21)	125.5(6)
H(31)-C(3)-C(2)	127.2(6)	C(4)-C(3)-H(31)	127.1(6)
H(41)-C(4)-C(3)	125.8(6)	C(5)-C(4)-H(41)	125.8(6)
H(51)-C(5)-C(1)	125.0(6)	H(51)-C(5)-C(4)	125.1(6)
C(7)-C(6)-H(61)	97.4(6)	C(11)-C(6)-H(61)	127.7(7)
H(102)-C(10)-C(9)	102.5(7)	H(101)-C(10)-C(9)	122.9(8)
H(101)-C(10)-H(102)	133.6(7)	H(111)-C(11)-C(6)	109.5(5)
H(112)-C(11)-C(6)	109.6(5)	H(112)-C(11)-H(111)	109.5
H(113)-C(11)-C(6)	109.3(5)	H(113)-C(11)-H(111)	109.5
H(113)-C(11)-H(112)	109.5	H(121)-C(12)-C(7)	109.5(5)
H(122)-C(12)-C(7)	109.4(5)	H(122)-C(12)-H(121)	109.5
H(123)-C(12)-C(7)	109.5(5)	H(123)-C(12)-H(121)	109.5
H(123)-C(12)-H(122)	109.5	H(131)-C(13)-C(8)	109.4(5)
H(132)-C(13)-C(8)	109.4(5)	H(132)-C(13)-H(131)	109.5
H(133)-C(13)-C(8)	109.6(5)	H(133)-C(13)-H(131)	109.5
H(133)-C(13)-H(132)	109.5	H(141)-C(14)-O(1)	108.7(9)
H(142)-C(14)-O(1)	110.3(10)	H(142)-C(14)-H(141)	109.5
H(143)-C(14)-O(1)	109.4(10)	H(143)-C(14)-H(141)	109.5
H(143)-C(14)-H(142)	109.5	H(151)-C(15)-O(2)	109.2(6)
H(152)-C(15)-O(2)	109.8(6)	H(152)-C(15)-H(151)	109.5
H(153)-C(15)-O(2)	109.4(6)	H(153)-C(15)-H(151)	109.5

H(153)-C(15)-H(152)	109.5	H(161)-C(16)-O(3)	109.5(7)
H(162)-C(16)-O(3)	109.5(7)	H(162)-C(16)-H(161)	109.5
H(163)-C(16)-O(3)	109.4(6)	H(163)-C(16)-H(161)	109.5
H(163)-C(16)-H(162)	109.5		

Table 6.27.

Selected non-bonded distances [Å] for (**38**).

Intramolecular:

O(1)-Mo(1)	3.564	O(2)-Mo(1)	3.374
O(3)-Mo(1)	3.521	H(11)-Mo(1)	2.992
H(21)-Mo(1)	2.936	H(31)-Mo(1)	2.922
H(41)-Mo(1)	3.052	H(51)-Mo(1)	3.096
H(61)-Mo(1)	2.687	C(10)-Mo(1)	3.312
H(102)-Mo(1)	3.348	C(11)-Mo(1)	3.388
C(12)-Mo(1)	3.614	C(13)-Mo(1)	3.627
Cl(1)-P(1)	3.320	C(2)-P(1)	3.251
C(3)-P(1)	3.198	H(31)-P(1)	3.096
C(8)-P(1)	3.155	C(9)-P(1)	3.195
C(13)-P(1)	3.422	H(133)-P(1)	3.115
C(14)-P(1)	2.647	H(142)-P(1)	2.966
H(143)-P(1)	2.959	C(15)-P(1)	2.646
H(152)-P(1)	2.905	H(153)-P(1)	2.902
C(16)-P(1)	2.634	H(162)-P(1)	2.897
H(163)-P(1)	2.895	C(3)-Cl(1)	3.429
C(4)-Cl(1)	3.146	H(41)-Cl(1)	2.994
C(6)-Cl(1)	3.277	C(7)-Cl(1)	3.168
C(11)-Cl(1)	3.424	H(111)-Cl(1)	2.705
C(12)-Cl(1)	3.276	H(122)-Cl(1)	2.833
C(14)-Cl(1)	3.505	H(142)-Cl(1)	2.757
O(2)-O(1)	2.528	O(3)-O(1)	2.238
C(13)-O(1)	3.139	H(133)-O(1)	2.384
H(141)-O(1)	1.916	H(142)-O(1)	1.935

H(143)-O(1)	1.924	C(15)-O(1)	3.000
H(153)-O(1)	2.647	O(3)-O(2)	2.536
C(3)-O(2)	3.040	H(31)-O(2)	2.423
C(14)-O(2)	3.219	H(151)-O(2)	2.099
H(152)-O(2)	2.106	H(153)-O(2)	2.101
C(16)-O(2)	3.199	C(15)-O(3)	2.954
H(152)-O(3)	2.602	H(161)-O(3)	2.001
H(162)-O(3)	2.001	H(163)-O(3)	2.000
H(21)-C(1)	2.208	C(3)-C(1)	2.306
C(4)-C(1)	2.275	H(51)-C(1)	2.202
C(9)-C(1)	2.779	C(10)-C(1)	3.192
H(102)-C(1)	2.529	C(2)-H(11)	2.217
C(5)-H(11)	2.216	C(9)-H(11)	2.684
C(10)-H(11)	2.657	H(102)-H(11)	1.879
H(31)-C(2)	2.258	C(4)-C(2)	2.278
C(5)-C(2)	2.247	C(9)-C(2)	3.094
C(3)-H(21)	2.243	C(16)-H(21)	2.764
H(163)-H(21)	2.181	H(41)-C(3)	2.234
C(5)-C(3)	2.274	C(4)-H(31)	2.246
H(51)-C(4)	2.188	C(5)-H(41)	2.195
C(6)-C(5)	2.920	C(6)-H(51)	2.823
H(113)-H(51)	2.248	C(8)-C(6)	2.432
C(9)-C(6)	2.674	H(111)-C(6)	2.124
H(112)-C(6)	2.125	H(113)-C(6)	2.122
C(12)-C(6)	2.592	H(121)-C(6)	2.648
C(7)-H(61)	1.934	C(8)-H(61)	2.389
C(9)-H(61)	2.231	C(11)-H(61)	2.349
C(9)-C(7)	2.397	C(11)-C(7)	2.573
H(111)-C(7)	2.783	H(121)-C(7)	2.140
H(122)-C(7)	2.138	H(123)-C(7)	2.140
C(13)-C(7)	2.551	H(132)-C(7)	2.845
H(133)-C(7)	2.846	C(10)-C(8)	2.519

H(101)-C(8)	2.856	C(12)-C(8)	2.556
H(122)-C(8)	2.847	H(123)-C(8)	2.848
H(131)-C(8)	2.127	H(132)-C(8)	2.126
H(133)-C(8)	2.128	H(102)-C(9)	1.947
H(101)-C(9)	2.099	C(13)-C(9)	2.575
H(131)-C(9)	2.639	H(163)-C(9)	2.780
C(13)-C(10)	3.255	H(163)-C(10)	2.666
H(101)-H(102)	2.018	H(163)-H(102)	2.396
C(12)-C(11)	3.022	H(121)-C(11)	2.495
H(112)-H(111)	1.764	H(113)-H(111)	1.764
C(12)-H(111)	2.836	H(121)-H(111)	2.169
H(113)-H(112)	1.764	H(121)-H(112)	2.419
C(13)-C(12)	3.018	H(122)-H(121)	1.764
H(123)-H(121)	1.764	H(123)-H(122)	1.764
H(142)-H(122)	2.323	H(132)-H(131)	1.764
H(133)-H(131)	1.764	H(133)-H(132)	1.764
C(14)-H(133)	2.846	H(142)-H(141)	1.764
H(143)-H(141)	1.764	H(143)-H(142)	1.764
H(153)-H(143)	2.331	H(152)-H(151)	1.764
H(153)-H(151)	1.764	H(153)-H(152)	1.764
H(162)-H(152)	2.369	H(162)-H(161)	1.764
H(163)-H(161)	1.764	H(163)-H(162)	1.764

Intermolecular:

H(153)-Cl(1a)	2.874	H(21)-Cl(1b)	2.911
H(163)-Cl(1b)	3.075	H(151)-O(3c)	2.732
H(132)-C(1d)	2.862	H(112)-H(11e)	2.356
H(132)-C(5d)	2.830	H(61)-H(51e)	2.279
H(113)-H(101f)	2.454	H(112)-H(111g)	2.445
H(121)-H(112g)	2.378	H(162)-C(14c)	2.824

H(162)-H(141c)	2.223	H(143)-H(143a)	2.379

Key to symmetry operations relating designated atoms to reference atoms at (x,y,z):

(a) -x,-y,-z

(b) x,0.5-y,0.5+z

(c) -x,0.5+y,0.5-z

(d) x,-1.0+y,z

(e) 1.0-x,-0.5+y,0.5-z

(f) 1.0-x,0.5+y,0.5-z

(g) 1.0-x,-y,-z

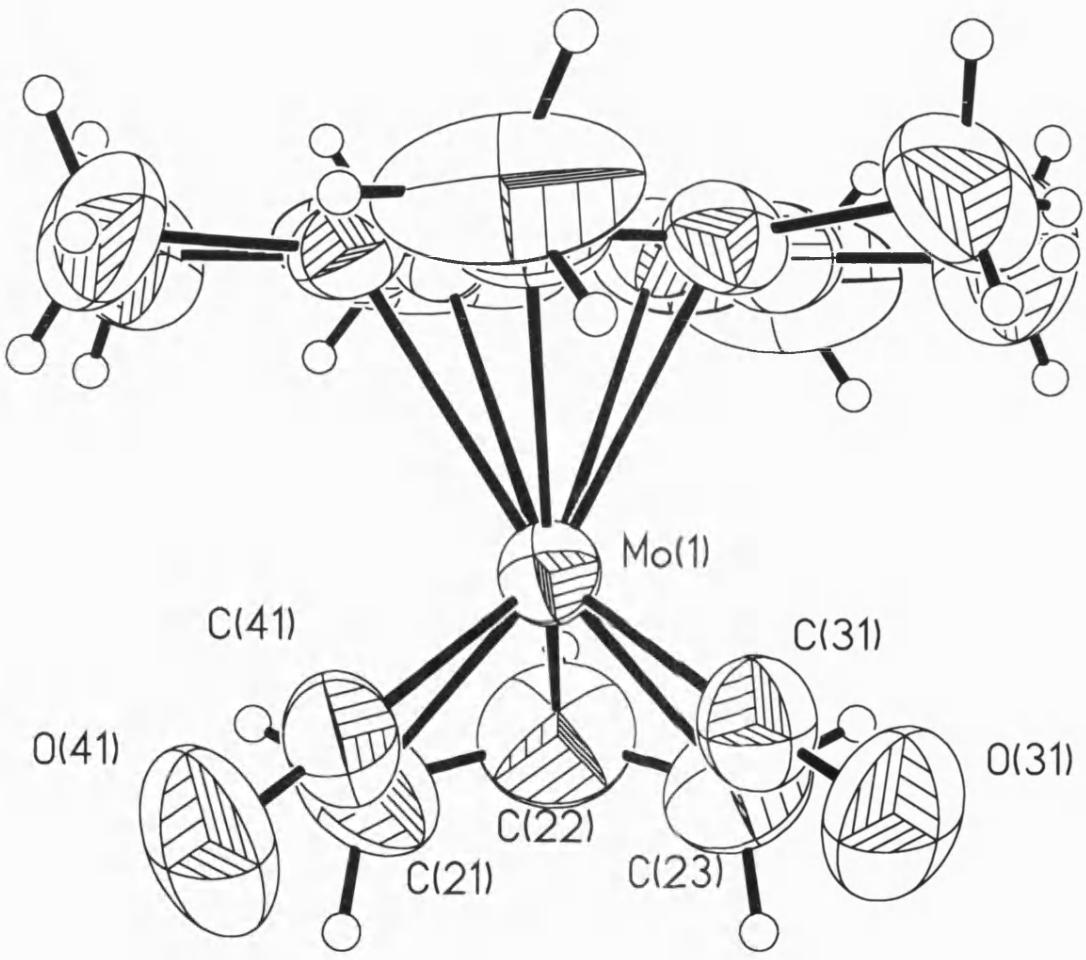

Figure 6.6. ORTEP representation of [Mo(η^3-C_3H_5)(CO)$_2$(η^5-C_9Me_7)] (**69**).

$[Mo(\eta^3\text{-}C_3H_5)(CO)_2(\eta^5\text{-}C_9Me_7)][BF_4]$ (69).

Large yellow *blocks* of (**69**) were obtained by cooling a pentane solution to -30°C. A crystal of approximate dimensions 0.4 x 0.4 x 0.2 mm was chosen for data collection. Data were measured at 293(2)K on a Siemens P4 automatic four-circle diffractometer operating in the ω-scan mode, with graphite-monochromated Mo K_α X-radiation ($\bar{\lambda}$ = 0.71073Å).

Crystal Data — $C_{21}H_{26}MoO_2$. M_r = 406.36, monoclinic, $P2_1/n$, a = 12.3952(13), b = 9.5466(9), c = 16.6038(13)Å, β = 104.746(5)°, U = 1900.0(3)Å^2, Z = 4, D_c = 1.625gcm^{-3}, μ = 0.70mm^{-1}, F(000) = 840. Cell parameters from 26 centred reflections in the range $5 \leq \theta \leq 13°$

Data Collection and Processing — One quadrant of diffracted data were measured for $1.84 \leq \theta \leq 25.00°$ ($-1 \leq h \leq 14$, $-1 \leq k \leq 11$, $-19 \leq l \leq 19$). Three standard reflections were redetermined after every 97 reflections measured, and revealed negligible crystal decay or movement. A total of 4348 data were measured, of which 3345 were unique [R_{int} = 0.0289]. A semi-empirical absorption correction (psi scans) was applied (T_{min} 0.3012, T_{max} 0.3436).

Structure Solution and Refinement — The structure was solved (Mo, O and most C atoms) without difficulty by direct methods (*SHELXS*-86)[93], and refined (*SHELXL*-93)[94] on F^2 by full-matrix least-squares methods; the remaining C atoms were readily located in the first difference Fourier synthesis. Although some of the H atoms could be found in subsequent difference Fourier maps, all were set riding in calculated positions [C—H = 0.98Å (CH of allyl), 0.97Å (CH_2 of allyl), 0.96Å (CH_3)] with isotropic thermal parameters calculated as 1.2 (C_3H_5) or 1.5 (CH_3) times the corresponding (equivalent) isotropic thermal parameter for the parent C atom. Following isotropic convergence, all non-H atoms were successfully allowed anisotropic thermal motion. The structure converged to a conventional [*i.e.*, based on 1891 data with $F_o > 4\sigma(F_o)$] R_1 = 0.0437 (0.0707 for all data) and wR_2 = 0.1142. Goodness of fit = 1.013. The maximum and minimum residual electron densities in the final difference map were 0.69 and -0.37e/Å^{-3} respectively.

Table 6.28.Atomic coordinates (x 10^4) and equivalent isotropic displacement parameters ($Å^2$ x 10^3) for (**69**) U(eq) is defined as one third of the trace of the orthogonalized Uij tensor.

	x	y	z	U(eq)
Mo(1)	2421(1)	7987(1)	489(1)	42(1)
C(1)	4281(4)	7261(6)	924(4)	61(2)
C(2)	3684(5)	6732(7)	1489(3)	65(2)
C(3)	2869(5)	5772(6)	1074(3)	57(1)
C(4)	2989(4)	5643(5)	238(3)	46(1)
C(5)	2383(5)	4826(7)	-453(5)	72(2)
C(6)	2689(8)	4898(9)	-1179(4)	87(2)
C(7)	3569(8)	5719(9)	-1264(4)	85(2)
C(8)	4166(6)	6564(7)	-638(5)	73(2)
C(9)	3862(4)	6548(5)	152(3)	47(1)
C(10)	5263(6)	8226(9)	1175(7)	115(3)
C(20)	3959(8)	7064(11)	2414(4)	123(4)
C(30)	2184(8)	4879(9)	1505(5)	101(3)
C(50)	1441(7)	3905(11)	-362(7)	130(4)
C(60)	2036(10)	4108(12)	-1952(6)	161(6)
C(70)	3914(11)	5685(13)	-2078(5)	169(6)
C(80)	5105(8)	7495(10)	-706(7)	134(4)
C(21)	2285(7)	9502(8)	-638(4)	83(2)
C(22)	1629(7)	8349(10)	-844(4)	92(3)
C(23)	765(6)	7963(9)	-551(4)	80(2)
C(31)	1277(5)	8189(6)	1096(4)	59(1)
O(31)	625(4)	8290(6)	1480(3)	87(2)
C(41)	2768(5)	9822(6)	987(4)	60(2)
O(41)	2986(5)	10883(5)	1318(4)	97(2)

Table 6.29. Bond lengths (Å) and angles (°) for (**69**).

Mo(1)-C(41)	1.938(6)	C(2)-Mo(1)-C(4)	57.9(2)
Mo(1)-C(31)	1.947(6)	C(23)-Mo(1)-C(4)	96.0(2)
Mo(1)-C(22)	2.209(6)	C(3)-Mo(1)-C(4)	35.2(2)
Mo(1)-C(2)	2.307(6)	C(21)-Mo(1)-C(4)	113.6(2)
Mo(1)-C(23)	2.322(6)	C(1)-Mo(1)-C(4)	58.0(2)
Mo(1)-C(3)	2.334(6)	C(41)-Mo(1)-C(9)	120.9(2)
Mo(1)-C(21)	2.337(6)	C(31)-Mo(1)-C(9)	148.3(2)
Mo(1)-C(1)	2.338(5)	C(22)-Mo(1)-C(9)	91.3(3)
Mo(1)-C(4)	2.414(5)	C(2)-Mo(1)-C(9)	57.9(2)
Mo(1)-C(9)	2.429(5)	C(23)-Mo(1)-C(9)	112.7(2)
C(1)-C(9)	1.427(8)	C(3)-Mo(1)-C(9)	58.1(2)
C(1)-C(2)	1.427(9)	C(21)-Mo(1)-C(9)	94.2(2)
C(1)-C(10)	1.499(8)	C(1)-Mo(1)-C(9)	34.8(2)
C(2)-C(3)	1.408(9)	C(4)-Mo(1)-C(9)	34.1(2)
C(2)-C(20)	1.518(8)	C(9)-C(1)-C(2)	107.0(5)
C(3)-C(4)	1.438(7)	C(9)-C(1)-C(10)	128.7(7)
C(3)-C(30)	1.508(9)	C(2)-C(1)-C(10)	123.7(7)
C(4)-C(9)	1.421(7)	C(9)-C(1)-Mo(1)	76.1(3)
C(4)-C(5)	1.432(8)	C(2)-C(1)-Mo(1)	70.9(3)
C(5)-C(6)	1.354(11)	C(10)-C(1)-Mo(1)	124.8(4)
C(5)-C(50)	1.500(11)	C(3)-C(2)-C(1)	109.6(5)
C(6)-C(7)	1.379(12)	C(3)-C(2)-C(20)	125.4(7)
C(6)-C(60)	1.530(10)	C(1)-C(2)-C(20)	124.8(7)
C(7)-C(8)	1.373(11)	C(3)-C(2)-Mo(1)	73.4(3)
C(7)-C(70)	1.518(9)	C(1)-C(2)-Mo(1)	73.3(3)
C(8)-C(9)	1.455(8)	C(20)-C(2)-Mo(1)	123.8(5)
C(8)-C(80)	1.492(10)	C(2)-C(3)-C(4)	107.0(5)
C(21)-C(22)	1.359(10)	C(2)-C(3)-C(30)	123.8(6)
C(22)-C(23)	1.337(11)	C(4)-C(3)-C(30)	128.3(6)
C(31)-O(31)	1.154(7)	C(2)-C(3)-Mo(1)	71.3(3)

C(41)-O(41)	1.152(7)	C(4)-C(3)-Mo(1)	75.5(3)
C(41)-Mo(1)-C(31)	78.5(2)	C(30)-C(3)-Mo(1)	127.4(5)
C(41)-Mo(1)-C(22)	106.2(3)	C(9)-C(4)-C(5)	120.6(5)
C(31)-Mo(1)-C(22)	107.9(3)	C(9)-C(4)-C(3)	108.2(5)
C(41)-Mo(1)-C(2)	97.2(2)	C(5)-C(4)-C(3)	131.2(6)
C(31)-Mo(1)-C(2)	97.4(2)	C(9)-C(4)-Mo(1)	73.5(3)
C(22)-Mo(1)-C(2)	148.2(3)	C(5)-C(4)-Mo(1)	121.8(4)
C(41)-Mo(1)-C(23)	112.6(3)	C(3)-C(4)-Mo(1)	69.3(3)
C(31)-Mo(1)-C(23)	76.3(3)	C(6)-C(5)-C(4)	118.5(7)
C(22)-Mo(1)-C(23)	34.2(3)	C(6)-C(5)-C(50)	121.4(8)
C(2)-Mo(1)-C(23)	147.1(3)	C(4)-C(5)-C(50)	120.1(7)
C(41)-Mo(1)-C(3)	129.6(2)	C(5)-C(6)-C(7)	121.9(7)
C(31)-Mo(1)-C(3)	90.1(2)	C(5)-C(6)-C(60)	120.9(10)
C(22)-Mo(1)-C(3)	123.8(3)	C(7)-C(6)-C(60)	117.2(9)
C(2)-Mo(1)-C(3)	35.3(2)	C(8)-C(7)-C(6)	122.9(6)
C(23)-Mo(1)-C(3)	111.9(3)	C(8)-C(7)-C(70)	117.8(10)
C(41)-Mo(1)-C(21)	75.2(3)	C(6)-C(7)-C(70)	119.3(9)
C(31)-Mo(1)-C(21)	116.1(3)	C(7)-C(8)-C(9)	117.7(6)
C(22)-Mo(1)-C(21)	34.6(3)	C(7)-C(8)-C(80)	125.0(8)
C(2)-Mo(1)-C(21)	142.7(3)	C(9)-C(8)-C(80)	117.3(8)
C(23)-Mo(1)-C(21)	62.7(3)	C(4)-C(9)-C(1)	108.2(5)
C(3)-Mo(1)-C(21)	148.7(2)	C(4)-C(9)-C(8)	118.3(5)
C(41)-Mo(1)-C(1)	92.4(2)	C(1)-C(9)-C(8)	133.4(6)
C(31)-Mo(1)-C(1)	131.3(2)	C(4)-C(9)-Mo(1)	72.4(3)
C(22)-Mo(1)-C(1)	120.5(3)	C(1)-C(9)-Mo(1)	69.1(3)
C(2)-Mo(1)-C(1)	35.8(2)	C(8)-C(9)-Mo(1)	125.2(4)
C(23)-Mo(1)-C(1)	147.4(3)	C(22)-C(21)-Mo(1)	67.5(4)
C(3)-Mo(1)-C(1)	59.4(2)	C(23)-C(22)-C(21)	127.9(9)
C(21)-Mo(1)-C(1)	107.2(3)	C(23)-C(22)-Mo(1)	77.5(4)
C(41)-Mo(1)-C(4)	150.3(2)	C(21)-C(22)-Mo(1)	77.9(4)
C(31)-Mo(1)-C(4)	117.7(2)	C(22)-C(23)-Mo(1)	68.3(4)
C(22)-Mo(1)-C(4)	92.7(3)	O(31)-C(31)-Mo(1)	177.7(6)

O(41)-C(41)-Mo(1) 176.9(6)

Table 6.30. Anisotropic displacement parameters ($Å^2$ x 10^3) for (**69**). The anisotropic displacement factor exponent takes the form:
$-2\pi^2 [h^2 a^{*2} U_{11} + ... + 2 h k a^* b^* U_{12}]$

	U_{11}	U_{22}	U_{33}	U_{23}	U_{13}	U_{12}
Mo(1)	43(1)	44(1)	40(1)	0(1)	9(1)	-1(1)
C(1)	40(3)	45(3)	86(4)	-6(3)	-5(3)	4(2)
C(2)	74(4)	69(4)	44(3)	-5(3)	-1(3)	24(3)
C(3)	67(3)	54(3)	54(3)	15(3)	26(3)	9(3)
C(4)	50(3)	41(3)	47(3)	2(2)	11(2)	2(2)
C(5)	66(4)	54(3)	82(4)	-13(3)	-9(3)	1(3)
C(6)	118(6)	80(5)	49(4)	-12(3)	-6(4)	39(5)
C(7)	134(7)	77(5)	48(3)	4(3)	32(4)	52(5)
C(8)	73(4)	67(4)	97(5)	36(4)	54(4)	29(3)
C(9)	46(3)	42(3)	54(3)	5(2)	15(2)	3(2)
C(10)	53(4)	81(6)	189(10)	-41(6)	-5(5)	-16(4)
C(20)	153(8)	148(8)	47(3)	-29(5)	-16(4)	76(7)
C(30)	129(7)	82(5)	114(6)	32(5)	70(6)	10(5)
C(50)	95(6)	100(7)	177(10)	-39(7)	1(6)	-38(6)
C(60)	199(12)	143(10)	98(7)	-72(7)	-44(7)	57(9)
C(70)	278(15)	179(11)	84(5)	51(7)	109(8)	141(11)
C(80)	122(8)	108(7)	213(12)	60(7)	119(8)	14(6)
C(21)	115(6)	69(4)	60(4)	19(3)	12(4)	-2(4)
C(22)	98(6)	118(7)	49(3)	15(4)	2(4)	9(5)
C(23)	67(4)	101(5)	58(3)	-3(4)	-8(3)	6(4)
C(31)	62(3)	58(4)	59(3)	-6(3)	20(3)	-8(3)
O(31)	78(3)	99(4)	100(3)	-18(3)	51(3)	-11(3)
C(41)	66(4)	53(3)	68(4)	-7(3)	29(3)	-10(3)
O(41)	122(4)	64(3)	122(4)	-37(3)	64(4)	-33(3)

Table 6.31. Hydrogen coordinates (x 10^4) and isotropic displacement parameters ($Å^2$ x 10^3) for (**69**).

	x	y	z	U(eq)
H(10C)	5337(6)	8544(9)	1735(7)	172
H(10B)	5154(6)	9016(9)	805(7)	172
H(10A)	5928(6)	7735(9)	1144(7)	172
H(20A)	4543(8)	7751(11)	2545(4)	185
H(20B)	4200(8)	6226(11)	2727(4)	185
H(20C)	3307(8)	7425(11)	2554(4)	185
H(30A)	1683(8)	4305(9)	1102(5)	152
H(30B)	1762(8)	5471(9)	1780(5)	152
H(30C)	2670(8)	4291(9)	1909(5)	152
H(50A)	1347(7)	3992(11)	192(7)	195
H(50B)	1606(7)	2949(11)	-464(7)	195
H(50C)	766(7)	4186(11)	-756(7)	195
H(60C)	2369(10)	4279(12)	-2406(6)	242
H(60A)	1277(10)	4428(12)	-2100(6)	242
H(60B)	2054(10)	3123(12)	-1835(6)	242
H(70B)	3434(11)	5059(13)	-2460(5)	253
H(70A)	4672(11)	5366(13)	-1976(5)	253
H(70C)	3856(11)	6609(13)	-2313(5)	253
H(80A)	5387(8)	7979(10)	-188(7)	201
H(80B)	4843(8)	8165(10)	-1143(7)	201
H(80C)	5689(8)	6942(10)	-829(7)	201
H(21A)	1910(7)	10389(8)	-620(4)	100
H(21B)	2931(7)	9567(8)	-866(4)	100
H(22A)	1839(7)	7698(10)	-1235(4)	110
H(23A)	439(6)	7054(9)	-723(4)	96
H(23B)	222(6)	8682(9)	-524(4)	96